Targeted-metabolomics Of Phytoplankton Blooms In The Gulf of Naples And Effects Of Algal Oxylipins On The Reproduction And Gene Expression Of The Copepod *Temora stylifera*

Thesis

Targeted-metabolomics of phytoplankton blooms in the Gulf of Naples and effects of algal oxylipins on the reproduction and gene expression of the copepod *Temora stylifera*

Ennio Russo (F4499657)

Thesis submitted for the degree of Doctor of Philosophy, XVIII Cycle

September 2019

The Open University, Milton Keynes (UK), School of Life, Health and Chemical Sciences

Stazione Zoologica Anton Dohrn, Naples (Italy), Department of Integrative Marine Ecology (IME)

Supervision Panel:

Director of Studies: **Dr. Ylenia Carotenuto** (Stazione Zoologica Anton Dohrn, Italy)

Internal Supervisor: Dr. Adrianna Ianora (Stazione Zoologica Anton Dohrn, Italy)

External Supervisor: Prof. Dr. Eric von Elert (University of Cologne, Germany)

Examiners:

External Examiner: Dr. Ana Bartual Magro (University of Cádiz, Spain)

Internal Examiner: Dr. Paolo Sordino (Stazione Zoologica Anton Dohrn, Italy)

Chair: Dr. Ulisse Cardini

Abstract

Diatoms, dominant phytoplankton in the world's ocean, synthesize a large number of oxylipins, fatty-acid-derived bioactive metabolites that impair cell proliferation. Oxylipins were originally proposed as defensive molecules hindering the reproductive success of grazer copepods through a maternal effect. In the present thesis, a targeted-metabolomics approach was applied to quantify six non-volatile oxylipins and the fatty acids from surface phytoplankton collected in the Gulf of Naples (Italy) along the year 2017. Potential effects of biotic and abiotic factors on the population dynamics of *Temora stylifera* (a dominating copepod species in the sampling area) were analysed in terms of reproductive potential and molecular responses of wild copepods captured in the sampling year. A *de novo* transcriptomic approach allowed comparing the transcriptional profiling of adult females at high and low naupliar survival rates. Expression of 13 sequences selected after the RNA-Seq analysis was quantified through RT-qPCR in wild copepod females along 2017. In the laboratory, physiological and molecular responses of *T. stylifera* females were analysed after feeding on four diatom mono-algal diets isolated from the Gulf of Naples and characterized in terms of oxylipin synthesis potential and nutritional value. Overall, the results shed more light on plankton ecology and in particular on diatom-copepod interactions. A potential role of oxylipins as signalling molecules in natural diatom communities is proposed and discussed, opening new scenarios in diatom chemical ecology studies. No clear effects of NVOs on the reproductive potential and the molecular responses of wild *T. stylifera* females were detected. A delayed negative effect of *Chaetoceros* (one of the most abundant diatom genera in the Gulf of Napels) on naupliar survival rates was observed, partially explaining the maximum population density of *T. stylifera* occurring in autumn. Transcriptional profiling suggested a gene regulation possibly aimed at maximizing the reproductive success of the copepod. The genes *ATP-Dependent RNA Helicase* (*me31b*), *Very Low-Density Lipoprotein Receptor* (*VLDLR*) and *cAMP-Responsive Element-Binding Protein* (*CREBL*) were significantly related to egg

production and could constitute sentinel sequences to estimate the reproductive potential of wild copepods in subsequent field surveys. Laboratory experiments suggested different physiological and molecular responses of *T. stylifera* females to the four diatoms, possibly indicating gene expression modulation in response to different chemical signatures of the diets.

Acknowledgements

I would like to sincerely thank my Director of Studies, Dr. Ylenia Carotenuto, for believing in me and for giving me this great opportunity. Also, I would like to thank her for her guidance, dedication and patience, for always discussing rather than imposing, for her consideration for my ideas and for always ensuring the best working conditions. I was lucky to meet her as person and researcher.

I also thank my supervisors, Dr. Adrianna Ianora and Prof. Eric von Elert, and the other researchers who supervised my work (Dr. Giuliana d'Ippolito, Dr. Angelo Fontana, Dr. Diana Sarno and Dr. Genoveffa Nuzzo) for their guidance and for always providing constructive comments and new ideas. I thank Dr. Maria Grazia Mazzocchi and Dr. Iole Di Capua for providing support and copepod abundance data and Dr. Francesca Margiotta for environmental data. I thank the MEDA Unit of Stazione Zoologica (Gianluca, Augusto, Ferdinando and Marco) for samplings and Francesco, Massimo, Mario, Fabrizio, Flora and Lucio for technical help during lab activities. I also thank my examination panel for useful suggestions provided during the *viva voce* examination.

I want to thank all my friends for their support during hard times…and especially Daniela and Paolo for borrowing me their apartment at the day of the interview!!!

I thank all people with whom I shared the path: Greta for the philosophical cups of water in the morning and the precise appointments at 12:30 for lunch; Angela, Vincenzo, Massimiliano, Lorenzo, Camilla and Lucia of course for barbecues, coffees and drinks (unforgettable the slushy gin lemon in Piazzetta Nilo!), but especially for the summer school organization! Special thanks to Vincenzo, Lorenzo, Massimiliano, Kevin, Filippo and Christian for all jokes and stupid stuff we made/said together at work and that alleviated the pressure.

I thank my parents and my sister for making all this possible. Thank you for supporting me in following my dreams; thank you for being happy if I am happy; thank you for the values you passed me and that allowed me succeeding in this tough task.

I thank Anna for always standing at my side, for her smiles and hugs that make me feel at home, for enlightening the way when I am in the dark, for remembering me what matters in life and for making me better every day.

I dedicate this thesis to all the people who ever told me to give up.

Table of Contents

List of figures

List of tables

Chapter 1

State of the art and thesis objectives

*The material in Chapter 1 forms the basis of the paper "**Russo E., Ianora A., Carotenuto Y. (2018). Re-shaping marine plankton communities: effects of diatom oxylipins on copepods and beyond**" published in "Marine Biology" to which I made major contributions*

1.1 Introduction

The global Net Primary Production (NPP) on Earth has been estimated to be 104 Pg-C/year, almost equally distributed between the land (53.8%) and the ocean (46.2%) (Field et al., 1998). Diatoms likely are the most important component of micro-phytoplankton (size between 20 µm and 200 µm) in terms of abundance and diversity and substantially contribute to the global NPP on our planet (Uitz et al., 2010). Although showing strong inter-annual and spatial variability (Alvain et al., 2008), diatoms are estimated to contribute to 1/5 of the global photosynthesis (Armbrust, 2009). Their role is particularly evident in summer periods at high latitudes, where diatoms have been observed to dominate phytoplankton communities (Uitz et al., 2010, Alvain et al., 2008), and in well mixed areas (such as coastal upwelling systems) (Armbrust, 2009), where cells synthesize conspicuous amounts of lipids in order to regulate buoyancy.

Diatoms play a fundamental role in ecological dynamics, interacting with different compartments of the aquatic systems. The carbon assimilated by diatoms can rapidly enter the aquatic food web through grazing or can alternatively sink towards the bottom, contributing to the biological carbon pump and to the formation of fossil carbon resources (Armbrust, 2009, Tréguer and Pondaven, 2000). While sinking to the deep ocean, algal cells are also colonized by an increasing fraction of heterotrophic bacteria, potentially introducing a source of variation in microbial communities (Grossart et al., 2006). Also, the extensive grazing on diatoms implies a great contribution of these microalgae to the classical food web, up to top predators, following the paradigm: diatoms – zooplankton - small pelagic fishes – large pelagic fishes - humans.

The role of diatoms in shaping plankton communities and in driving ecological dynamics has received even more attention after that (Miralto et al., 1999) isolated three polyunsaturated aldehydes (PUAs, two decatrienal isomers and the decadienal; Figure 1.1) from two diatom species blooming in the Northern Adriatic Sea. The teratogenic effect of

these molecules drove the authors to highlight detrimental insidious consequences on the egg viability of two grazers, the copepods *Acartia clausi* and *Calanus helgolandicus*, possibly explaining the bulk of annual copepod recruitment surprisingly observed in the diatom post-bloom phase. This milestone study increasingly drew scientific attention to the negative effects of diatoms for secondary producers and challenged the validity of the classical trophic chain (primary producers – grazers – top predators). In addition, it also stressed the importance of chemical ecology for a more comprehensive understanding of ecological dynamics in plankton studies.

Nowadays, it is generally accepted that several diatom species produce many diverse oxylipins, generally defined as fatty acid-derived oxygenated compounds, synthesized through enzymatic oxygenation (Cutignano et al., 2011). Even if these same authors divide oxylipins into three major families (hydroxyl fatty acids, carbonil-containing fatty acids and epoxy-alcohols fatty acids), a more general differentiation divides them into non-volatile oxylipins (NVOs) and volatile oxylipins (Barreiro et al., 2011).

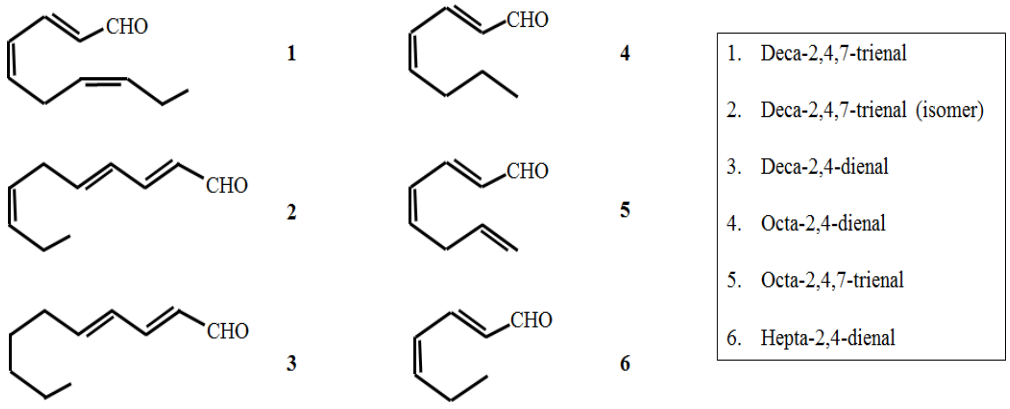

Figure 1. 1: The main polyunsaturated aldehydes produced by diatoms (modified after Fontana et al., 2007a).

Studying oxylipin production and the effects of these molecules on meso-zooplankton represents an extremely important and complex topic. Results presented so far have been

sometimes contradictory and the actual role of oxylipins in shaping plankton communities has been debated (Flynn and Irigoien, 2009, Irigoien et al., 2002).

Among zooplankton, copepods represent one of the most various and important groups in both marine and freshwater systems. Globally, around 13,000 morphospecies have been estimated to actively colonize both the pelagic and the benthic domains as well as to adapt to parasitic life strategies (Boxshall and Defaye, 2007). Most of the copepod taxonomic richness is found at sea, where they show geographic patterns in species distribution based on environmental gradients: maximal diversity seems to occur at low latitudes, relating positively with temperature and salinity, while negatively with chlorophyll-a concentrations (Rombouts et al., 2010, Rombouts et al., 2009).

As marine copepods dominate pelagic metazoan communities, they play a central role in food webs, remarkably affecting carbon transfer to higher and lower trophic levels (Boxshall and Defaye, 2007, Verity and Smetacek, 1996). Copepods not only actively graze/prey on large phytoplankton/ciliates, but they also affect directly and indirectly carbon transfers to microbes and top-predators (Figure 1.2). They directly contribute to the microbial food web mainly through the export of carbon from epipelagic layers to deep waters: organic matter can reach the bottom as faecal pellets (these aggregates tend to sink quickly) or in response to active migrations of copepods to lower depths (Turner, 2015). Moreover, copepod carcasses have been shown to be hot spots of denitrifying bacteria communities (Glud et al., 2015), probably also in response to the high N concentrations that characterize these animals (Meunier et al., 2016). Indirectly, variations in the grazing pressure exerted by copepods can alter the transfer of phytoplankton detritus to the deep waters as marine snow (Turner, 2015, Zöllner et al., 2009). Copepods are also among the favourite preys of many pelagic and more demersal fishes: they are actively predated by anchovies (Palomera et al., 2007) and variations in their availability have been shown to significantly affect the population dynamics of the Atlantic cod (Beaugrand et al., 2003).

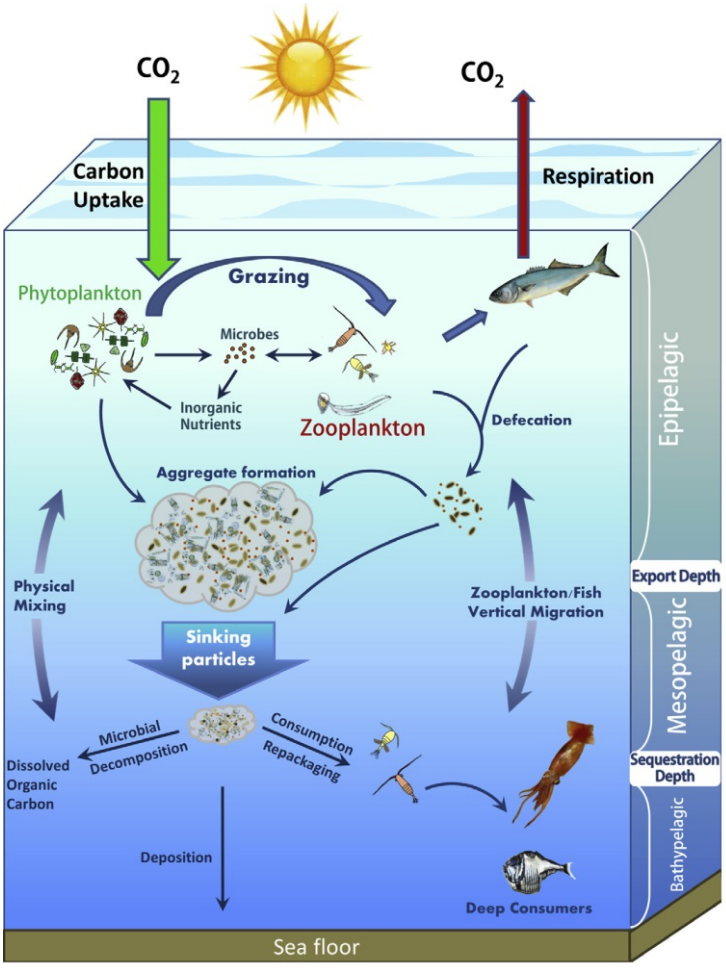

Figure 1. 2: Schematic representation of carbon flow in marine systems (Turner, 2015).

This brief description probably already illustrates how much changes in copepod abundance and composition can profoundly affect ecological dynamics at different levels of the marine food web.

1.2 Oxylipin production in diatoms

Oxylipins are reactive molecules produced through the oxygenation of fatty acids. While almost all metazoan lineages are lacking any oxylipin synthesis potential, it has been estimated that genes involved in oxylipin biosynthetic pathway were present in the last common ancestor of plants and animals (Lee et al., 2008). In diatoms, oxylipins are synthesized through an enzymatic cascade activated after cell breaking (d'Ippolito et al., 2004, Pohnert, 2002) with the production of: 1) free polyunsaturated fatty acids (PUFAs);

2) oxygenation of PUFAs by lipoxygenases (LOX) with subsequent production of fatty acid hydroperoxides (FAHs); 3) transformation of FAHs into oxylipins by further enzymatic activity. In diatoms, the main fatty acid classes that are utilised/that serve as substrate for oxylipin synthesis seem to be Eicosapentaenoic-acid (EPA, C20:5) and both Hexadecatrienoic-acid and Hexadecatetraenoic-acid (HTrA, C16:3 and HTA, C16:4, respectively) (Ianora et al., 2012b, d'Ippolito et al., 2002), even if it has been recently demonstrated that *Leptocylindrus* spp. can synthesize oxylipins also from the Docosahexaenoic-acid (DHA) (Nanjappa et al., 2014). Phospholipids and glycolipids are the main sources of free fatty acids in diatoms and non-specific phosholipases catalyse the cleavage from the sn-1 and the sn-2 sites of the glycerol head (Fontana et al., 2007a). Within a few minutes after cell disruption, LOXs efficiently oxygenize up to 69% of the available PUFAs (Wichard et al., 2007), prompting formation of FAHs. Subsequently, enzymes, such as hydroperoxidelyases (HPLs), reductases and epoxyalcohol synthases, further catalyse the synthesis of a wide array of oxylipins, both PUAs and NVOs (d'Ippolito et al., 2009, Ianora and Miralto, 2010).

Interestingly, oxylipin production in diatoms is known to be an extremely variable process. Differences have been highlighted at the genus, species, population and clonal level (Gerecht et al., 2013, Gerecht et al., 2011), in response to a) variations in the LOX activity (Cutignano et al., 2011) and b) physiological and genetic factors (Lamari et al., 2013). Examples reporting production of different oxylipins among genera and species are numerous. For instance, few *Chaetoceros* are known to produce PUAs (Fontana et al., 2007b, Wichard et al., 2005b), while a LOX activity focused at the C-11 of the EPA mediates the formation of the PUA decatrienal in the diatom *Thalassiosira rotula* (Fontana et al., 2007a). These same authors described *Skeletonema costatum* (now *Skeletonema marinoi*) to synthesize the PUA heptadienal after peroxidation at the C-14 of this same fatty acid; additionally, a LOX activity at the C-9 of the Hexadecatrienoic (HTrA) and the Hexadecatetraenoic (HTA) acids was observed to catalyse formation of octadienal and

octatrienal, respectively, in *T. rotula* and *S. costatum* (Fontana et al., 2007a). Remarkably, 15S-LOX peroxidation has been documented to drive the synthesis of oxylipins from DHA in *Leptocylindrus* spp. (Nanjappa et al., 2014). At the species level, *Skeletonema pseudocostatum* has been reported to synthesize only NVOs, differently from *S. marinoi* (Barreiro et al., 2011). Additionally, *Thalassiosira pseudonana* does not seem to express the LOX genes at all and to produce oxylipins, in contrast with the PUA-producing *T. rotula* (Wichard et al., 2005b, Wichard et al., 2005a). Strong differences have been reported also at the population level, since *T. rotula* occurring in the Gulf of Naples seems to produce high amounts of aldehydes, while the population off the coast of California likely does not (Paffenhöfer et al., 2005). Differences in PUA production were also found in *T. rotula* by (Barreiro et al., 2011), who observed one population to produce the PUAs octatrienal, octadienal and heptadienal, while only a second one to synthesize decatrienal. (Gerecht et al., 2013, Gerecht et al., 2011) suggested that oxylipin production could represent differences even among clones of the same algae (in their experiment *S. marinoi*) characterized by similar protein contents and growth rates.

Some studies indicate different oxylipin production also at different growth stages of the same diatom strain: (d'Ippolito et al., 2009), for example, concluded that the diatom *Pseudo-nitzschia delicatissima* can produce the 15-oxoacid especially during the stationary phase, while (Vidoudez and Pohnert, 2012) by means of a comparative metabolomics approach, observed the highest occurrence of PUAs during the exponential and the stationary growth phases of a *S. marinoi* culture. (Vidoudez and Pohnert, 2008) reported even an active release of oxylipins by *S. marinoi* before the cells entered the declining phase. This finding may suggest that oxylipins can act as info-chemicals in diatom communities or populations, raising compelling questions about their role in marine food webs (Bidle, 2016, Bidle, 2015). Recently, evidence was provided about the ability of diatoms to genetically respond to mechanical forces. (Amato et al., 2017), in fact, demonstrated that diatoms can rapidly adjust their biochemical pathways depending on the

turbulence regime of the system. These authors observed an increased expression of genes involved in fatty acid biosynthesis at higher turbulence regimes. Even if the levels of fatty acids do not seem to directly correlate with the amount of oxylipins produced by diatoms (Vidoudez and Pohnert, 2012), likely caused by different expression potential of LOX genes, variations in oxylipin synthesis may also indirectly depend on environmental mechanical forces because of the enhanced availability of substrata.

1.3 Effects of oxylipins on copepods

Oxylipins have been demonstrated to exert teratogenic effects on a wide range of organisms, including Echinodermata, Mollusca and Crustacea (Adolph et al., 2004), suggesting that their activity is due to unselective biochemical reactions influencing generic biological processes shared by eukaryotes.

Copepods are generally clustered among the most important active grazers feeding on diatoms in pelagic aquatic systems. Oxylipins have been demonstrated to impair embryonic development in copepods and potentially to drive reduced fitness in natural populations of these metazoans by affecting gametogenesis, fertilization, embryogenesis and larval fitness (Ianora et al., 2012a, Caldwell, 2009, Ianora et al., 2004). (Wolfram et al., 2014) showed that oxylipins can selectively accumulate in the gonads of copepods, where they chemically react with nucleophiles (such as proteins and DNA) and impair reproduction (Figure 1.3). (Wolfram et al., 2014), in particular, monitored the accumulation of fluorescent probes containing α,β,γ,δ-unsaturated aldehyde structures (tetramethylrhodamine based fluorescent reporter, TAMRA-PUA) and a set of control probes containing saturated aldehyde structures (TAMRA-SA) in the internal tissues of the copepod *Acartia tonsa*. The authors showed that whether TAMRA-PUA probes accumulated in copepod female gonads, TAMRA-SA were mainly located in the lipid sac.

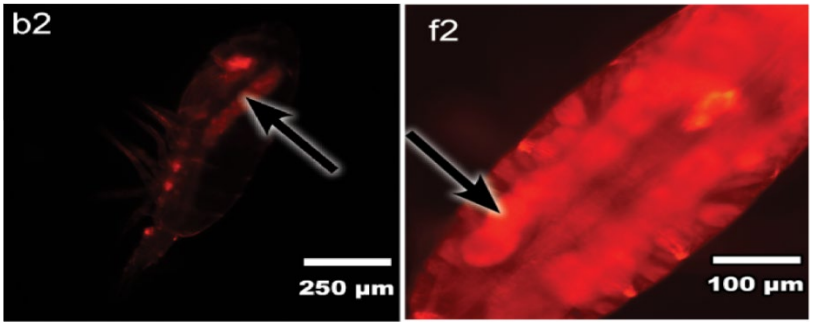

Figure 1. 3: Accumulation of TAMRA-SA (b2) and TAMRA-PUA (f2) in the lipidic sac and the gonads of the copepod *Acartia tonsa,* respectively (modified after Wolfram et al., 2014).

Even if PUAs presumably are the most harmful molecules due to their short carbon structure (Adolph et al., 2004), in recent years evidence has accumulated on teratogenic effects mediated by a wider spectrum of other substances of diatom origin. In fact, oxygenation of unsaturated fatty acids catalysed by LOX enzymes triggers the formation of powerful Michael's acceptors in addition to PUAs. For example, FAHs (molecules clustered in the hROS, highly Reactive Oxygen Species, family) are intermediates generated during LOX activity that can determine both oxidative stress and reduced reproductive potential in copepod grazers (Fontana et al., 2007b). Moreover, FAHs can be further enzymatically modified to form a wide array of NVOs (d'Ippolito et al., 2005), which, as PUAs, easily react with nucleophiles (Pohnert, 2002). (Fontana et al., 2007b) were likely the first who clearly demonstrated that NVOs synthesized by non-PUA producing diatoms (e.g. *Skeletonema pseudocostatum*) can induce apoptosis and reduce hatching success in grazer copepods.

In consideration of such a marked teratogenic potential expressed through the synthesis of many diverse oxylipin classes, it is not surprising that several authors keep reporting how a diatom-rich diet can induce significant decreases in egg production rates, hatching success and naupliar survival (even with 100% of larval mortality) in several copepod species (Md Amin et al., 2011, Ianora et al., 2011, Poulet et al., 2006, Vargas et al., 2006, Ianora et al., 2004).

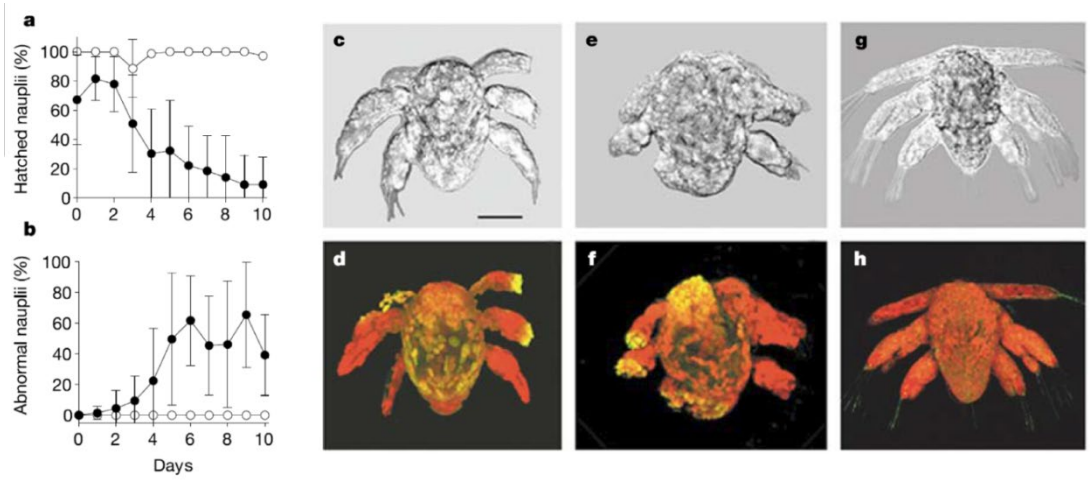

Figure 1. 4: a) Percentage of eggs viability spawned after *Calanus helgolandicus* 10 days feeding on *Skeletonema costatum* (filled circles) and *Prorocentrum minimum* (open circles). b) Percentage of abnormal nauplii after feeding on *S. costatum* and *P. minimum*. c)-d)-e)-f) Abnormal nauplii after feeding on *S. costatum* (yellow areas indicate apoptosis after TUNEL staining). g)-h) Nauplii after feeding on *P. minimum* (Ianora et al., 2004).

Teratogenesis represents the main consequence for copepods upon diatom ingestion (Figure 1.4), but the effects seem to go even beyond. For example, (Brugnano et al., 2016) recently documented negative influences also on larval biomass in the copepod *Paracartia latisetosa*, after feeding on *Skeletonema marinoi*. These authors tested the effects of this diatom on developmental rates of *P. latisetosa* nauplii applying four experimental conditions: a control where both females and nauplii were reared on *Prorocentrum minimum*, a treatment where both females and nauplii fed only on *S. marinoi* and two additional switching feeding conditions for females/nauplii (*P. minimum*/*S. marinoi* or *S. marinoi*/*P. minimum*). Results showed that the most significant differences in naupliar biomass were evident between the control and the treatment diet, after 24h and 48h of maternal feeding. In particular, growth rates varied from a maximum of 0.32 µg-C/day (control diet) to a minimum of 0.04 µg-C/day (both females and nauplii reared with *S. marinoi*). Additional effects of oxylipin producing diatoms on copepods may also relate to sex ratios, since (Carotenuto et al., 2011) observed skewed ratios in the copepod *Temora stylifera* fed on the PUA producing diatoms *Thalassiosira rotula* and *S. marinoi*.

Despite the evident negative effects of oxylipins on the larval stages of their grazers (i.e. nauplii), mortality of adult specimens has been observed only in rare occasions (Buttino et al., 2008), probably because adult copepods can up-regulate specific detoxification enzymes to limit the negative effects of these molecules (Carotenuto et al., 2014). In fact, oxylipin production is generally interpreted as a chemical defence not intended to directly kill predators, but rather to negatively affect the offspring (n+1 generation) through the mothers (i.e. the so called "maternal effect") (Ianora et al., 2004). By contrast, oxylipins have been observed to have direct negative influences on those post-embryonic stages that actively feeding on diatoms (Carotenuto et al., 2011, Carotenuto et al., 2002), suggesting that distinct developmental stages of the same copepod species can express different abilities to mitigate the negative effects of harmful chemicals.

1.3.1 Copepod responses at a molecular level

The application of molecular tools to measure the effects of oxylipin-producing diatoms on copepods is a particularly useful approach to study the effects of diatoms on grazers. Expression analyses of specific Genes of Interest (GOIs) using a Real Time quantitative PCR approach (RT-qPCR), led (Lauritano et al., 2011a, Lauritano et al., 2011b) to conclude that only two days of feeding of *Calanus helgolandicus* females on the diatom *Skeletonema marinoi* can drive a 2-fold down-regulation of *α-tubulin* (*A-TUB*) coding gene, a 3-fold down regulation of *β-tubulin* (*B-TUB*) gene and a reduction of primary defence genes (e.g. chaperones) against toxins. For these experiments, *C. helgolandicus* specimens were collected in the Northern Adriatic Sea and then fed for 2 days *ad libitum* in the laboratory with either diatoms (*S. marinoi* or *Chaetoceros socialis*) or flagellates (*Prorocentrum minimum* or *Rhodomonas baltica*). Results revealed stronger responses after feeding on *S. marinoi* than the other diets (*C. socialis*, *P. minimum* and *R. baltica*), with significant down-regulation of the *Heat Shock Protein 40* (*HSP 40*) coding gene, of genes involved in apoptosis regulation (*Cellular Apoptosis Susceptibility*, *CAS*,

and *Inhibitor of Apoptosis*, *IAP*, proteins), of several aldehyde dehydrogenase isoforms (*ALDH6*, *ALDH8* and *ALDH9*; Lauritano et al., 2011b), and of *A-TUB* and *B-TUB* coding genes (Lauritano et al., 2011a, Lauritano et al., 2011b). Interestingly, *C. socialis*, a non-PUA producing diatom, was not observed to significantly alter gene expression patterns in the same copepod (Lauritano et al., 2011a). These effects were also confirmed *in situ*, as down-regulation of *A-TUB* and *B-TUB* as well as of *CAS* coding genes were detected in *C. helgolandicus* females collected in the Adriatic Sea during a sampling cruise (Lauritano et al., 2016). The down-regulation of these genes can be the putative trigger of tubulin polymerization inhibition, with consequent deleterious effects on the appropriate spindle formation during cell division and final apoptosis events in the embryos (Lauritano et al., 2016, Lauritano et al., 2011b). These studies validate on a molecular basis previous results indicating PUA producing diatoms as adverse food items for the correct development of copepod larval stages and in final instance for recruitment. Nonetheless, they also require further experimental validation: effects at the molecular level have been revealed only for *C. helgolandicus* in response to a limited array of diatom species, populations and strains. A wider number of non-PUA producing diatoms needs to be tested under different experimental conditions, analysing the effects on copepods also after longer feeding periods.

The copepod molecular response to oxylipin-producing diatoms was also investigated using other approaches. (Carotenuto et al., 2014) were the firsts who analysed the whole transcriptional profile of *C. helgolandicus* through a Suppression Subtractive Hybridization approach (SSH), demonstrating that 2 days of feeding on *S. marinoi* significantly altered the whole transcriptomic machinery of the females, when compared to specimens raised on a control diet (i.e. *R. baltica*). These authors sequenced a total of 947 Expressed Sequence Tags (ESTs), which were further assembled into 376 unigenes of *C. helgolandicus*. Results highlighted a strong stress response (expression of genes involved in protein folding/degradation, re-organization of tubulin filaments and in processing

environmental and cellular information) in *C. helgolandicus* fed with *S. marinoi*, leading the authors to reconstruct the possible pathway explaining the short-term effects of oxylipins on copepods. In brief, ingestion of *S. marinoi* may inhibit *ALDH*, *IAP*, *CAP* and *A*/*B-TUB* coding genes with a consequent accumulation of aldehydes in copepod tissues (possibly the gonads) (Wolfram et al., 2014) and final apoptosis; subsequently, a Cellular Stress Response (CSR) is activated by the adults in order to re-establish homeostasis as well as both structure and function of macromolecules. Such molecular and physiological responses can support successful reproduction of *C. helgolandicus* feeding for 2 days on *S. marinoi* (Ianora et al., 2004). These data also suggest that adaptive responses of adult copepods to oxylipin ingestion cannot be effective for long periods of feeding on oxylipin producing diatoms, because *S. marinoi* has been shown to induce dramatic declines in both egg viability and naupliar survival in *C. helgolandicus,* after 48 hours (Fontana et al., 2007b, Ianora et al., 2004). In addition, results presented by (Carotenuto et al., 2014) could also offer interesting clues to explore species-specific responses of copepods to oxylipin producing diatoms (Ianora et al., 2008, Fontana et al., 2007b). An intriguing perspective is to inspect molecular responses of different developmental stages of selected copepod species; such an approach could potentially reveal why feeding nauplii seem to be more sensitive to oxylipins than the adults, after ingesting diatoms (Carotenuto et al., 2011). RNA extraction protocols have been recently optimized for the calanoid copepods *Temora stylifera* and *Centropages typicus* from the Gulf of Naples (Asai et al., 2015). Such methods can now be applied to a wider range of copepod species, thereby revealing molecular responses of these metazoans through gene expression analysis or transcriptomic approaches.

1.3.2 Variation in copepod responses to diatoms

Some authors, after both laboratory experiments (Buttino et al., 2008; Fontana et al., 2007b) and field surveys (Ianora et al., 2008; Vargas et al., 2006), have proposed that

distinct copepod species may be differently affected by oxylipins, but little information is available in this sense. In fact, results mainly derive from experiments focusing on a relatively limited number of copepod genera/species (i.e. mainly *Calanus* spp., *Temora* spp. and *Acartia* spp.) and only a few studies have simultaneously examined more than one species. For example, the copepods *Centropages typicus*, *Acartia clausi* and *Temora stylifera* showed dissimilar reproductive outputs after feeding on the PUA producing diatom *Thalassiosira rotula* (Ianora and Miralto, 2010). (Buttino et al., 2008) observed different responses of *T. stylifera* and *Calanus helgolandicus* in terms of egg production, hatching success and naupliar survival, after ingestion of decadienal (DD)-loaded giant liposomes. Similarly, unequal egg production and hatching success were detected in the same copepod species fed with *Chaetoceros socialis*, *Chaetoceros affinis* and *Skeletonema marinoi* (Fontana et al., 2007b). Different reproductive potentials among distinct copepod species have been also highlighted in the field. (Ianora et al., 2008) suggested that reproductive success of *A. clausi* could have been less affected than those of *C. helgolandicus* and *Temora longicornis*, in the Northern Adriatic Sea. Differences in egg production, hatching success and naupliar survival were found also in the copepods *Acartia tonsa*, *Paracalanus parvus* and *Centropages brachiatus* collected off the coast of Chile (Vargas et al., 2006). More recently, species-specific sensitiveness to oxylipins has been demonstrated also on a molecular basis, analysing the expression of selected genes of interest in *C. helgolandicus* and *Calanus sinicus* (Lauritano et al., 2015). These authors, in particular, evaluated the molecular responses of *C. sinicus* after 2 and 5 days of feeding on *S. marinoi.* Target genes encompassed some of those involved in primary defensive mechanisms, such as heat shock proteins *HSP70* and *HSP40*, *Cytochrome P450-4*, *Glutathione S-Transferase* (*GST*), *Glutathione Synthase* (*GSH-S*), *Superoxide Dismutase* (*SOD*) and *Catalase* (*CAT*) as well as others involved in aldehyde detoxification (*ALDH2*, *ALDH3*, *ALDH6*, *ALDH7*, *ALDH8* and *ALDH9*). The authors reported a reduction in the expression levels of *CAT*, *HSP70*, *B-TUB* and one *aldehyde dehydrogenase* after 2 days,

while after 5 days an up-regulation of *B-TUB*, *ADLH2*, *ALDH9*, *CAT* and *GSH-S*, suggesting recovery from the harmful effects. Such results were discussed in comparison to variations in gene expression patterns of *C. helgolandicus* exposed to the same oxylipin producing diatom for the same time period, revealing strong species-specific differences (Lauritano et al., 2012, Lauritano et al., 2011a, Lauritano et al., 2011b). In general, these results demonstrate that copepods may respond differently to harmful compounds of diatom origin because of variable detoxification potentials, posing important evolutionary, physiological and ecological questions.

In addition to species-specific effects of diatoms on grazing copepods, a recent study also demonstrated population-specific responses in the copepod *C. helgolandicus*. Analysing specimens originating from populations of the Atlantic Ocean, the North Sea and the Mediterranean, (Lauritano et al., 2012) showed that the Atlantic and the North Sea individuals (which were demonstrated to share the same haplotype) could actively up-regulate detoxification enzymes, while the Mediterranean ones did not. These authors, in particular, offered either the non-oxylipin producing algae *Rhodomonas baltica* or the PUA-producing diatom *S. marinoi* to *C. helgolandicus* specimens collected in the three different regions, assessing molecular responses of the animals after 24 or 48 hours. An up-regulation of radical detoxification enzymes was recorded in *C. helgolandicus* specimens from the North Sea and the Atlantic Ocean, but not in those from the Mediterranean Sea. Similarly, no aldehyde detoxification enzymes were expressed in copepods from the Adriatic Sea, in contrast to the up-regulation of *ALDH2*, *ALDH7*, *ALDH8* and *ALDH9* in the samples from the Swedish coast and the Atlantic, after 24 hours. This study provided compelling evidence about even a population-specific sensitiveness of *C. helgolandicus* to oxylipins, possibly in response to divergent evolution of defensive mechanisms. Such information constitute precious clues to appropriately approach the topic and indicate that assessing the global role of diatoms in marine plankton food webs through a comparative analysis of their effects on copepod reproductive potential alone could be misleading.

Evaluation of copepod responses to harmful diatoms now needs to be supported by appropriate molecular analyses; by their application, it would be possible to generate global databases of species-/population-specific responses, which could provide key guidelines to the understanding of marine plankton food webs at discrete spatial-temporal scales.

Even if laboratory experiments inspecting the effects of single diatom species on copepods are of key importance for a clearer understanding of diatom-copepod interactions, the effects of potentially harmful phytoplankton on the population dynamics of these metazoans should be inspected in consideration of their complex ecology. In fact, diet composition undoubtedly constitutes another relevant source of variation in determining reproductive failure in copepods. For instance, mixed diets including low diatom concentrations have been demonstrated to improve copepod growth with relatively limited reduction in hatching success (Carotenuto et al., 2012). These authors demonstrated that low concentrations (0.17 mg C/L) of *Thalassiosira weissflogii* added to a mixed flagellate diet (*Isochrysis galbana*, *R. baltica*) favoured recruitment of *C. helgolandicus* during short feeding periods (<2 months). Previously, other experiments tested the effects of both mixed diets and a switch in prey items on the reproductive success of copepods (Poulet et al., 2007a, Poulet et al., 2007b). (Poulet et al., 2007b), for example, observed low egg production in the calanoid *Calanus chilensis*, when a diatom enriched diet was provided. This effect was not reversible, when *Prorocentrum minimum* was offered to the females. Conversely, negative impacts of diatoms on the egg production rate of *C. helgolandicus* females (from the Western English Channel) were dampened, when *P. minimum* was provided (Poulet et al., 2007a). More recently, while the diatoms *T. rotula* and *S. marinoi* used as pure cultures were observed to arrest development from nauplii to adult stages in the copepod *T. stylifera*, a mixed diet (*P. minimum* + *T. rotula*) erased the effect, irrespective of maternal feeding (Carotenuto et al., 2011). However, such patterns can strongly depend on the oxylipin profile of the diatom ingested, because *P. minimum*

provided along with *S. marinoi* was not efficient in alleviating negative effects on the copepod (Carotenuto et al., 2011). Positive influence of a mixed diet on egg production rates was recently presented also by (Vehmaa et al., 2011), who tested the effects of a reduced diatom:dinoflagellate (*S. marinoi*:*Scrippsiella hanogei*) ratio on the egg production of the copepod *Acartia bifilosa* collected in the Baltic Sea. After subjecting the copepods to 11 diets at varying diatom:dinoflagellate ratios (from 1:0 to 0:1), the authors concluded that a mixed assembly of these two phytoplankton species could benefit egg production of the copepod.

After this brief presentation, it is clear that extrapolating a general pattern about the effects of diatoms and oxylipins on grazer copepods is extremely difficult. Considering the complexity of the topic and the number of questions which are still pending, further experimental efforts are needed. An important step would be the definition of oxylipin production potentials in more diatom species and the study of their effects on a higher number of different grazing copepods in well-defined spatio-temporal scales, in order to explore such variability in more detail. Field experiments supported by laboratory approaches integrating physiological, molecular and chemical variables, in particular, will constitute key approaches in order to shed more light on the actual role of diatoms in shaping plankton communities.

1.3.3 In situ *diatom-copepod interactions*

Field data supporting evidence of negative effects of oxylipins on copepods are still relatively scarce and limited in spatial replication. Nonetheless, *in situ* experiments inspecting diatom-copepod interactions are accumulating in recent years, progressing from an initial effort correlating diatom phenology to copepod reproductive outputs (Irigoien et al., 2002, Miralto et al., 1999) towards the inclusion of both chemical and molecular analyses as response variables. Figure 1.5 highlights globally distributed areas where effects of diatoms on copepod have been evaluated so far.

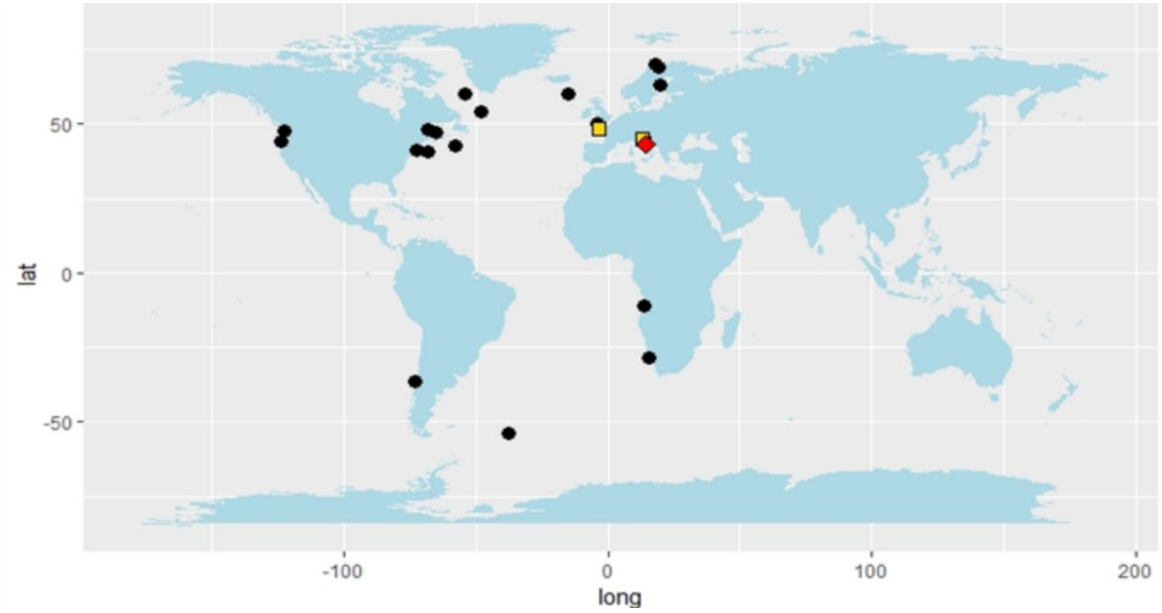

Figure 1. 5: Representation of the globally distributed areas, where effects of diatoms on copepods were estimated. Black circles: sampling locations where diatom phenology has been related to copepod reproductive success (Irigoien et al., 2002; Halsband-Lenk et al., 2005; Halsband-Lenk, 2005; Pierson et al., 2005; Ask et al., 2006; Vargas et al., 2006; Koski, 2007); yellow squares: sampling locations encompassing chemical characterization of phytoplankton extract (i.e. Wichard et al., 2008 in the English Channel; Ianora et al., 2015 in the Adriatic Sea); red diamond: sampling sites considering both chemical analyses of phytoplankton extracts and molecular responses of copepods (i.e. Lauritano et al., 2016 in the Adriatic Sea). Image reported from (Russo et al., 2019).

Results presented by (Irigoien et al., 2002) offered for the first time a spatially wide overview of copepod-diatom interactions. These authors analysed hatching success in 17 copepod species across 12 globally distributed areas, in relation to diatom biomass and dominance. (Irigoien et al., 2002) concluded that the classic food web paradigm was still valid, because no clear negative correlation was detected between hatching success and diatom biomass. (Koski, 2007) performed a 10 day field cruise in three Norwegian fjords (Balsfjord, Ullsfjord and Malangen) where egg production rates, hatching success, naupliar development and food selection of the copepod *Calanus finmarchicus* were analysed. The copepod seemed to actively graze on diatoms such as *Thalassiosira* and *Chaetoceros* as well as on ciliates and dinoflagellates depending on their availability. Nonetheless, high feeding selections for diatoms did not seem to affect the reproductive potential. (Ask et al., 2006) analysed hatching success and clutch size in the calanoid copepod *Eurytemora affinis* from the Gulf of Bothnia (Baltic Sea), reporting the lowest hatching frequencies to

occur at the final stage of the spring diatom bloom, while the highest when ciliates were abundant and diatoms represented less than the 50% of the phytoplankton community. Interestingly, a negative correlation between the hatching success and the total abundance of diatoms was reported; more in particular, *Chaetoceros* spp. were indicated as the main drivers for the impaired reproductive success. (Ianora et al., 2008) estimated the effects of the diatom *Cerataulina pelagica* (a non PUA-producing diatom) on the egg viability of *Calanus helgolandicus*, *Temora longicornis* and *Acartia clausi* in the Northern Adriatic Sea and observed low reproductive potential in the first two species, but not in *A. clausi*. In this study, concentration levels of FAHs (which are oxylipin precursors) were estimated to range between 30 and 100 ng/μg protein. A series of field experiments have also been performed in Dabob Bay (Washington, USA), where the reproductive potential of the copepods *Pseudocalanus newmani*, *Metridia pacifica* and *Calanus pacificus* was studied in relation to diatom composition and abundance, between February 2002 and May 2004 (Halsband-Lenk, 2005, Halsband-Lenk et al., 2005, Pierson et al., 2005). (Halsband-Lenk et al., 2005) concluded that when the diatoms *Thalassiosira pacifica* and *Thalassiosira aestivalis* dominated phytoplankton blooms, egg viability of *P. newmani* fell below 50% and naupliar survival below 1%, suggesting that a) the effects of diatoms on the reproductive success of grazer copepods may be cumulative and that b) the abundance of aldehyde-producing diatoms (rather than total diatom abundance) may be the most appropriate factor for estimating copepod reproductive success. Similar results were also described for the reproductive success of the copepod *C. pacificus* (Pierson et al., 2005), since naupliar survival was the variable that best allowed detecting potential harmful effects of oxylipin-producing diatoms. In particular, lower survival rates were recorded in concomitance with the bloom of *Thalassiosira* spp. Similarly, also (Vargas et al., 2006) observed naupliar survival variations in *Acartia tonsa*, *Paracalanus parvus* and *Centropages brachiatus* to be more marked than those in hatching success, in Dichato Bay

(Chile). In this area, PUA concentrations were estimated to vary between 3.12 fmol/cell and 11.2 fmol/cell, in 2004 (Poulet et al., 2007a).

More recently, *in situ* experiments have been carried out including a higher number of variables, progressing from chemical analyses of phytoplankton extracts towards the evaluation of molecular responses of copepods at sea. (Wichard et al., 2008), for example, inspected the reproductive potential of *C. helgolandicus* from the coastal waters off Roscoff, through an integrative approach including toxic and nutritional analyses of food items. Here, the authors reported a PUA concentration of 0-8 fmol/diatom cell. The data indicated that hatching success did not depend on temperature, chlorophyll-a, PON, POC, PUA production or DHA/EPA (Docosahexaenoic-acid:Eicosapentaenoic-acid) ratio. In turn, the authors concluded that PUA-producing diatoms in the study area were not negatively impacting reproductive success of *C. helgolandicus*, possibly in response to adaptive detoxification mechanisms activated by the animals after ingestion (Wichard et al., 2008). This hypothesis could be realistic, because (Lauritano et al., 2012) have recently demonstrated that *C. helgolandicus* from the North Sea shows faster molecular responses to PUA-producing diatom ingestion than the Mediterranean population. In 2004 and 2005, field cruises were performed in the Northern Adriatic Sea, inspecting the effects of both volatile (PUAs) and non-volatile oxylipins on the reproductive potential of the copepods *C. helgolandicus* and *A. clausi* (Ianora et al., 2015). These authors, in particular, tested the effects of late-winter diatom assemblages on the reproductive output of the two copepod species, evaluating results in consideration of PUA and NVO concentration. The relevance of this study relies not only on the temporal replication, but also on the contemporary evaluation of two copepod species and the chemical analyses of phytoplankton samples. With this multidisciplinary approach, (Ianora et al., 2015) described copepod species-specific responses in two separate time windows and showed how NVOs could be of high impact on the reproductive success of copepods at sea (cf. Barreiro et al., 2011). In fact, in 2004, a lower amount of oxylipins (around 4.5 μg/mg protein) was detected in comparison

to the year 2005 (around 11 μg/mg protein), in the sampling stations considered; most oxylipins were not classified as PUAs, but rather as NVOs, which were considered as the main chemicals driving low hatching success in *C. helgolandicus* and *A. clausi*. In this same basin, particulate PUAs (i.e. PUAs produced after cell braking) were estimated to range between 0 and 5.37 fmol/cell between 2002 and 2006 (Ribalet et al., 2014). More recently, (Lauritano et al., 2016) studied the responses of *C. helgolandicus* to diatom occurrence in the Northern Adriatic Sea through the application of both chemical and molecular analyses to characterize, respectively, a) chemicals potentially harmful for copepod grazers and b) expression of stress genes in the target copepod species at sea, at different spatial-temporal scales. This survey led to the characterization of new oxylipins of phytoplankton origin (a maximum amount of 1.39 μg/mg protein was detected) and demonstrated that wild *C. helgolandicus* feeding on diatoms can show 1) down-regulations of genes involved in mitosis and 2) activation of stress responses through the expression of *glutathione S-transferase* (*GST*), *catalase* (*CAT*) and *aldehyde dehydrogenase* (*ALDH8*) enzymes. In general, very useful methodological and conceptual information can be gained from results collected after these field experiments. Results obtained by (Halsband-Lenk et al., 2005, Halsband-Lenk, 2005, Pierson et al., 2005) may suggest that an effective evaluation of copepod population dynamics could be assessed only including the naupliar survival rate among the explanatory variables. A common feature of the field experiments described is that relationships between diatom abundances and copepod reproductive success are rarely evident through direct correlation analyses. This lack of correlation could be due to several reasons among which are: a) the great variability for oxylipin synthesis by different species and even by the same species growing under different physiological conditions; b) differences in the capability of copepod species to deal with these compounds, including differences in their detoxification capacity. Therefore future *in situ* studies aiming to evaluate copepod fitness should also consider quantifying oxylipins. Possibly, chemical analyses should be supported also by molecular quantifications of the

expression of specific genes of interest in copepods. Stepping stones in this process would be the definition of standard protocols for oxylipin description and quantification as well as the design and optimization of molecular primers for a wider array of target genes, in order to successfully test stress responses in a higher number of copepod species. Alternatively, -omic approaches encompassing both chemical (metabolomics) and molecular (next-generation sequencing) analyses of phytoplankton samples and copepods, respectively, may represent important resources in the future (Amato and Carotenuto, 2018). More generally, further experimental effort is needed, because such integrative approaches have been only rarely applied so far.

1.4 Metabolomics in chemical ecology

The metabolome is defined as the sum of the small metabolites produced in a given species (Kuhlisch and Pohnert, 2015, Patti et al., 2012) and metabolomics is the discipline studying low-molecular metabolites in biological systems (Kido Soule et al., 2015). In the recent years, the application of metabolomics approaches in biological studies has progressively received more attention. One of the main advantages in the application of metabolomics is that the analysis of expressed genes and proteins does not account for epigenetics and post-translational modifications, while focusing on metabolites allows directly evaluating the actual concentrations of metabolites regulated in the organisms (Patti et al., 2012). This means that through metabolomics analyses it is possible to acquire a functional snapshot of the metabolic processes activated in a given species to evaluate relationships between the organisms and the environment (Llewellyn et al., 2015, Patti et al., 2012). Even if the analysis of targeted metabolites has been extensively performed in the past, the term “metabolomics” is rather new (Patti et al., 2012 and references therein). Recent improvements in mass spectrometry now offer the chance to finely characterize a wide array of molecules in a limited amount of time, then

contributing to routine applications of metabolomics in ecological studies. Nonetheless, extensive metabolomics analyses in aquatic science are still limited (Kido Soule et al., 2015).

1.4.1 Targeted and untargeted metabolomics

Metabolomics studies can be generally divided in two main categories: targeted and untargeted, the first characterized by the analysis of selected molecules and the second aiming at measuring the highest number of metabolites at the same time (Patti et al., 2012). These authors compellingly reviewed the application of both targeted and untargeted metabolomics studies, describing how their application varies in response to the experimental purposes. In fact, while targeted metabolomics is particularly indicated in testing well defined hypotheses, untargeted metabolomics rather leads to formulation of new experimental hypotheses (Patti et al., 2012).

Targeted and untargeted metabolomics studies are applied in different experimental approaches; among them, (Kuhlisch and Pohnert, 2015), reviewed "comparative metabolomics", "systems biology" and "comprehensive metabolomics" as the three main approaches applied to metabolomics studies. The first approach aims at describing how production of a subset of targeted metabolites varies in the studied organism(s). (Vidoudez and Pohnert, 2012), for example, analysed the metabolic changes in the diatom *S. marinoi* at different developmental stages. They reported, through a comparative approach, significant changes in compound production over time, highlighting that cells at the exponential and the stationary growth phases were characterized by similar amounts of PUAs. Comparative metabolomics studies have been recently performed also in the field, tracking changes in the lipid profiles of the coastal phytoplankton community collected for one year in the Western English Channel (White et al., 2015). This study described not only how different oceanographic conditions could alter lipid composition in phytoplankton, but also that physiological adaptations to

nutrient availability could also occur in these organisms. Furthermore, inspecting the presence of protease inhibitors in freshwater phytoplankton successfully revealed seasonal succession of cyanobacterial chemotypes (Sadler et al., 2014).

Differently from the comparative metabolomics, a systems biology approach is based on the application of different –omics techniques (such as metabolomics, genomics and transcriptomics) in order to reconstruct the metabolic map leading to the synthesis of the targeted metabolites. This approach has been seldom applied. Recently, allelopathic effects mediated by the dinoflagellate *Karenia brevis* on the diatom *Thalassiosira pseudonana* were reported (Poulson-Ellestad et al., 2014). Also, a metabarcoding analysis coupled with a metabolomics approach recently highlighted that selective grazing of *Calanus* sp. copepods was related to prey physiology rather than abundances (Ray et al., 2016).

The last approach in metabolomics studies, i.e. the comprehensive metabolomics approach, is generally applied in untargeted studies, because changes in a wide array of metabolites are recorded. A comprehensive analysis of different metabolites poses hard methodological challenges since no protocol is available yet for the simultaneous extraction of all the metabolite classes (Kido Soule et al., 2015, Llewellyn et al., 2015), but such approach allows identifying new compounds produced by the organism(s) (Patti et al., 2012). (Barofsky et al., 2009), for example, reported that cells of *S. marinoi* in the early growth phase were metabolically distinguishable from those in the late phase. More recently, a combination of targeted and untargeted metabolomics applied to intracellular and extracellular metabolites was used in order to characterize dissolved organic matter released by the cyanobacterium *Synechococcus elongatus* into the medium (Fiore et al., 2015). Acquisition of fragmentation spectra through MS/MS analysis allowed the authors to identify untargeted metabolites not predicted to be generated from the metabolic processes of *S. elongatus*, such as kyneurine (i.e. a tryptophan oxidation product). These molecules, likely released as side compounds produced as a “waste” of the basal

metabolic activity, can be possibly now targeted in hypothesis-driven metabolomics studies (Fiore et al., 2015, Patti et al., 2012).

1.4.2 Targeted-metabolomics in oxylipin analysis

Analysis of oxylipins mostly represents a case of a targeted metabolomics study, because a well-defined class of molecules, that is fatty-acid derived oxygenated compounds, is the object of hypothesis-driven experimental designs. Oxylipins are characterized in their chemical structure and abundance through Liquid Chromatography analysis associated with Mass Spectrometry (LC-MS). In order to identify these molecules at a finer scale, fragmentation (MS/MS) patterns and UV absorbance can be also analysed (Cutignano et al., 2011). After that molecules have been synthesised through enzymatic reaction, they are methylated and then separated by chromatography. In this way, compounds can be separated on the basis of their chemical structure, eluting from the column to the mass detector at different times. A both quantitative and qualitative characterization of the targeted molecules through LC-MS/MS occurs after that compounds pass through the source, the analyser(s) and the detector mounted on the instrument (Figure 1.6). At the beginning, an ion source ionizes the different compounds through electrospray (ESI), allowing the user to select a different ionization system (ESI^+ or ESI^-) on the basis of the chemical nature of the molecules analysed. After successful ionization, molecules may also be fragmented and then sent to the analyser.

Masses of precursors as well of the product ions (those generated after fragmentation of precursor molecules) are then determined by the detector, which in single quadrupole systems is represented by four parallel bars generating different tensions. By modulation of the forces applied to the quadrupole, it is then possible to select the ions funnelled to the detector. This component finally translates the mass of the different ions (both precursors and products) to a signal and generates the final chromatograms. The

higher the ion intensity arriving to the detector, the bigger the area of the correspondent peak will be displayed on the chromatogram.

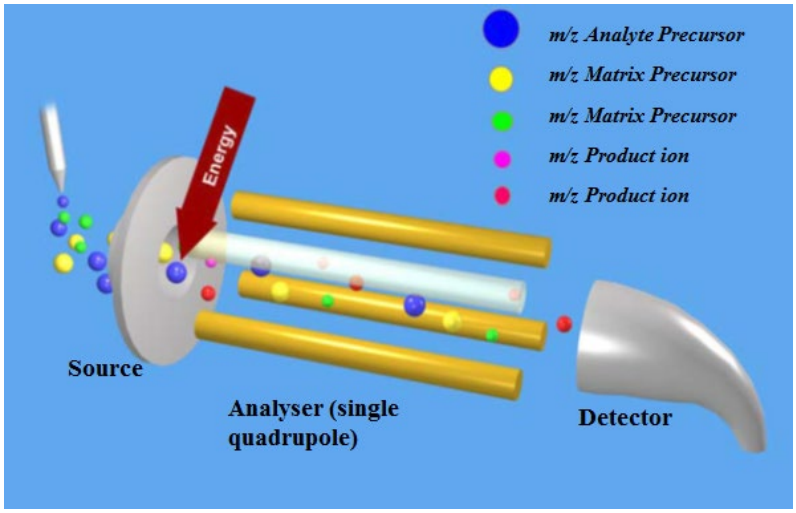

Figure 1. 6: Schematic representation of single quadrupole LC-MS/MS functioning. The abbreviation m/z indicates the mass-to-charge ratio.

While the final quantification of the targeted ions is achieved after direct comparison with the area of an internal standard at known concentration (Kido Soule et al., 2015), oxylipins are qualitatively distinguished on the basis of both the retention time and the mass of the ions. In particular, it has been shown that the chemical structure of epoxy-alcohols, keto-acids and hydroxyl-acids (the main NVO classes) lead these molecules to sequentially elute from the column, being characterized by distinct retention times (Cutignano et al., 2011). These authors, applying a ESI^+ source based on sodium ion (mass-to-charge, m/z, M + 23), also describe how the different masses (m/z) help to define oxylipins on the basis of their precursors: hydroxyl-acids deriving from EPA (i.e. HEPEs), HTA and HTrA, for example, are characterized by the m/z 355, 303 and 301, respectively, whereas epoxy-alcohols deriving from the same precursors by the m/z 371, 319 and 317, respectively. Additionally, MS/MS fragmentation patterns give the possibility to specifically reconstruct the biochemical activity of specific lipoxygenases: for instance, the 13,14-HEpETE typically fragments into three product ions of m/z 259, 273 and 289, while the 16,14-HEpETE into one single ion of m/z of 273 because the OH group bonds with

different carbons along the chain of the fatty acid (Figure 1.7; Cutignano et al., 2011). As a result, MS/MS fragmentation patterns can provide information about the specific LOX activity which generated the correspondent NVO.

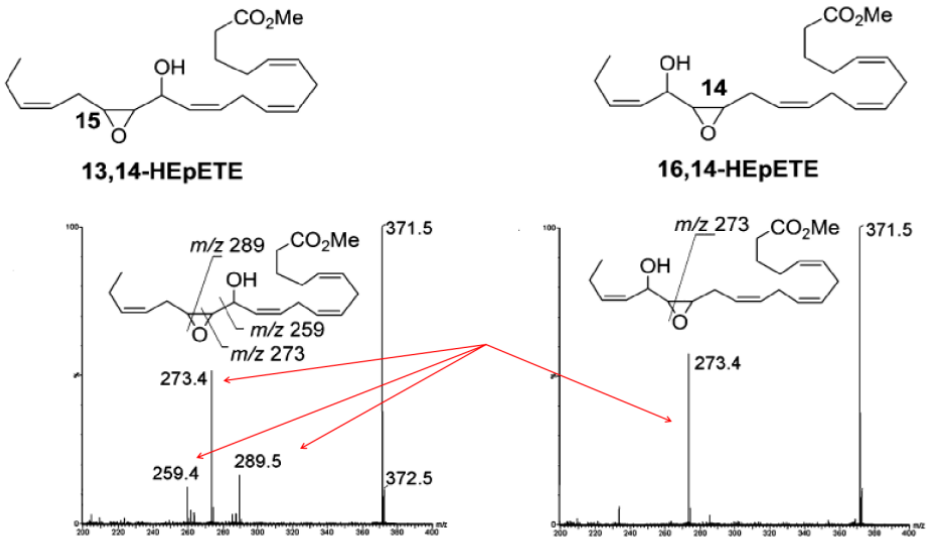

Figure 1. 7: MS/MS analysis of 13,14-HEpETE and 16,14-HEpETE in diatoms extracts. Red arrows highlight how the two molecules, characterized by the same m/z of the precursor ion (i.e. 371.5), differently fragment (modified after Cutignano et al., 2011).

1.5 The study area

1.5.1 The Gulf of Naples

The Gulf of Naples (GoN) is a semi-enclosed SW-oriented embayment located in Southern Italy. It encompasses an area of around 900 km^2 characterized by an average depth of 170 m. The Gulf is delimited at its Northern border by the islands Procida and Ischia, at East by hills and the Vesuvius (over 1200 m) and at the Southern border by the Sorrento peninsula and the island of Capri. The openings to the Tyrrhenian Sea are mainly two, named "Bocca Grande" and "Bocca Piccola": the former is identified as the sea portion between Ischia and Capri, while the second as the sea portion between Capri and the Sorrento peninsula (Figure 1.8). "Bocca Grande" involves two canyons (the Magnaghi and the Dohrn ones), reaching a maximum depth of around 800 m, while "Bocca Piccola"

is characterized by a single sill of 72 m depth. Another important topographic feature of the Gulf of Naples is the presence of a continental shelf ranging between 100 and 180 m in depth and between 2.5-20 km in width (Cianelli et al., 2015).

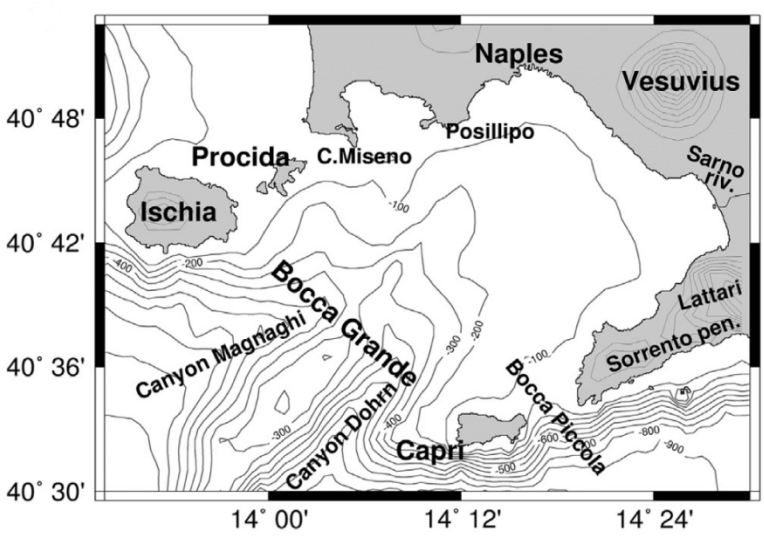

Figure 1. 8: Topography and orography of the Gulf of Naples (Cianelli et al., 2015).

In addition to a high population density along the coast as well as to intense touristic and commercial activities, freshwater discharges coming from the Sarno River contribute to make the inner region of the GoN very eutrophic. This condition is in net contrast with the oligotrophic nature of the Tyrrhenian waters affecting the Gulf offshore; therefore two sub-basins can be identified and their boundary varies in dimension and position depending on seasonal dynamics (Cianelli et al., 2015).

In general, remote and local factors can be identified as the main forces influencing hydrology in the area. Advection of water masses from the Tyrrhenian Sea (such as the Modified Atlantic Water and the Levantine Intermediate Water) represents the remote factor determining two main circulation schemes: while a counterclockwise circulation leads to an offshore advection of water masses in January-March, the formation of a cyclonic gyre in the central part of the Gulf occurring in July-September determines the isolation of the offshore waters from the coastal ones (de Ruggiero et al., 2016, Uttieri et al., 2011). By contrast, winds are the local factor that forces variations in the surface

currents: NE- and SW-oriented winds lead to offshore and inshore surface currents, respectively, while breezes provide scarce water exchanges during summer months (Cianelli et al., 2015).

In general, seasonal changes in remote and local factors occur and co-act in shaping an extremely challenging study area, highly variable in its oceanographic, chemical and biological features.

1.5.2 LTER-MC

The Long-Term Ecological Research station MareChiara (LTER-MC) is a sampling site located two miles away from the coastline in the Gulf of Naples (Figure 1.9) and represents a dynamics area characterized by ecological dynamics influenced by both coastal and open-ocean waters, then mirroring the mutable conditions occurring in the Gulf.

MareChiara is one of the few long-term stations available in the Mediterranean Sea and is the only one along the Tyrrhenian coast of Italy; here, physical, chemical and biological data are being collected since 1984 (with a major interruption from 1991 to 1995). Since 2006, MareChiara is part of the international network of the Long Term Ecological Research (LTER) (Morabito et al., 2018). In general, phytoplankton peaks are registered in February-March (before the stratification of the water column), in May and in October (Mazzocchi et al., 2011, Zingone et al., 2009), while phytoflagellates and diatoms, although showing inter-annual and seasonal oscillations, generally represent the most abundant groups characterizing the area (Zingone et al., 2009).

In winter, phytoplankton biomass and chlorophyll-a concentration reach their minima because of strong water mixing and low PAR availability (Zingone et al., 2009). However, episodic blooms of few diatom species (mainly *Chaetoceros* spp*., Pseudo-nitzschia delicatissima* and *Thalassionema bacillaris*) (Ribera d'Alcalà et al., 2004) occur

with different intensities and frequencies in this season at LTER-MC (Zingone et al., 2009).

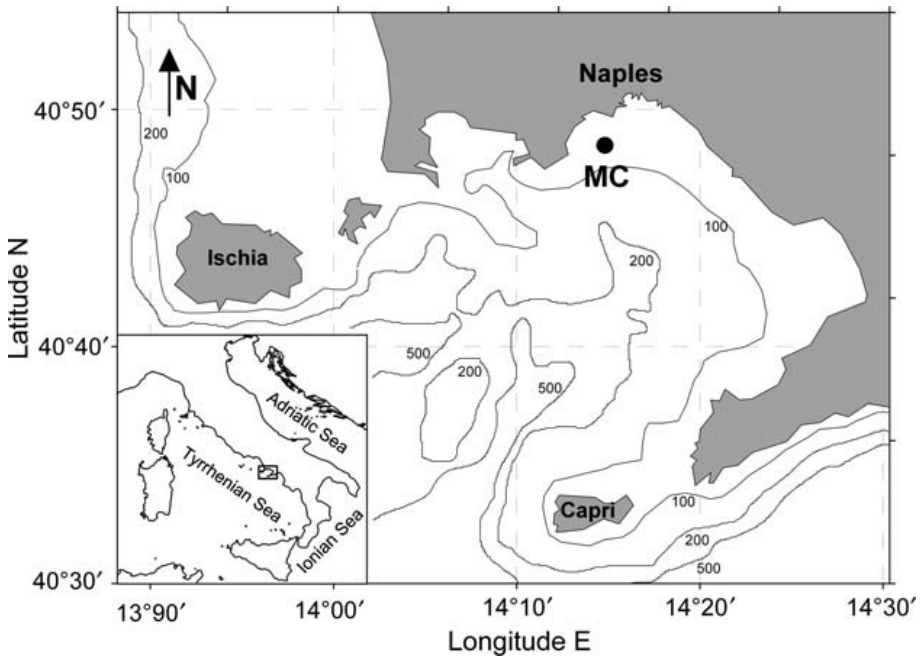

Figure 1. 9: LTER-MC sampling site (black circle) in the Gulf of Naples (Mazzocchi et al., 2011).

In spring, a high nutrient availability mediated by offshore transports of coastal waters triggers the maximal phytoplankton abundance. Small sized diatoms, such as *Skeletonema pseudocostatum*, *Chaetoceros tenuissimus* and *Chaetoceros socialis*, dominate phytoplankton community and persist in the following months (Ribera d'Alcalà et al., 2004).

During the summer, the water column is well stratified and multi-specific phytoplankton blooms are mediated by intermittent lateral water advections that replenish the Gulf with nutrients. As a result, oligotrophic and eutrophic conditions alternate, driving flagellates and diatoms (in particular *Leptocylindrus* spp. and *Skeletonema* spp.) to dominate, respectively (D'Alelio et al., 2015).

In autumn, nutrients of terrestrial origin are dispersed by a wide circulation pattern and summer diatoms (e.g. *T. rotula* and *P. delicatissima*) peak again, co-occurring with

other Bacyllariophyceae (*Skeletonema menzelii*, *Pseudo-nitzschia multistriata* and *Leptocylindrus minimus*).

Zooplankton at LTER-MC is characterized by the regular alternation of four main copepod species: *Acartia clausi*, *Centropages typicus*, *Paracalanus parvus* and *Temora stylifera* (Ribera d'Alcalà et al., 2004). In fact, similarly to phytoplankton, also zooplankton communities follow recurrent seasonal patterns along the year at this long-term station. In winter, secondary producers are at their minimum; small calanoids, cyclopoids, oncaeids and corycaeids seem to be the main zooplankton groups, represented especially by the genera *Clausocalanus*, *Calocalanus*, *Oithona* and *Oncaea*.

In spring, *A. clausi* and *C. typicus* mostly characterize zooplankton community at LTER-MC, even if occasional intrusions of the large grazer *Calanus helgolandicus* from the offshore waters are observed. During summer months, the marked stratification of the water column prompts the occurrence of cladocerans (especially *Penilia avirostris*) and suspension-feeding calanoids (i.e. *P. parvus*); in addition, intermittent nutrient inputs favour the growth of *A. clausi* and *C. typicus*. By the end of the summer and throughout the autumn, the major contributors to zooplankton communities are doliolids and the copepods *T. stylifera*, *Clausocalanus furcatus* and *Oithona plumifera*.

1.6 The target copepod species: *Temora stylifera* (Dana, 1849)

Temora stylifera is one of the most abundant neritic calanoid copepod species, occurring globally in tropical and subtropical waters (Bradford-Grieve et al., 1999). This species is characterized by sexual dimorphism and males can be easily distinguished from females because of modified antennular segments used by males to clasp females during reproduction and by the absence of somite fusion in the urosome (Ferrari and Dahms, 2007) (Figure 1.10). Little information is available about the feeding preferences of this copepod, but *T. stylifera* is generally described as a broadcast filter feeder (Benedetti et al.,

2018, Benedetti et al., 2016, Paffenhöfer, 1998), privileging herbivory with some degree of omnivory (Benedetti et al., 2018, Paffenhöfer and Knowles, 1980).

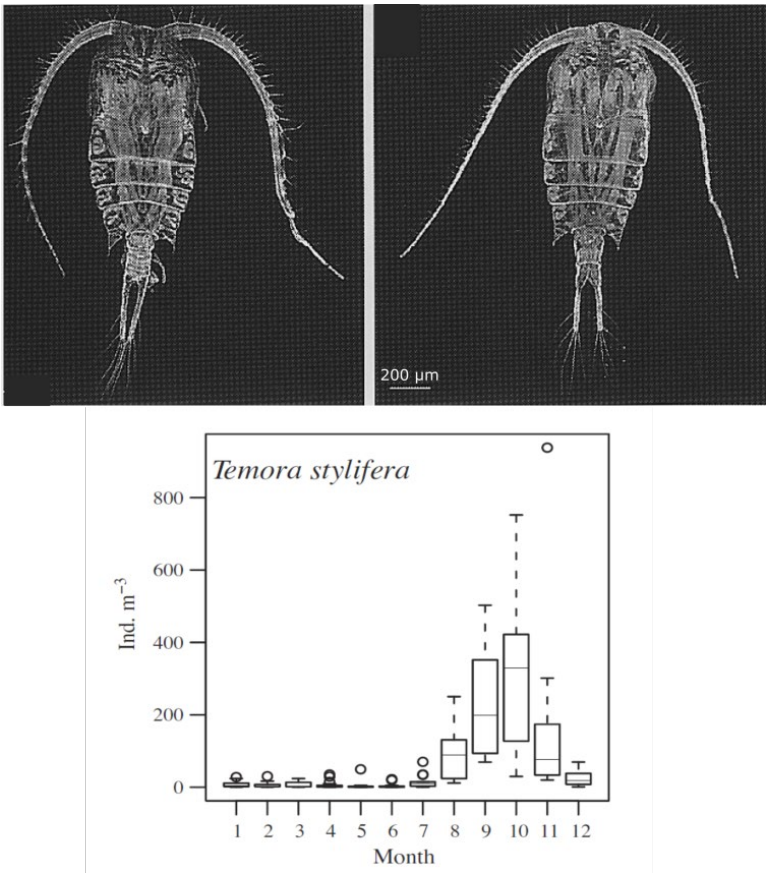

Figure 1. 10: Top: *Temora stylifera* adult male (left picture) and female (right picture) (Carotenuto, 1999). Bottom: annual population dynamics of *T. stylifera* in the Gulf of Naples (LTER-MC) from 1984 to 2006 (Mazzocchi et al., 2012).

Because of the widespread distribution, several studies have investigated population dynamics of this copepod species in the field. In the Gulf of Naples, in particular, the annual cycle of *T. stylifera* has been widely characterized and in this area the population is known to increase in late summer (June-July), reaching the maximum density in autumn. Subsequently, a brisk decline in abundance is observed in winter (Mazzocchi et al., 2012; Figure 1.10).

To assess how life-history traits influence seasonal fluctuations of *T. stylifera* population, several studies have inspected variations of egg production rates, egg viability and larval survival rates through both *in situ* and laboratory studies. (Carotenuto et al., 2006), in particular, characterized weekly physiological responses (faecal pellet

production, egg production rate, hatching success and naupliar I (NI) survival were reported) of *T. stylifera* collected at LTER-MC along one sampling year. These authors observed the maximum production of 120 eggs/female-day, highlighting marked differences in comparison to the maximum of 33.3 eggs/female-day produced by *T. stylifera* females in the North-Western Mediterranean Sea (Halsband-Lenk et al., 2001). In the Gulf of Naples, a constantly high hatching success was observed (above 80%), while percentage of NI viable nauplii showed wide oscillations and on average 12% of nauplii moulted to NII stages along the sampling year (Carotenuto et al., 2006). Although chlorophyll-a (chl-a) did not represent a good predictor to infer hatching success and naupliar survival in the field (Carotenuto et al., 2006), laboratory experiments have revealed sensitivity of *T. stylifera* to diatom diets, because these algae impaired reproductive success through maternal effects or direct effects on larval feeding stages (Carotenuto et al., 2011, Fontana et al., 2007b, Ianora et al., 1995). Laboratory results have been useful to highlight that assessing survival rates of *T. stylifera* developmental stages is of key importance to predict fluctuations in copepod abundance *in situ* (Mazzocchi et al., 2006), even if the seasonal dynamics of this copepod has been related to temperature variations (Lindley and Daykin, 2005, Di Capua and Mazzocchi, 2004). Considering the wide distribution, the occurrence of precursor field studies in the Gulf of Naples, the herbivorous feeding preferences and the relative ease in its manipulation, the copepod *T. stylifera* was selected as the target copepod species for this thesis. Besides providing new information about biotic and abiotic drivers influencing the reproductive success of this copepod in the Gulf of Naples, and potentially in other distribution areas, a *de novo* transcriptome analysis contributed to enlarge public genomic resources for plankton crustaceans and copepods.

1.7 Aims of the project

The overarching aim of this Ph.D. project is to investigate whether and how diatoms affect population dynamics of grazing copepods in the Gulf of Naples. The survey encompassed a targeted-metabolomics approach for quantification of phytoplankton-derived NVOs and fatty acids (FAs) as well as transcriptomic and gene expression analyses to evaluate *T. stylifera* responses. In addition, laboratory experiments with this copepod species and four diatoms were run to analyse copepod reproductive responses at a finer scale as well as to inspect oxylipin production in new diatoms isolated from the Gulf of Naples.

Only few studies inspecting the effects of oxylipins on the reproductive potential of copepods have been carried out in the field so far. The Gulf of Naples is generally described as an oligotrophic basin where diatoms are constantly present all over the year, showing two major multi-specific blooms in spring and winter (Ribera d'Alcalà et al., 2004). The first aim of the project is to characterize, through a one-year field study, oxylipin and fatty acid profiles of phytoplankton at a fixed research station in the Gulf of Naples, in order to relate these data to both phytoplankton community composition and biological responses of the selected copepod species, namely *Temora stylifera*.

Phytoplankton samples were collected at a weekly basis at the Long Term Ecological Research station MareChiara (LTER-MC) for 12 months. Phytoplankton collected through surface water samples was a) identified in its community composition, characterizing diatoms to a species-specific level as well as other relevant phytoplankton groups and b) processed for a community metabolomics analysis targeting oxylipins and fatty acids, by means of Liquid Chromatography-Mass Spectrometry (LC-MS/MS) and Gas Chromatography-Mass Spectrometry (GC-MS/MS) analyses. Even if standardized protocols already exist for the extraction of oxylipins (Cutignano et al., 2011), slight modifications of the laboratory procedure were required for an efficient analysis of the

phytoplankton samples. Besides offering possible explanations about *T. styifera* population dynamics along the year in the sampling site, the targeted-metabolomics data should help elucidate the possible role of oxylipins in phytoplankton communities as well as possible influence of biotic and abiotic factors on oxylipin production and phytoplankton physiological responses (in terms of fatty acid contents) along weekly intervals in one sampling year.

The second aim is to investigate the *in-situ* biological responses, in terms of reproductive output and gene expression, of the copepod *T. stylifera* collected weekly from concurrent zooplankton samples at LTER-MC during the studied year. Faecal pellets, number of eggs, hatching success and naupliar I (NI) survival were measured in *T. stylifera* as standard variables for estimating copepod reproductive potential (Carotenuto et al., 2006). A *de novo* transcriptomic analysis was also performed on *T. stilifera* copepod females collected at two subsequent weeks in which survival rates of NI nauplii were significantly different. Therefore, results could allow unveiling which molecular pathways are potentially affected by biotic and abiotic factors and which responses might be expressed by the copepods to counteract such negative effects. Additionally, a number of genes of interests (GOIs) were selected and optimized among the differentially expressed sequences observed after the transcriptomic analysis. The selected GOIs were related to biochemical pathways strictly involved in reproductive processes. GOI expression was quantified through Real Time – quantitative Polymerase Chain Reaction (RT-qPCR) following methods developed by (Lauritano et al., 2011a; Lauritano 2011b) and measured in copepod females collected along the year 2017. Expression levels were analysed in relation to environmental and biotic variables (such as NVOs, FAs and phytoplankton) to assess whether these factors significantly influenced copepod physiological and molecular responses.

The third aim of this Ph.D. project is to evaluate effects of new oxylipin-producing diatoms isolated from the Gulf of Naples on local copepods at a finer scale through

laboratory experiments. The family *Leptocylindraceae*, for example, has been recently characterized as a diatom group able to synthesize oxylipins from docoshexaenoic acid (DHA) (Nanjappa et al., 2014). However, the effects of *Leptocylindrus* spp. on grazer copepods have never been tested so far. Therefore, biological responses in terms of reproductive output and quantitative gene expression were measured in *T. stylifera* after feeding on *Leptocylindrus* cf. *danicus* in comparison to the control diet *Prorocentrum minimum*. Such experiments were extended to three additional diatom species: *Asterionellopsis glacialis*, *Chaetoceros curvisetus* and *Chaetoceros pseudocurvisetus*. *Asterionellopsis glacialis* does not occur at high concentrations in the Gulf of Naples, but (Wichard et al., 2005a) reported that this diatom from the English Channel was a PUA-producing species. Harmful effects of *A. glacialis* on copepod grazers are still unknown. The other two diatom species, *C. curvisetus* and *C. pseudocurvisetus*, were selected because of the important contribution of the genus *Chaetoceros* at LTER-MC. The effects of *C. affinis* and *C. socialis* have been already tested on *T. stylifera* (Fontana et al., 2007b); assessing the harmful potential of other two *Chaetoceros* species on the same copepod allows widening our understanding of the interactions among dominating diatom and copepod taxa in the Gulf of Naples.

1.7.1 Specific research questions

1. How do phytoplankton chemical traits change in the Gulf of Naples along one entire year?
2. What is the role of diatom oxylipins in the Gulf of Naples and in marine pelagic systems?
3. How does the copepod *Temora stylifera* respond in terms of reproductive potential and gene expression in relation to environmental variables, phytoplankton abundance and phytoplankton chemical traits?

4. What is the harmful potential of diatom species which have never been tested so far in relation to their chemical traits?

Chapter 2

Targeted-metabolomics of phytoplankton community at LTER-MC

*The material in Chapter 2 forms the basis of the paper "**Russo E., d'Ippolito G., Fontana A., Sarno D., D'Alelio D., Busseni G., Ianora A., von Elert E., Carotenuto Y. (2019). Density-dependent oxylipin production in natural diatom communities: possible implications for plankton dynamics**" accepted for publication in "The ISME Journal" in which I played a major role*

2.1 Introduction

Metabolomics is the characterization of low-molecular weight (<1000 Da) primary and secondary metabolites (Viant, 2008). The main advantage of metabolomics approaches is that they allow describing biochemical pathways irrespective of post-translational modifications of proteins (Patti et al., 2012), thus offering a snapshot of organism physiology at different conditions. Recent improvements in analytical methods (such as single-cell metabolomics through laser-desorption/ionization-mass spectrometry, LDI-MS) (Baumeister et al., 2019) and instrument sensitivity have elicited chemical investigations in biological and ecological studies (Poulin and Pohnert, 2019). However, there are still relatively few examples of metabolomics analyses applied to aquatic systems (Kido Soule et al., 2015).

In marine environments, secondary metabolites regulate organism interactions in benthic and pelagic domains; these chemicals are known to play a crucial role in the ecology of phytoplankton, because they are involved in defensive strategies, allelopathic activities and cell death synchronization (Pohnert, 2009 and references therein). Therefore, metabolomics analyses are precious to reveal how plankton responds to biotic and abiotic pressures and how physiological modifications may regulate cell-cell interactions. The vast majority of metabolomics studies on phytoplankton are based on laboratory experiments focusing on selected model species. In such experiments, both targeted and untargeted metabolomics approaches have been applied to answer a wide range of experimental questions. These include surveys of physiological adaptation of phytoplankton to abiotic variables, such as nutrient and CO_2 concentrations (Wördenweber et al., 2017, Popko et al., 2016, Bromke et al., 2015, Lu et al., 2013, Renberg et al., 2010), variations in metabolic profiling of single phytoplankton strains along the growth phases (Fiore et al., 2015, Mausz and Pohnert, 2015, Vidoudez and Pohnert, 2012) and organism interaction, including

allelopathy (Poulin et al., 2018, Poulson-Ellestad et al., 2014), phytoplankton-bacteria relationships (Paul et al., 2012) and prey-predator relationships (Ray et al., 2016).

In contrast to the increasing number of laboratory-based metabolomics studies, field surveys investigating physiological variations of phytoplankton communities *in situ* are still relatively few. Such discrepancy is likely due to the challenging experimental conditions, due to a limited availability of biomass for chemical analyses and the difficulty of testing direct effects of controlled factors. In this perspective, despite few examples of non-targeted metabolomics *in situ* (Lutz et al., 2015, Sadler et al., 2014), most field-based surveys relied on targeted metabolomics approaches aiming at characterizing specific pathways in phytoplankton communities.

Analysis of lipid and fatty acid profiling of phytoplankton is of key importance in plankton ecology. Fatty acids deriving from complex lipids such as intact polar diacylglycerols (IP-DAGs) and triacylglycerols (TAGs) represent the most abundant lipid fraction in plankton organisms (Wakeham et al., 1997). Besides their relevance in terms of relative abundance, lipids and fatty acids represent efficient chemotaxonomic markers of phytoplankton groups (Taipale et al., 2013, Lang et al., 2011, Dijkman and Kromkamp, 2006, Brett and Müller-Navarra, 1997) as well as trophic markers in food web plankton ecology (Müller-Navarra et al., 2004, Dalsgaard et al., 2003). Moreover, fatty acids assimilated by copepod grazers after feeding on phytoplankton have been shown to significantly affect the reproductive success of the animals and these effects seem to be mainly related to the assimilation of ω-3 poly-unsaturated fatty acids (PUFAs), such as C18:3, C20:5 and C22:6 (Jónasdóttir et al., 2009, Arendt et al., 2005, Hazzard and Kleppel, 2003). For these reasons, targeted characterization of complex lipids and fatty acids in phytoplankton communities has received more attention than the products of other biochemical pathways. In fact, several studies investigated variations in lipid and fatty acid concentration and composition in different marine systems, including the South Pacific Ocean (Van Mooy and Fredricks, 2010), the Atlantic Ocean (Hazzard and Kleppel, 2003),

the Mediterranean Sea (Popendorf et al., 2011) and the Labrador Sea (Copeman and Parrish, 2003). More recently, (White et al., 2015) analysed lipid and fatty acid profiles of phytoplankton collected for one year, at a weekly basis and from surface waters, at the long-term station L4 in the English Channel. The aim of the study was to investigate how abiotic variables and phytoplankton community composition affected the lipid profiles. The authors reported phytoplankton physiological adaptations to nutrient stress conditions in addition to information about variations in the nutritional value of phytoplankton for grazers.

Among micro-phytoplankton, diatoms are indeed the most representative group (Malviya et al., 2016), playing a fundamental role in marine biogeochemical cycles (Tréguer et al., 2017). One of the most extensively studied biochemical pathways in diatoms is the one involved in oxylipin synthesis (Cutignano et al., 2011). In marine systems, diatoms probably are the most abundant phytoplankton group known to actively synthesize both volatile polyunsaturated aldehydes (PUAs) (Miralto et al., 1999) and non-volatile oxylipins (NVOs[1]) (Fontana et al., 2007a) from PUFAs (d'Ippolito et al., 2009, d'Ippolito et al., 2004, Pohnert, 2002). The actual role of oxylipins in diatom ecology is still under debate. In fact, the complex relations of diatoms with the surrounding environment and other organisms coupled with an unspecific effect of these molecules on cells (Adolph et al., 2004) do not allow to univocally associate oxylipin production to a single function. There is sound laboratory evidence that diatom-derived PUAs and NVOs dramatically hinder fitness of zooplankton grazers, both micro-zooplankton (Lavrentyev et al., 2015) and copepods (Ianora et al., 2004), suggesting the evolution of oxylipin

[1] Non-Volatile Oxylipins (NVOs) has been traditionally used to indicate this heterogeneous family of substances. This definition is appropriate to the description of these compounds in terrestrial environments but it is strongly misleading in water systems where the concepts of solubility and volatility are very different because of the different properties of the milieu (GIORDANO, G., CARBONE, M., CIAVATTA, M. L., SILVANO, E., GAVAGNIN, M., GARSON, M. J., CHENEY, K. L., MUDIANTA, I. W., RUSSO, G. F., VILLANI, G., MAGLIOZZI, L., POLESE, G., ZIDORN, C., CUTIGNANO, A., FONTANA, A., GHISELIN, M. T. & MOLLO, E. 2017. Volatile secondary metabolites as aposematic olfactory signals and defensive weapons in aquatic environments. *Proceedings of the National Academy of Sciences,* 114**,** 3451. Therefore, a new definition, such as Linear Oxygenated Fatty Acids (LOFAs), should be introduced.

production as a defensive strategy. In addition to negative influences on zooplankton grazers, laboratory studies have demonstrated effects of diatom-derived PUAs also on the growth of diatom-associated bacteria (Balestra et al., 2011, Ribalet et al., 2008), with wide implications for remineralization rates and for the global carbon cycle (Edwards et al., 2015). Interestingly, PUAs also influence several phytoplankton taxa, including prymnesiophytes, chlorophytes, dinophytes, prasinophytes and diatoms (Ribalet et al., 2007, Casotti et al., 2005), inhibiting growth in a dose dependent manner (Vardi et al., 2008, Ribalet et al., 2007a, Vardi et al., 2006). These results might imply a role of these molecules as either allelopathic compounds produced to exclude competitors or info-chemicals synchronizing cell death in diatom blooms (Bidle, 2016, Pohnert, 2009).

Potential ecological relevance of oxylipins in marine systems has stimulated an increasing number of studies investigating field variations of these molecules through targeted approaches. Repeated samplings carried out in limited time windows in subsequent years in the Northern Adriatic Sea are available and offer a snapshot of temporal variations of oxylipin production in the same area (Ribalet et al., 2014, Vidoudez et al., 2011). A recent survey performed in the Atlantic Ocean (43°N to 33°S), instead, maximized spatial resolution of oxylipin variations (Bartual et al., 2014). Also, characterization of oxylipin profiles was provided at two tidal regimes in the Strait of Gibraltar (Morillo-García et al., 2014). Despite such experimental efforts, field experiments only reported concentrations of PUAs, which not always constitute the dominant fraction of diatom-derived oxylipins (Ianora et al., 2015). Quantification and qualitative characterization of phytoplankton-derived NVOs from natural communities have been only attempted in the Northern Adriatic Sea, so far (Ianora et al. 2015, Lauritano et al., 2016). As PUAs, NVOs are highly reactive (Fontana et al., 2007b) and may play a crucial role in structuring both diatom interactions and general ecological dynamics in marine systems.

The aim of the present survey is to provide a targeted characterization of FAs and NVOs from the phytoplankton community in the Gulf of Naples. Phytoplankton samples were collected and analysed in their taxonomic and chemical composition for one year at a weekly basis. Results were analysed to assess how FAs and NVOs varied in relation to phytoplankton abundance and composition as well as to assess how environmental variables influenced the chemical traits of phytoplankton.

2.2 Materials and methods

2.2.1 Collection and processing of water samples

From January 2017 to December 2017, samplings were carried out weekly at the Long-Term Ecological Research Station MareChiara (LTER-MC, 40°48.5'N, 14°15'E) by the SZN Unit Monitoring and Environmental Data Unit (MEDA) on-board of the motorboat "Vettoria". Environmental variables at surface (0.5 m), such as water temperature, transmittance, fluorescence, oxygen concentration, pH, salinity and water density were measured with a CTD probe SBE911 mounted on a rosette sampler deployed vertically along the water column. Surface (0.5 m) concentration of chlorophyll-a (chl-a) and phaeopigment-a (phaeo-a) were analyzed with a spectrofluorometer (see Ribera d'Alcalà et al., 2004, for further methodological information).

Water samples were collected from the surface (0.5 m) deploying two 10 L plastic bucket directly from the ship. After collection, samples were kept cool in an insulated box and transported to the laboratory within a few hours. Here, the water was well mixed and then pre-filtered onto a 200 µm mesh nylon net in order to remove large debris and meso-zooplankton. Subsequently, a sub-sample of 250 ml was transferred into a brown glass bottle, fixed with 10 ml of neutralized formaldehyde (40%) to a final concentration of ~1.6% and stored at 4°C in the dark until later phytoplankton composition analysis. For non-volatile oxylipin (NVO) and fatty acid (FA) analyses, a variable volume of water

depending on the sample density (0.5-2 L) was filtered on Millipore (Merck, Darmstadt, Germany) polycarbonate filters (PC, 47 mm diameter, 2 µm mesh size; *N = 4-6*) using a multiple vacuum filtration, 3-place manifold Whatman apparatus (Merck, Darmstadt, Germany) mounting three 500 ml magnetic filter funnel beakers (VWR International S.r.l., Milan, Italy). The phytoplankton size range of 2-200 µm selected for this analysis, therefore, included both micro-plankton (20-200 µm) and nano-plankton (2-20 µm). Finally, PC filters were folded using clean steel tweezers, transferred to 2 ml eppendorf tubes, immediately frozen in liquid nitrogen and stored at -80 °C until chemical analysis.

2.2.2 Phytoplankton identification

Phytoplankton species composition and abundance were estimated from the surface water samples previously fixed in formaldehyde. In particular, fixed phytoplankton was concentrated in sedimentation chambers following the Utermöhl method (Edler and Elbrächter, 2010). After gently mixing the 250 ml sample, a variable volume (3-50 ml, depending on weekly phytoplankton abundance) was transferred to Utermöhl sedimentation chambers and left undisturbed for 24-72 h, depending on the volume considered. Phytoplankton was observed under an inverted microscope (Zeiss Axiovert200) at 400x magnification. When possible, diatoms were identified to the species level, while most of the other organisms were clustered in major taxonomic groups. Their relative abundance was estimated along both the vertical and the horizontal transects of the chamber. Additionally, the whole first half of the sedimentation chamber was also observed at a lower magnification (200x) to quantify the organisms larger than 20 µm and those species which could have been wrongly estimated during the first counting steps.

For biomass calculation, average bio-volumes available for the different species from LTER-MC data series were converted in carbon content (µg-C/L) using formulas by (Menden-Deuer and Lessard, 2000).

2.2.3 NVO and FA analyses

Chemical analyses were performed in collaboration with Dr. Giuliana d'Ippolito and Dr. Angelo Fontana of the Institute of Biomolecular Chemistry of the National Research Council (ICB-CNR, Pozzuoli, Italy). In this study, PUAs were not considered, because *in situ* observations have demonstrated that NVOs can potentially represent the main part of the oxylipins synthesized by phytoplankton (Ianora et al., 2015). Furthermore, PUA-producing diatoms (such as *Skeletonema marinoi* and *Thalassiosira. rotula*) are known not to occur (e.g. *S. marinoi*) or to only partially contribute (e.g. *T. rotula*) to the phytoplankton community in the Gulf of Naples (Ribera D'Alcalà et al., 2004).

Extraction and quantification of non-volatile oxylipins and fatty acids was performed following a standardized protocol (Cutignano et al., 2011), adequately modified in order to analyse the material collected on the PC 2 µm filters (Gerecht et al., 2013). Specifically, PC filters were washed with 1 ml of Milli-Q water using a glass Pasteur pipette. After several washes with the same aliquot of water, the filters were submerged in the eppendorf tubes and sonicated for 1 min in ice bath in order to damage the cells and to allow oxylipin synthesis to initiate. After sonication, the water sample was transferred to a 50 ml falcon tube. The entire procedure was repeated again in order to maximize collection of the biological material from the filter, then adding an additional volume (1 ml) of sonicated seawater into the same falcon tube. When the phytoplankton biomass on one filter was too little, two or more filters were processed together and merged in a single falcon tube. Sonicated samples were left at room temperature for 30 min in order to obtain a sufficient amount of molecules to be detected by the instrument. Subsequently, the enzymatic reaction was stopped by adding acetone in the same amount of the water volume; 1 µg of 16-Hydroxyhexadecanoic acid (1 mg:10 ml) and 10-20 µg of Nonadecaenoic acid (1 mg:1 ml) were dissolved into the sample as internal standards for non-volatile oxylipins and fatty acids, respectively. The samples were further extracted

with dichloromethane (CH_2Cl_2), then drying the organic phase under vacuum. Material was re-suspended with 1 ml of CH_2Cl_2 and transferred to a calibrated glass vial. Subsequently, the sample was methylated by adding 2 ml of diazomethane directly into the vial, which was left loosely closed in an ice bath for 30 min or more. After diazomethane was evaporated under N_2 flow, the methylated material was re-suspended in 200-300 µl of methanol and finally transferred into a glass insert. Targeted NVOs were quantified in ESI+ mode through Q-Exactive Hybrid Quadrupole-Orbitrap (Thermo Scientific, USA) equipped with an Infinity 1290 UHPLC System (Agilent Technologies, USA) mounting a reverse phase Aquity BEH C18 column (1.7 µm, 2.1 x 50 mm; Waters, USA). Elution was set following methods described in d'Ippolito et al. (2018). NVOs deriving from C16:3 (Hexadecatrienoic-acid, HTrA), C20:5 (Eicosapentaenoic-acid, EPA) and C22:6 (Docosahexaenoic-acid, DHA) fatty acids were specifically targeted.

The same extract used for oxylipin quantification was exploited for FA analysis. Ten FA species were targeted, the Myristic acid (C14:0), Palmitic acid (C16:0), Palmitoleic acid (C16:1), Hexatrienoic acid (C16:3), Stearic acid (C18:0), Oleic acid (C18:1), Linoleic acid (C18:2), Octadecatrienoic acid (C18:3), Eicosapentaenoic acid (C20:5) and Docosahexaenoic acid (C22:6). These molecules were quantified through EI^+ GC-MS/MS (Thermo Scientific, USA) mounting an Agilent (Agilent Technologies, USA) HP-1 column (0.17 µm, 25 m x 0.32). Elution method was set following description provided by d'Ippolito et al. (2018).

In order to obtain a quantitative measure of both NVOs and FAs, molecular masses codifying for the targeted molecules were selected in the chromatogram. Retention times were annotated, then integrating the areas of the different molecular ions. Fatty acids were identified based on their retention times and fragmentation spectra through the online database NIST MS Search 2.0.

Both NVOs and FAs were quantified in comparison to the standard added to the sample, according to the formula:

$$ng_{(x)} = \frac{a_{(x)} \times ng_{(S)}}{a_{(S)}}$$

where *x* indicates the oxylipin or the fatty acid of interest, *S* is the standard and *a* is the area of the peak of interest in the chromatogram or of the standard. The absolute amount of each NVO and FA species was normalized by the volume of water filtered and expressed as ng-NVOs/L. NVOs were also expressed as fg-NVOs/diatom-cell considering the total diatom abundance in the sample (diatom-cells/L), following calculation by (Ribalet et al., 2014).

2.2.4 Data analysis

To assess monthly variations of environmental variables, a Principal Component Analysis (PCA) was performed considering standardized values. Standardization was performed following the formula $(x - \mu)/\sigma$, where x is the observation, μ is the mean value of the variable and σ is the standard deviation. Monthly variations in diatom community composition and fatty acid composition measured at LTER-MC along 2017 were also assessed through multivariate analysis. ANalysis Of SIMilarities (ANOSIM; permutations: N=9999, Euclidean distance or Bray-Curtis dissimilarity) was coupled with non-metric Multi-Dimensional Scaling (nMDS) representation. Balanced observations were produced considering group means as missing observations (Anderson and Walsh, 2013). ANOSIM and nMDS analyses are based on rank transformation of the data and are free from normality assumptions needed for parametric approaches (Palyi and Shankar, 2016). The advantage of nMDS is that the entire variability of the data is resumed in a reduced number of axes. Effective representation of the data is evaluated by the stress, which summarizes how the observed values fit with the expected ones (Palyi and Shankar, 2016). Both FA concentration and diatom abundance data were log-transformed before analysis.

Regression patterns among variables were inspected through simple and multiple regressions. In particular, dependence of phytoplankton, NVOs and FAs to environmental variables were inspected through Generalized Additive Models (GAM) analysis. “A GAM uses a link function to establish a relationship between the mean of the response variable and a “smoothed” function of the explanatory variable(s)” (Guisan et al., 2002). The great advantage of GAM is that data are not forced to follow a parametric relation; rather, the fit is defined by the data scattering. Therefore, GAM allows detecting relationships among the dependent variable and predictor(s) even when non-linear distributions occur. The main drawback of this analysis is the interpretation of the data, as the pattern could not be explained biologically because of limited information available about the study systems. In this perspective, linear regression analyses were applied, when possible. Significant results were obtained after inspecting linear variations of NVOs as function of diatom density. To validate the predominant role of diatom density in driving NVO-per-litre concentrations and NVO-per-cell production, multiple linear regressions considering environmental variables and diatom density as possible predictors were performed. Environmental variables included temperature (°C), transmittance (%), fluorescence (RFU), oxygen-saturation (i.e. SbeOxOps, %), oxygen (mg/L), salinity (PSU), density (kg/m^3) and chlorophyll-a (mg/m^3). Variables showing Variance Inflation Factor (VIF)>10 were removed from the model.GAMs were applied also to inspect relationships between the total amount of FAs and phytoplankton groups (i.e. diatoms, dinoflagellates, coccolithophores and phytoflagellates). Moreover, Spearman’s correlations were calculated to inspect variations of the FA species in relation to diatom groups and the other three major taxonomic groups (i.e. dinoflagellates, coccolithophores and phytoflagellates).

Among the FA species quantified, three of them (i.e. HTrA C16:3, EPA C20:5 and DHA C22:6) were specifically considered in relation to diatom abundance and NVO concentrations. In fact, these fatty acid species are known to constitute the main pool in diatoms (Fontana et al., 2007a, Brett and Müller-Navarra, 1997) and are direct precursors

of NVOs (Fontana et al., 2007a). To inspect relations between the total concentration of these three FA species and both diatoms and NVOs, simple linear regression analyses were performed.

To explore how NVOs and phytoplankton were related, simple and multiple linear regression tests were performed. For these analyses, observations available for the 8th February and 20th June were not considered, because they fell outside the 95% distribution interval. Data were log-transformed to obtain linearity from initial power-law distributions. To identify the main phytoplankton groups driving NVO production, a backward multiple linear regression test was run considering log-transformed data of main phytoplankton taxonomic groups (i.e. diatoms, dinoflagellates, phytoflagellates and coccolithophores) as predicting variables. A quality verification of the parameters of this regression test was performed through the "gvlma" package implemented in R. VIF did not exceed the value of 10 and suggested no multi-collinearity among predicting variables. Considering that diatoms alone explained almost 90% of NVO variation, subsequent analyses only considered diatoms, which represented the main contributors to the production of the targeted oxylipins.

Simple linear regressions were conducted to test dependency of both NVOs/L and NVOs/diatom-cell on diatom concentration variations. Such linear models were refined through backward multiple linear regression tests considering main diatom taxa as predicting variables. For the multiple linear regression analyses, rarer species were clustered in the respective genus in order to reach a number of predicting variables (35 taxa) lower than the number of observations. Validity of the tests was verified through the "gvlma" package implemented in R. In these occasions, VIF was ignored, because the purpose was to refine the general model rather than characterize contribution of each taxon (Grahm, 2003).

To test if variations in oxylipin production, expressed as NVOs/diatom-cell, were driven by changes in diatom community composition along the study period, three oxylipin

production ranges were arbitrarily identified based on the observed results: “low”, “medium” and “high”, corresponding to 0-100, 100-300 and >300 fg-NVOs/diatom-cell, respectively. Then, each phytoplankton sample was clustered to the respective oxylipin production range. Significant variations were tested through a one-way ANOSIM test (permutation: N=9999; Bray-Curtis index for raw data and Jaccard index for presence/absence data), balanced in replicate numbers as described before. Non-metric multidimensional scalings (nMDS) were then produced to visualize the results. ANOSIM tests were supported by Similarity Percentages (SIMPER) analysis to isolate the main drivers of variations (White et al., 2015). ANOSIM, nMDS and SIMPER analyses were performed in PAST 3.0 (Hammer et al., 2001), linear regression tests and visualization in R (version 3.3.2, packages gvlma, car and ggplot2). All tests were run considering two-tailed distributions.

2.3 Results

2.3.1 Environmental variables

Weekly values of each environmental variable measured at LTER-MC during 2017 are shown in Figure 2.1. Surface water temperature followed a unimodal pattern. Low temperatures were recorded in winter and values above 15 °C were detected only after 21st of March. Temperature progressively increased towards the summer, reaching the highest value of more than 28 °C on 8th of August. From that date onwards, temperature progressively decreased to a final value of 16 °C on 19th of December. Water density followed the inverse pattern of temperature values. In particular, the highest densities were observed in winter (on average, 1028 kg/m^3 were detected from January to the end of March), while values progressively decreased from the beginning of spring (1027 kg/m^3) until the end of summer (1026 kg/m^3). In autumn, water density at surface progressively increased again.

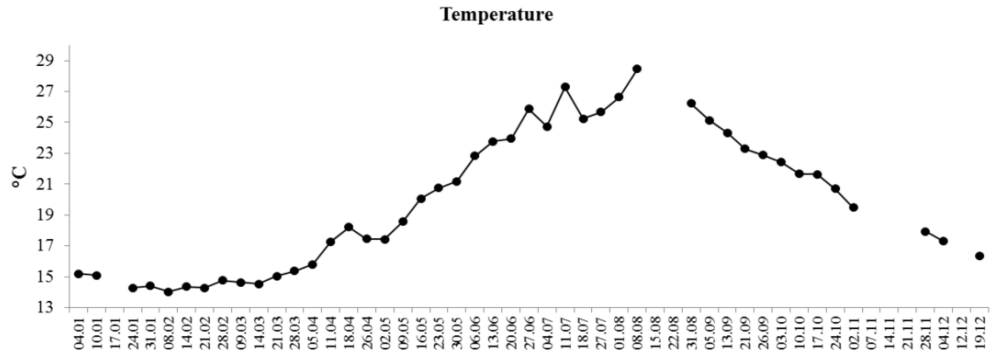
Temperature
°C
29
27
25
23
21
19
17
15
13

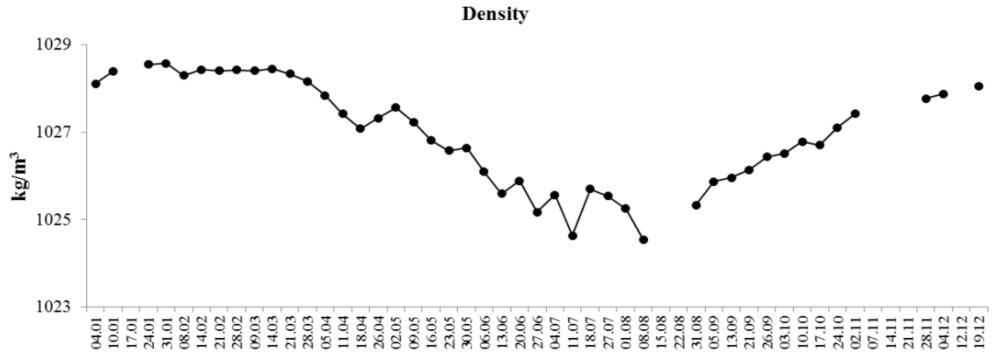
Density
kg/m³
1029
1027
1025
1023

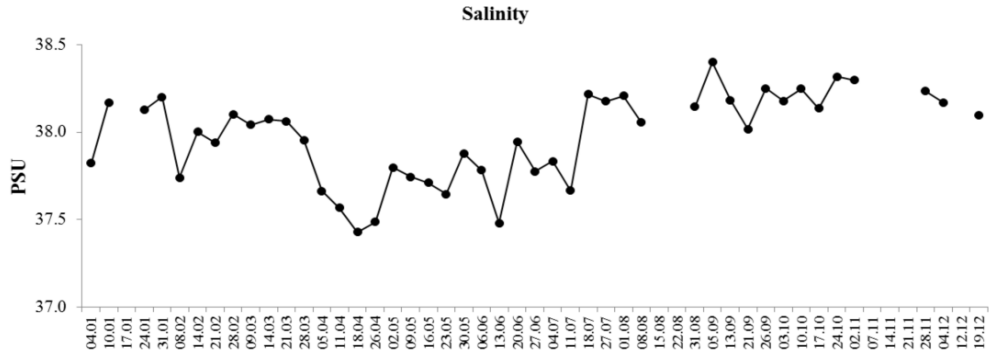
Salinity
PSU
38.5
38.0
37.5
37.0

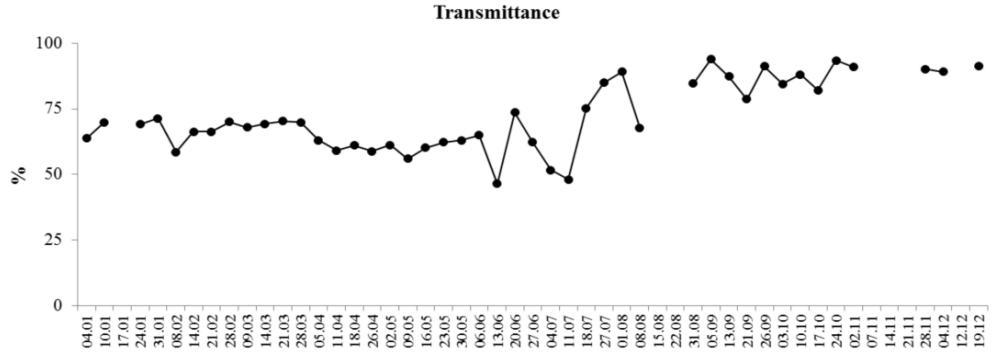
Transmittance
%
100
75
50
25
0

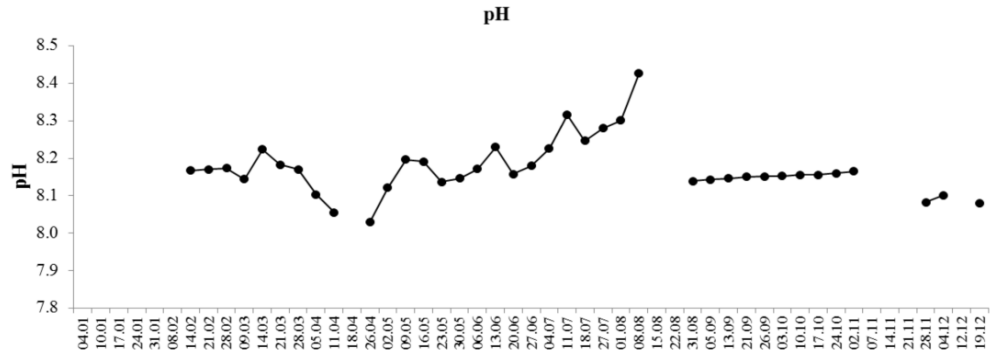
pH
pH
8.5
8.4
8.3
8.2
8.1
8.0
7.9
7.8

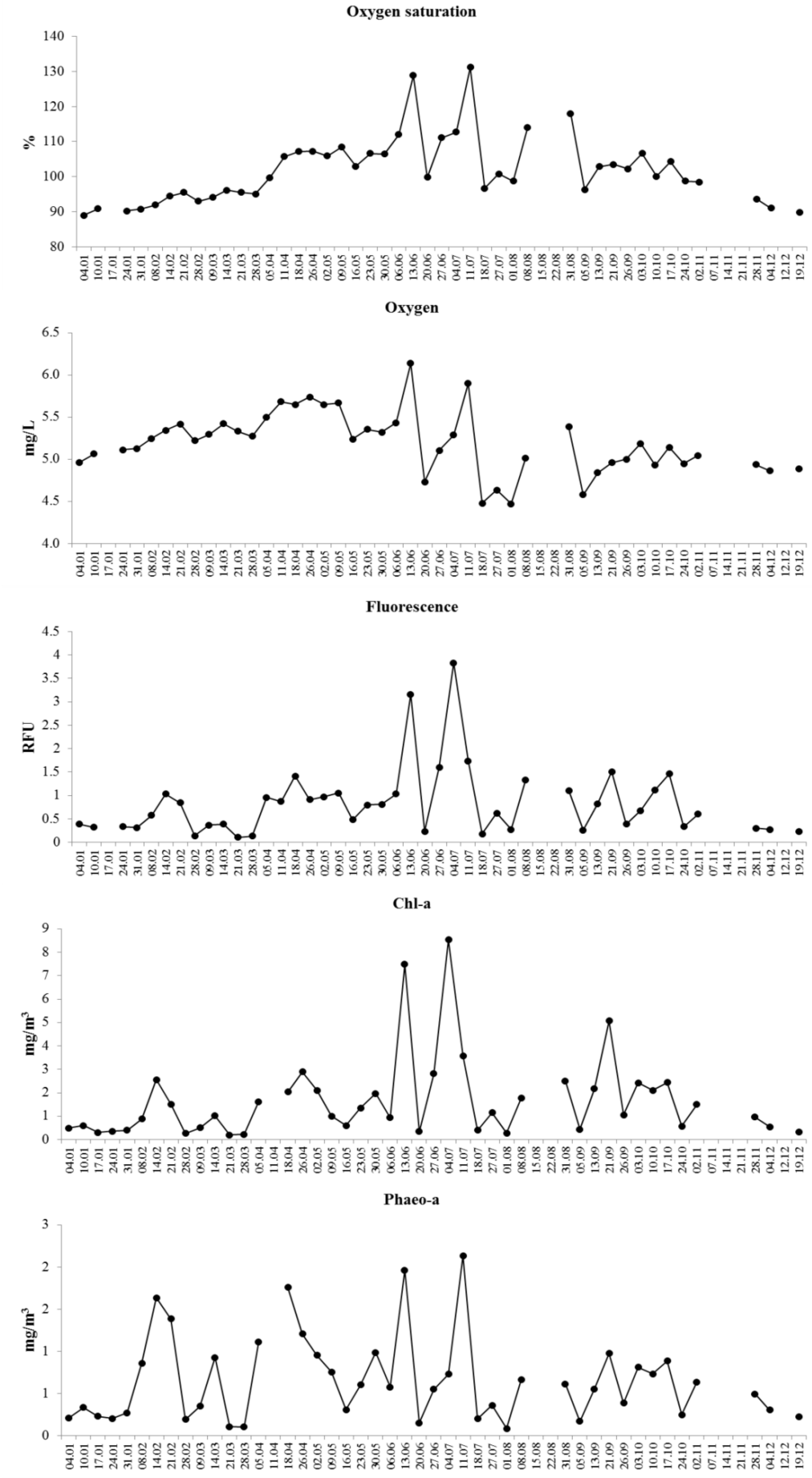

Figure 2. 1: Weekly variations of the environmental variables measured at LTER-MC along 2017. Ordinates indicate the value measured for each variable, abscissas the sampling dates.

Salinity variations were highly oscillatory, but, in a seasonal perspective, the lowest values were recorded in early spring (37.43 PSU on 18th of April) and during spring-summer months (from 28th of March to 11th of July salinity never reached 38 PSU). Towards the end of summer, salinity values were generally higher than the previous months (always above 38 PSU).

Transmittance is defined as the effectiveness in transmitting the radiant energy through a water sample in comparison to a pure water sample. At LTER-MC, transmittance was always above 45%, but reached the highest values towards the end of the year: between September and the end of December, values ranged from 78% and 93%.

Variations of surface water pH ranged between 8 and 8.5, reaching the maximum of 8.43 on 8th of August. In autumn, pH was constantly around 8.1.

At surface, oxygen concentration ranged between 5 mg/L and 6 mg/L until 6th of June, then decreasing in the rest of the year. In spring-summer, wider oscillations were observed. Oxygen saturation (SbeOxOps) followed a similar pattern: percentages progressively increased until spring-summer periods, when strong oscillations were detected, then decreasing towards the end of the year.

Chlorophyll fluorescence, the emission of light by a substance that has absorbed light, estimates the abundance of autotrophic organisms at surface. Weekly recordings highlighted an oscillating pattern along the sampling period, with the maximal peaks detected in spring-summer (above 3 Relative Fluorescence Units, RFU, on 13th of June and 4th of July). In the rest of the year, values ranged between 0.1 RFU and 1.5 RFU.

Chl-a and phaeo-a pigments tightly followed weekly fluorescence variations, often oscillating at consecutive observations. Chl-a was more abundant than phaeo-a, because chl-a values ranged 0.28 mg/m^3 to the maximal values of 7.49 mg/m^3 and 8.53 mg/m^3 measured on 13th of June and 4th of July, respectively. By contrast, phaeo-a varied between 0.08 mg/m^3 and 2.14 mg/m^3.

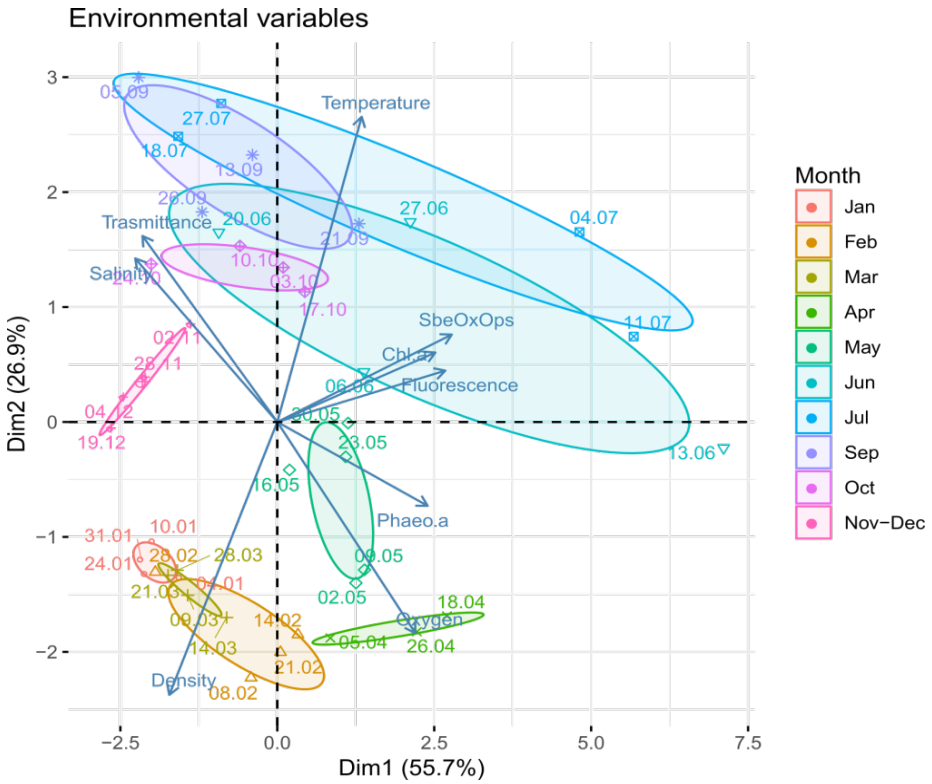

Figure 2. 2: PCA plot of monthly standardized environmental variables. The first two axes are shown and the percentage of variance explained is indicated. In this analysis, pH was not considered because many missing values occurred in the first part of the sampling periods. Month abbreviations: Jan=January, Feb=February, Mar=March, Apr=April, Jun=June, Jul=July, Sep=September, Nov-Dec=November-December.

PCA representation was effective for synthesizing variation of the environmental variables, because the first two principal components (PC1 and PC2) explained more than the 80% of variance (Figure 2.2). The PCA plot showed monthly variations of surface waters depending on environmental variables. Winter months (January, February and March) were very similar and were mainly defined by high water densities (and low temperatures). April and May were separated from the other months because of oxygen and phaeo-a concentrations. June and July were characterized by wide variations, but were more similar to each other than the other months, because of the high values for temperature, fluorescence, oxygen saturation and chl-a. September was a month showing intermediate features between June/July and October/November-December. October and November-December were more similar to each other because of high salinity and transmittance values.

2.3.2 Phytoplankton abundance and composition

Phytoplankton community at LTER-MC from January to December 2017 was dominated by phyto-flagellates and diatoms, which alternated in abundance (Figure 2.3).

As shown is Figure 2.3, Sudden changes in phytoplankton cell concentrations were often observed (e.g. 5th of April, 20th of June and 18th of July). Maximal phytoplankton abundances reached 30x10^{6} cells/L (on May 9th), while the lowest phytoplankton abundance was 0.15x10^{6} cells/L (on January 31st). In particular, maximal concentrations of phytoplankton cells were observed in May, June and July (minimum 2.6x10^{6} cells/L, maximum 30.3x10^{6} cells/L), while low values were detected in winter (from January to March, between 0.15x10^{6} and 0.5x10^{6}cells/L) and late autumn (November and December, between 0.46x10^{6} and 0.51x10^{6}cells/L). In addition to phyto-flagellates and diatoms, Prymnesiophyceae (mainly *Emiliania huxleyi* and other coccolithophores) were considerably present in September (between 0.54x10^{6} cells/L and 1.2x10^{6} cells/L) and dinoflagellates in June-July (between 0.1x10^{6} cells/L and 1x10^{6}cells/L). Percentage values confirmed alternated dominances of phyto-flagellates and diatoms in phytoplankton communities. Phyto-flagellates mainly dominated in February-March (representing 65-94% of phytoplankton composition), while diatoms in June-July (46-70%) and September-October (46-65%), showing an isolated maximum dominance peak on April 5th (90%). Percentage values revealed relevant relative contributions of coccolithophores in winter (3-38%) and early autumn (6-19%) and a constant occurrence of dinoflagellates along the year (on average 2.6% ±1.4, with the maximum value of 6.8% on 13th of September).

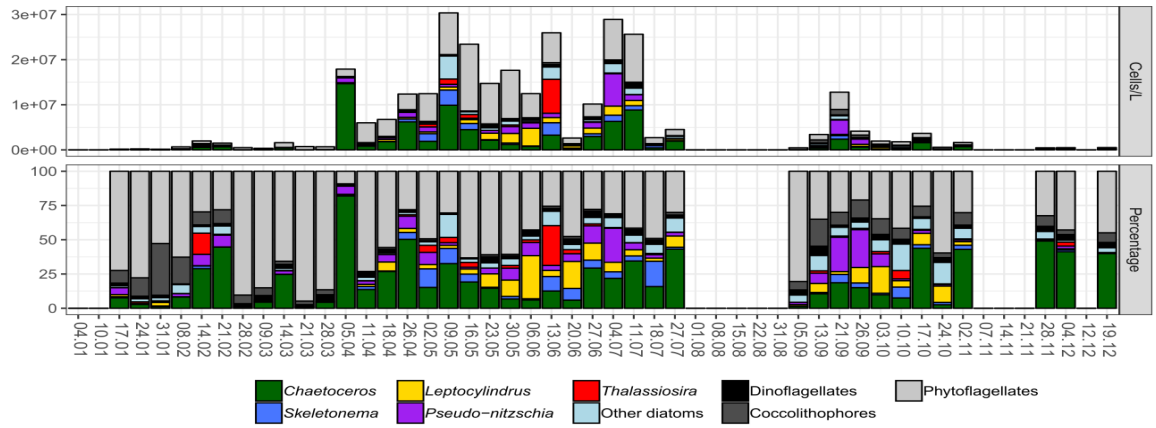

Figure 2. 3: Weekly surface phytoplankton abundance (upper panel) and percentage (lower panel) at LTER-MC along 2017. The five most abundant diatom genera are showed; the rest of diatom diversity is resumed in the group "Other diatoms". Ordinate of the barplot at the top indicates cell concentration (cells/L); ordinate of the barplot at the bottom indicates percentage (%).

Table 2. 1. List of diatom taxa identified from surface water samples collected at LTER-MC along 2017. The maximal concentration (cells/L) observed for each group is indicated.

Species	Max. (cells/L)	Species	Max. (cells/L)
Asterionellopsis glacialis	131,744	*Guinardia striata*	14,127
Bacteriastrum furcatum	2018	*Haslea* spp.	29,642
Bacteriastrum jadranum	6587	*Haslea wawrickae*	200
Bacteriastrum parallelum	1,063,527	*Hemiaulus hauckii*	4709
Bacteriastrum spp.	19762	*Hemiaulus sinensis*	2635
Centric diatoms < 10 µm	5,051,752	*Lauderia annulata*	25,563
Centric diatoms < 5 µm	487,450	*Leptocylindrus convexus*	1,883,328
Centric diatoms > 10 µm	354,509	*Leptocylindrus danicus*	2,038,426
Cerataulina pelagica	1,307,252	*Leptocylindrus mediterraneus*	8800
Chaetoceros affinis	254,803	*Leptocylindrus* spp.	398,823
Chaetoceros anastomosans	66,470	*Lithodesmium* cf. *variabile*	2200
Chaetoceros brevis	800	Pennate diatoms < 10 µm	33,235
Chaetoceros curvisetus	265,882	Pennate diatoms > 10 µm	110,784
Chaetoceros dadayi	200	*Pleurosigma* spp.	80
Chaetoceros danicus	3364	*Proboscia alata*	2691
Chaetoceros decipiens	14,800	*Pseudo-nitzschia delicatissima*	2,525,876
Chaetoceros diversus	44,314	*Pseudo-nitzschia fraudulenta*	26,909
Chaetoceros minimus	22,157	*Pseudo-nitzschia galaxiae*	2,902,542
Chaetoceros peruvianus	2691	*Pseudo-nitzschia multistriata*	46,418
Chaetoceros protuberans	51,400	*Pseudo-nitzschia pseudodelicatissima*	952,743
Chaetoceros pseudocurvisetus	23,000	*Pseudo-nitzschia* spp.	1,750,388
Chaetoceros simplex	155,098	*Rhizosolenia* spp.	673
Chaetoceros socialis	443,136	*Skeletonema pseudocostatum*	3,367,834
Chaetoceros spp.	8,818,409	*Skeletonema* spp.	2,747,444
Chaetoceros tenuissimus	9,904,092	*Skeletonema tropicum*	42,800
Chaetoceros throndsenii	1,794,701	*Thalassionema frauenfeldii*	800
Cylindrotheca closterium	288,038	*Thalassionema nitzschioides*	73,999
Dactyliosolen blavyanus	155,098	*Thalassiosira* cf.*allenii*	1,174,311
Dactyliosolen fragilissimus	14,600	*Thalassiosira mediterranea*	4036
Dactyliosolen phuketensis	23,055	*Thalassiosira rotula*	17,600
Eucampia cornuta	2691	*Thalassiosira* spp.	7,533,314

In total, 62 diatom taxa were identified and counted, of which the five most abundant diatom genera are shown in Figure 2.3. *Chaetoceros* was the most persistent diatom genus along the year. In winter, *Chaetoceros* were mostly represented by large colonial species (e.g. *C. affinis*, *C. curvisetus*, *C. protuberans* and *C. pseudocurvisetus*), while in the rest of the year small single species occurred in higher abundances (mainly *C. tenuissimus* and *C. throndsenii*). Undetermined *Chaetoceros* (clustered as *Chaetoceros* spp.) were found all over the year at considerable concentrations (mean value of $1.1x10^6$ cells/L). Other diatom genera, such as *Pseudo-nitzschia*, *Leptocylindrus*, *Skeletonema* and *Thalassiosira*, showed occasional dominance. *Pseudo-nitzschia* (represented by *P. fraudulenta*, *P. galaxiae* and two species complexes, i.e. *P. delicatissima* and *P. pseudodelicatissima*) was present throughout the sampling year and was mainly found from spring to autumn (maximum $7.2x10^6$ cells/L, on 4th July). The genus *Leptocylindrus* mainly occurred in late spring-summer and autumn. In the Gulf of Naples, the genus *Leptocylindrus* includes *L. convexus* and three cryptic species, i.e. *L. danicus*, *L. hargravesii* and *L. aporus*, here grouped as *L.* cf. *danicus*. Occurrence of *L. convexus* was mainly limited to spring-summer months (maximum $1.9x10^6$ cells/L, on June 6th), while *L.* cf. *danicus* was found mostly all over the year (maximum $2x10^6$ cells/L, on June 6th). *Skeletonema pseudocostatum* was abundant in late spring-summer (from April to July) and *S. tropicum* occurred in October/November. *Thalassiosira* mainly occurred in summer and autumn. Blooms of small sized *Thalassiosira* (<10 μm) were observed in isolated weeks (maximum abundance of $7.5x10^6$ cells/L on June 13th). *Asterionellopsis glacialis* was found in winter (from January to the end of March) and in autumn (from 13th of September until the end of the year), reaching the maximum concentration of 131,744 cells/L on 17th of October. Rare diatom taxa (e.g. *Bacteriastrum* spp., *Dactyliosolen* spp., *Hemiaulus* spp., *Rhizosolenia* spp., *Thalassionema* spp.) were clustered together in the group of "Other diatoms". Their contribution was particularly relevant on discrete dates in summer. Main diatom taxa identified in the phytoplankton sample are listed in Table 2.1.

ANOSIM test revealed a general difference in diatom community composition and abundance, on a monthly basis, because the general R (Global R=0.67, p<0.001) indicated moderate separation among groups (Table AI. 1). Non-significant results were obtained in comparing February and March, February and November-December, October and November-December. Monthly differences in diatom community composition and concentration were also highlighted by nMDS representation based on log-transformed data. In particular, winter (January, February and March) and autumnal (October and November-December) communities were quite similar among each other, while spring and summer assemblages separated from the other groups. April and May diatom communities clustered together, as did June and July ones (Figure 2. 4).

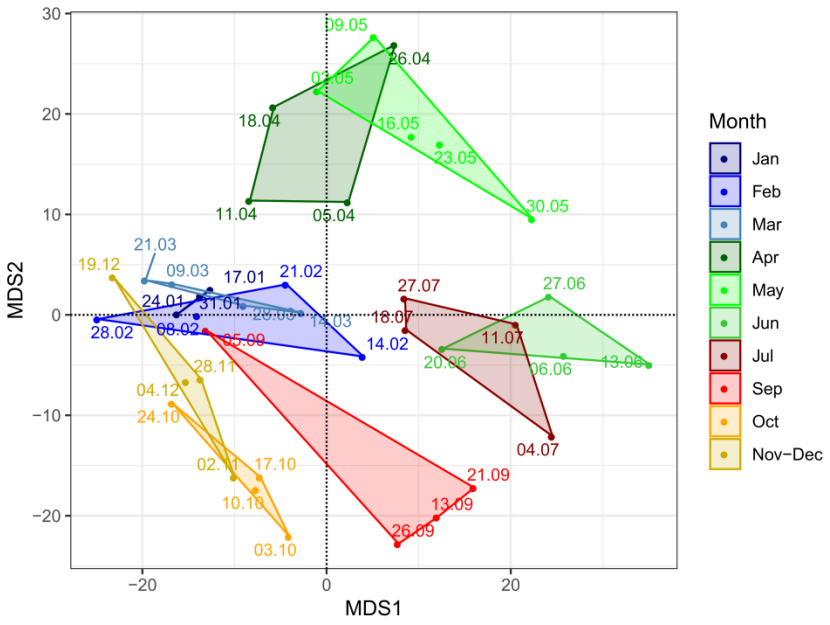

Figure 2. 4: nMDS plot of monthly diatom community composition at LTER-MC along 2017. Representation is based on log-transformed data and Euclidean distance measure (stress=0.15). Abbreviations: Jan=January, Feb=February, Mar=March, Apr=April, May=May, Jun=June, Jul=July, Sep=September, Oct=October, Nov-Dec=November-December.

2.3.3 FA concentration and composition

Mean annual concentrations, as well as maximal and minimal values, of FA species measured in the phytoplankton collected at LTER-MC are shown in Table 2.2. Weekly and monthly concentrations of each FA species are shown in Figure 2.5. Saturated fatty acids

(i.e. the Myristic, 14:0, Palmitic, 16:0, and Stearic, 18:0) were the most persistent species in the phytoplankton collected at LTER-MC along 2017, because they were always detected in the samples. Among them, the Palmitic acid was the most abundant fatty acid, reaching a maximal concentration of more than 200 µg/L on May 23rd. This chemical species was found in an annual mean concentration of 28.7 µg/L and on average constituted almost half of total FA concentration (i.e. 47.84%), never exceeding the 55% of the total composition. The Stearic acid (C18:0) was the second most abundant and dominating fatty acid along the data series, reaching the maximum concentration of 168 µg/L (on May 23rd). On average, its concentration was above 22 µg/L and it represented 38% of total fatty acid species. On a monthly basis, these two FA species followed a similar pattern, with higher concentrations in spring. However, differently from the Palmitic acid (C16:0), the Stearic acid (C18:0) was never detected below 3 µg/L and represented at least 26% of total abundance. In contrast, the minimal concentration of the Palmitic acid was 0.45 µg/L.

Table 2. 2. Fatty acid (FA) species measured in the phytoplankton at LTER-MC along 2017. Annual mean concentrations (ng/L ±SD) and percentages of total fatty acids (% ±SD), together with maximal (Max.) and minimal (Min.) values are reported.

FA	Annual mean ng/L (±SD)	Max. ng/L	Min. ng/L	Mean % (±SD)	Max. %	Min. %
C14:0	1372.63 (±1205)	6114.61	65.52	2.89 (±1.71)	9.07	0.2
C16:0	28,668.3 (±38,018)	227,415.7	445.84	47.84 (±7.47)	55.60	8.83
C16:1	1644.54 (±1852)	6604.9	0	3.14 (±3.14)	11.17	0
C16:3	159.71 (±319)	1035.67	0	0.32 (±0.6)	2.05	0
C18:0	22,269 (±29,569)	168,544.65	3034.34	38.41 (±6.71)	72.86	26.57
C18:1	1501.85 (±1569)	9801.98	0	3.66 (±2.03)	8.75	0
C18:2	275.92 (±348)	2075.35	0	0.69 (±0.45)	1.49	0
C18:3	57.03 (±132)	599.81	0	0.16 (±0.33)	1.35	0
C20:5	418.85 (±610)	2319.82	0	0.89 (±1.05)	3.97	0
C22:6	285.54 (±392)	1390.31	0	0.58 (±0.71)	2.35	0

Among unsaturated fatty acids, the Palmitoleic (C16:1) was the most abundant species (annual mean concentration of 1.64 µg/L and maximum of 6 µg/L on May 9th). This fatty acid was mainly detected from April onwards and constituted, on average, 3.14% of total fatty acids, reaching a maximum of 11% of total composition. These values were similar to those observed for the Oleic acid (C18:1), which was found in an average concentration of 1.5 µg/L (maximum of 9 µg/L on January 4th) and that represented, on average, 3.7% of total fatty acid abundance (maximum of 8.75%). In contrast to the Palmitoleic (C16:1), C18:1 reached the highest concentrations in winter, then occurring at lower densities in the rest of the year. C18:2 and C18:3 fatty acids occurred in lower concentrations than the saturated and the mono-unsaturated counterparts (average concentration of 0.27 and 0.06 µg/L, respectively; average percentage 0.69% and 0.16%, respectively). Monthly concentrations of these two PUFAs were completely different among each other, because densities of C18:2 were the highest in January (then occurring at similar concentrations in the rest of the year), while C18:3 showed very low abundances until the end of the summer, occurring from June to December.

Among PUFAs, main attention was dedicated to Hexadecatrienoic acid (C16:3, HTrA), Eicosapentaenoic acid (C20:5, EPA) and Docosahexaenoic acid (C22:6, DHA), which are known to be the fatty acid precursors of the six NVO species targeted in the survey. On average, HTrA concentration was 159.7 ng/L (0.32%, maximum of 2.05%), ranging from a maximum of 1035 ng/L observed on 9th of May to a minimum of 0 ng/L. In particular, this FA species was mainly detected in summer and autumn (in particular from June to October), while it was not observed in winter (from January to March) and occasionally in spring. The Eicosapentaenoic acid (EPA) occurred in an average concentration of 418.85 ng/L (0.89%, maximum value of almost 4%) and at the maximum concentration of 2319.82 ng/L (observed on 9th of May). Occurrence of this FA species did not show a clearly seasonal pattern, but abundances were lower in winter than spring-summer and autumn. The Docosahexaeonic acid (DHA) occurred in an average

concentration of 285.54 ng/L (0.58% and maximum of 2.35%), reaching the maximum density of more than 1390 ng/L on May 9th. Variations of DHA were slightly different from EPA, because DHA was detected only in spring-summer and first autumn, but not in winter.

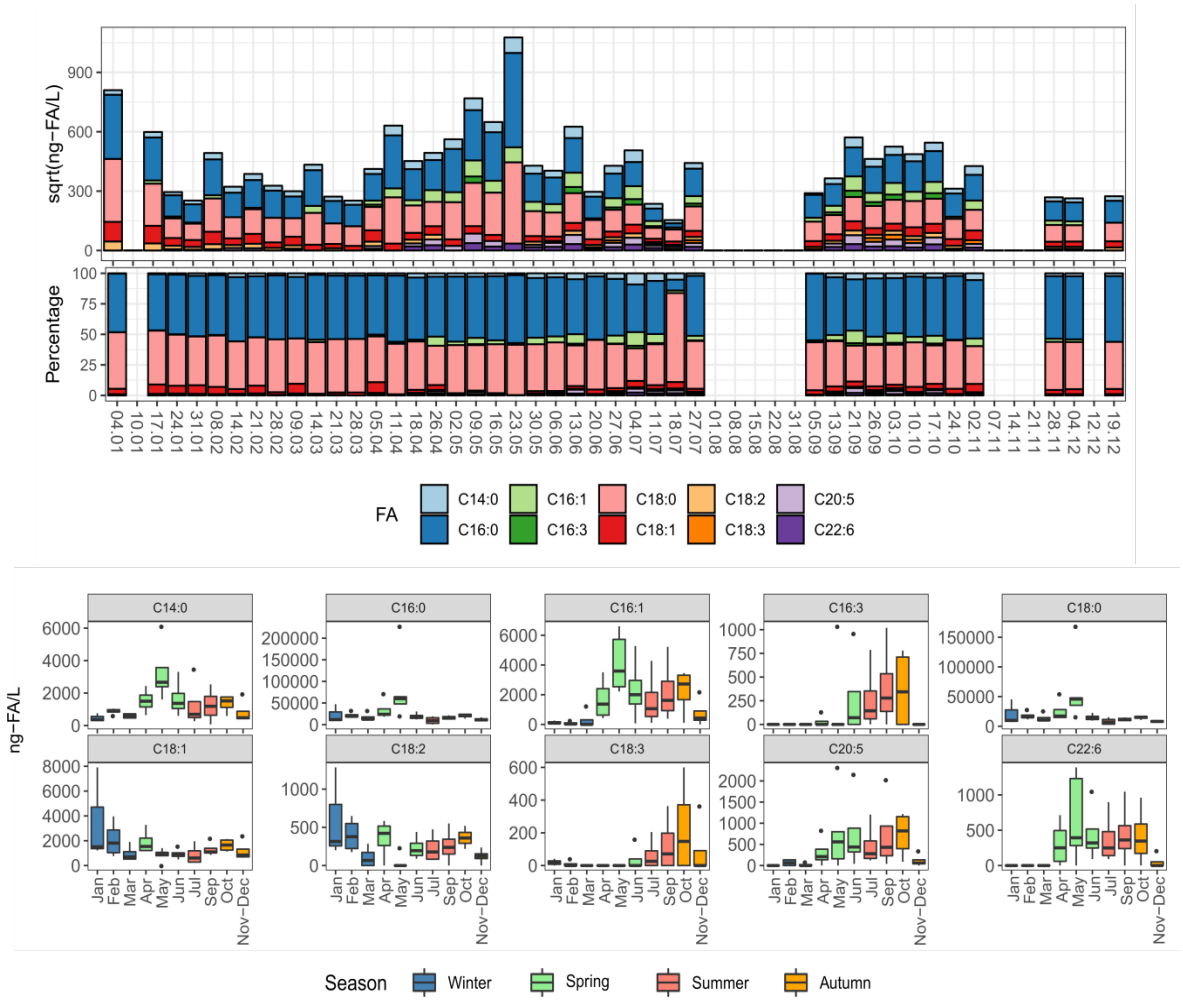

Figure 2. 5: Weekly and monthly variations of the ten fatty acid group of species at LTER-MC along 2017. Top panel indicates square root-transformed fatty acids concentrations (ng/L) and percentage composition. In the bottom panel, the ten FA species are plotted separately, reporting average per month concentrations. Colours of the boxplot mirror the seasons.

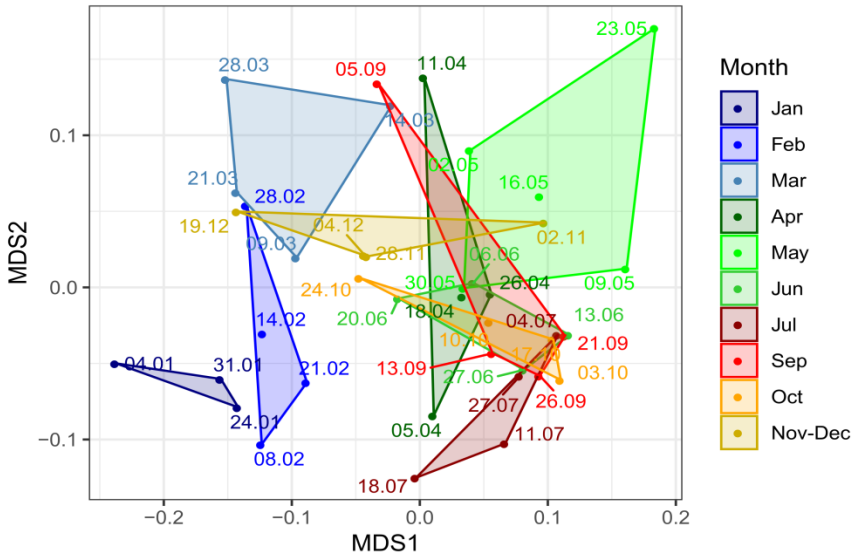

Figure 2. 6: nMDS representation synthesizing variations in fatty acid concentration and composition at LTER-MC along 2017 (Stress=0.04). Log-transformed data and Bray-Curtis dissimilarity were used.

The ANOSIM test highlighted moderate variations of fatty acid concentration and composition along 2017 (Global R=0.47, $p<0.001$). In particular, January and February significantly differed to all the other months. March was not significantly different only in comparison to November-December. April significantly separated from winter months as well as from July and September. May showed similar fatty acid composition to April and June, while differing from all the other months. June, July, September, October and November-December were not dissimilar among each other (Table AI. 2). NMDS representation summarizing differences in fatty acid composition and concentration on a monthly basis stressed separation of January, February and March from the rest of the year (Figure 2.6).

2.3.4 Particulate NVO concentration and composition

Six non-volatile oxylipin (NVO) species including Epoxy-alcohols and Hydroxy-acids originating from HTrA (Hydroxy-Hexadecatrienoic-acid, HHTrE and Hydroxy-Epoxy-Hexadecatrienoic-acid, HEpHTrE), EPA (Hydroxy-Eicosapentanoic-acid, HEPE and Hydroxy-Epoxy-Eicosapentanoic-acid, HEpETE) and DHA (Hydroxy-

Docosahexanoic-acid, HDoHE and Hydroxy-Epoxy-Docosapentanoic-acid, HEpDoPE) fatty acids were detected in the phytoplankton collected at LTER-MC during 2017. In general, the particulate NVO amount obtained from phytoplankton extracts was not sufficient to determine molecule structures at a finer scale through UV absorbance or characteristic MS/MS fragmentation of epoxy-alcohols (Cutignano et al., 2011). Therefore, no information about position of the hydroxy and the epoxy functional groups along the alkyl chains was collected. Nonetheless, it is remarkable that NVOs were detected and quantified at all dates, even when their total abundance was below10 ng/L.

Table 2. 3. Non-volatile oxylipin (NVOs) concentrations expressed as ng/L and as fg/diatom-cell observed in the sampling period (January-December 2017) at LTER-MC. Values are reported for each NVO species, group (hydroxyl-acids and epoxy-alcohols) and fatty acid precursor (HTrA, EPA and DHA). Concentrations are given as mean ±SD, while ranges indicate the absolute minima and maxima. Highest values are highlighted in bold.
HEpDoPE=Hydroxyl-Epoxy-Docosapentanoic-acid;
HEpETE=Hydroxyl-Epoxy-Eicosapentanoic-acid;
HEpHTrE=Hydroxyl-Epoxy-Hexadecatrienoic-acid;
HDoHE=Hydroxyl-Docosahexanoic-acid;
HEPE=Hydroxyl-Eicosapentanoic-acid;
HHTrE=Hydroxyl-Hexadecatrienoic-acid.

NVOs	**Concentration**		**Range**	
	ng/L	fg/diatom-cell	ng/L	fg/diatom-cell
HEpDoPE	3.82 ±4.02	1.69 ±2.51	0-14.92	0-9.97
HDoHE	22.56 ±23.79	45.42 ±86.32	0-99.02	0-359.66
HEpETE	29.61 ±26.61	55.05 ±98.53	0-88.67	0-414.36
HEPE	**74.71 ±68.37**	**109.43 ±188.68**	0-**245.66**	0-**820.31**
HHTrE	1.96 ±3.14	1.46 ±3.12	0-12.17	0-14.49
HEpHTrE	3.11 ±5.05	1.47 ±3.46	0-22.04	0-16.78
TOTAL	***135.95 ±118.5***	***214.51 ±346.47***		
Hydroxyl-acids	**33.08 ±51.64**	**52.10 ±126.86**	0-**340.21**	0-**1097.50**
Epoxy-alcohols	12.18 ±19.98	19.40 ±61.87	0-108.29	0-414.36
HTrA-derivatives	2.54 ±0.81	1.46 ±3.27	0-32.12	0-31.27
EPA-derivatives	**52.16 ±31.89**	**82.24 ±152.04**	3.26-**320.62**	6.12-**1133.58**
DHA-derivatives	13.19 ±13.25	23.55 ±64.54	0-107.68	0-359.66

Total NVO concentration widely varied along the year, ranging from a maximum concentration of 417 ng/L (on June13th) to a minimum of 3.6 ng/L (on January 24th; Figure 2.7). Concentrations briskly changed weekly along the year, even if, globally, three main periods of maximal abundance were identified, in February (8-223 ng/L), April-July (11-417 ng/L) and September-October (9-333 ng/L). The most abundant oxylipin species were Hydroxy-acids (average annual concentration of 33.1 ±52 ng/L and maximal concentration of 340 ng/L on May 9th), while Epoxy-alcohols were less concentrated (average annual concentration of 12.2 ±20 ng/L and maximal concentration of 108 ng/L on June 13th; Table 2.3).

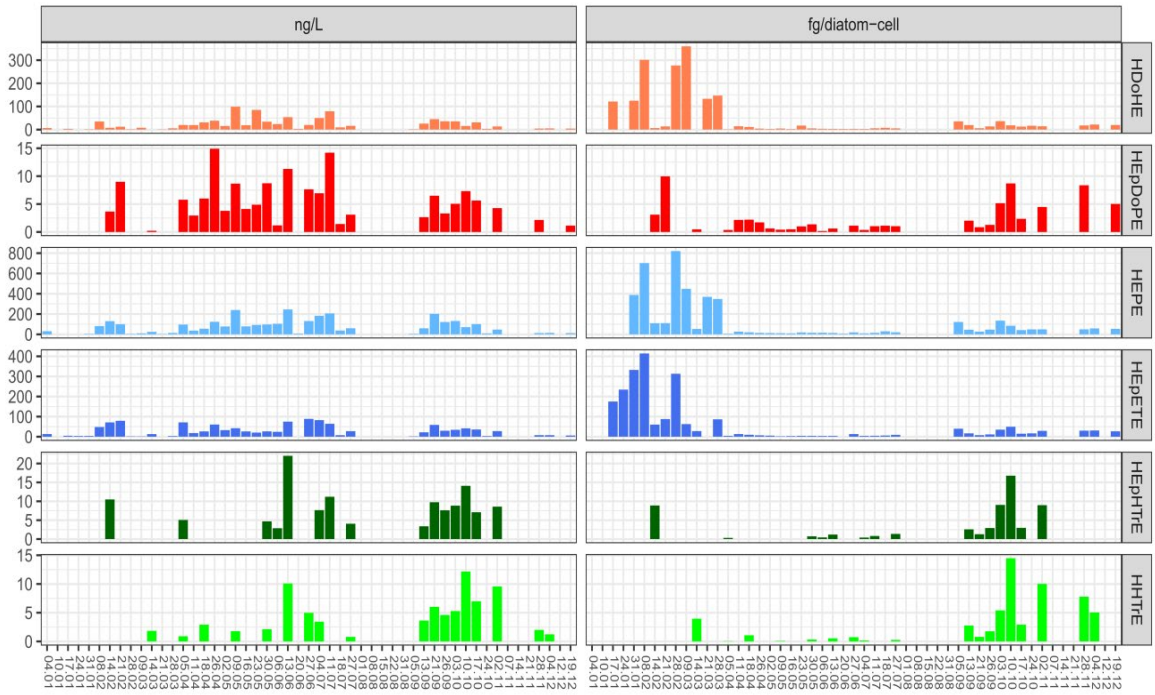

Figure 2. 7: Particulate NVO variations at LTER-MC along 2017. Comparisons between ng-NVOs/L and the respective fg-NVOs/diatom-cell are shown for each oxylipin species. Scales of "y" axes differ among NVO species.

The main fatty acid precursor for synthesis of NVOs was EPA, followed DHA and HTrA: the annual average of EPA derivatives was 52.2 ±32 ng/L, while 13.2 ±13 ng/L derived from DHA and 2.5 ±0.8 ng/L from HTrA. More in particular, HEPE was the most abundant NVO in the data series, being detected in an average concentration of 74.7 ±68 ng/L; by contrast, the other oxylipin species ranged from 3.1 ±5 ng/L (HHTrE) to 29.6 ±27

ng/L (HEpETE). HEPE, HEpETE and HDoHE were the most persistent oxylipin species, because each of them was detected in all samples but two along the weekly samplings (Figure 2.7).

A one-way ANOSIM test showed overall significant changes in oxylipin concentration (ng/L) and composition (Global R=0.14; $p<0.05$), but the R score was rather low (Table AI. 3). In fact, main differences were revealed when January and March were compared to the other months. Similarly, the group November-December was generally distant from the others. No significant differences were revealed among the other groups. SIMPER analysis helps revealing main contributors to the total variation. In the case of oxylipins, HEPE and HEpETE, the two C20:5 derivatives, contributed to almost 75% of total dissimilarity and represented the main drivers of variation leading to the differences observed between winter months and the rest of the year.

Overall, nMDS representation highlighted the low monthly differences in NVO composition and abundance revealed by the ANOSIM test, because no clear separation among monthly NVO composition was observed (Figure 2.8).

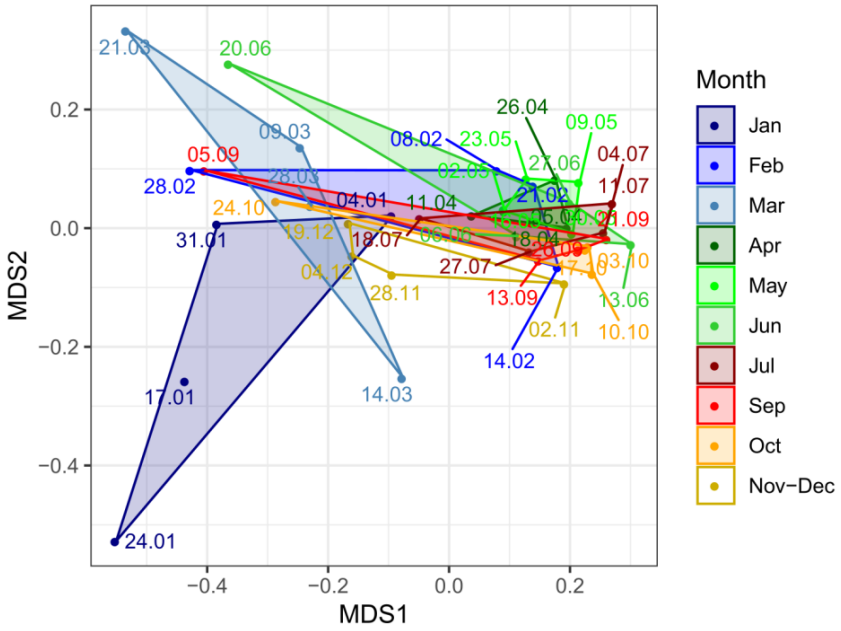

Figure 2. 8: nMDS representation synthesizing variations in NVO concentration and composition at LTER-MC along 2017 (Stress=0.07). Log-transformed data and Bray-Curtis dissimilarity were used.

Oscillations of NVOs were dramatically different, when fg-NVOs/diatom-cell were calculated. This normalization offers information about variations in oxylipin synthesis potential in each diatom cell. The highest cellular production potential was detected in winter, when each diatom cell was estimated to synthesize more than 1400 fg-NVOs (1417 fg/diatom-cell on February 8th and 1410 fg/diatom-cell on February 28th; Figure 2.7). In this season, other peaks of lower intensity were observed: 871 fg/diatom-cell on March 9th, 845 fg/diatom-cell on January 31st, 581 fg/diatom-cell on March 28th and 502 fg/diatom-cell on March 21st. No peaks of such high intensities were detected in the rest of the year, but a general potential to synthesize more than 100 fg/cell was detected in diatoms occurring in autumn (between 43 fg/diatom-cell and 226 fg/diatom-cell). In spring-summer months, cellular oxylipin production never exceeded 60 fg/cell and values ranged between 9 fg/diatom-cell and 57 fg/diatom-cell. The annual average cellular production of Hydroxy-acids was higher than Epoxy-alcohols (52.1 ±126.88 fg/diatom-cell vs 19.4 ±61.9 fg/diatom-cell, respectively). EPA led to an average production of 82.2 ±152 fg-NVOs/diatom-cell, while 23.6 ±64.5 fg-NVOs/diatom-cell and 1.5 ±3.3 fg-NVOs/diatom-cell were produced from DHA and HTrA precursors, respectively (Table 2.3). HEPE was the most abundant oxylipin produced by each diatom cell (annual average of 109.4 ±188.7 fg/diatom-cell), followed by HEpETE (55 ±98.5 fg/diatom-cell) and HDoHE (45.4 ±86.3 fg/diatom-cell). The average cellular production of HEpDoPE, HHTrE and HEpHTrE was sensibly lower (1.7 ±2.5 fg/diatom-cell, 1.46 ±3.1 fg/diatom-cell and 1.47 ±3.5 fg/diatom-cell, respectively) (Figure 2.7).

2.3.5 Interactions of environmental variables with diatoms and FA

Considering that diatoms were the core of the survey, analyses mainly focused on this phytoplankton group. Variations of total diatom abundance were inspected in relation to the environmental variables measured at LTER-MC.

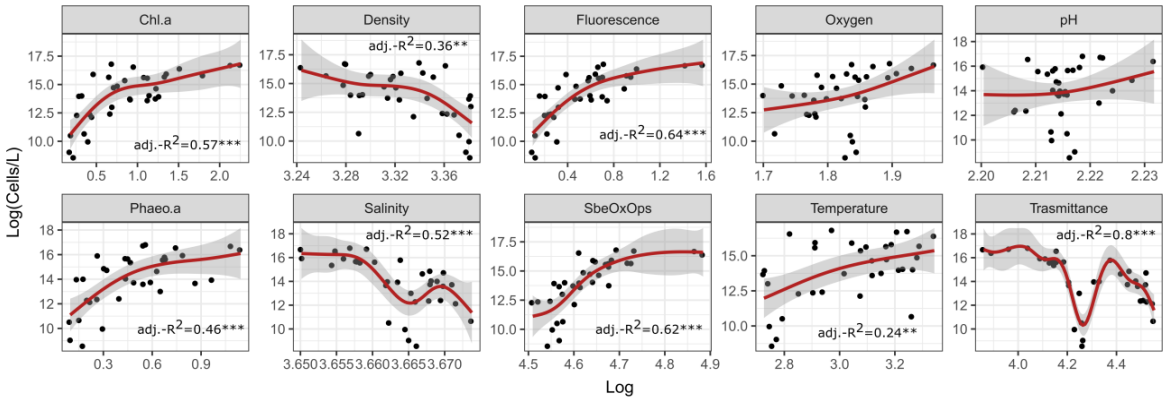

Figure 2. 9: Generalized Additive Model (GAM) results resuming relationships among total diatom concentration and environmental variables. When significant, the adjusted-R^2 (adj.-R^2) of the regression is indicated along with the significance level (*=p<0.05, **=p<0.01, ***=p<0.001). Dark shadings indicate 95% confidence intervals.

The Generalized Additive Model (GAM) results suggested that oxygen and pH did not significantly drive variations in diatom densities. Transmittance, fluorescence and oxygen saturation (SbeOxOps) showed the best relation with the dependent variable (adj.-R^2=0.8, 0.64 and 0.62, p<0.001, respectively). Salinity, Chl-a, phaeo-a, water density and temperature were also significantly related to diatom abundances, but the adj.-R^2 was lower than the predictors mentioned above (Figure 2.9).

Effects of environmental variables on FA concentrations were also tested. In fact, it was hypothesized that environmental predictors could have affected phytoplankton physiology, leading to different chemical traits with respect to FA production. Among environmental predictors, oxygen and pH best described total fatty acid variations (adjusted-R^2=0.64, p<0.001 and adjusted-R^2=0.6, p<0.001, respectively), even though fluorescence and transmittance were also well related to total fatty acid concentrations (adjusted-R^2=0.44, p<0.01 and adjusted-R^2=0.36, p<0.05, respectively). Phaeo-a concentrations, salinity and oxygen saturation were also significantly related to total fatty acids, but these variables explained little variation in comparison to the previous ones. Chl-a, water density and temperature were not significantly related to total fatty acid abundance (Figure 2.10).

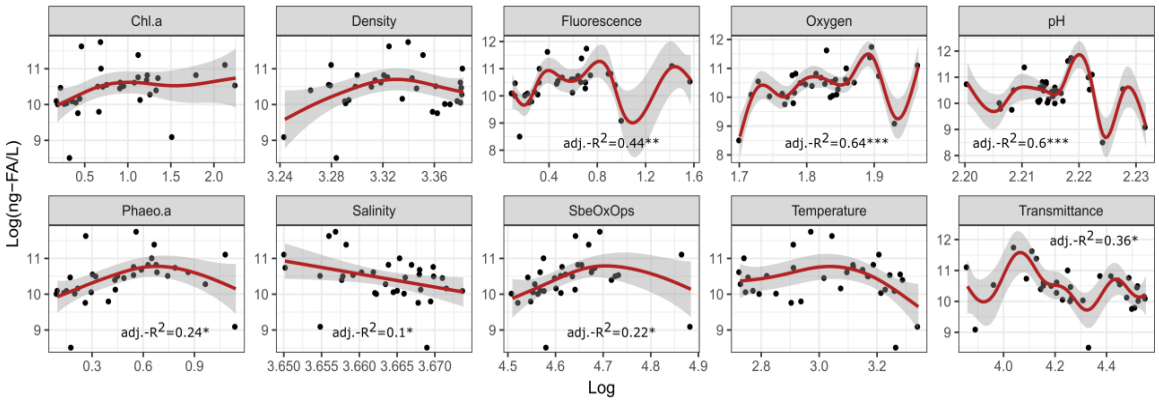

Figure 2. 10: Generalized Additive Model (GAM) results resuming relationships among total fatty acids per litre and environmental variables. When significant, the adjusted-R^2 (adj.-R^2) of the regression is indicated along with the significance level (*=p<0.05, **=p<0.01, ***=p<0.001). Dark shadings indicate 95% confidence intervals.

HTrA, EPA and DHA have been reported as the main fatty acid species in diatoms and they are the precursor fatty acid species for production of the six NVOs considered in this survey (Nanjappa et al., 2014, Fontana et al., 2007a). On this basis, relationship of these diatom-derived FAs with environmental variables was inspected through GAM analyses (Figure 2.11). The assumption that HTrA, EPA and DHA mainly derived from diatoms was also supported by results shown in section 2.3.6.

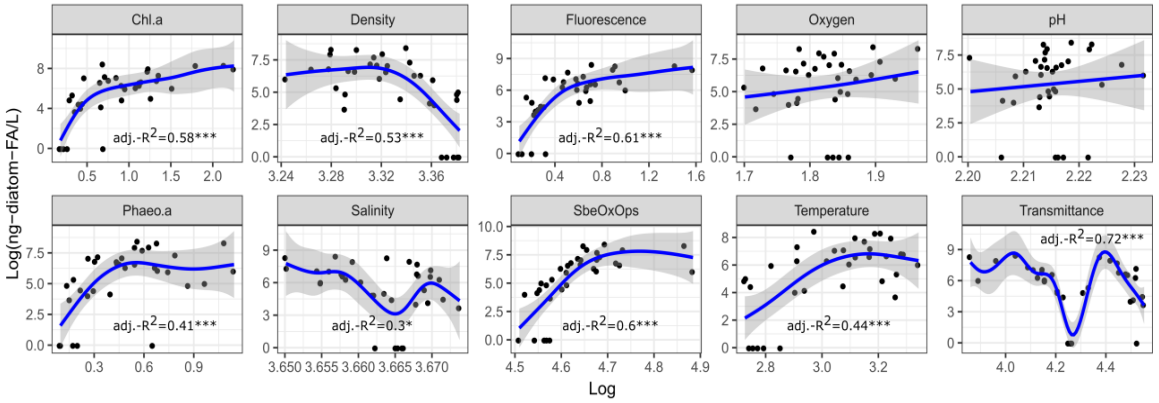

Figure 2. 11: Generalized Additive Model (GAM) results resuming relationships among diatom-derived fatty acids (HTrA, EPA and DHA) and environmental variables. When significant, the adjusted-R2 (adj.-R2) of the regression is indicated along with the significance level (*=p<0.05, ***=p<0.001). Dark shadings indicate 95% confidence intervals.

GAMs highlighted substantially different patterns than those observed when considering total fatty acid concentrations. In fact, oxygen and pH did not provide significant effects. Rather, transmittance (adj.-R^2=0.72, p<0.001), fluorescence (adj.-

R^2=0.61, p<0.001), oxygen saturation (adj.-R^2=0.6, p<0.001), chl-a (adj.-R^2=0.58, p<0.001), water density (adj.-R^2=0.53, p<0.001), temperature (adj.-R^2=0.44, p<0.001), phaeo-a concentrations (adj.-R^2=0.41, p<0.001) and salinity (adj.-R^2=0.3, p<0.05) were all significantly related to the three selected fatty acid species.

Effects of environmental variables on NVO concentrations were also inspected, but results suggested that variations in the synthesis of the six NVOs could have been mainly driven by diatom concentrations. Therefore, variation of these molecules is mainly discussed in relation to diatom density rather than other predictors (see section 2.3.7).

2.3.6 Interactions of FAs with phytoplankton and NVOs

To understand which phytoplankton group mainly drove total FA concentrations, GAM analyses were performed considering each major taxonomic group (i.e. diatoms, dinoflagellates, coccolithophores, phytoflagellates) as independent variable.

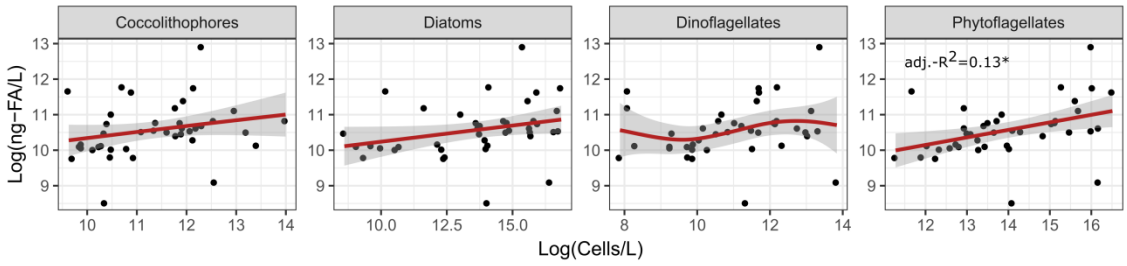

Figure 2. 12: Generalized Additive Model (GAM) results resuming relationships among fatty acids and major phytoplankton taxonomic groups. When significant, the adjusted-R^2 (adj.-R^2) of the regression is indicated along with the significance level (*=p<0.05). Dark shadings indicate 95% confidence intervals.

Phytoflagellates were the only phytoplankton group which were significantly related to total fatty acid concentrations (Figure 2.12), but the adj.-R^2 was low (0.13, p<0.05). More detailed information about the contribution of phytoplankton groups and diatom genera to FA concentrations was achieved through Spearman's correlation tests (Figure 2.13) calculated considering the single FA species, the five most abundant diatom groups and the other major phytoplankton taxa. All correlations but the one between Oleic acid (C18:1) and dinoflagellates were positive. Linoleic (C18:2) and Octadecatrienoic

(C18:3) acids showed no significant correlation with the phytoplankton groups considered. Myristic acid (C14:0) was well related to all major phytoplankton groups, but, among diatoms, the genera *Skeletonema* and *Thalassiosira* showed weaker correlations. Similarly, also Palmitoleic (C16:1), Hexadecatrienoic (C16:3), Eicosapentaenoic (C20:5) and Docosahexaenoic (C22:6) acids were well correlated with all phytoplankton taxa considered. Nonetheless, the highest correlation involving Palmitoleic (C16:1) acid was observed with the mixed group "Other diatoms". "Other diatoms" and coccolithophores showed the highest correlations with Hexadecatrienoic acid (C16:3). Correlations involving dinoflagellates, phytoflagellates and Eicosapentaenoic acid (C20:5) were lower than the other groups, while the Docosahexaenoic acid (C22:6) correlated the best with "Other diatoms" and the worst with the genus *Thalassiosira*.

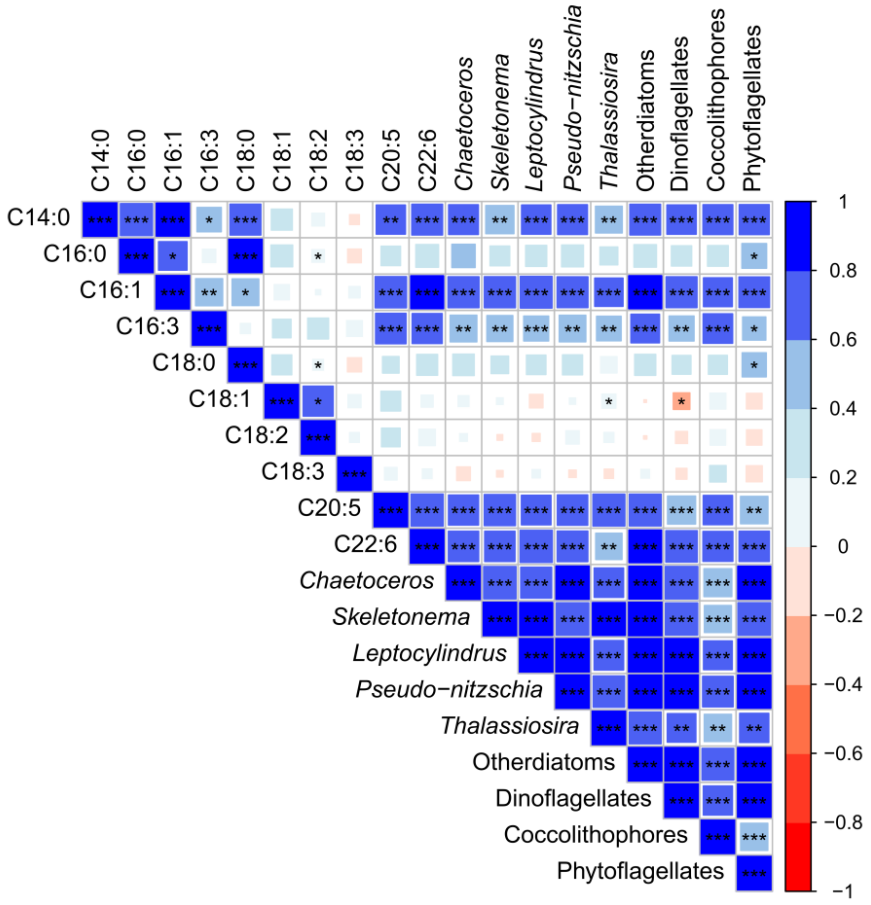

Figure 2. 13: Correlation plots (Spearman's correlations) among FA species, phytoplankton groups and main diatom genera. Diatoms are divided in the five most abundant genera and the multispecies group "Other diatoms". Square colours correspond to correlation (Spearman's ρ), asterisks indicate the significance value.

The total concentration of HTrA, EPA and DHA fatty acids in relation to total diatom concentration was inspected by applying a simple linear regression analysis and results highlighted a significant relation (adj.-R^2=0.65, y=2.81+0.33x, F=75.43, d.f.=38, p<0.001). To analyse more in detail which of the six main diatom groups (i.e. the genera *Chaetoceros*, *Leptocylindrus*, *Pseudo-nitzschia*, *Skeletonema* and *Thalassiosira* as well as the heterogeneous group "Other diatoms") mainly drove diatom-derived FA concentrations, GAM analyses were applied considering the total abundance of these molecules as the dependent variable and abundances of the six diatom groups as predictors (Figure 2.15). All six diatom groups showed a high and significant relation with the fatty acids selected. In particular, the group "Other diatoms" as well as the genera *Skeletonema* and *Leptocylindrus* described more variability than the other groups, as indicated by the highest adjusted-R^2 values (Figure 2.15).

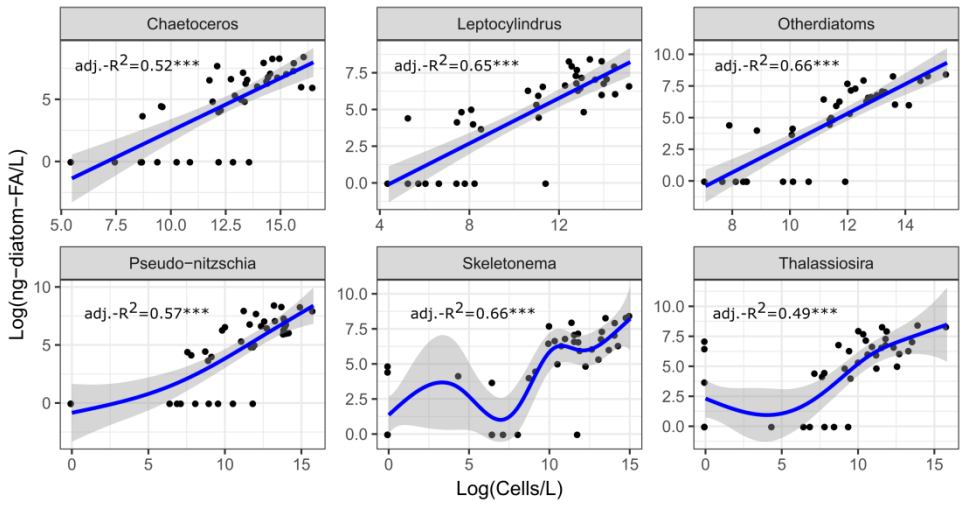

Figure 2. 14: Generalized Additive Model (GAM) results resuming relationships among the concentration of diatom-derived fatty acids (HTrA, EPA and DHA) and the six main diatom groups. The adjusted-R^2 (adj.-R^2) of the regression is indicated along with the significance level (***=p<0.05). Dark shadings indicate 95% confidence intervals.

Diatoms synthesize oxylipins from fatty acid precursors and in the present survey NVOs deriving from HTrA, EPA and DHA were specifically targeted for quantitative analysis. On this basis, a simple linear regression analysis was applied to inspect whether NVO concentration (ng/L) related to diatom-derived fatty acid abundance (ng/L). Outputs

indicated a significant relationship (adjusted-R^2=0.6, y=73.5+0.07x, F=60.21, d.f.=39, p<0.001), describing how the total concentrations of the targeted NVOs increased at increasing concentrations of HTrA, EPA and DHA (Figure 2.16).

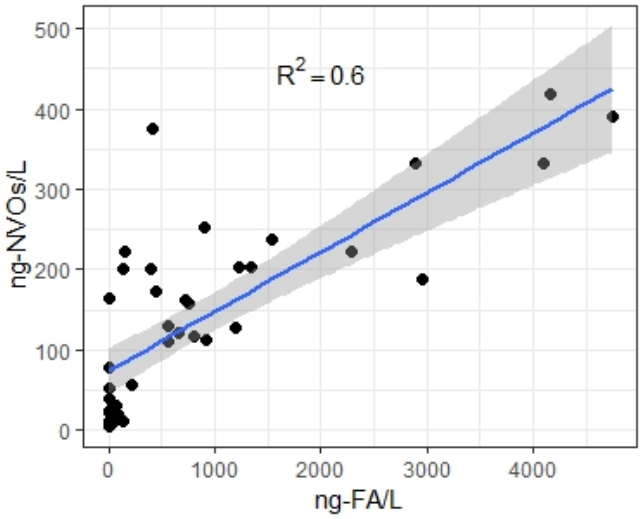

Figure 2. 15: Linear regression between diatom-derived fatty acids (i.e. the sum of HTrA, EPA and DHA) expressed as ng-FA/L and NVO concentrations (ng-NVOs/L).

2.3.7 Interactions of NVOs with phytoplankton

Backward multiple linear regression analysis was used to elucidate the main phytoplankton groups responsible for production of the targeted oxylipins. Diatoms and coccolithophores offered the best prediction (multiple-adjusted-R^2=0.92, F=217, d.f.=35, p<0.001), while the contribution of dinoflagellates and phytoflagellates was not significant. The predominant role of diatoms in driving NVO variations was further supported by the non-significant effects (p>0.05) of the environmental variables considered in the multiple linear models. In particular, gradients in both ng-NVOs/L and fg-NVOs/diatom-cell were significantly explained by diatoms and chl-a, but not by the other environmental variables (Table 2.4).

To determine whether diatoms or coccolithophores offered the best prediction of NVO-per-litre variations, single linear regression analyses were performed, considering these two groups separately. Diatoms (y=0.52x+2.7; adjusted-R^2=0.87; F=253.6; d.f.=36; p<0.001) (Figure 2.16a) explained more variability of ng-NVOs/L than coccolithophores

(y=0.93x+6.2; adjusted-R^2=0.61; F=59.44; d.f.=36; p<0.001). Considering also the low abundance of coccolithophores (cells/L) at LTER-MC in 2017, the linear relationship between NVOs/L and phytoplankton abundance was further analysed only in relation to diatoms. The linear regression between diatoms and ng-NVOs/L was refined through a multiple linear regression analysis: those diatom taxa that did not significantly contribute to oxylipin production were excluded, and the model resulted in a multiple-adjusted-R^2=0.98 (F=93.61, d.f.=27 and 10, p<0.001).

Table 2. 4. Multiple linear regressions testing the combined effects of environmental variables and diatoms on the concentration of NVOs (ng/L and fg/cell). The environmental variables were selected after removing factors showing VIF>10. After backward removal of the non-significant (p>0.05) variables from the model, only chl-a and diatoms resulted as significant predictors of the oxylipin concentrations.

Model	**NVOs~Trasmittance+Oxygen+Salinity+Density+Chl.a+Diatoms**			
Dependent variable	ng-NVOs/L		fg-NVOs/diatom-cell	
	t	p	t	p
Chl-a	3.023	0.0048	2.855	0.0074
Diatoms	9.398	7.49^{-11}	-12.283	7.42^{-14}
	Adj.-R^2=0.89, F=144.5, d.f.=2 and 33, p<0.001; N=38		Adj.-R^2=0.87, F=113.1, d.f.=2 and 33, p<0.001; N=38	

A significant inverse regression was observed (y=-0.46x+10.75; R^2=0.84; F=192.8; d.f.=36; p<0.001) between diatom abundance and NVO-per-cell production (fg/diatom-cell) (Figure 2.16b). In this case, a multiple-linear-regression test slightly improved the general model (multiple-adjusted-R^2=0.89, F=33.39, d.f.=9 and 28, p<0.001). Such inverse linear regressions were lost, when calculations were performed considering phytoflagellates (adjusted-R^2=0.18), dinoflagellates (adjusted-R^2=0.21) and coccolithophores (adjusted-R^2=0.004). To verify whether the inverse regression with NVOs was valid also for changes in diatom biomass, the total bio-volume of diatoms in the phytoplankton sample was plotted against fg-NVOs/ng-diatom-C. The relation was inverse and significant (y =-0.39x+5.13; R^2=0.71; F=90.24; d.f.=36; p<0.001). However, this value was considerably lower than the regression with diatom abundance (adjusted-R^2=0.84 vs adjusted-R^2=0.71).

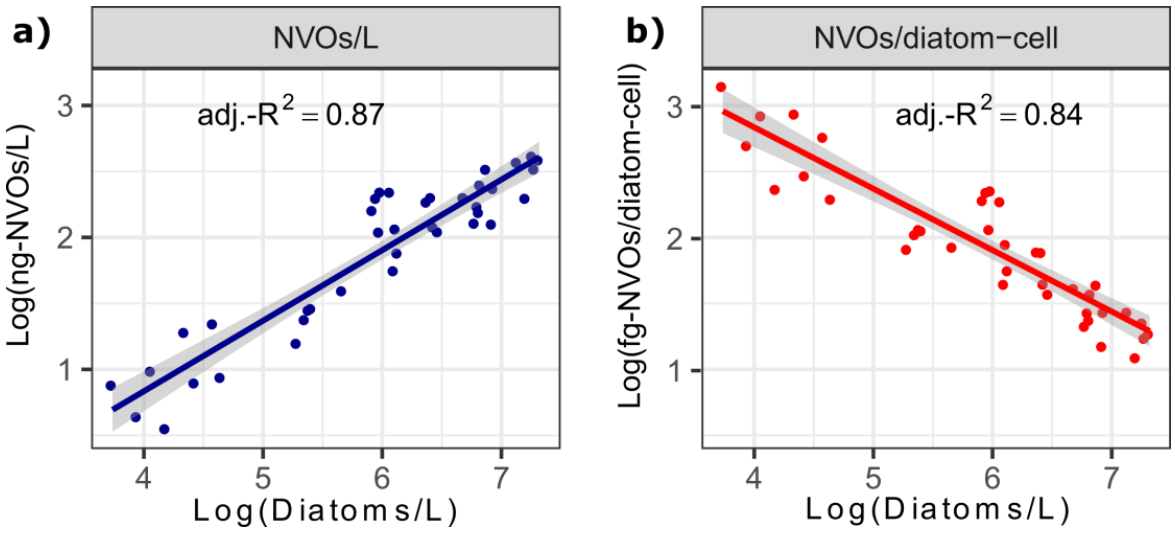

Figure 2. 16: Linear regressions between diatom abundances and non-volatile oxylipin (NVO) concentration and production. a) Blue dots and line indicate the relationship between ng-NVOs/L and diatoms/L. b) Red dots and line indicate the relationship between fg-NVOs/diatom-cell and diatoms/L. In both a) and b) grey shadings indicate the 95% confidence interval of the linear regressions. Log-transformed data are shown.

The balanced ANOSIM test inspecting whether changes in fg-NVOs/diatom-cell were driven by variations in diatom community composition highlighted overall highly significant differences (Global R=0.75, p<0.001). Diatom composition characterizing the group "high" was mostly separated from the group driving the "low" oxylipin production (R=0.96, p<0.001). By contrast, the "medium" group showed intermediate values (R=0.51 vs "low"; R=0.76 vs "high"). NMDS was effective in ANOSIM result representation, showing a stress=0.07 (Figure 2.17a). To verify if this difference was driven by diatom abundance rather than composition, the ANOSIM test was repeated on presence-absence data: such transformation allowed accounting only for differences in species composition (Figure 2.17b). Overall, the test revealed low differences (R=0.22, p<0.001), and group similarity was much higher than the one observed for raw data (R=0.26, p<0.001 "low" vs "high"; R=0.25, p<0.001 "medium" vs "low"; R=0.19, p<0.001 "medium" vs "high").

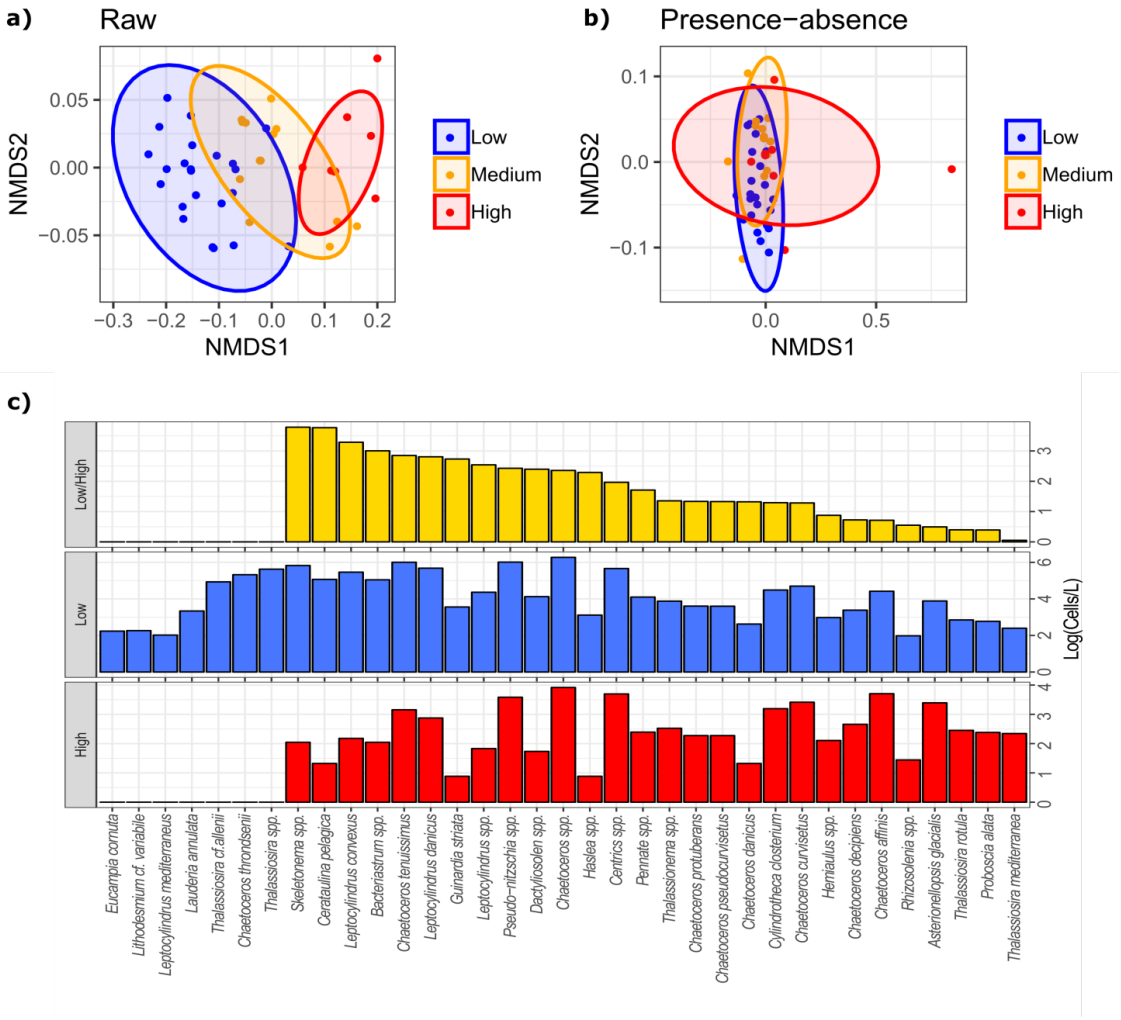

Figure 2. 17: a) nMDS representing three oxylipin production groups on the basis of their similarities in diatom community composition considering raw abundance data (Stress = 0.07). b) nMDS representing three oxylipin production groups on the basis of their similarities in diatom community composition considering presence/absence data (Stress = 0.2). 95% ellipses are shown; ellipse colours indicate observations characterized by different NVO-per-cell production: blue = "low" (0-100 fg/diatom-cell), orange = "medium" (100-300 fg/diatom-cell), red = "high" (>300 fg/diatom-cell). c) SIMPER analysis results based on raw diatom abundances. Diatom taxa are listed on "x" axes, cellular concentrations (log-transformed) are shown on "y" axis. Red bars indicate abundance of the respective diatom species contributing to community of "high" (>300) fg-NVOs/diatom-cell. Blue bars indicate abundance of the respective diatom species contributing to community of "low" (0-100) fg-NVOs/diatom-cell. Yellow bars indicate the ratio between diatom densities in the "low" and the "high" condition and are ordered from the highest to the lowest values. Higher ratios indicate higher differences in cellular concentrations of the respective species in the "low" and the "high" observations.

SIMPER analysis indicated that only a few diatom taxa did not contribute at all to the diatom composition of the "high" production group in comparison to the "low" group: *Thalassiosira* spp., *Chaetoceros throndsenii*, *Thalassiosira* cf. *allenii*, *Lauderia annulata*, *Leptocylindrus mediterraneus*, *Lithodesmium* cf. *variabile* and *Eucampia cornuta*. By

contrast, *Thalassiosira mediterranea*, *Proboscia alata*, *Thalassiosira rotula*, *Asterionellopsis glacialis* and *Rhizosolenia* spp. showed the lowest concentration differences in the "low" and the "high" oxylipin-per-cell production groups (Figure 2.17c).

2.4 Discussion

2.4.1 Phytoplankton abundance and composition

Diatoms and phyto-flagellates, which alternated in dominance in 2017 at LTER-MC, are well known to constitute the main taxa of the surface phytoplankton assemblage at this sampling site (Zingone et al., 2009). The annual dynamics did not completely mirror the canonical phytoplankton pattern observed at LTER-MC, in that the first peak, detected in April 2017, was shifted later in time (Zingone et al., 2009) (Figure 2.3). The Gulf of Naples is a basin showing both oligotrophic and eutrophic features driven by alternating oceanographic influences of nutrient-depleted offshore Tyrrhenian waters and nutrient-enriched coastal waters (Cianelli et al., 2012). Phytoplankton variations at LTER-MC in 2017 well reflected those described for eutrophic systems by the Plankton Ecology Group Model (PEG Model) (Sommer et al., 2012). Such eutrophic characteristics may also explain why phytoplankton cell abundances exceeded $1x10^7$ cells/L in spring-summer, reaching similar cell concentrations observed in the Northern Adriatic Sea (Ianora et al., 2015). Phytoplankton minima observed in January-March and October-December were possibly explained by high water mixing and/or by limited nutrient availability (Zingone et al., 2009), while weekly changes by sudden influence of different water masses (Cianelli et al., 2015). Diatom succession observed in 2017 well reflected the general annual patterns reported at LTER-MC (Ribera d'Alacalà et al., 2004), where large colonial diatoms mostly dominate in water mixing conditions, such as winter and autumn, while small solitary species dominate during high stratification periods (spring and summer). Among environmental predictors driving variations in diatom densities, transmittance showed the

highest effect (adj.-R^2=0.8; Figure 2.9). However, biological mechanisms driving such variations are difficult to explain, because a sudden dip in diatom concentrations occurred at intermediate transmittance values. By contrast, effects of temperature and salinity are easier to discuss on the basis of literature information. In fact, a linear increase of diatom growth rates at higher water temperatures has been demonstrated (Montagnes and Franklin, 2001) and higher diatom concentrations at warmer conditions observed at LTER-MC in 2017 could be explained by enhanced cellular growth rates. With respect to salinity, an inverse relation with diatom concentration was found, indicating that at higher salinity diatom cells decreased. This result likely relies on the mutable oceanographic features characterizing the sampling site LTER-MC. That is, lower salinities are explained by the influence of nutrient enriched coastal waters, while higher salinities by the influence of oligotrophic oceanic waters (Cianelli et al., 2015, Cianelli et al., 2012). However, the data collected do not allow distinguishing when variations in diatom community composition and abundance were driven by oceanographic dilution effects or by diatom species succession (Cianelli et al., 2015).

2.4.2 Fatty acid variations

Many laboratory and field studies have investigated variations in fatty acid concentration and composition from marine phytoplankton because of the high ecological relevance of these molecules. In fact, both essential and non-essential fatty acids are assimilated by herbivores through grazing (Müller-Navarra, 2008, Brett and Müller-Navarra, 1997). Fatty acids represent key nutritional resources for heterotrophic organisms in the pelagic domain, because they sustain physiological functions and reproductive success of zooplankton and fishes (Jónasdóttir et al., 2009, Arendt et al., 2005, Dalsgaard et al., 2003). Fatty acids are also key precursors in the synthesis of oxylipins in diatoms (Cutignano et al., 2011). In contrast to the positive effects of fatty acids on the reproduction of secondary producers, oxylipins potentially impair grazer fitness through

teratogenic effects (Russo et al., 2018). On this basis, assessing natural variations of fatty acids is useful to evaluate the physiological status of phytoplankton and their grazers as well as the reproductive potential of secondary producers in marine systems.

Although fatty acids may be useful chemotaxonomic indicators (Taipale et al., 2013, Dijkman and Kromkamp, 2006) and can offer information about food web dynamics (Kainz et al., 2004), quantitative characterization from natural phytoplankton communities is not always straightforward. For example, the low biomass available from natural samples could represent a limiting factor for the analytical power and the variability of fatty acids detected could not offer sufficient resolution to clearly infer phytoplankton composition (Galloway and Winder, 2015, Reuss and Poulsen, 2002). FAs constitute an integral part of neutral (such as triacylglycerol and wax esters) and polar lipids (for example phospholipids and glycolipids) (Dalsgaard et al., 2003) and their release from these complex molecules occurs through enzymatic and non-enzymatic hydrolysis. To favour release of free FA from complex lipids, saponification is usually required to gain higher accuracy in the quantification of free FAs. Due to the limited biomass available for the samples collected in the present survey and to the occurrence of spontaneous hydrolysis reactions during the extraction process, no saponification treatment was applied. Therefore, FA quantification here presented is particularly useful to validate oxylipin occurrence by quantifying their precursors, but this analysis could have suffered of incomplete hydrolysis of free FAs from complex lipids. The good relation between FA and NVO concentrations supported oxylipin quantification and further analyses constitute an attempt to investigate whether quantitative data of FAs from the present survey could have supported evidence for chemotaxonomic markers or for influence of abiotic predictors in their synthesis.

In general, the common *de novo* process of fatty acid synthesis in marine algae leads to the formation of Palmitic (C16:0) acid from Acetyl-CoA and of saturated fatty acids containing 18 and 20 carbon atoms through chain elongation of this primary product

(Cagliari et al., 2011, Guschina and Harwood, 2006, Dalsgaard et al., 2003). Biosynthesis of monounsaturated fatty acids such as 16:1, 18:1 and 20:1 occurs through aerobic desaturation (catalysed by Δ9 desaturase enzyme) of the saturated precursors, introducing a double bond between the 9^{th} and the 10^{th} carbon along the acyl chain. Plants are then able to synthesize C18:2 and C18:3 PUFAs and these fatty acids represent the substrates for the synthesis of C20:4n-6 (from C18:2n-6), EPA and DHA (from C18:3n-3) fatty acids. Moreover, diatoms are typically characterized by the synthesis of C16 PUFAs through desaturation of Palmitoleic acid (C16:1) (Dalsgaard et al., 2003).

Fatty acid concentrations observed at LTER-MC along 2017 partially mirrored patterns observed in other field surveys. For example, (Pond et al., 1996) analysed concentrations of 13 fatty acids from samples of different particle size (<20 μm and 20-200 μm) collected in the North Sea. They reported that Palmitic (C16:0), Palmitoleic (C16:1 *n*-7+9) and Myristic (C14:0) acids were the most abundant fatty acids. Similarly, saturated and monounsaturated fatty acids constituted the bulk of the fatty acid species in phytoplankton collected off the West Greenland coast and off Southern Iceland (Jónasdóttir et al., 2002, Reuss and Poulsen, 2002). Similarly, Palmitic (C16:0) and Palmitoleic (C16:1 *n*-7) acids were among the most abundant species detected in Svalbard (Norway) also by (Leu et al., 2010, Leu et al., 2006). As highlighted by results collected in the present survey, concentrations of these same species largely exceeded those of the other FAs also in the Gulf of Naples. Even though several studies reported the dominating contribution of saturated and mono-unsaturated fatty acids to the total pool, other surveys focusing on natural phytoplankton communities suggested that EPA and DHA could represent a relevant fraction of the total fatty acid abundance (Leu et al., 2010, Leu et al., 2006, Copeman and Parrish, 2003, Napolitano et al., 1997, Pond et al., 1996). These evidences differ from data reported for the Gulf of Naples, where EPA and DHA were much less concentrated than C16:0, C16:1, C14:0, C18:0 and C18:1, representing at maximum 4% and 2.4%, respectively, of the total fatty acid pool. These discrepancies

could be driven by differences in phytoplankton community composition as well as by a different physiological status of phytoplankton in response to abiotic or biotic factors (Galloway and Winder, 2015).

For example, negative effects of irradiance and temperature have been observed on the synthesis of PUFAs in marine phytoplankton (Leu et al., 2010, Thompson et at., 1992, Thompson et al., 1990). Results from the present survey indicated that fluorescence and transmittance were significantly related to total fatty acid concentrations, but patterns were highly oscillatory (Figure 2.10) and of difficult interpretation. Instead, the effects of temperature on the total fatty acid pool were not significant, while diatom-derived PUFAs (HTrA, EPA and DHA) significantly increased at higher temperature values. The simple linear regression analysis demonstrated that, at LTER-MC, these three PUFAs are mainly derived from diatoms. Results also suggested that the synthesis of these three PUFAs could commonly occur in all diatom taxa, because the main five diatom genera (*Chaetoceros*, *Leptocylindrus*, *Pseudo-nitzschia*, *Skeletonema* and *Thalassiosira*) and the mixed group "Other diatoms" well explained variations of these three fatty acids (Figure 2.15).

By considering the concentration of these three PUFAs instead of the total fatty acid concentrations, more marked variations depending on environmental variables were detected (Figure 2.11). Even if no linear effect occurred, a dip in the sum of HTrA, EPA and DHA was observed at intermediate transmittance values. These results could suggest that transmittance could have exerted a negative effect on the synthesis of the three PUFAs in the Gulf of Naples, but a similar effect of this environmental predictor was also observed on diatom abundance. Therefore, such dip could indicate alternation of diatom abundance and community composition (Leu et al., 2010, Brett and Müller-Navarra, 1997) along transmittance values, with consequent variations in the FA signature.

The concentration of the three diatom-derived fatty acids initially increased with increasing fluorescence and temperature, but reached a plateau at high values of these variables. These patterns could indicate saturation of these three selected PUFAs (i.e.

HTrA, EPA and DHA; Figure 2.11) (Thompson et al., 1992) at discrete fluorescence and temperature values, rather than a negative effect. Indeed, nutrient availability could have played a role in shaping the observed patterns, but nutrient data at LTER-MC are not available for 2017.

More recently, evidence has been provided also about the effect of pH on fatty acid concentrations because of variations in phytoplankton community composition (Leu et al., 2013). In the current survey, effects of pH on HTrA, EPA and DHA fatty acids were not significant, but this environmental variable well explained oscillatory pattern of total fatty acid concentration (Figure 2.10). This result suggests a possible non-linear effect of pH on total FA concentration. However, it remains unclear whether influences on phytoplankton physiology or community composition occurred.

Although FA are usually investigated as phytoplankton biomarkers in pelagic food webs (Gallowy and Winder, 2015, Müller-Navarra, 2008, Dijkman and Kromkamp, 2006, Dalsgaard et al., 2003, Napolitano et al., 1997), data collected at LTER-MC did not allow to clearly identify how the major phytoplankton groups identified differentially contributed to fatty acid synthesis. Palmitic and Stearic acids were significantly correlated only with phytoflagellates, possibly indicating the predominant synthesis of these fatty acids by this phytoplankton group.

2.4.3 NVO variations

Qualitative and quantitative characterization of particulate NVOs from our data confirm that HTrA and EPA represent relevant oxylipin precursors in diatoms (d'Ippolito et al., 2009, Fontana et al., 2007a, d'Ippolito et al., 2006, d'Ippolito et al., 2005, Pohnert, 2005, d'Ippolito et al., 2003), but also suggest that the relative contribution of DHA at sea (Nanjappa et al., 2014) may be more relevant than previously thought (Figure 2.7). In fact, previous information is based on a rather limited number of diatom species, which were not found (e.g. *Skeletonema marinoi*) or slightly contributed (e.g. *Pseudo-nitzschia*

delicatissima, *Skeletonema pseudocostatum, Thalassiosira rotula*) in the diatom community at LTER-MC. The higher concentrations of Hydroxy-acids compared to Epoxy-alcohols reported in this study were already described in the NVOs characterized in the Northern Adriatic Sea (Lauritano et al., 2016) and might indicate a common over-expression of reductases in natural diatom communities, because these enzymes catalyse synthesis of Hydroxy-acids from Hydro-peroxides (Fontana et al., 2007a). Analyses of mono-specific diatom cultures have revealed a wide variety of LOX pathways in the lineage even if the distribution of these enzymes is rather species-specific. Unfortunately, the lack of information about position of hydroxy and epoxy functional groups hinders sound consideration on the occurrence of different LOX pathways in the natural assemblage of the Gulf of Naples.

Macro-ecological dynamics can be inferred only by comparing new evidence with those already presented. However, one major limitation in comparing oxylipin production in distinct sampling systems is that there is no common methodological procedure for oxylipin analysis and normalization. Oxylipin quantification expressed as ng-NVOs/L and fg-NVOs/diatom-cell in this study allows discussing our results in comparison with those presented in previous field surveys from distinct marine systems.

Particulate NVO concentrations (ng-NVOs/L) detected at LTER-MC were higher than those detected in systems other than the Northern Adriatic Sea. For example, particulate PUAs measured in the Atlantic Ocean showed a mean concentration of 28.35 ±82.47 pg/L (Bartual et al., 2014), while those measured in the Strait of Gibraltar ranged between 6.44-1584.98 pg/L during the Spring tide and between 5-1264 pg/L during the Neap tide (Morillo-García et al., 2014). By contrast, total particulate PUA concentration (ng/L) observed in 2008 in the Adriatic Sea was sensibly higher than the NVO abundance detected at LTER-MC in 2017. In fact, the highest heptadienal and ocatienal concentrations were 1993 ng/L and 1303 ng/L in the Adriatic Sea, respectively (Vidoudez et al., 2011), while particulate NVOs never exceeded 417 ng/L, in the Gulf of Naples.

Patterns are different, when cellular oxylipin production is taken into account: values always range in the magnitude of fg-NVOs/cell and variations depend on system productivity (Cózar et al., 2018). Cellular production of NVOs in the Gulf of Naples exceeded the synthesis of particulate PUAs observed in the Northern Adriatic Sea (Ribalet et al., 2014). In fact, average particulate PUA productions were observed to vary from 87 fg/cell (in 2004) to a maximum of 209 fg/cell (in 2002), while maximal production never exceeded 638 fg/cell (observed in 2006) (Ribalet et al., 2014). In the present survey, annual average cellular production was of 214 fg-NVOs/diatom-cell, with the maximum value of 1417 fg-NVOs/diatom-cell observed on 8th of February. (Morillo-García et al., 2014) also indicated that, in the Strait of Gibraltar, PUAs varied between 0-1262 fg/cell during the Spring tide and between 12.89-940.68 fg/cell during the Neap tide, then showing comparable, but lower, cellular production of oxylipins than the present study. Similarly, particulate PUAs ranged between 0-1276 fg/cell in the coastal waters off Roscoff (Wichard et al., 2008).

NVO concentrations from this survey cannot be compared to those reported by (Ianora et al., 2015) and (Lauritano et al., 2016) from phytoplankton samples collected in the Northern Adriatic Sea. Those are, so far and to the best of our knowledge, the only two field surveys reporting NVO variations, but in those cases oxylipins were normalized by mg of protein, then hindering data comparison based on our normalizations.

Overall, comparison of oxylipin production in different systems shows that while oxylipin concentration expressed as weight/L widely varies depending on the study area (from pg/L to µg/L) (Bartual et al., 2014, Morillo-García et al., 2014, Vidoudez et al., 2011), cellular oxylipin production always varies within the same magnitude (fg/cell). This might suggest that while total oxylipin concentration in the water volume depends on system productivity (the highest productivity in the hypertrophic Northern Adriatic Sea, the lowest in the Atlantic Ocean) (Bartual et al., 2014, Vidoudez et al., 2011), oxylipin-per-cell production is modulated by physiological conditions of the oxylipin producers. In fact,

oxylipin-per-cell productions were always detected in the range of fg/cell and never exceeded the maximal production of 1417 fg-NVOs/diatom-cell detected in this study.

Such interpretation is supported by the regression analyses (Figure 2.16). The tests describing variations of ng-NVO/L as function of phytoplankton groups and diatom concentrations provide evidence that the selected oxylipins from our samples derive almost exclusively from diatoms, thus allowing discussing oxylipin patterns in relation to diatom community structure. This is the first time that such a positive relation between ng-NVOs/L and diatom/L is reported from a single field survey and implicates that the more diatoms were present at sea and collected on the filter, the higher concentrations of the targeted NVOs were detected. In this perspective, particulate oxylipin-per-litre concentrations observed at LTER-MC may show higher similarity with those reported in the Northern Adriatic Sea (Vidoudez et al., 2011) because of comparable diatom concentration maxima. Besides proving a tight connection between NVOs and the natural diatom community, the reported simple linear regression equation can represent a reference equation to evaluate oxylipin synthesis potential over time in other systems, by comparing slopes of the curves. Such information can provide precious clues to infer the oxylipin synthesis tendency and therefore to better understand the ecology of diatoms in the study systems.

The evidence that cellular oxylipin production is inversely related to diatom concentration is more remarkable, especially because of the wide evolutionary, biological and ecological implications that can be extrapolated from this pattern. In fact, adjustment of oxylipin synthesis depending on diatom density might imply a major role of NVOs as info-chemicals potentially influencing diatom-diatom interactions. In this perspective, higher oxylipin-per-cell synthesis potential at minimal diatom concentrations may be driven by the necessity of diatoms to communicate with each other with stronger signals when they are highly dispersed in the water medium. Rather, reduction of the oxylipin potential production by diatoms at increasing diatom abundances can guarantee effective

communication even when molecule synthesis is lower. Sub-lethal doses of decadienal were observed to induce stress resistance in diatom cells (Vardi et al., 2006) and this intraspecific effect could resemble more realistically the actual effects of oxylipins on diatom cells at sea.

In this perspective, oxylipin concentration and production (expressed as pg or ng/L or as fg/cell, respectively) detected in other field surveys seem in line with our interpretation that oxylipin production is reduced as diatom concentration increases: a lower oxylipin-per-cell production was detected in the Northern Adriatic Sea (Ribalet et al., 2014), while in the Gulf of Naples the highest per-cell production was recorded at the lowest diatom abundance. As a result, the high diatom densities often observed in the Northern Adriatic Sea could dampen cellular oxylipin production, which, by contrast, is at its maximum when cells are highly diluted in the medium. Such dynamics well reflects also evidences recently reported by (Cózar et al., 2018), who described PUA production tendency to decrease along the trophic status of the systems (lower tendency in eutrophic systems, higher in oligotrophic ones). However, such a pattern was interpreted by the authors as a strategy to improve remineralization rate in nutrient limited conditions, supporting experimental evidence that PUAs can boost remineralization rates (Edwards et al., 2015). (Cózar et al., 2018), in particular, presented an inverse relation between µg-PUAs/g-*chl* and total µg-*chl*/L.

Interestingly, results from this survey in the Gulf of Naples indicate that changes in cellular oxylipin production are not associated with changes in diatom community composition, as demonstrated by the ANOSIM test performed among the three oxylipin production clusters (Figure 2.17). This evidence highlights that similar diatom communities can modulate oxylipin production depending on diatom cell concentration. By contrast, the results do not allow to understand precisely whether all diatom cells adapt oxylipin synthesis in a comparable way or not. In particular, two main scenarios can be hypothesized (Figure 2.18) 1) A “cheater” scenario: while some diatom species always

produce oxylipins, others suppress oxylipin synthesis, thereby reducing energy consumption and cheating on oxylipin producers, because these cheaters still take advantage of the information mediated by the chemical signal (Figure 2.18a). 2) A "common physiology" scenario: all diatom species share the same physiology and are capable of changing oxylipin production depending on the abundance of diatom cells (Figure 2.18b).

Each of these two scenarios may also have wide ecological implications with respect to the fitness of copepod grazers. In the cheater scenario, the relative abundance of cheaters will increase with diatom cell densities, since the chemical signal mediated by NVOs is efficiently mediated by oxylipin producers. When in the cheater scenario grazers ingest diatoms occurring at low abundances (cells/L; Figure 2.18a), they have a high probability of ingesting a high amount of oxylipins, because the diatom community is dominated by cells with a high oxylipin synthesis potential. Therefore, grazer fitness can briskly decline along time after selective feeding (Ianora et al., 2004) or progressively decline after unselective diatom ingestion. When, instead, feeding on diatoms occurs at high abundances, the probability of ingesting high amounts of oxylipins is reduced, because cheaters are relatively more abundant in the community. In this case, copepod fitness after selective feeding can be oscillatory because of alternated ingestion of cheaters and cells showing high oxylipin synthesis potential. After unselective feeding, instead, copepod fitness can slowly decline along time because of mean low oxylipin ingestion.

Alternatively, when grazers ingest diatoms occurring at low abundances (cells/L) in the "common physiology" scenario (Figure 2.18b), a high oxylipin uptake will occur independently of the diatom cell ingested. Thus, grazer fitness would progressively decrease along time irrespective of selective or unselective feeding strategies. Instead, when feeding occurs on diatoms at high abundances in this scenario, the amount of oxylipins ingested will be lower, because all diatom cells reduce oxylipin synthesis. In this

case, grazer fitness can be supposed to resemble the one proposed in the "cheater" scenario at high diatom concentrations, independently of selective or unselective feeding.

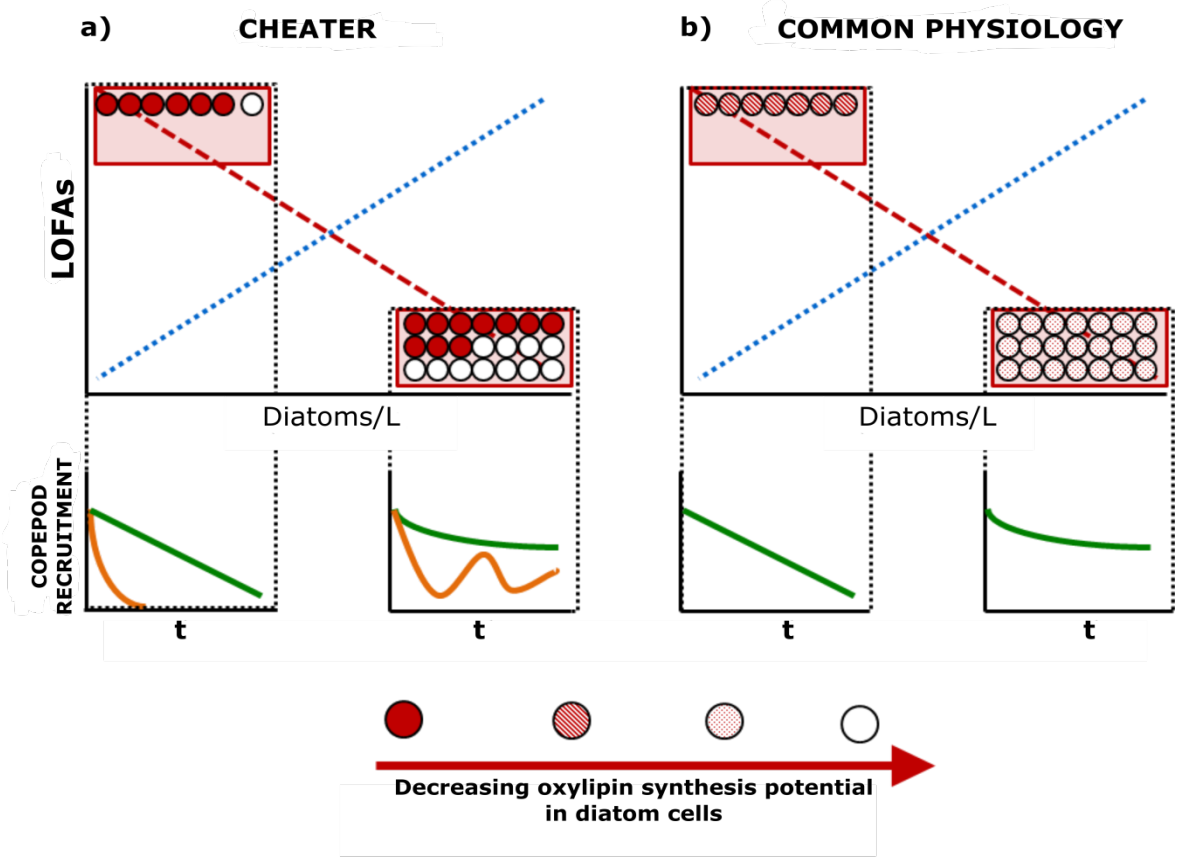

Figure 2. 18: Conceptual model synthesizing two possible dynamics describing variations in non-volatile oxylipin (NVO) synthesis potential along diatom density gradient. Circles indicate diatom cells and fill gradient indicates the oxylipin synthesis potential (red is the highest, white is the lowest). Dotted blue lines show the positive relation between ng-NVOs/L and diatom-cells/L; dashed red lines show the inverse relation between fg-NVOs/diatom-cell and diatom-cells/L. a) "Cheater" dynamics: some diatom cells can reduce oxylipin synthesis depending on the abundance of diatom cells with constantly high oxylipin synthesis potentials. After grazing on diatom cells at low and high abundances, copepod grazer recruitment can vary depending on selective (orange lines) or unselective (green lines) feeding strategies. b) "Common physiology" dynamics: all diatom cells share the same physiological adaptation and synthesize the same amount of molecules. Copepod grazer recruitment after feeding on diatom cells at low and high abundances is different because of different ingestion of harmful molecules, but it does not vary depending on selective or unselective feeding strategies.

Even if the results demonstrate a tight connection between oxylipin concentration and production and diatom abundances, one main limitation in the present study is that it was not possible to integrate nutrient variations in the analyses. Influence of nutrient limitation on oxylipin production has been documented in relation to N, P and Si (Ribalet et al., 2009, Ribalet et al., 2007b).

Moreover, oxylipins are produced from fatty acid precursors, but this survey does not reveal whether oxylipin variations were driven by different expression of genes involved in oxylipin synthesis or by changes in intra-cellular fatty acid composition (Grosse et al., 2018). Even if a significant relationship was found between ng-FA/L and ng-NVOs/L, this result could rely on the methodological procedure, which led to higher PUFA production at high phytoplankton densities, after cell disruption.

Despite these uncertainties, (Cózar et al., 2018) reported the effects of N:P ratio on PUA production to be of secondary importance, if compared to those mediated by chl-a (which is a proxy of phytoplankton biomass). Additionally, diatoms have evolved sophisticated mechanisms to perceive and respond to environmental signals (Falciatore et al., 2000) and, in an oxylipin context, they have been demonstrated to activate complex intra-cellular mechanisms after exposure to these molecules (Vardi et al., 2008, Vardi et al., 2006). On this ground it is unlikely that variations in oxylipin production that we detected are a side consequence of altered PUFA levels in diatom cells. Rather, our data support a major role of oxylipins, in our case NVOs, as info-chemicals playing a role in chemical communication within natural diatom communities, with cascading implications for copepod recruitment.

Chapter 3

Physiological and molecular responses of the copepod *Temora stylifera* at LTER-MC

3.1 Introduction

Among zooplankton, copepods represent one of the most various and important groups in both marine and freshwater systems, where they constitute 70-90% of meso-zooplankton abundance (Steinberg and Landry, 2017). Copepods play a central role in food webs and biogeochemical cycles, because they affect carbon transfer to higher and lower trophic levels and modulate nutrient recycling (Boxshall and Defaye, 2007, Verity and Smetacek, 1996). In this perspective, assessing biotic and abiotic factors influencing copepod population dynamics can be of primary importance in the analysis of the entire marine pelagic food web.

3.1.1 Physiological, molecular and transcriptomic approaches in copepod population dynamics

The importance of copepods in marine ecosystems explains why investigating variations in copepod community and population dynamics is relevant from an ecological perspective. Identifying significant factors influencing natural copepod populations is challenging, also in consideration of the interactive nature of biotic and abiotic drivers in natural environments (Deschutter et al., 2017, Lima-Mendez et al., 2015).

Studies investigating major forces driving copepod population dynamics are mainly based on long-term data series in which oscillations in the abundance of juveniles and adults are analysed (Mazzocchi et al., 2012, Beaugrand et al., 2003). Copepod development from egg hatching to adult passes through six larval and six copepodid stages (the last copepodid stage is the adult) (Allan, 1997). Hence, understanding how hatching success of eggs and survival rates of nauplii and copepodids vary is of key importance for predicting copepod recruitment (Carotenuto et al., 2002). On this ground, many studies have investigated variations in copepod egg production, hatching success and survival of non-feeding nauplii (NI/NII) through field surveys (Lauritano et al., 2016, Ianora et al.,

2015, Wichard et al., 2008, Poulet et al., 2007, Poulet et al., 2006, Carotenuto et al., 2006, Irigoien et al., 2002).

In the context of diatom-copepod interactions, these approaches are of particular relevance to understand the negative effects of diatom oxylipins on copepod populations. Negative impacts of diatom monospecific diets on the reproductive output of copepods were widely reported by (Ban et al., 1997) and these effects were due to oxylipins synthesized by diatoms upon cellular wounding (Miralto et al., 1999). Importantly, adult copepod females can activate detoxification mechanisms (Carotenuto et al., 2014), overcoming direct short-term negative influences due to oxylipins. Rather, these compounds are known to affect copepod embryos through a maternal effect, determining reduction of egg hatching and of early-hatched nauplii survival (Ianora et al., 2004).

Investigating physiological and molecular responses of adult copepod females is essential to understand factors regulating copepod reproductive success and potential recruitment. Nowadays, technical advances allow fast and low-cost access to molecular information. Next Generation Sequencing (NGS) technology of whole transcriptomes based on high-throughput sequencing of short-reads (RNA-Seq) and Real-Time quantitative PCR (RT-qPCR), for example, are now precious tools to disentangle molecular mechanisms driving the physiological responses of copepods. In particular, characterizing variations in the transcriptional profile of these metazoans is arising as a successful approach for this purpose. A transcriptome is the complete set of messenger RNA (mRNA) and non-coding RNA (ncRNA) transcripts produced by a particular cell, cell type or organism (Morozova et al., 2009). Due to the lack of a reference genome for copepods (Havird and Santos, 2016), their transcriptomes are commonly assembled following a *de novo* approach. This method strives to find overlaps among short reads in order to assemble them into transcripts. A typical RNA-Seq workflow includes, first, fragmentation and conversion of the total or fractionated RNA population (poly A^+) into a library of cDNA fragments and then ligation of primer adaptors to both ends of the

fragments to be sequenced. Each molecule is sequenced in single or paired-end options in a high-throughput NGS machine, typically Illumina, to generate millions of short reads representing the transcriptome. The reads are typically 30–400 bp long, depending on the sequencing technology used. Following sequencing, there are generally two ways to process the short reads, either they are aligned to a reference genome or reference transcriptome, or they are *de novo* assembled, if no proper reference genome or transcriptome is available. Recently, the *de novo* transcriptomes of several pelagic copepods, such as *Temora longicornis* (Semmouri et al., 2019), *Acartia tonsa* (Zhou et al., 2018), *Eurytemora affinis* (Legrand et al., 2016), *Calanus finmarchicus* (Christie et al., 2014b), and *Calanus sinicus* (Ning et al., 2013), were published. The transcriptome of *C. finmarchicus* was also further analysed in respect to the expression of nitric oxide transmitter signalling (Christie et al., 2014a) and of enzymes involved in amine biosynthesis (Christie et al., 2014b) at different developmental stages (Tarrant et al., 2014). Moreover, a transcriptomic approach was applied to analyse regulators of diapause in this same copepod species (Tarrant et al., 2016).

A next-generation sequencing approach exploring differential gene expression analysis based on the transcriptome of copepod females fed diatom monospecific cultures is still lacking. In this perspective, the study by (Carotenuto et al., 2014) represents the only example of a transcriptomic analysis based on a suppression subtractive hybridization (SSH) technique (Diatchenko et al., 1996). Briefly, this method generates subtracted cDNA libraries, by combining normalization and subtraction in a single procedure. In this process, normalization equalizes abundance of cDNA, while subtraction excludes the common sequences between the target and the control cDNA populations. Despite the great analytical potential of NGS sequencing, most experiments investigating potential effects of diatom oxylipins on the molecular responses of copepod females were based on quantitative expression analysis of a series of target genes of interest (GOIs), which were *a priori* hypothesized to be important in copepod stress responses (Lauritano et al., 2015,

Lauritano et al., 2012, Lauritano et al., 2011a, Lauritano et al., 2011b). Remarkably, only one field survey investigated whether the expression of selected GOIs could have explained variations in the reproductive success of adult females of the species *Calanus helgolandicus* in natural conditions (Lauritano et al., 2016). A thorough description of the main studies inspecting the effects of diatom oxylipins on copepods through molecular approaches can be found in Chapter 1.

In this chapter, I describe and discuss results estimating the reproductive potential of the copepod *Temora stylifera* collected weekly at LTER-MC along 2017, on the basis of egg production, egg hatching success and survival rates of early hatched nauplii. Also, a RNA-Seq approach, followed by differential gene expression analysis, was applied to generate a *de novo* assembled transcriptome of *T. stylifera* females collected during two consecutive sampling weeks, to understand whether their transcriptomic response drove different naupliar survival rates. The reference transcriptome was further used as a benchmark to analyse temporal variations in the expression of selected GOIs through RT-qPCR in *T. stylifera* females collected weekly along 2017.

The calanoid copepod *T. stylifera* is a broadcast filter feeder (Benedetti et al., 2018, Benedetti et al., 2016, Paffenhöfer, 1998) that dominates the autumnal copepod community in the Gulf of Naples (Mazzocchi et al., 2012). Several studies have already investigated the population dynamics of this copepod in the Gulf of Naples, exploring whether abiotic factors and life-history traits could explain the marked seasonality in this area (Carotenuto et al., 2006, Mazzocchi et al., 2006, Di Capua and Mazzocchi, 2004). The aim of this survey is to identify biotic and abiotic factors that might drive different physiological responses of *T. stylifera* in the attempt to explain the seasonal occurrence of this species at LTER-MC. Transcriptome and gene expression analyses can offer the chance to understand molecular pathways regulated by *T. stylifera* in response to biotic and abiotic pressures and to relate such molecular responses to copepod physiology and reproductive success.

3.2 Materials and methods

3.2.1 Sampling and physiological responses of Temora stylifera

Along 2017, zooplankton samples were collected by the SZN Unit every week at LTER-MC through oblique towing of a 200 µm Nansen net (113 cm mouth diameter) equipped with a 200 µm filtering cod-end, on-board of the R/V "Vettoria". Samples were poured in glass jars, diluted with surface seawater and transported to the laboratory in an insulated box within few hours. In the laboratory, 15 females of *T. stylifera* were picked from the zooplankton sample using a wide mouth pipette. These specimens were individually incubated in crystallizing dishes filled with 100 ml of surface seawater collected at LTER-MC and pre-filtered through a 50 µm mesh. Pre-filtration of seawater was necessary in order to remove large debris and to avoid undesired incubation of eggs and nauplii of different copepod species. Crystallizing dishes were incubated in a temperature-controlled room kept at 20 °C and on a 12h:12h dark:light cycle. After 24 hours, the females were removed from the crystallizing dishes and the number of spawned and chewed eggs, as well as the number of faecal pellets, were counted under an inverted microscope (Zeiss Axiovert25) at 25x magnification. While the faecal pellets have been considered as a proxy of the feeding rate of the animal, the sum of spawned and chewed eggs offered a measure of the reproductive potential of the species in the studied period (Ianora et al., 1989).

After counting eggs and faecal pellets, the crystallizing dishes were kept at 20 °C, on a 12h:12h dark:light cycle, for an additional 48 hours to allow eggs hatch to first nauplii (NI) and to develop to the second stage (NII). At this time point, the number of dead nauplii stage NI laying on the bottom of the crystallizing dishes was counted under the inverted microscope, in order to assess survival of first non-feeding nauplii (NI), and thus, maternally-related larval survivorship. Subsequently, the content of the crystallizing dish was fixed by adding 15 ml of ethanol (96%), and the number of hatched membranes, the

non-viable eggs and total nauplii present in the container were counted. Hatching success of the eggs as well as naupliar survival rates were calculated following (Carotenuto et al., 2006):

$$Hatching\ success = \frac{N\ (membranes)}{N\ (laid\ eggs)}\ 100$$

$$Naupliar\ survival = 100 - (\frac{N\ (dead\ nauplii)}{N\ (membranes)}\ 100)$$

To investigate if measurements of *in situ* fecundity, hatching success and early naupliar survival allowed accurate prediction of natural copepod oscillations, weekly abundances (individuals/m^3) of *T. stylifera* males, females and copepodids were also considered. These data are routinely collected at LTER-MC as part of the long-term observations in the Gulf of Naples (Ribera D'Alcalà et al., 2004). Weekly data of egg production, hatching success, early-naupliar survival and female abundance, were combined to calculate secondary production (1) and potential recruitment (2, 3) of natural populations of *T. stylifera* at LTER-MC during 2017, following (Poulet et al., 1995) and (Carotenuto et al., 2006).

(1) $Eggs_{(SEA)} = Eggs_{(LAB)} \times Abundance_{(T.STYLIFERA\ FEMALES)}$

(2) $Recruited\ eggs_{(SEA)} = (Eggs_{(SEA)} \times Hatching)/100$

(3) $Recruited\ NI_{(SEA)} = (Recruited\ eggs_{(SEA)} \times NI\ Survival)/100$

3.2.2 Molecular responses of Temora stylifera*: RNA extraction and* de novo *transcriptome assembly*

On several occasions during 2017, 30-60 females of *T. stylifera* were picked from the zooplankton sample collected weekly at LTER-MC and transferred to three replicate 1.5 ml eppendorf tubes. Samples were immediately frozen in liquid nitrogen after removing excess water, and finally stored at -80 °C for later total RNA extraction. These samples have been used to investigate quantitative gene expression changes of selected

Genes of Interests (GOIs) in wild-caught *T. stylifera* females over an annual sampling period. In order to identify the panel of putative target genes, a reference transcriptome of *T. stylifera* was generated. In particular, adult females collected on 23rd and 30th of May 2017 were used for RNA-Seq analysis and *de novo* assembly, followed by differential gene expression analysis. These dates were selected because of the opposite naupliar survival rates measured in these two consecutive samples (25% and 98%, respectively; t-test considering unequal variances, N=15). Samples consisted of three replicates each containing 8-10 adult females. For differential analysis of gene expression, females collected on 30th of May were considered the control sample because of the high maternally-related naupliar survivorship.

Total RNA of *T. stylifera* was extracted using the RNeasy Micro Kit (Qiagen, Hilden, Germany), following the manufacturer's specification. Briefly, frozen copepods were homogenized with a heat-sterilized Teflon micropestle in the presence of 1 ml of RLT buffer and 10 µl of β-mercaptoethanol (Merck, Darmstadt, Germany). The homogenate was centrifuged for 3 min and the supernatant was collected in a new tube. An equal volume of 70% ethanol was added to the lysate and mixed by pipetting. Seven hundred microliters of sample were transferred to an RNeasy MinElute spin column placed in a 2 mL collection tube and RNA was extracted following the manufacturer's protocol. On-column DNaseI treatment was also performed. The RNA was finally eluted in 12-15 µL of RNase-free water. RNA concentration (ng/µl) and purity were assessed through Nanodrop ND-1000 UV-Vis spectrophotometer (Marshall Scientific, Hampton, USA), reporting maximum absorbance at 260 nm, A260/230 nm ratio (a measure of phenol contamination, optimum ~2) and A260/280 nm ratio (a measure of protein contamination, optimum ~2). Overall RNA integrity and DNA contamination was checked by electrophoresis of at least 200 ng of RNA on a 1% agarose gel in 0.5 × Tris Borate EDTA buffer (TBE). RNA integrity was also evaluated by analysing 150-200 ng of RNA in a 6000 Nano LabChip of an Agilent Bioanalyzer 2100 (Agilent Technologies, Santa Clara,

USA), which defines RNA quality in term of RNA Integrity Number (RIN), computed by comparing the peak areas of 18S and 28S rRNA, the height of the 28S rRNA peak and the fast area ratio (Schroeder et al., 2006). RIN values >8 were considered suitable for NGS analysis (Pérez-Portela and Riesgo, 2013).

At least 2 µg of extracted RNA per sample (200 ng/µL) were delivered to Genomix4Life S.r.l. (Laboratory of Molecular Medicine and Genomics of the University of Salerno, Salerno, Italy) for library preparation, sequencing and *de novo* transcriptome assembly. Six cDNA libraries were prepared using TruSeq RNA Sample Prep Kit (Illumina) according to the manufacturer's recommendations and pooled such that each index-tagged sample was present in equimolar amounts. The pooled samples were subject to cluster generation and multiplexed sequencing using an Illumina HiSeq 2500 platform (Illumina, San Diego, USA) in a 2x100 paired-end format. Raw reads were cleaned, trimmed and clipped with BBDuk (https://jgi.doe.gov/data-and-tools/bbtools/) setting a minimum *phred score* (*Q*) of 20 (base call accuracy of 99%), and a minimum length of 35 nucleotides. The quality of the reads before and after trimming was checked with the software FASTQC (http://www.bioinformatics.babraham.ac.uk/projects/fastqc/). High quality paired-end reads from all samples were used as input for transcriptome assembly using Trinity (Grabherr et al., 2011) with the following options: --SS_lib_type RF--no_normalize_reads --min_kmer_cov 1 --KMER_SIZE 32, to generate the reference transcriptome of *T. stylifera*. A filter for contaminants was performed by BLASTing the transcripts against the NCBI nr database, discarding all the sequences having a significant hit (e-value ≤0.0001) against bacteria or vegetal cells.

3.2.3 Differential expression analysis and functional annotation of Temora stylifera *transcriptome*

Quantification of transcripts (isoforms) and unigene (the longest isoform of each gene cluster) abundance for each sample was assessed using RSEM software provided by

the Trinity package (Li and Dewey, 2011), after mapping back the reads on the assembled transcriptome using STARS (Dobin et al., 2012). Mean expression levels of isoforms' and unigenes' read counts, expressed as Counts Per Million (CPM), were used as input to perform differential expression analysis between samples collected on 23rd of May 2017 (experimental condition) with respect to samples collected on 30th of May 2017 (control condition), using the Trinity DeSeq2 package (Love et al., 2014). Significance values were obtained by performing a hypergeometric test and corrected p-value using the False Discovery Rate (FDR) method (Benjamini and Hochberg, 1995), and isoforms or genes having a FDR ≤0.05 were considered differentially expressed.

Functional annotation of *T. stylifera* transcriptome (whole set of transcript isoforms) was performed using the comprehensive bioinformatics tool Blast2Go (Conesa and Götz, 2008, Conesa et al., 2005). The software provides a user-friendly interface for Gene Ontology annotation and offers a wide array of graphical and analytical tools for data manipulation and mining. Blast2Go uses the Basic Local Alignment Search Tool (BLAST, https://blast.ncbi.nlm.nih.gov/Blast.cgi) to find sequences similar to the query set in FASTA format. The BLAST program used was BLASTx (E-value cut-off set to 1^{-3}) (Altschul et al., 1990), which compares a nucleotide query sequence translated in all reading frames against a non-redundant protein sequence database (nr) used to find potential translation products of an unknown nucleotide sequence. Default parameters were selected, with a number of HITs equal to 1. Different BLAST statistics charts can be generated for a global visualization of the results. Blast2Go extracts the GO terms associated to each of the obtained HITs and returns an evaluated GO annotation for the query sequence(s). GO annotation can be visualized reconstructing the structure of the Gene Ontology relationships, which assigns specific Biological Process (BP), Molecular Function (MF) and Cellular Component (CC) terms to each transcript. A typical basic use case of Blast2Go consists of different steps: BLAST (1), InterProScan Annotation (2), Gene Ontology Mapping (3), Gene Ontology Annotation (4).

3.2.4 Quantitative expression of selected genes of interest (GOIs) through RT-qPCR

RT-qPCR is a technique based on the general principle of the polymerase chain reaction (PCR) and is used to amplify and simultaneously quantify a targeted DNA sequence. It allows detecting variations of cDNA (complementary DNA segments synthesized from mRNAs) levels based on the measurement of a fluorescent signal produced during the PCR cycles. The most commonly used fluorescent detection dye is SYBR Green, a double-stranded DNA intercalating dye that fluoresces at 520 nm once bound to the DNA. The amount of dye incorporated and the fluorescence emitted during the last amplification step is proportional to the amount of target DNA generated (Arya et al., 2005). The more DNA present at the beginning, the fewer number of PCR cycles are required to reach a significant increase of fluorescence above a statistical background threshold. The threshold cycle (Ct) is therefore the number of amplification cycles needed to reach a specific threshold level of detection and is used to identify differences in transcript expression levels among different samples. Quantification of the expression levels of the selected gene of interest (GOI) is then normalized by the expression of one or more reference genes, i.e. transcripts codifying for stable genes, i.e. those genes whose expression does not significantly change across samples and treatments.

In order to validate Illumina sequencing and differential expression results, six reference genes (RGs) previously optimized in *Calanus helgolandicus* (Lauritano et al. 2011a), were tested in *T. stylifera* through RT-qPCR to identify the most stable genes in samples used for transcriptome assembly: *Actin* (*ACT*), *Histone 3* (*IST*), three ribosomal units (*18S* RNA, ribosomal protein *S7*, ribosomal protein *S20*) and *Ubiquitin* (*UBI*). First, primer specificity and amplification efficiency of the six reference genes were assessed. Complementary DNA (cDNA) needed as template for RT-qPCR analysis was retrotranscribed from 1 µg of *T. stylifera* total RNA in a final volume of 20 µL using iScriptTM cDNA Synthesis Kit (Bio-Rad, Hercules, USA) following the manufacturer's

instructions, using the GeneAmp PCR System 9700 (Applied Biosystems, Foster City, USA). Briefly, the reverse-transcription reaction was carried out with 4 µl 5X iScript reaction mix buffer, 1 µl iScript Reverse Transcriptase enzyme, 1 µg template RNA and H_2O provided by the manufacturer. The mix was first incubated 5 min at 25°C, followed by 20 min at 46°C and finally heated at 95°C for 1 min. RT-qPCR reactions were then performed in MicroAmp Optical 384-Well reaction plates (Applied Biosystem, Foster City, USA) with optical adhesive covers (Applied Biosystem, Foster City, USA), using a Viia7 Real Time PCR system (Applied Biosystem, Foster City, USA). The final PCR volume for each sample was 10 µl, with 5 µl of SensiFAST SYBR Green Master Mix (Meridian Inc., Cincinnati, USA), 1 µl of cDNA template and 4 µl (concentration of 0.7 pmol/µl) of each primer pair. All RT-qPCR reactions were carried out in triplicate to capture intra-assay variability. Three negative controls (consisting of 1 µl of water instead of the cDNA template) were considered for each primer pair. PCR conditions for all samples analysed were set as follows: 95 °C for 20 s, 40 cycles of 95 °C for 1 s, and 60 °C for 20 s. Dissociation protocol with a gradient (0.5 °C every 30 s) from 65 °C to 95 °C was also used to investigate the specificity of the primers and presence of primer dimers. Gene-specific amplification was confirmed by a single peak in the melting curve analysis. To quantify gene expression, primer amplification efficiencies were calculated through six serial dilutions of cDNA (1, 1:5, 1:10, 1:50, 1:100 and 1:500) for all primer pairs. The reference equation for efficiency calculation is $E = 10^{-1/slope}$, where the slope is obtained from a standard curve between Ct values and the log10 of each dilution factor.

Stability of the six reference genes in *T. stylifera* samples used for transcriptome analysis was finally identified through RT-qPCR analyses as described above, using 1 µl of cDNA template (dilution 1:5) obtained by retro-transcription of the same total RNA employed for the Illumina sequencing. The most stable reference genes were then evaluated using RefFinder (http://leonxie.esy.es/RefFinder/), a user-friendly web-based tool for evaluating and screening reference genes from extensive experimental datasets. It

integrates three different computational programs: geNorm (Vandesompele et al., 2002), Normfinder (Andersen et al., 2004), BestKeeper (Pfaffl et al., 2004), and the comparative ΔCt method (Silver et al., 2006), and it allows comparing and ranking the tested candidate reference genes using Ct values as direct input. Based on the rankings from each program, RefFinder assigns an appropriate weight to an individual gene and calculates the geometric mean of their weights for the overall final ranking.

Once the most stable reference genes were identified, 9 unigenes and 3 isoforms were selected from the list of DEGs generated by Illumina sequencing and subsequent differential expression analysis and these sequences were used as genes of interest (GOIs) to: i) validate differential expression analysis and ii) analyse quantitative gene expression changes in *T. stylifera* samples collected along 2017, through RT-qPCR. In particular, the sequences selected were: the *Putative Odorant Binding Protein A5* (*A5*), the *cAMP-Responsive Element-Binding Protein-Like2* (*CREBL*), the *putative ATP-Dependent RNA Helicase* (*me31b*), the *Serine/Threonine Protein Phosphatase* (*Ppa2*), the *Protein Obstructor E-Like* (*Obst-E*), the *E3 Ubiquitin-Protein Ligase Arih1-Like* (*ARIH1*), the *Arylsulfatase B-Like* (*ARSB*), the *Heat-Shock Protein 70* (*HSP70*), the *Very Low-Density Lipoprotein Receptor-Like* (*VLDLR*), the *MOB Kinase Activator 1B* (*MOB1B*), the *ATP-Dependent RNA Helicase Vasa-Like* (*Vasa*) and the *Platelet-Activating Factor Homolog 2* (*PAFAH*). The sequences of these genes and isoforms were selected on the basis of fold-change between samples collected on 23rd of May 2017 (experimental condition) with respect to samples collected on 30th of May 2017 (control condition), sequence length, E-value (indicating the correspondence probability of a sequence with its annotation) and similarity percentage (indicating how much of the query sequence corresponds to the reference one in public databases) reported after DE analysis and functional annotation of the transcriptome. These selected sequences were then used to design specific forward and reverse primers through the online available platform Primer3web 4.1.0 (http://bioinfo.ut.ee/primer3/) and synthesized by Sigma-Aldrich (Merk, Germany).

Desired primer size was set in the range of 18-24 bp (optimum 20) and melting temperature (Tm) between 59-61 °C (optimum 60 °C). Amplification products ranged between 110-240 bp. To verify primer specificity, PCRs were performed on GeneAmp PCR System 9700, with 2 µl 10× PCR reaction buffer (Roche), 2 µl 10×2 mM dNTPs (Roche), 0.8 µl 5U/µl Taq polymerase (Roche), 1 µl 20 pmol/µl of each primer (forward and reverse), 1 µl of *T. stylifera* template cDNA and nuclease-free water to 20 µl final volume. The PCR program consisted of a denaturation step at 95 °C for 3 min, 40 cycles at 95 °C for 30 s, 60 °C for 1 min and 72 °C for 30 s, and a final extension step at 72 °C for 7 min (Lauritano et al., 2011a). Amplified PCR products were analysed by electrophoresis on 1.5% agarose gel in 0.5x TBE buffer to check proper length specificity of the products. Each corresponding band on the agarose gel was excised and extracted according to the GenEluteTM Gel extraction Kit protocol (Sigma-Aldrich, Merk, Germany) for sequencing, in order to verify the correct identity. Sequencing reactions were performed at the Molecular Biology & Bioinformatics Service of SZN, following Big Dye Terminator Cycle Sequencing Technology (Applied Biosystems) instructions, on the Automated Capillary Electrophoresis Sequencer 3730 DNA Analyzer (Applied Biosystems). BLASTx homology search was then used to confirm the identity of each sequence. Subsequently, specificity and amplification efficiencies of the primers were further tested in RT-qPCR, using serial dilutions (1, 1:5, 1:10, 1:50, 1:100) of *T. stylifera* cDNA template. Settings of qPCR reactions were the same as described before. As for RGs, gene-specific amplification was confirmed by a single peak in the melting curve analysis.

To validate differential expression analysis results, cDNA obtained from *T. stylifera* samples used for transcriptome analysis was used as template (1:10 dilution) for RT-qPCR reactions. RNA 18S and UBI were used as reference genes for the analyses, because they were indicated as the most stable ones (see Results section). Relative expression levels of each target gene in the treated samples (i.e. those collected on 23rd of May) was compared to control samples (i.e. those collected on 30th of May) through the Pfaffl equation (

et al., 2002), using the tool REST (Relative Expression Software Tool) (Pfaffl 2009; Pfaffl et al. 2002). This tool uses a mathematical model based on the PCR efficiencies and the Ct deviation between the sample and the control group. Results were analysed based on the following equation, where the relative expression of a target gene is compared in a sample (copepod collected on 23rd of May) versus a control (copepod collected on 30th of May), normalized to a reference gene (Pfaffl 2002):

$$Ratio = \frac{E(Target)^{\Delta Ct\ target(Control-Sample)}}{E(Reference)^{\Delta Ct\ reference(Control-Sample)}}$$

The E(target) is the RT-qPCR efficiency of target gene primers; E(ref) is the RT-qPCR efficiency of the reference gene primers; $\Delta Ct_{(target)}$ is the Ct deviation of control-sample of the target gene transcript; $\Delta Ct_{(reference)}$ is the Ct deviation of control-sample of reference gene transcript.

Temporal variations in the expression levels of these 12 target genes were also analysed through RT-qPCR in *T. stylifera* females collected at LTER-MC along 2017. In addition to these genes we also included the sequence annotated as *Methylene-tetrahydrofolate-dehydrogenase* (*MTHFD*), which was present in the whole transcriptome but not in the DEGs dataset. However, this gene was selected for its putative involvement in the deleterious effect of oxylipins on copepod fitness (Y. Carotenuto, pers. com.). Primer specificity and amplification efficiency was also evaluated for this new sequence. RT-qPCR reactions for all 13 GOIs were performed as described before, using as template the cDNA (1:5 dilution) obtained from wild *T. stylifera* females collected along the sampling period. For these samples, the Mean Normalized Expression (MNE) of each target gene was calculated using the tool QGene software (Simon, 2003) according to formula (2).

$$Ratio = \frac{(E\ reference)^{CT\ reference,mean}}{(E\ target)^{CT\ target,mean}}$$

QGene is an excel based software which calculates means and standard errors for the reference as well as for the target genes and determines a MNE using efficiencies of PCR amplification for the target and the reference genes and converts the logarithmic scaled Cycle Threshold (Ct) values to linear normalized expressions. Where E(reference) and E(target) are the efficiencies of PCR amplification of reference and target genes and CT(reference, mean) and CT(target, mean) are the corresponding Ct mean values of reference and target genes, respectively. This calculation was chosen because the purpose of the analysis was the assessment of normalized gene expression variability along time without having a control condition.

3.2.5 Data analysis

Co-variations of the four physiological variables (faecal pellet production, egg production, hatching success and naupliar survival) measured for *T. stylifera* were inspected through non-parametric correlation tests (permutation N=9999). Monthly variations in *T. stylifera* physiological responses were analysed through ANOSIM test (N=9999, Euclidean distance) performed on standardized values balanced in replicate number by group mean substitutions (Anderson and Walsh, 2013). Wilcoxon's t-tests were applied to inspect significant differences in the four physiological variables across the four seasons. Gene expression variations were investigated on a seasonal basis (winter, spring, summer and autumn). This clustering was performed because of the scattered occurrence of samples for RT-qPCR analyses. A PCA was performed to analyse multivariate variation in gene expression in the four seasons. For PCA analysis MNE values were multiplied by a factor 10^6 to obtain integers and subsequently log-transformed. In addition, Wilcoxon's t-tests were applied to inspect significant differences in the MNE of each target gene across the four seasons.

Single Generalized Additive Models (GAM) were applied to test if the physiological responses of *T. stylifera* were explained by each environmental variable (i.e.

temperature, density, salinity, transmittance, pH, oxygen saturation, oxygen concentration, fluorescence, chl-a and phaeo-a), each major phytoplankton group (i.e. diatoms, dinoflagellates, coccolithophores, phytoflagellates), FAs and oxylipin concentrations (expressed as ng/L and fg/diatom-cell). Oxylipins were considered as the total of the six chemical species identified and the concentration of each chemical species so as to investigate whether different oxylipin species could have driven different responses in the adult copepod females. A simple linear regression analysis was performed considering abundance of the five most abundant diatom genera (i.e. *Chaetoceros*, *Leptocylindrus*, *Thalassiosira*, *Pseudo-nitzschia*, *Skeletonema*) and a sixth multi-specific diatom group as the predicting variables for naupliar survival rates observed at t+1 (the subsequent week in respect to the diatom abundance). Data were manipulated in this way to inspect a delayed effect of diatoms on the survival rates of *T. stylifera* larval stages. *Temora stylifera* physiological responses were then analysed in relation to gene expression variations through single GAM analyses. For subsequent analyses investigating variations of gene expression in relation to biotic and abiotic factors, only those genes which significantly related to the physiological responses of copepods were considered. In fact, it was assumed that physiological responses of *T. stylifera* depended on gene expression, whose variations were driven by biotic and abiotic factors. Five genes significantly relating to *T. stylifera* physiological responses were taken into account for further GAM analyses considering environmental variables, phytoplankton abundance, FAs and oxylipin/cell concentrations as independent variables. Data of pellets and eggs have been log-transformed before the analyses. While analysing gene expression data, observations available for the genes *A5* (*Odorant Binding Protein*) and *Pafah* (*Platelet-Activating Factor Homolog2*) on 20th of February were not included in the analysis, because this observation was considered an outlier in the data series.

3.3 Results

3.3.1 Physiological responses and population dynamics of Temora stylifera *at LTER-MC*

Faecal pellet and egg production were the only physiological variables significantly correlated with each other ($r=0.6$, $t=44.7$, $p<0.001$). Maximal peaks of these two variables were observed from April to the end of May, while lower production was detected in the rest of the year (Figure 3.1). On average, 44.17 ±25.64 faecal pellets were produced by each copepod female in a day, with a maximum of 102.4 (in May) and a minimum of 10.1 (in January) pellets/female-day. The total number of laid eggs was similar to the number of faecal pellets (average of 47.29 ±25.07, max. 111 and min. 10.6 eggs/female-day). Egg hatching was high along the year, because on average 88.45% ±8.8 of eggs successfully hatched (max. 98.5% in March, min. 63.4% in May). Hatching success oscillations were mainly observed in spring and summer months. By contrast, high differences in the naupliar survival rates (average 77% ±30.16, max. 100% and min. 9.93%) were observed. After a progressive decrease, the first dip in naupliar survival was detected in winter (January 17th).

This minimum was followed by a progressive increase in the subsequent three weeks. Additional negative peaks were observed in spring (April 11th, May 2nd, May 16th and May 23rd), while high naupliar survival rates were measured in the rest of the year. Interestingly, naupliar survival oscillations observed in spring differed from the pattern observed in winter, because sudden negative and positive peaks alternated along the sampling weeks.

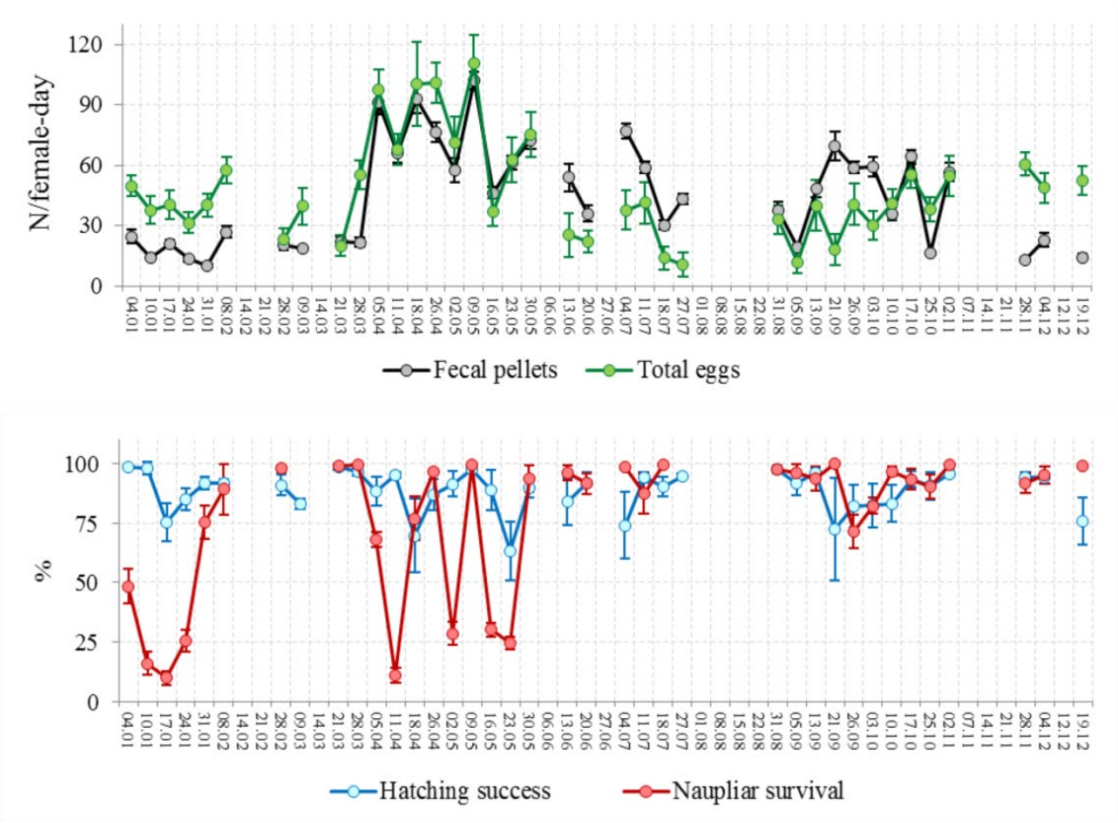

Figure 3. 1. Weekly fluctuations of *Temora stylifera* physiological responses (faecal pellet and egg production is indicated in the top panel; hatching success and naupliar survival rates are indicated in the bottom panel) at LTER-MC. Average (±SE) values are reported.

To better quantify seasonal differences in faecal pellet production, egg production, hatching success and naupliar survival rates, Wilcoxon's t-test were performed. For these analyses, differences in the physiological response variables of *T. stylifera* were tested across seasons, which were defined temporally (winter: January-March; spring: April-June; summer: July-September; autumn: October-December; Figure 3.2).

Results indicated that the number of faecal pellets produced in winter significantly differed from spring and summer and that faecal pellets observed in spring were significantly higher than the number observed in autumn. Egg production in spring was significantly higher than winter and summer. Subsequently, egg production rates in autumn significantly increased from summer values. No seasonal differences were observed in hatching success and naupliar survival rates, even though wide variations were evident. For

example, oscillations in hatching success occurred in summer and autumn, while marked variations in naupliar survival rates occurred in winter and spring.

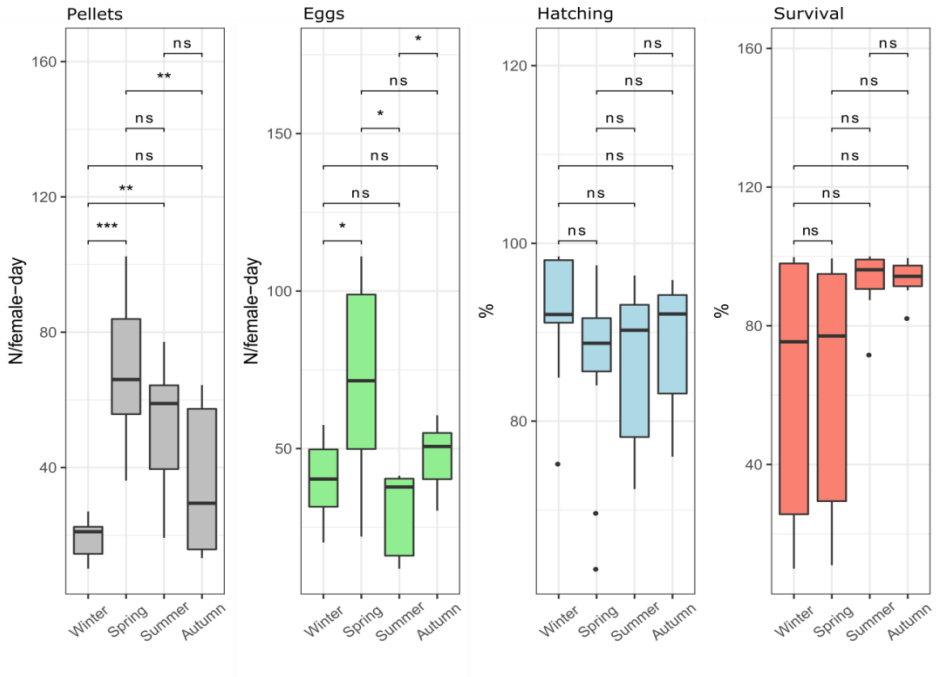

Figure 3. 2. Boxplot representing seasonal production of faecal pellets and eggs as well as of hatching success and naupliar survival of *Temora stylifera*. Asterisks indicate significant differences of monthly averages from a reference value.

The ANOSIM test suggested low monthly differences in the physiological responses of *T. stylifera* (Global R=0.39, p<0.001; Table 3.1). Copepod physiology characterized in January significantly differed from all the other months. February and March were not significantly different from each other and the responses observed in November-December. Similarly, April and May were significantly dissimilar from the other months, but not with each other. June, July, September and October showed low distances among them.

Table 3. 1. ANOSIM results (permutation N=9999, Euclidean distance) showing monthly differences in *Temora stylifera* physiological responses. Abbreviations: Jan=January, Feb=February, Mar=March, Apr=April, Jun=June, Jul=July, Sep=September, Oct=October, Nov-Dec=November-December. Asterisks indicate significance levels: *=p<0.05, **=p<0.01, ns=not significant. Standardized values are considered.

R=0.39 p<0.001	Feb	Mar	Apr	May	Jun	Jul	Sep	Oct	Nov-Dec
Jan	**	**	**	*	**	**	**	**	**
Feb		ns	**	**	**	**	*	*	ns
Mar			**	**	**	**	*	*	ns
Apr				ns	**	*	**	**	**
May					**	**	**	**	**
Jun						ns	ns	**	**
Jul							ns	ns	**
Sep								ns	*
Oct									ns

The total abundance of *T. stylifera* at LTER-MC was low (max. 46.51 ind./m^3) until the end of August 2017. In autumn, the population progressively increased to 262.34 ind./m^3 on 10th of October and subsequently to the maximum of 297.1 ind./m^3 on 2nd of November. Concentrations were low in November and December, although data for most of November weeks are not available due to bad weather conditions. In general, adult stages (both females and males) were present in lower abundances than juveniles (copepodids), which often constituted the largest fraction of *T. stylifera* population (Figure 3.3).

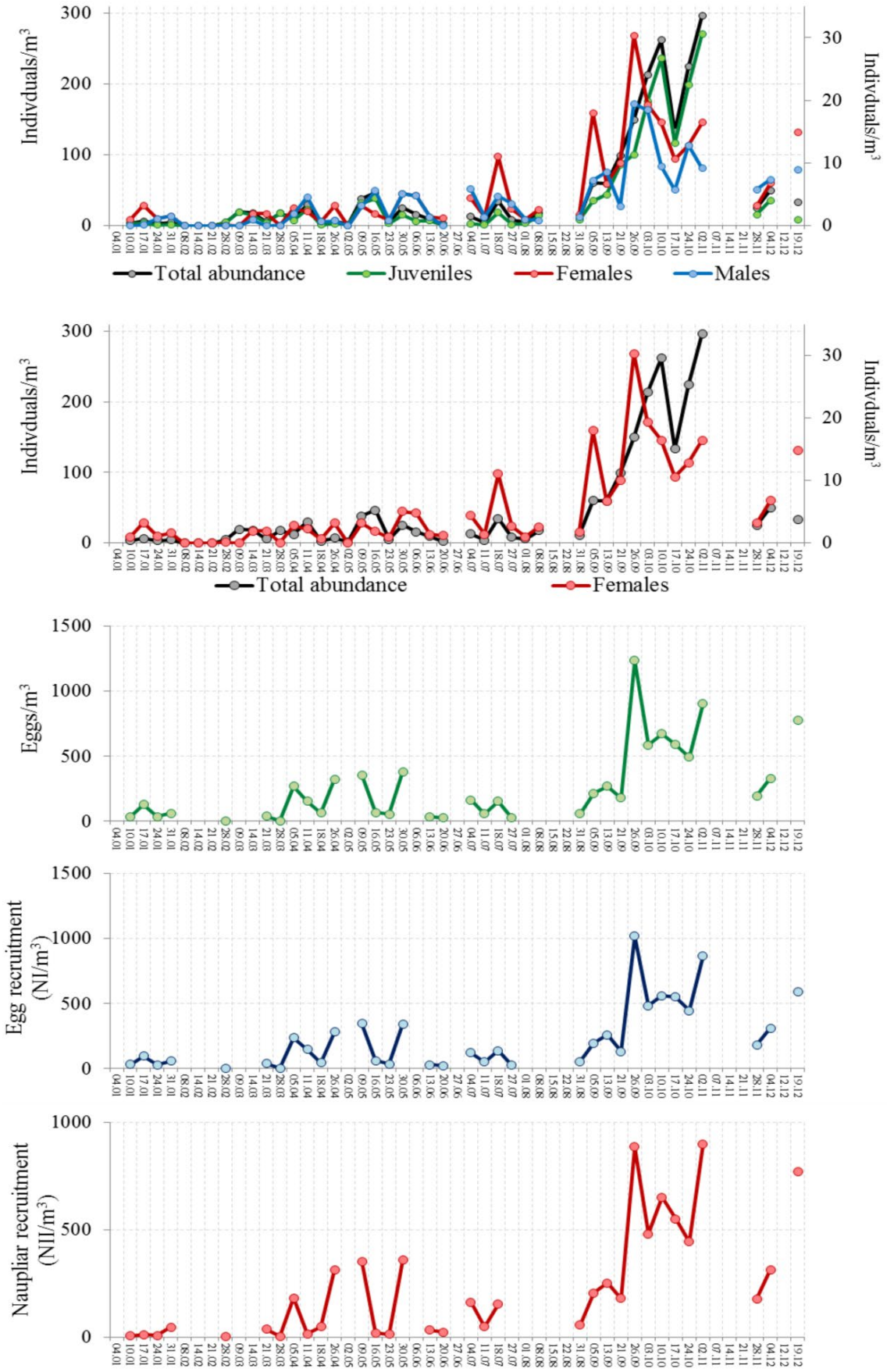

Figure 3. 3. Estimates of *Temora stylifera* population density, egg abundance (green dots), hatching success (blue dots) and naupliar survival rates (red dots) at LTER-MC along 2017 as function of adult female abundance in the natural population. NI and NII indicate naupliar stage.

Calculations estimating *in situ* egg abundance (eggs/m^3), egg recruitment (NI nauplii/m^3) and early-nauplii recruitment (NII nauplii/m^3) at sea partially mirrored female concentrations, confirming low abundances in winter, spring and summer, in contrast to the higher values observed in autumn (Figure 3.3). Due to little variations in hatching success along the year, egg recruitment at sea (average 229.69 ±252.43 NI/m^3, max. 1016.27 NI/m^3, min. 1.92 NI/m^3) well reflected the calculated number of eggs produced (average 263.22 ±293.54 eggs/m^3, max. 1235.3 eggs/m^3, min. 2.11 eggs/m^3). The pattern was rather conserved also in early-nauplii recruitment (average 234 ±265.33 NII/m^3, max. 897.46 NII/m^3, min. 2.07 NII/m^3), which peaked on 26th of September and 2nd of November. Interestingly, the peak on September 26th just preceded the peak in juvenile abundance on 10th of October (two-weeks delay), which was possibly related to development time from NI to copepodites. Unfortunately, due to bad weather conditions copepod abundance data are lacking till the end of November, thus it is not possible to establish whether the high NI recruitment on 2nd of November was followed by further increase in juvenile abundance.

3.3.2 De novo *assembly and functional annotation of* Temora stylifera *transcriptome*

As demonstrated by t-test results, the reproductive potential of *T. stylifera* females collected on 23rd and 30th of May significantly differed only for the survival rates of NI nauplii (Figure 3.4).

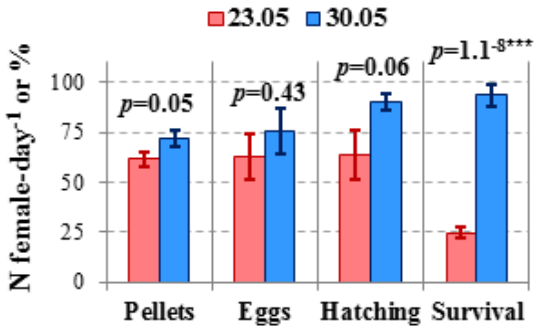

Figure 3. 4. Reproductive potential of *Temora stylifera* females collected on 23rd May (treated samples) and 30th May (control samples). Abscissa shows values of N/female-day (referred to faecal pellets and eggs) and % (referred to hatching success and naupliar survival). The p-value shows significance of the t-tests for each variable (α=0.05). Values are means (±SE).

Therefore, differential expression of genes as highlighted by the transcriptomic analysis can help reveal molecular mechanisms activated by adult copepod females to maximize naupliar survival, because the NI nauplii of *T. stylifera* are non-feeding stages that rely on maternal energy reserves until moulting to the subsequent feeding larval stage (NII).

Table 3. 2. RNA quantity (ng/µl) and quality assessed by Nanodrop measurement (260/280 and 260/230 ratio) and by Bioanalyzer (RIN) for samples of *Temora stylifera* collected at LTER-MC on 23rd and 30th of May 2017.

Samples	*Nr.*	*ng/µl*	*260/280*	*260/230*	*RIN*
Test_1	1	236.0	2.01	2.63	10
Test_2	2	244.6	2	2.64	N/A
Test_3	3	214.2	2.07	1.25	10
Control_1	4	229.2	2.03	1.97	10
Control_2	5	237.8	1.97	2.33	N/A
Control_3	6	234.3	2.02	1.63	10
MEAN		***232.7***	***2.02***	***2.1***	

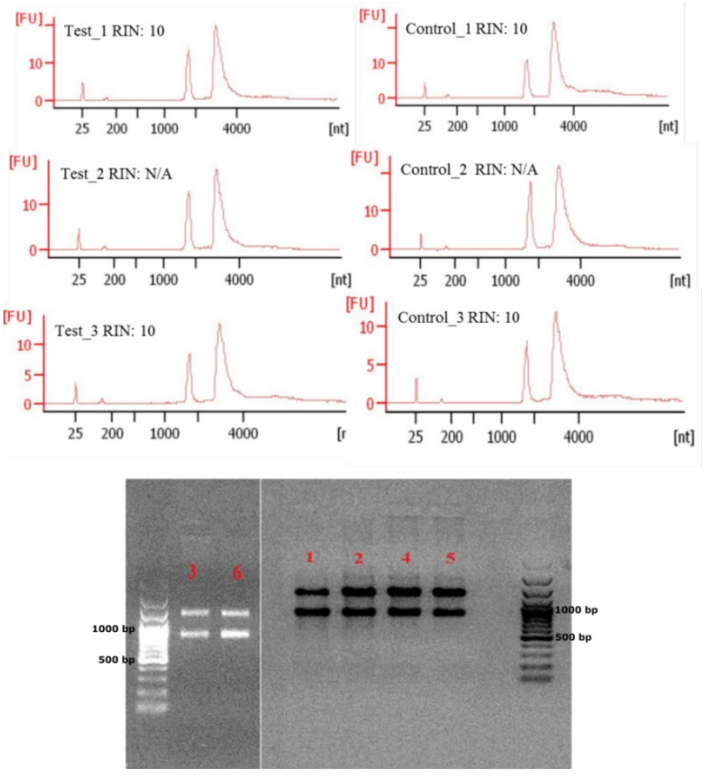

Figure 3. 5. Bioanalyzer results (RIN is indicated) are reported in the six spectra at the top. Gel electrophoresis of *Temora stylifera* RNA samples for specimens collected on 23rd (1, 2, 3) and 30th (4, 5, 6) of May are reported in the bottom picture. Left bands are the ladder-100 and the reference number of 500 and 1000 base pairs (bp) is reported.

RNA extracted from *T. stylifera* females collected on 23rd and 30th of May was in an average concentration of 232.7 ng/µl, with RIN = 10 (when detected) and 260/280 as well as 260/230 ratios ~2. The third replicates of treated and control samples, however, showed a lower 260/230 ratio (Table 3.2). As demonstrated also by gel electrophoresis, RNA extraction procedure did not alter RNA integrity (Figure 3.5). Therefore RNA samples were used for cDNA library construction and Illumina sequencing.

Illumina-based RNA-Seq generated a total of ~132 million reads, after quality cleaning. The same number of reads was achieved for both the forward and the reverse cDNA filaments, supporting consistency in the sequencing output. The *de novo* assembly made with Trinity on high quality reads generated 268,665 transcript (average length of 517.6 bp, N_{50}=665), which were further clustered into 120,749 unigenes to reduce redundancy due to multiple transcript isoforms (Table 3.3). This list of unigenes, that represented the longest isoform of each gene cluster, was considered our *T. stylifera* reference transcriptome and was processed for further functional annotation.

Table 3. 3. Summary statistics of *Temora stylifera* RNA-Seq analysis.

Category	Number/Length
Number of Reads R1	131,993,195
Number of Reads R2	131,993,195
Number of Transcripts	268,665
Average Transcripts Length	517.6 bp
Median Transcripts Length	310 bp
N_{50}	655 bp
Number of Genes	120,749

Functional annotation of *T. stylifera* transcriptome performed by BLASTx resulted in 62,648 matching sequences in the non-redundant protein database out of 120,749 unigenes (51.88%; Figure 3.6).

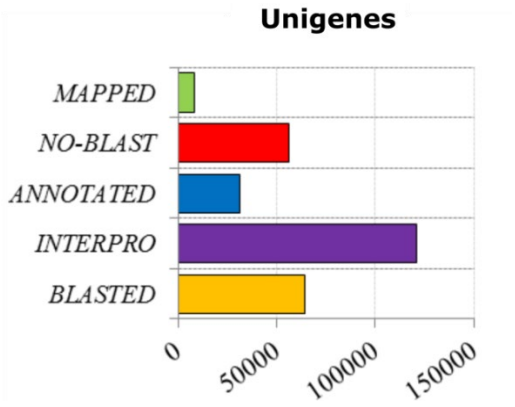

Figure 3. 6. Blast2Go statistics output for functional annotation of *Temora stylifera* transcriptome (unigenes). The number of sequences which found matching by BLASTx is indicated as blasted (in yellow), in contrast to the sequences that did not find positive matching (i.e. no-blast in red). Violet bars indicate Inter Pro Scan annotated sequences. The number of mapped and annotated sequences is indicated in green and blue, respectively.

E-values (which measure probability of protein identity), indicated that almost 10% of the matching unigenes showed very high homology ($0<\text{E-value}<10^{-100}$) to similar sequences in the non-redundant protein database. Overall, more than 42% of the sequences showed high probability of homology ($0<\text{E-value}<10^{-30}$). Similarity values express the similarity percentage between the *de novo* assembled sequence and proteins in the non-redundant database. A low fraction (1.7%) of the total unigenes were almost identical (similarity between 95-100%), while 76.1% of the sequences had a similarity ranging from 100% to 60% (Figure 3.7).

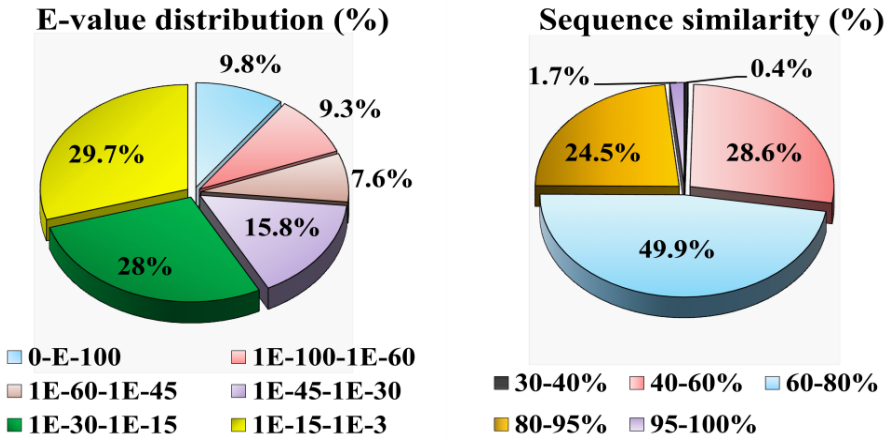

Figure 3. 7. Statistics of homology BLASTx search of *Temora stylifera* unigenes against the non-redundant protein database. E-value distributions with cut-off at 10-3 (left panel) and similarity distribution of the top BLAST hits for each unigene (right panel) are shown.

The species distribution of the best matches (top-hit) against the non-redundant protein database indicated that the largest fraction of matching unigenes showed similarities with sequences of the copepod *Eurytemora affinis*, followed by the copepod *Acartia pacifica*, the cladocerans *Daphnia pulex* and *D. magna* and the copepod *Pseudodiaptomus poplesia*. The other top-hit species were mainly crustaceans or Arthropoda, while three molluscs and one brachiopod were among the other first 20 top-hit species (Figure 3.8).

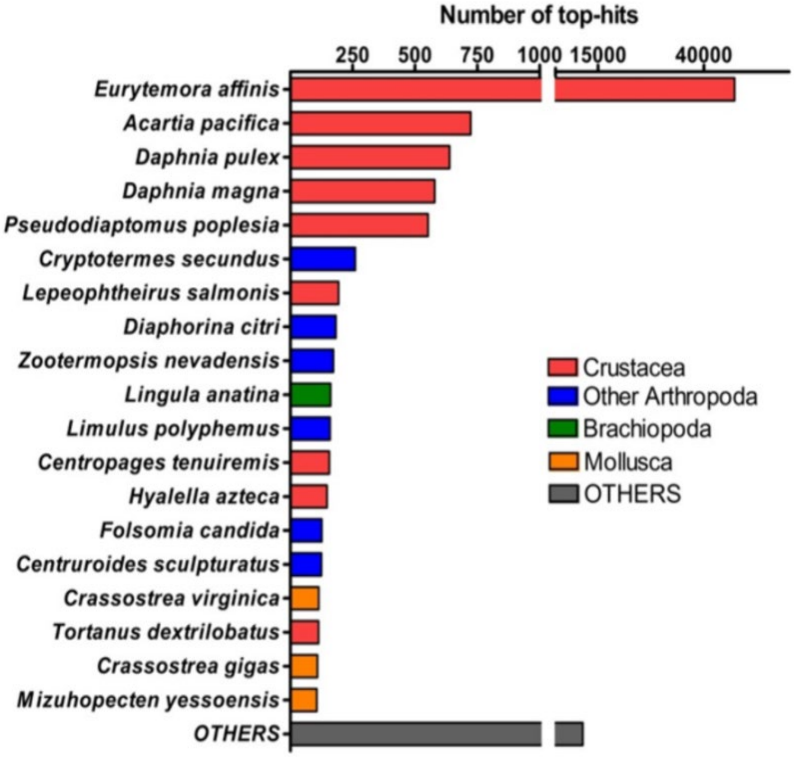

Figure 3. 8. Top-hit species distribution of BLASTx similarity search for *Temora stylifera* transcriptome. Taxonomic groups are defined by colours: Crustacea (red), Arthropoda (blue), Brachipoda (green), Mollusca (orange).

Blast2Go outputs showed that 31,346 unigenes, out of 62,648 that received significant matching in BLASTx, were functionally annotated. In total, 126,358 GO annotation terms were assigned and distributed among Biological Process (BP, 36.77%), Molecular Function (MF, 35.57%) and Cellular Component (CC, 27.66%) GO categories

(Figure 3.9). The majority of annotated unigenes were assigned to metabolic and cellular processes (10.7%), binding (13.7%) and cell part (7.17%).

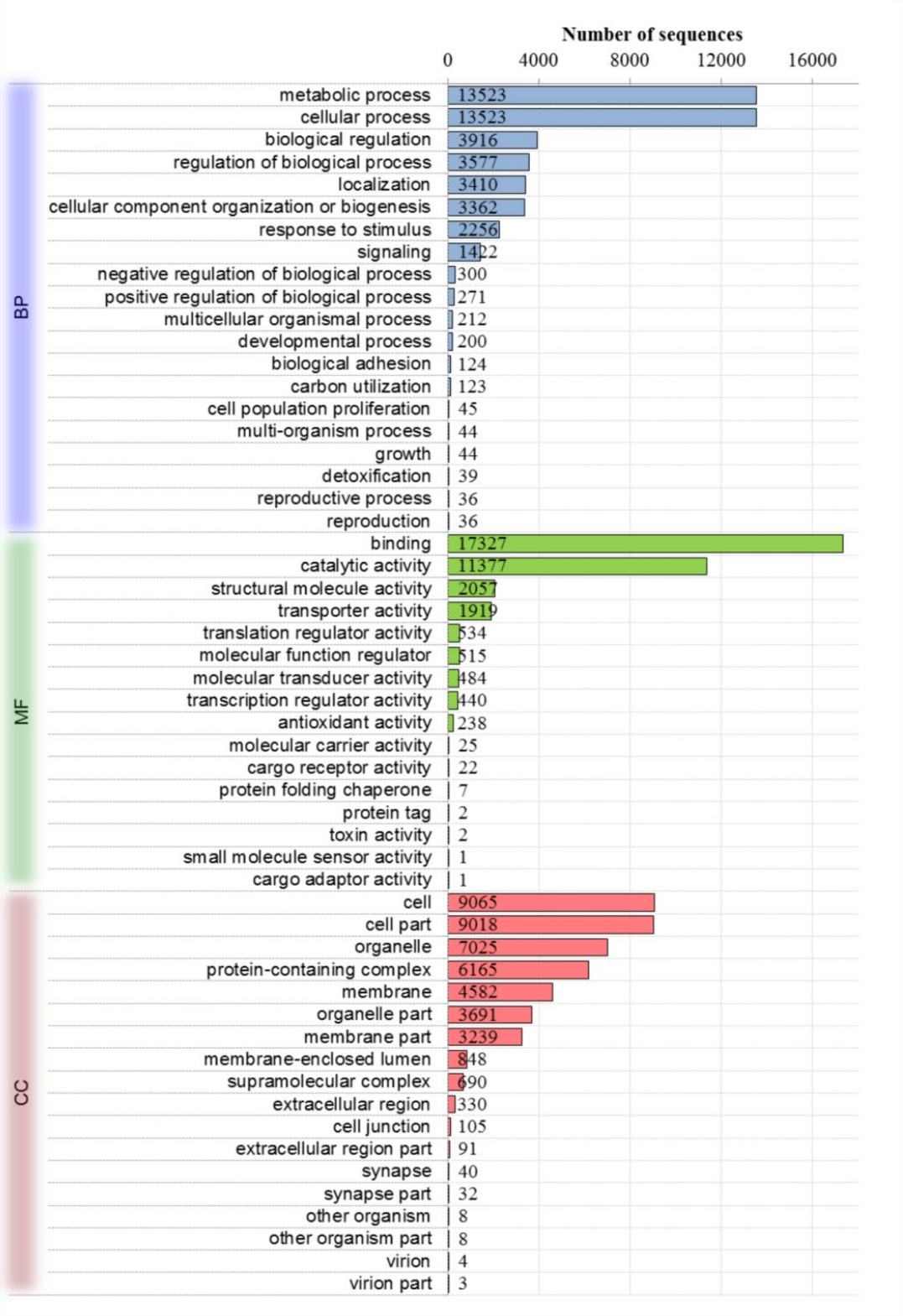

Figure 3. 9. Gene Ontology (GO) categories of annotated unigenes of *Temora stylifera* transcriptome. GO terms are distributed among three main categories: Biological Process (BP), Molecular Function (MF) and Cellular Component (CC).

3.3.3 Differential expression analysis and transcriptome validation

Analysis of expression levels of *T. stylifera* unigenes between samples collected on 23rd of May (treated) and 30th of May (control) showed that a total of 144 unigenes were differentially expressed (FDR $p<0.05$). In particular, 108 genes were down-regulated, while 36 genes were up-regulated, in treated with respect to control samples. Of the total 144 differentially expressed sequences, only 33 received GO assignment and functional annotation. When transcript isoforms were also analysed, 331 sequences were differentially expressed (FDR $p<0.05$), 199 were down-regulated and 132 were up-regulated. Among these sequences, 106 received GO assignment and were functionally annotated.

Most of the significantly down-regulated unigenes were described as *putative Odorant Binding Proteins*. Other down-regulated unigenes were annotated as sequences related to developmental metabolic processes (involving chitin and collagen), protein ubiquitination, response to stress (mainly *Heat Shock Protein 70*), oxidation-reduction reactions and hydrolase activities. The significantly up-regulated unigenes, instead, were mainly involved in reproduction as well as cell development and proliferation (e.g. *Vitellogenin-like* unigenes, *RNA Helicase* and *Lipoprotein Receptor* unigenes). Moreover, sequences involved in transmembrane transport and reception activity were also included. The distribution of statistically significant differentially expressed unigenes among the three main GO categories BP, MF and CC is reported in Figure 3.10, whereas the differentially expressed unigenes annotated for the BP category are listed in Table 3.4. The full list of DE unigenes with the corresponding statistics is available in Appendix II (Table AII.1).

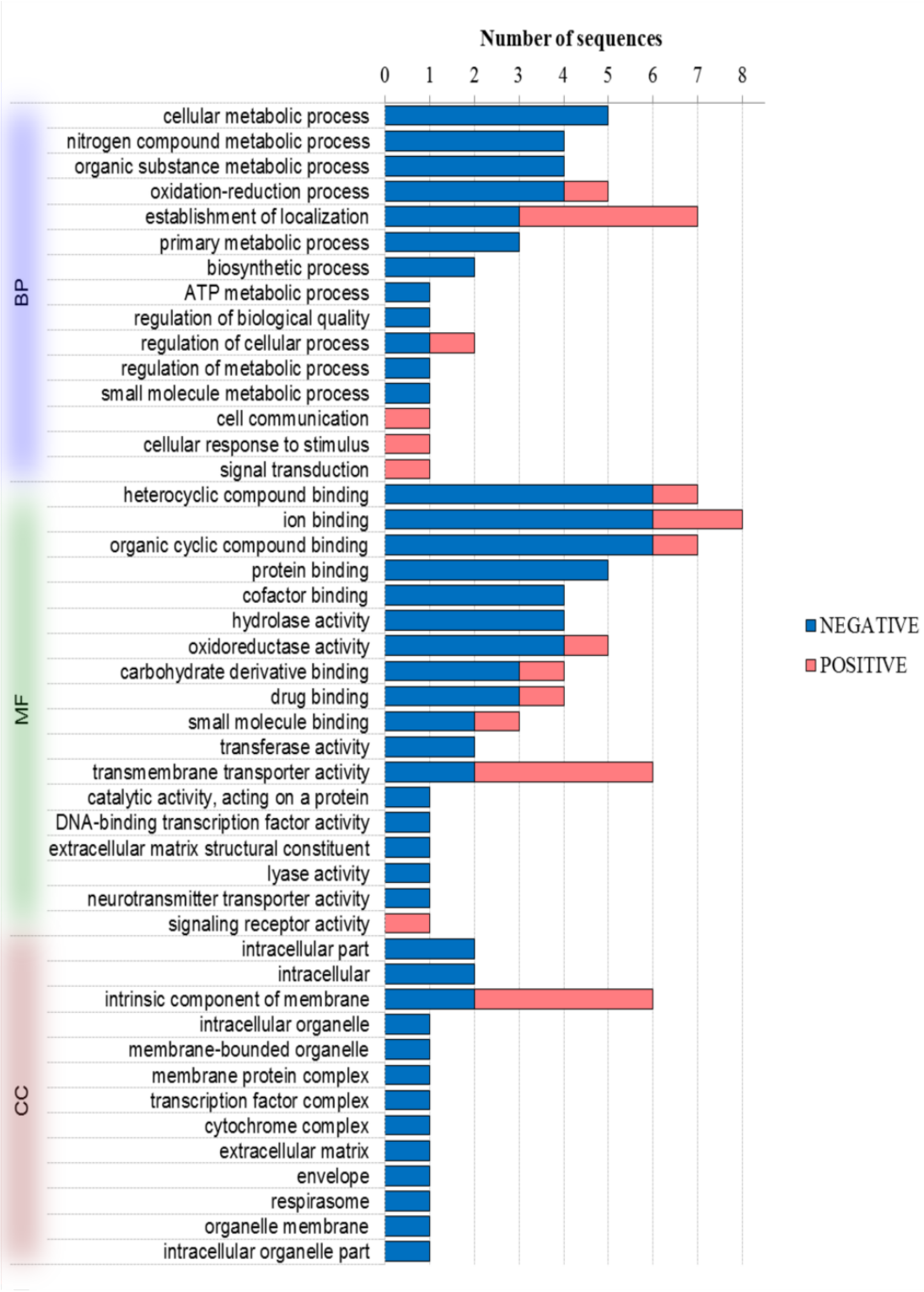

Figure 3. 10. Gene Ontology (GO) classification of the differentially up-regulated and the down-regulated unigenes in *Temora stylifera* females (FDR≤0.05). Red bars indicate up-regulated sequences; blue bars indicate down-regulated sequences. Colour shadings differ depending on GO categories (CC, MF or BP).

Table 3. 4. List of differentially expressed unigenes in *Temora stylifera*, annotated in the Biological Process (BP) GO category. BP sub-categories are reported. The name of each annotated sequence along with log_2-fold change (log_2-FC), adjusted-p-value (adj.-p), e-value, similarity (Sim.) and length (in bp, L) is indicated. Down-regulated sequences are indicated by green text; up-regulated sequences are indicate by red text.

Biological Process	Sequence name	Description	log_2-FC	adj.-p	L
Mitochondrial electron transport, cytochrome c to oxygen	TRINITY_DN44278_c0_g1	*Cytochrome c Oxidase Subunit I*	**-2.31**	0.033	204
Oxidation-reduction process	TRINITY_DN48367_c6_g8	*Malate Dehydrogenase*	**-1.87**	0.043	224
	TRINITY_DN50562_c0_g1	*Cytochrome P450 2C9*	**-1.87**	0.002	930
	TRINITY_DN50562_c0_g2	*Cytochrome P450 CYP3034A1*	**-1.74**	0.002	866
Cation transport	TRINITY_DN55897_c0_g1	*Sodium-Dependent Nutrient Amino Acid Transporter*	**-1.38**	0.007	2619
Chitin metabolic process	TRINITY_DN46142_c0_g1	*Peritrophins 3-A1 Precursor*	**-1.62**	9.03^{-05}	228
Phospholipid biosynthetic process	TRINITY_DN50806_c1_g2	*Phosphatidylserine Decarboxylase Proenzyme*	**-1.27**	0.028	2085
Metabolic process	TRINITY_DN37862_c0_g1	*Arylsulfatase B*	**-1.45**	0.047	292
	TRINITY_DN61324_c6_g3	*Arylsulfatase B*	**-1.29**	0.002	552
	TRINITY_DN61324_c6_g1	*Arylsulfatase B*	**-1.29**	0.004	1130
	TRINITY_DN56814_c0_g1	*Arylsulfatase B*	**-1.13**	0.005	876
Protein ubiquitination	TRINITY_DN60002_c1_g1	*Ariadne*	**-1.76**	0.002	2425
Regulation of transcription, DNA-templated	TRINITY_DN46002_c0_g1	*cAMP-Responsive Element-Binding*	**-2.03**	0.002	370
Signal transduction	TRINITY_DN44116_c1_g1	*Neuronal Acetylcholine Receptor*	**3.76**	0.0003	1536
Transmembrane transport	TRINITY_DN59770_c0_g1	*Solute Carrier Organic Anion Transporter*	**-0.96**	0.02	2702
	TRINITY_DN58926_c0_g1	*Organic Cation Transporter*	**1.12**	0.005	2210
	TRINITY_DN56235_c0_g1	*Facilitated Trehalose Transporter*	**1.5**	0.002	867
	TRINITY_DN53823_c0_g4	*Facilitated Trehalose Transporter*	**1.58**	0.02	1704

In order to have a wider spectrum of gene functions and to allow a more detailed description of the molecular responses of *T. stylifera* females in the two sampling dates, we also performed differential expression analysis of transcript isoforms. In total, 588 GO terms were associated to the differentially expressed isoforms and were assigned to the three main GO categories, which were almost equally divided among BP (37.18%) and MF (34.66%), while a smaller fraction described the CC category (28.16%). Analysis of GO distribution among the three main categories was also repeated dividing up- and down-regulated isoforms (Figure 3.11).

Interestingly, few transcripts associated to different GO terms were exclusively up- or down-regulated in comparison to the control samples. Among BP sub-categories, sequences involved in ATP metabolism, cellular localization, organism interaction and signal transduction were specifically down-regulated (Table 3.5). In contrast, sequences involved in catabolic processes, cellular organization, reproduction and microtubule processes were exclusively up-regulated (Table 3.5). The full list of DE transcript isoforms with the corresponding statistic is listed in Appendix II (Table AII.2).

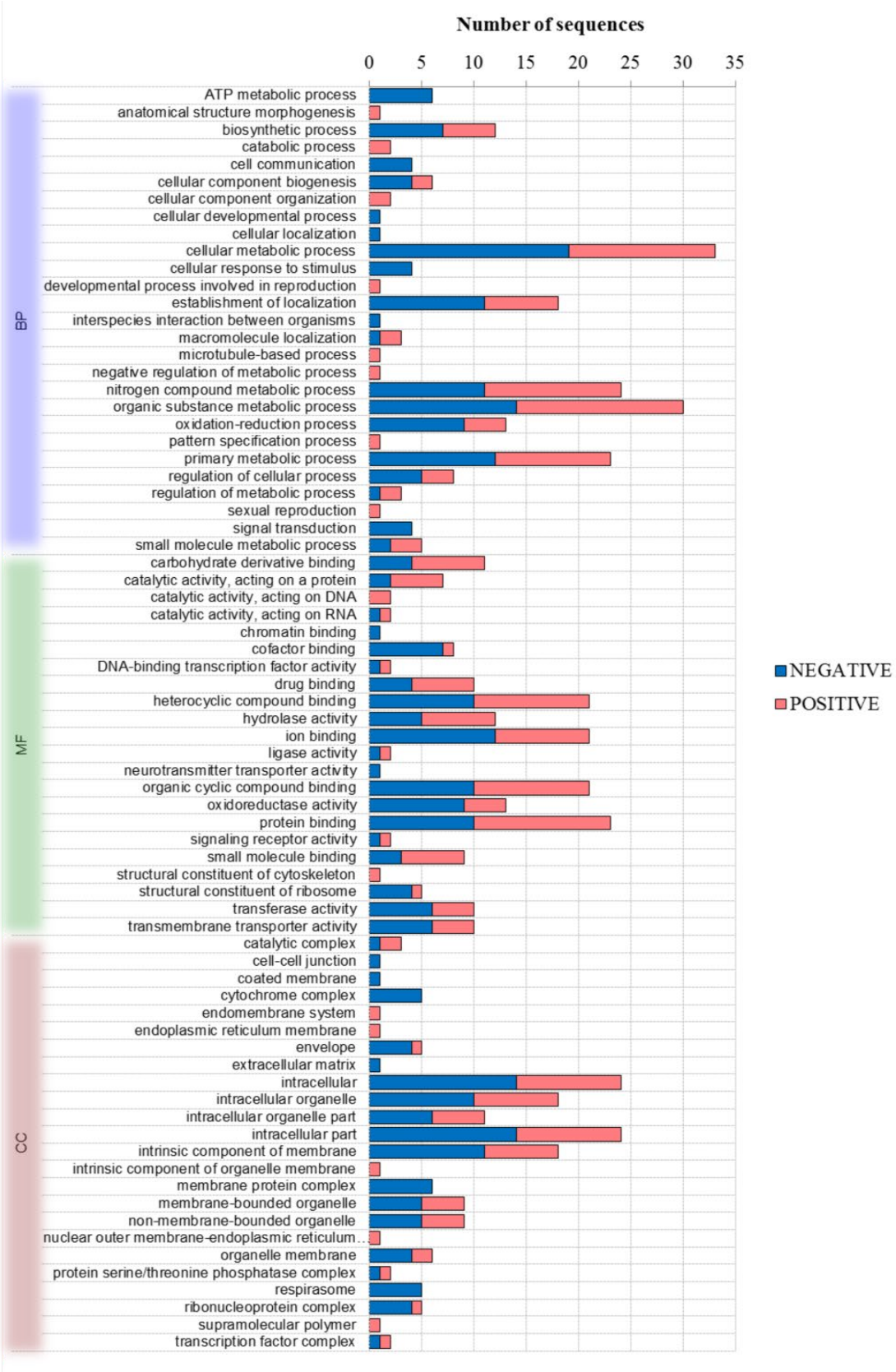

Figure 3. 11. Gene Ontology (GO) classification of the differentially up-regulated and the down-regulated isoforms in *Temora stylifera* females. Red bars indicate up-regulated sequences; blue bars indicate down-regulated sequences. Colour shadings differ depending on GO categories (CC, MF or BP).

Table 3. 5. Differentially expressed isoforms in *Temora stylifera*, annotated in the Biological Process (BP) GO category and showing exclusive up- or down-regulation in *Temora stylifera*. Trinity name, log2 fold-change (log2FC), adjusted p-values (adj.-p) and sequence description are reported.

Biological Process	Sequence name	log_2-FC	adj.-p	Description
		Down-regulated sequences		
ATP metabolic process	TRINITY_DN45761_c1_g1_i10	-3.65	9.57^{-03}	*Cytochrome Oxidase Subunit I*
	TRINITY_DN53513_c3_g1_i1	-3.10	4.15^{-02}	*Cytochrome Oxidase Subunit I*
	TRINITY_DN44787_c0_g1_i11	-5.75	7.28^{-03}	*Cytochrome Oxidase Subunit II*
	TRINITY_DN63585_c4_g1_i2	-2.73	5.65^{-05}	*Cytochrome Oxidase Subunit I*
	TRINITY_DN58044_c3_g1_i2	-4.70	1.43^{-02}	*NADH Dehydrogenase Subunit 4*
Cellular developmental process	TRINITY_DN52419_c1_g1_i4	-8.08	1.58^{-05}	*Trinucleotide Repeat-Containing Gene 18 Protein-like*
Cellular localization	TRINITY_DN60795_c6_g1_i2	-7.41	4.26^{-04}	*AP-2 Complex Subunit Alpha-like*
Interspecies interaction among organisms	TRINITY_DN57113_c0_g1_i2	-6.55	7.54^{-03}	*Dermatopontin-like isoform X1*
Signal transduction	TRINITY_DN61915_c1_g1_i2	-10.34	9.55^{-12}	*1-Phosphatidylinositol 3-Phosphate 5-Kinase-like*
	TRINITY_DN61595_c2_g1_i1	-9.39	1.01^{-07}	*Serine/Threonine-Protein Phosphatase 2A*
	TRINITY_DN54699_c0_g1_i3	-6.45	9.62^{-03}	*cAMP-Specific 3',5'-Cyclic Phosphodiesterase 4C-like*
	TRINITY_DN61841_c6_g1_i4	-9.29	1.73^{-08}	*Protein Trapped in Endoderm-1-like*
		Up-regulated sequences		
Catabolic process	TRINITY_DN56355_c0_g1_i3	6.93	1.71^{-03}	*Platelet-Activating Factor Acetyl hydrolase Homolog 2-like*
Microtubule-based process	TRINITY_DN44685_c4_g1_i4	7.82	2.09^{-05}	*Tubulin Beta-2C Chain*
Negative regulation of metabolic process	TRINITY_DN59104_c0_g2_i1	6.22	3.91^{-02}	*Protein Maelstrom 2-like isoform X1*
Sexual reproduction	TRINITY_DN59517_c0_g1_i1	4.35	4.19^{-03}	*Uncharacterized Protein Dvir_GJ21895, isoform A*

Depending on function, fold-change, significance (adjusted p-values), sequence length, E-value and sequence similarity percentage, 9 unigenes and 3 transcript sequences were selected for transcriptome validation, while one additional transcript (i.e. *MTHFD*) was added for subsequent temporal variation analysis in the expression levels of targeted sequences. Although unigenes offered a narrower array of functions codified by the sequences in comparison to transcripts, most primers were selected from unigenes. In fact, transcript expression detected through RT-qPCR analysis was more variable because of the presence of several isoform sequences in the same gene cluster. Primer products were all in the range of 111-228 bp and showed good amplification efficiencies (E, 1.87-2.14). RT-qPCR analyses performed to test amplification efficiencies (E) of the reference genes in the same *T. stylifera* samples revealed good efficiencies in primer product amplification (E=1.99 for *18S*; E=1.99 for *UBI*; E=1.9 for *ACT*; E=1.93 for *IST*; E=1.97 for *S20*). The full list of primer sequences for reference genes (Lauritano et al., 2011a, Lauritano et al., 2011b) is shown in Table 3.6; the list of the selected gene of interest (GOIs) is shown in Table 3.7.

Table 3. 6. Primer sequences of the six Reference Genes (RGs) selected for transcriptome validation and for annual expression analysis through RT-qPCR analysis. Name of RGs, function, length of the products (P_L), primer sequences (Forward and Reverse) and amplification efficiency (E) are reported.

Name	Function	P_L (bp)		Primers	E
Actin	Cytoskeleton structure	128	F	GGCACCACACTTTCTACAACG	1.9
			R	GTTGAAGGTCTCGAACATGATC	
Histone3	Chromatin structure	137	F	GAGGAGTGAAGAAGCCCCAC	1.93
			R	TGAAGTCCTGAGCAATCTCCC	
18S	Ribosome unit	164	F	GAAACCAAAGCATTTGGGTTC	1.99
			R	GCTATCAATCTGTCAATCCTTCC	
S7	Ribosome unit	147	F	CGTGAGCTGGAAAAGAAGTTC	2.14
			R	CAGGATGGAGTTGTGGACAG	
S20	Ribosome unit	113	F	CGTAAGACTCCTTGTGGTGAGG	1.97
			R	GAAGTGATCTGCTTCACGATCTC	
Ubiquitin	Protein degradation	113	F	GCAAGACCATCACCCTTGAG	1.99
			R	CAGCGAAAGATCAACCTCTG	

Table 3. 7. Primer sequences for unigenes and transcript isoforms selected for transcriptome validation, as well as for reference genes to be used for normalization of RT-qPCR analysis. Name and acronym of sequence, length of the primer products (P_L), log-transformed fold-change of the sequence (log_2-FC), significance value (adjusted p-values), primer sequences (Forward and Reverse) and amplification efficiency (E) are reported.

Name	P_L (bp)	log_2-FC	p-adj.		Primers	E
*A5**	130	-4.61	9^{-12}	F	GCCTGTTGCCGGAAACTTTT	2.1
				R	TTCTGGGCCGTCATTGACTC	
*CREBL**	111	-2.04	2^{-3}	F	GTACAAGCTGGAGAGGAGTCG	2.03
				R	GCCTTATTTGCCCTCTCCCT	
*me31b**	136	5.42	4^{-3}	F	TTCTGGACGAAGCGGACAAG	2.14
				R	CGCATGAAGGACTCGACTGT	
*Ppa2**	140	-3.72	1^{-3}	F	GCTTTGCCTTAAACTGCGCT	2.14
				R	CGGCAGGTAGTCAAACAGGT	
*Obst-E**	228	-1.62	9^{-5}	F	CAAGATCGACTGTCTGGGCA	2.04
				R	CGAGCCTTTCCACTCCACTT	
*ARIH1**	200	-1.76	2^{-3}	F	AGATGTGGGGCTGCAACTAC	2.06
				R	CTCAATCTTCTCCAGCGGCA	
*ARSB**	116	-1.29	4^{-3}	F	AACAACAGGGGCTTCAACCA	2.08
				R	TCAAACTCTGGCACCCTGTC	
*Hsp70**	133	-1.25	3^{-2}	F	CCATTCAGGTCTACGAGGGC	2.02
				R	TTGGCGTCAATGTCGAAGGT	
*VLDLR**	132	1.44	4^{-2}	F	ATCGCAGGGTCATTGTCCAG	2.13
				R	TGCGTATGTCTCGACCAGTG	
MOB1B#	156	-9.48	4^{-10}	F	TTGTCCTGTCATGTCGGCAG	1.9
				R	TTGCTGGGGAACAAGGACTC	
Vasa#	138	7.14	3^{-4}	F	CGCCTTCAACGATCTCCAGT	2.04
				R	GCCGAGAACATAAGGGTGGT	
PAFAH#	163	6.93	2^{-3}	F	GCCTTCACCTCGCTCTTCAG	1.87
				R	AGGCGTATCGATTGCAACCT	
MTHFD#	121	4.45	6^{-3}	F	ATGTGTGGCAGTCAGAAGGG	2.01
				R	CAACAAGACTGCGGCCAATC	

*: Unigenes
#: Transcripts

For RT-qPCR analysis, the expression of GOIs was normalized considering *18S ribosomal RNA* (*18S*) and *Ubiquitin* (*UBI*) as reference genes. These two genes were indicated as the most stable ones among the five candidates selected as potential reference sequences according to results provided by RefFinder (Figure 3.12).

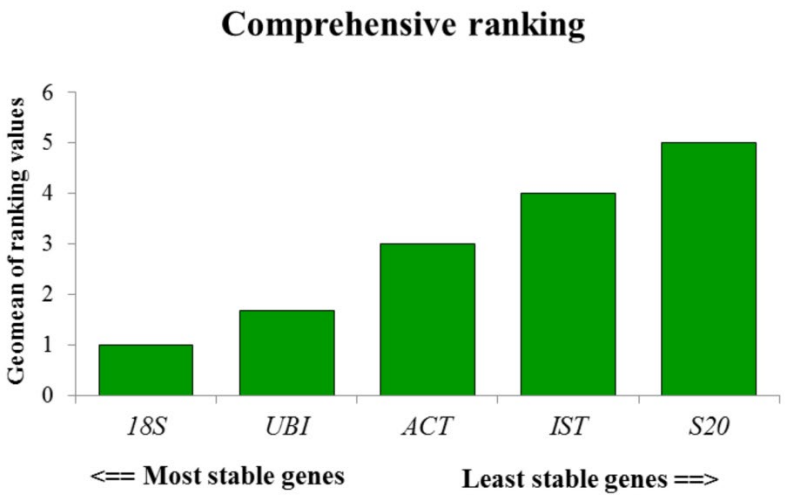

Figure 3. 12. Comprehensive ranking of the most stable genes in *Temora stylifera* samples considered for transcriptomic analysis (i.e. females collected on 23rd of May and 30th of May).

Normalized expression of the selected GOIs for transcriptome validation supported RNA-Seq results, because 9 sequences out of 12 reflected the same up- or down-regulation patterns as in the differential expression analysis. However, the genes *Protein Obstructor E* (*Obst*) and *Heat-Shock Protein 70* (*Hsp70*) as well as the transcript *MOB Kinase Activator 1B* (*MOB1B*) showed an opposite trend in comparison to RNA-Seq results (Figure 3.13). In general, differential expression was more pronounced in the RNA-Seq output than RT-qPCR results. Among the selected sequences, the transcripts *MOB1B*, *Vasa* and *Pafah* showed the highest fold-changes, which were close to 8. The expression ratio obtained after RT-qPCR analysis for the unigene *Odorant Binding Protein A5* (*A5*) was almost identical to the RNA-Seq output (log2-FC ~ -4).

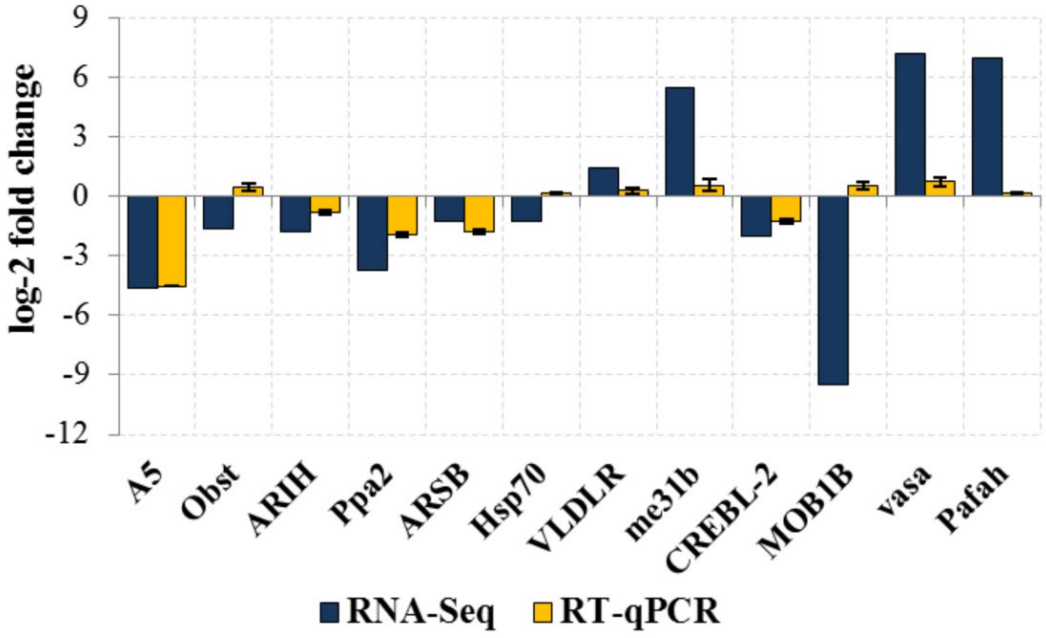

Figure 3. 13. Normalized expression (log-scale) of the 9 unigenes and 3 transcripts selected for transcriptome validation. Blue bars indicate expression as result of the RNA-Seq analysis; yellow bars indicate expression of unigenes and transcript isoforms (i.e. *MOB1B, Vasa* and *Pafah*) after RT-qPCR reactions. RT-qPCR results are means of triplicates (±SD).

3.3.4 Temporal variations in the expression of selected GOIs at LTER-MC

Expression analysis of the 13 sequences selected was performed on 22 samples of *T. stylifera* adult females collected along 2017 at LTER-MC. Most values are a mean of three replicates, except for the observation of 28th of February, which consisted of one single replicate because of low natural abundance of the animals and consequent lack in replication. Expression was not calculated in respect to control samples (see section 3.2). In fact, definition of control samples along the year would have been arbitrary and of difficult identification. Rather, mean expression normalized by the two reference genes (*18S* and *UBI*) is reported (Figure 3.14). Mean normalized expression (MNE) ranged between values lower than 0.0002 (e.g. for *Ppa2*) to values close to 1 (for *Obst*).

Among the 13 sequences, those coding for *Obst* and *Hsp70* showed the highest expression along the data series (0.1-0.9 MNE). Similar MNE rates were measured also for the sequences of *A5*, *me31b*, *MOB1B* and *PAFAH* as well as for *ARIH1*, *VLDLR*, *CREBL*

and *Vasa*. The sequences for *Ppa2*, *ARSB* and *MTHFD* showed the lowest expression values (less than 0.005 to a maximum of 0.0015 MNE; Figure 3.15).

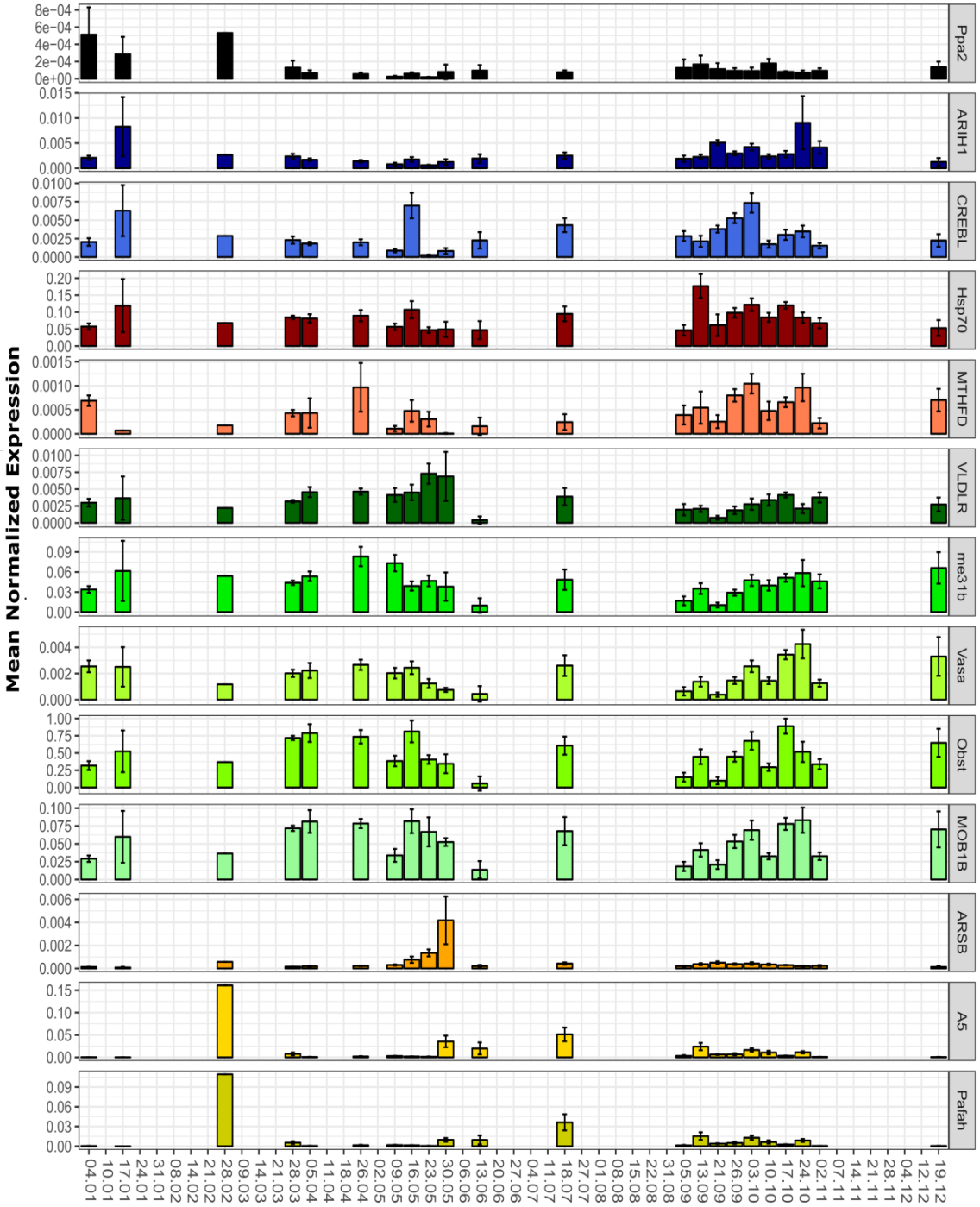

Figure 3. 14. Mean normalized expression (MNE) along 2017 at LTER-MC of the 9 genes and the 4 transcripts selected as target GOIs. Colours indicate clusters based on positive correlations expressing similarity in expression patterns.

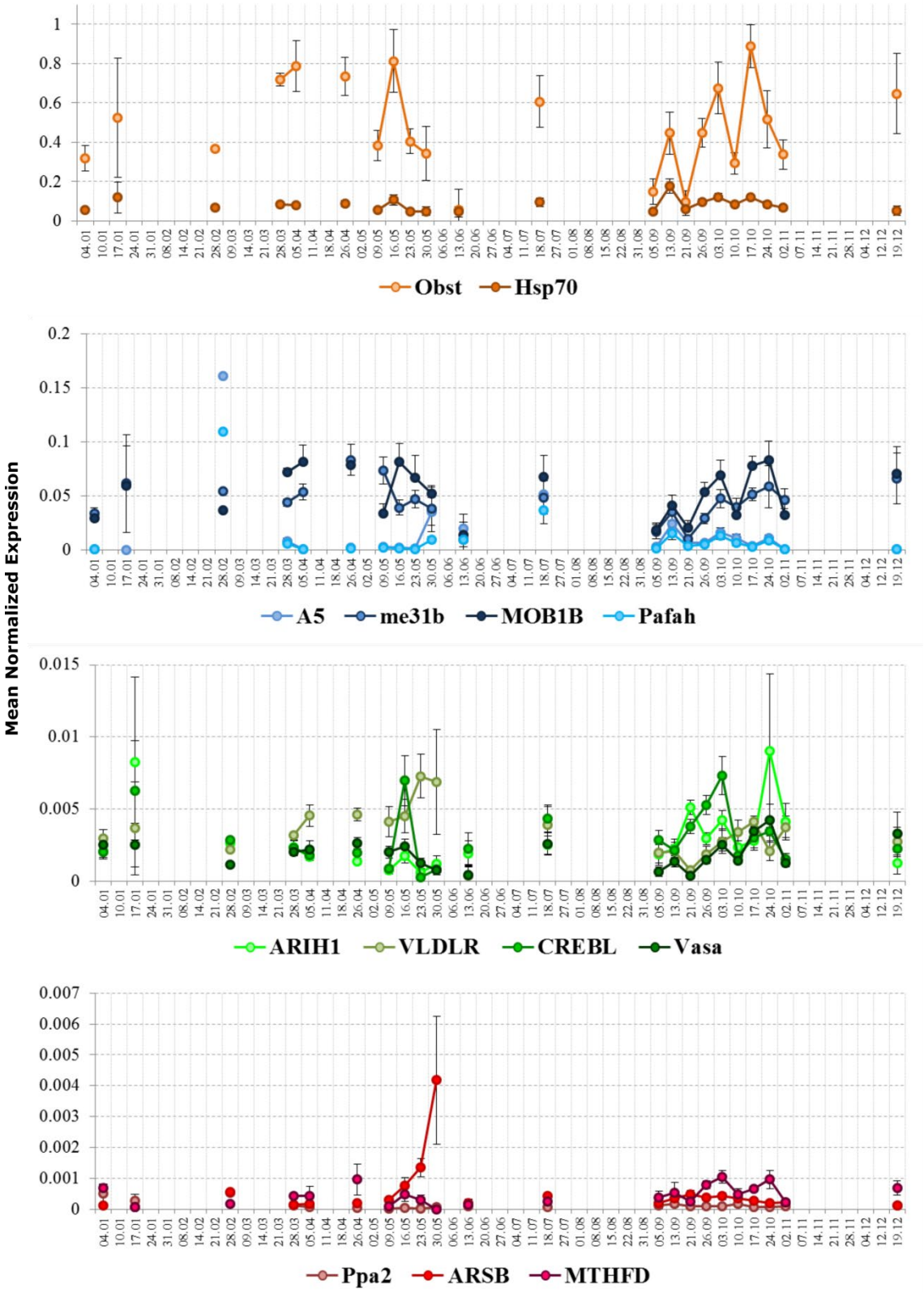

Figure 3. 15. Mean Normalized Expression (MNE) along 2017 at LTER-MC of the 9 genes and the 4 transcripts selected as target GOIs. Sequences are clustered in the same plot depending on MNE values to maximize clearness in expression variations.

To better synthesize the data and have a clearer picture about temporal variations in the MNE of the 13 selected sequences, MNE was inspected at a seasonal scale. Seasons were defined temporally (winter: January-March; spring: April-June; summer: July-September; autumn: October-December). To explore multivariate variations across the four seasons, a PCA analysis was performed on log-transformed values. The first two axes resumed more than half of total variation, with the first PC axis summarizing 45.7% of variation and the second axis 19.1%. MNE of sequences in winter mainly differed from the expression values detected in spring. By contrast, MNE observed in autumn slightly separated from summer samples (Figure 3.16).

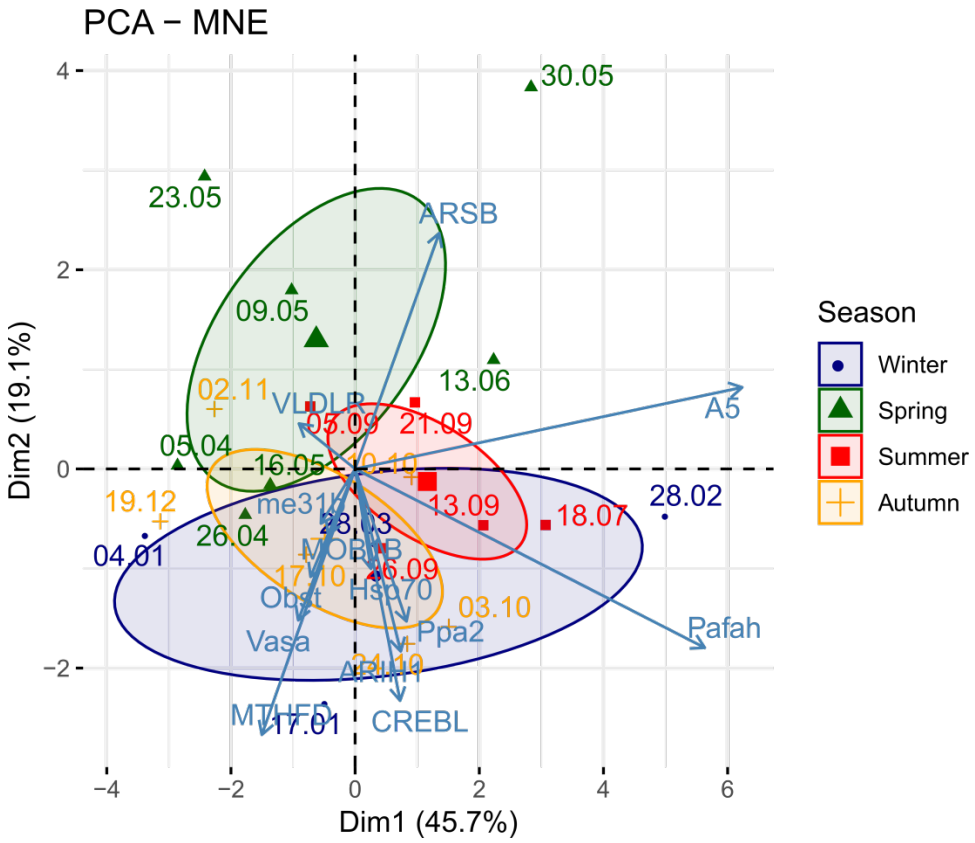

Figure 3. 16. PCA analysis made on the 13 sequences selected as GOIs for expression analysis. Ellipse colours and point shapes indicate the seasons. Representation is based on log-transformed values.

Boxplot displaying MNE variations along the four seasons showed that *Ppa2*, which was not included in a cluster of correlating genes, was highly expressed in winter, while its MNE was lower in the rest of the year. *ARIH1* and *CREBL* had the lowest

expression in spring and higher expression in the other seasons, while expression of *Hsp70* and *MTHFD* showed a progressive increase along the year. *VLDLR*, *me31b*, *Vasa*, *Obst* and *MOB1B* had the lowest MNE in summer and the highest in spring and autumn. *ARSB*, *A5* and *Pafah* showed slightly higher expressions in winter (Figure 3.17).

To analyse in a quantitative way monthly variations in the MNE of each sequence, a series of Wilcoxon's tests was run to test differences in MNE across seasons (Figure 3.18). No significant difference was detected in seasonal MNE of *Hsp70*, *Obst*, *MOB1B*, *ARSB*, *A5* and *Pafah* sequences. Expression of *MTHFD* significantly varied only between winter and autumn, while MNE of Vasa only between summer and autumn. The low expression on *CREBL* detected in spring significantly differed from summer and winter. Expression of *me31b* observed in summer was significantly different to autumn and winter values, while summer expression of *ARIH1* significantly differed from autumn, winter and spring. MNE of *VLDlR* significantly varied among all seasons, but not between winter and autumn. Similarly, non-significant difference in the expression of *Ppa2* was observed between summer and autumn.

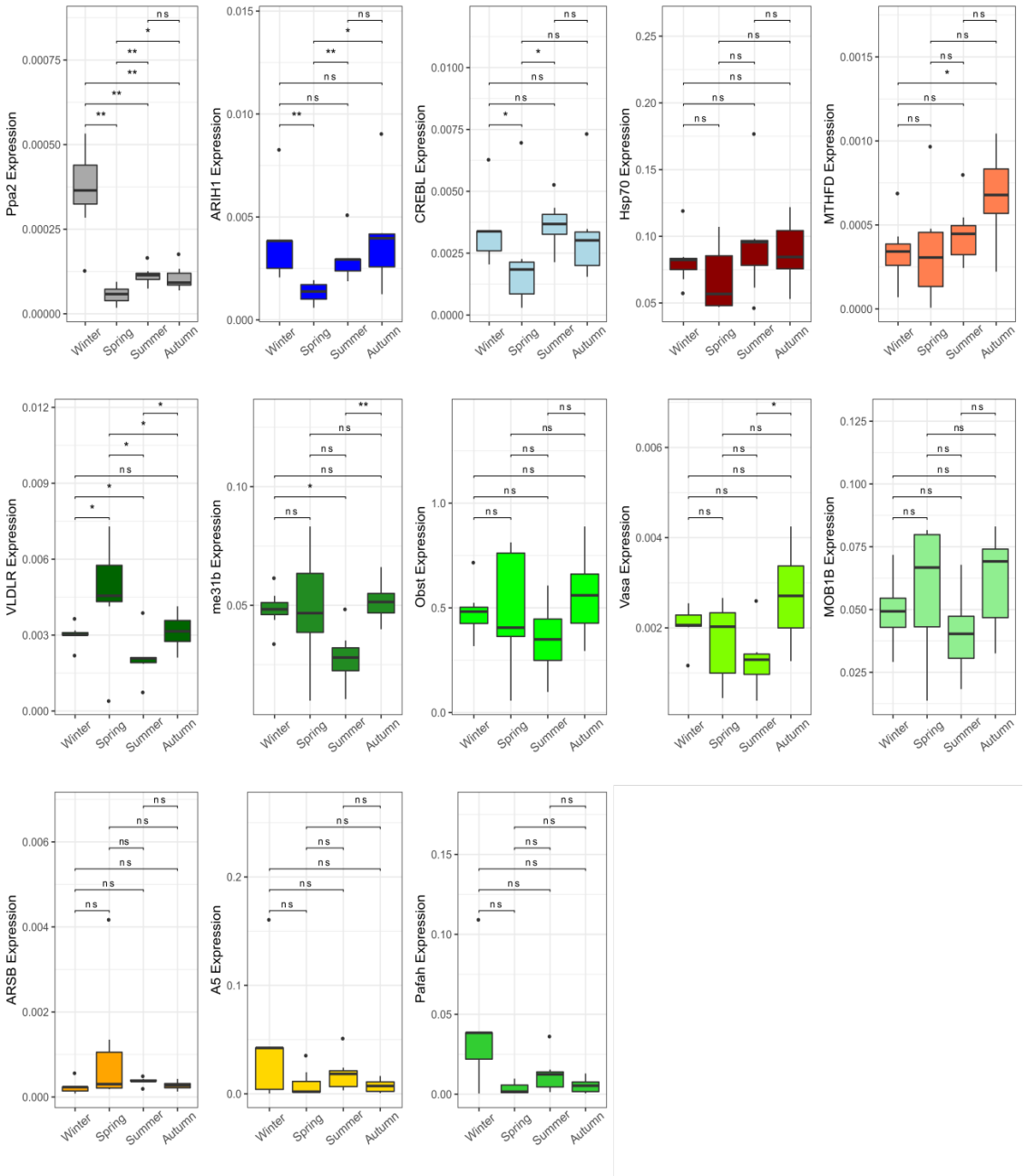

Figure 3. 17. Boxplots showing seasonal variations in the Mean Normalized Expression (MNE) of the 13 sequences selected for RT-qPCR analyses. Asterisks indicate significance of Wilcoxon's tests performed among seasonal values. Probability values: *<0.05; **<0.01; ns=not-significant.

3.3.5 Interaction of physiological responses of Temora stylifera *with biotic and abiotic variables measured at LTER-MC*

Firstly, interactions among the physiological responses of *T. stylifera* (i.e. faecal pellet production, egg production, hatching success and naupliar survival rates) were tested in relation to abiotic variables measured at LTER-MC in the same sampling dates (see Chapter 2; Figure 3.18). Variations in egg and pellet production were well explained by

environmental variables. In particular, faecal pellets were positively related to oxygen saturation, fluorescence, phaeo-a concentrations and chl-a (R^2=0.7, 0.62, 0.58 and 0.49, respectively; $p<0.001$). When inspected in relation to these variables, faecal pellet production initially increased, then reaching a plateau at intermediate values of these predictors. Variations along transmittance and pH were significant (R^2=0.55, $p<0.01$ and R^2=0.39, $p<0.05$, respectively), but oscillatory. By contrast, faecal pellets varied linearly with oxygen (positive relationship, R^2=0.24, $p<0.01$) and salinity (negative relationship, R^2=0.3, $p<0.01$). Egg production was mostly described by water temperature (R^2=0.52, $p<0.01$) and water density (R^2=0.55, $p<0.001$), which showed opposite patterns. In fact, egg production was the highest at low temperatures and high water densities, diminishing at high temperatures and low water densities. Egg production also increased along with oxygen and phaeo-a concentrations (R^2=0.53, $p<0.01$ and R^2=0.23, $p<0.05$, respectively). Instead, eggs slightly decreased at high chl-a concentrations (R^2=0.29, $p<0.05$) and followed an oscillatory pattern in relation to transmittance (R^2=0.49, $p<0.01$). In contrast to faecal pellet and egg production, environmental variables offered poor prediction of hatching success and naupliar survival variations. Lower hatching was observed at increasing chl-a concentrations (R^2=0.13, $p<0.05$), while a dip in the survival rates of *T. stylifera* nauplii was observed at intermediate transmittance values (R^2=0.35, $p<0.05$).

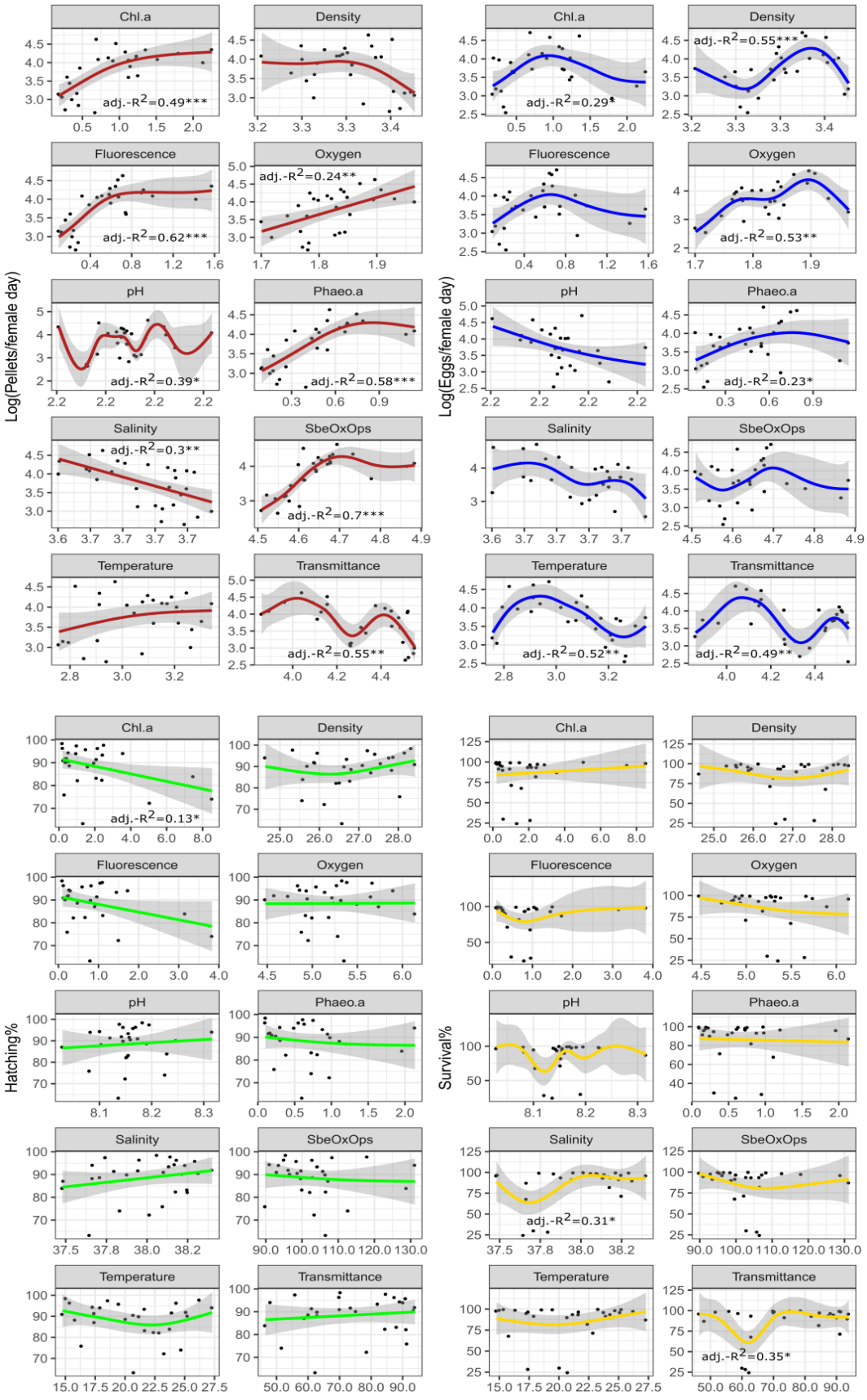

Figure 3. 18. Output of Generalized Additive Model (GAM) analyses investigating the relationship among variables explaining *Temora stylifera* physiological responses and abiotic variables measured at LTER-MC along 2017. Colours of regression lines indicate the different physiological variables (red for pellets, blue for eggs, green for hatching, yellow for naupliar survival). If significant, the R^2 of the regression and respective significance values are indicated.

Variations of *T. stylifera* physiological responses were investigated also in relation to the concentrations of the four main phytoplankton taxonomic groups, i.e. diatoms, coccolithophores, dinoflagellates and phytoflagellates (mainly cells <10 µm; Figure 3.19). Faecal pellet production significantly related to all these groups (R^2=0.84, 0.76, 0.75 and 0.43 for diatoms, dinoflagellates, phytoflagellates and coccolithophores, respectively; $p<0.001$), increasing at higher cell concentrations. However, egg production rates significantly related only to diatoms through a slightly positive relationship (R^2=0.11, $p<0.05$). Similarly, hatching success was significantly related only to dinoflagellates through a slightly negative regression (R^2=0.24, $p<0.05$). Phytoplankton concentrations did not explain variations in naupliar survival rates.

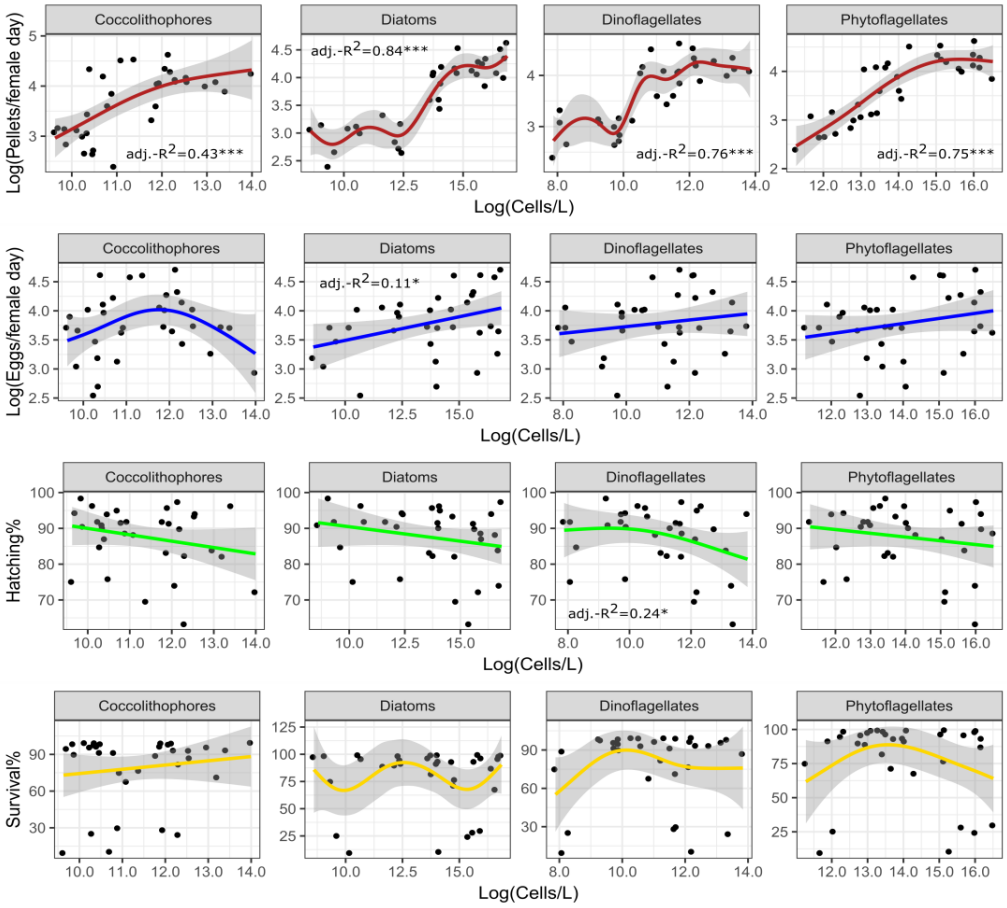

Figure 3. 19. Output of Generalized Additive Model (GAM) analyses investigating the relationship among *Temora stylifera* physiological responses and phytoplankton concentrations at LTER-MC, along 2017. Colours of regression lines indicate the different physiological variables (red for pellets, blue for eggs, green for hatching, yellow for naupliar survival). If, the R^2 of the regression and respective significance values are indicated.

To explore if a delayed maternal effect mediated by phytoplankton ingestion occurred, naupliar survival rates at t+1 (one week later) were considered in relation to phytoplankton cell abundances. Among all phytoplankton groups, only the genus *Chaetoceros* drove negative variations of naupliar survival rates in *T. stylifera* (adjusted-R^2=0.41; y=-1^{-7}x+4.53; F=20.6; d.f.=27, N=29, p<0.001; Figure 3.20).

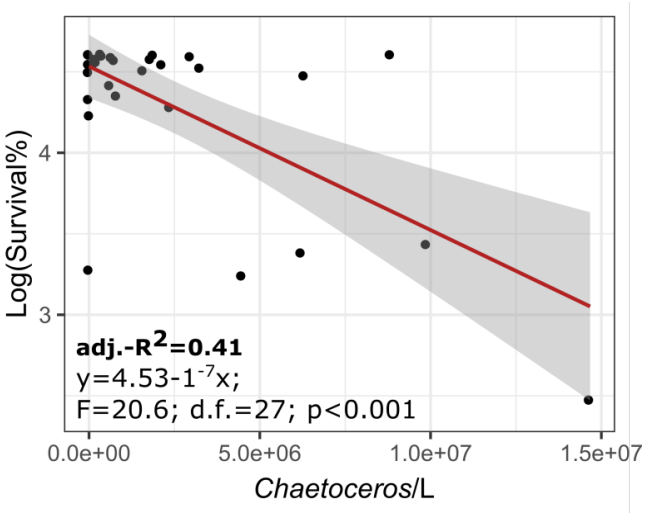

Figure 3. 20. Naupliar survival rates (%) as function of the abundance of *Chaetoceros* spp. (cells/L). The red line indicates linear regression between *Chaetoceros* abundance and naupliar survival rates at t+1 (i.e. one week later). Grey shading indicates 95% interval of the linear regression.

Further GAM analyses were performed to explore potential effects of chemical variables on the physiological responses of *T. stylifera*. The total concentration of both NVOs/L and NVOs/diatom-cell was considered as the predicting variable. Significant relations, but with an opposite trend, were found between faecal pellet production and NVO concentrations (R^2=0.75 when analysing NVOs/L and R^2=0.49 when analysing NVOs/diatom-cell; p<0.001). A significant, but weak, positive relationship was found between egg production and NVOs/L (R^2=0.1, p<0.05). GAM results were not significant when hatching success and naupliar survival were considered as dependent variables (Figure 3.21).

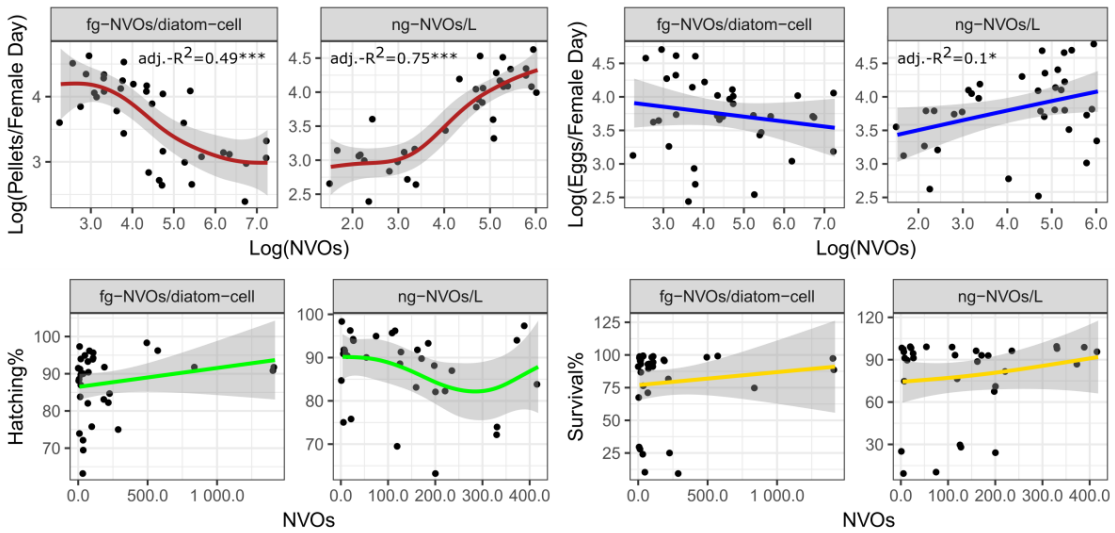

Figure 3. 21. Output of GAM analyses investigating the relationship among *Temora stylifera* physiological responses and total NVO concentrations at LTER-MC, along 2017. Both NVOs/L and NVOs/diatom-cell are considered as predicting variables. Colours of regression lines indicate the different physiological variables (red for pellets, blue for eggs, green for hatching, yellow for naupliar survival). When significant, the R^2 of the regression and respective significance values are indicated.

Non-significant relationships between hatching success, naupliar survival and oxylipin concentrations were also observed when GAM analyses were repeated considering the single NVO species as independent variables.

Possible effects of FAs on *T. stylifera* physiological responses were also analysed (Figure 3.22). All fatty acids but the group of C18:1, C18:2 and C18:3 were significantly related to faecal pellet production (the highest relationships were found with C16:1 and C22:6, R2=0.62 and 0.64, respectively, $p<0.001$). Egg production was significantly related to three FA species, the C14:0 ($R^2=0.16$, $p<0.05$), the C16:0 ($R^2=0.14$, $p<0.05$) and the C18:0 ($R^2=0.1$, $p<0.05$) with slightly positive regression patterns. Hatching success varied negatively along FA concentration increments. In particular, significant negative regressions were observed with C14:0 ($R^2=0.22$, $p<0.01$), C16:0 ($R^2=0.33$, $p<0.01$), C18:0 ($R^2=0.27$, $p<0.05$), C18:1 ($R^2=0.36$, $p<0.05$) and C22:6 ($R^2=0.15$, $p<0.05$). High concentrations of C16:0, C18:0 and C18:2 seemed to drive significant reduction also in naupliar survival rates ($R^2=0.55$, 0.46 and 0.28; $p<0.001$, $p<0.001$ and $p<0.05$, respectively).

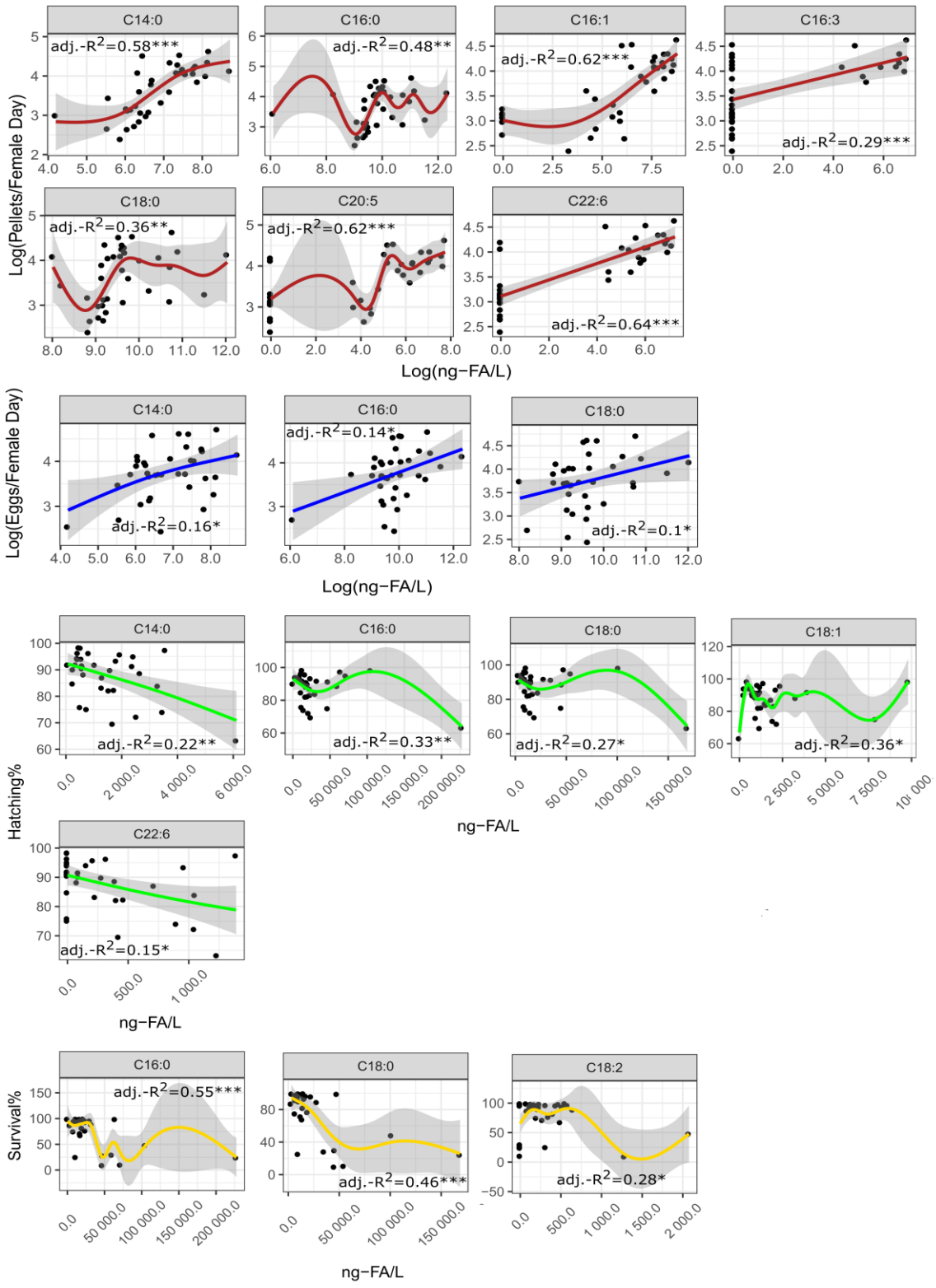

Figure 3. 22. Output of GAM analyses investigating relationships among *Temora stylifera* physiological responses and FA concentrations at LTER-MC, along 2017. Line colours indicate the different physiological variable measured (red for pellets, blue for eggs, green for hatching, yellow for survival). Only significant relations are depicted. The R^2 of the regression and respective significance values are indicated.

3.3.6 Interaction of molecular responses of Temora stylifera *with biotic and abiotic variables measured at LTER-MC*

To identify, among the 13 selected GOIs, those sequences that could have explained variations in *T. stylifera* physiological responses, a series of single GAM analyses was performed. MNE of each sequence was considered as the independent variable, while the physiological variables as the dependent ones (Figure 3.23). In total, only 5 genes showed significant relations with the physiological responses of copepod females. In particular, the *Very Low-Density Lipoprotein Receptor* (*VLDLR*) and the *Serine/Threonine Protein Phosphatase* (*Ppa2*) were significantly related to faecal pellet production (R^2=0.38 and 0.35, respectively; $p<0.05$). While lower pellets were counted at higher expressions of *Ppa2*, their number increased at higher expression rates of *VLDLR*. Egg production rate was significantly related with three genes, showing a reduction at high *CREBL* expression values (R^2=0.36; $p<0.05$) in contrast to an increment at higher expression rates of *me31b* and *VLDLR* (R^2=0.37 and 0.33, respectively; $p<0.01$). Reductions in hatching success seemed to be partially driven by higher expressions of *ARSB* (R^2=0.36; $p<0.05$), while variations in naupliar survival rates by expression of *ARSB* (R^2=0.71, $p<0.001$) and *Ppa2* (R^2=0.45; $p<0.05$).

On the basis of these results, further analyses focused specifically on the five genes that significantly related to physiological responses of *T. stylifera* females. These five selected genes were initially inspected in relation to the abiotic variables measured at LTER-MC through single GAM analyses.

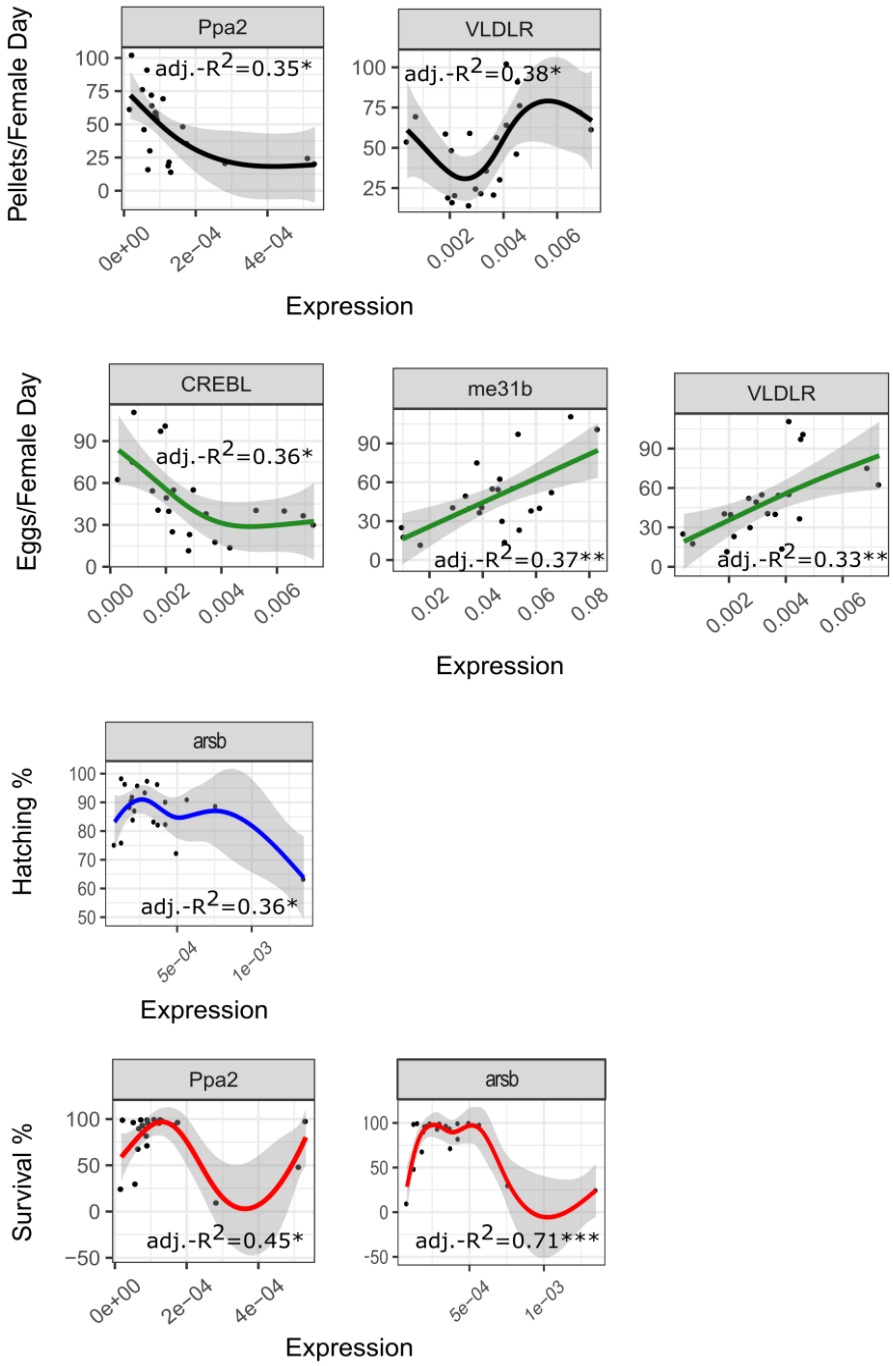

Figure 3. 23. Output of single GAM analyses inspecting the relationship between the expression of GOIs (MNE) and physiological responses of *Temora stylifera*. Only significant relations are depicted. The R^2 of the regression and respective significance values are indicated. Line colours vary depending on the dependent physiological variable considered. Sequence name: *Ppa2*=Serine/Threonine Protein Phosphatase; *VLDLR=Very Low-Density Lipoprotein Receptor*; *CREBL=cAMP-Responsive Element-Binding Protein*; *me31b=Putative ATP-Dependent RNA Helicase*; *ARSB=Arylsulfatase B*.

Significant regressions were observed when water density, temperature and oxygen saturation values were plotted against *Ppa2* and *me31b*. In particular, the expression of both genes increased at higher water densities, while decreasing at higher temperatures.

Expression pattern as function of oxygen saturation, instead, showed an expression peak of the two genes at discrete values of the independent variable (Figure 3.24). Expression of *VLDLR* significantly depended on oxygen concentrations (R^2=0.48; p<0.05) and transmittance (R^2=0.56; p<0.01). No significant relations were found between *ARSB*, *CREBL* and the environmental variables.

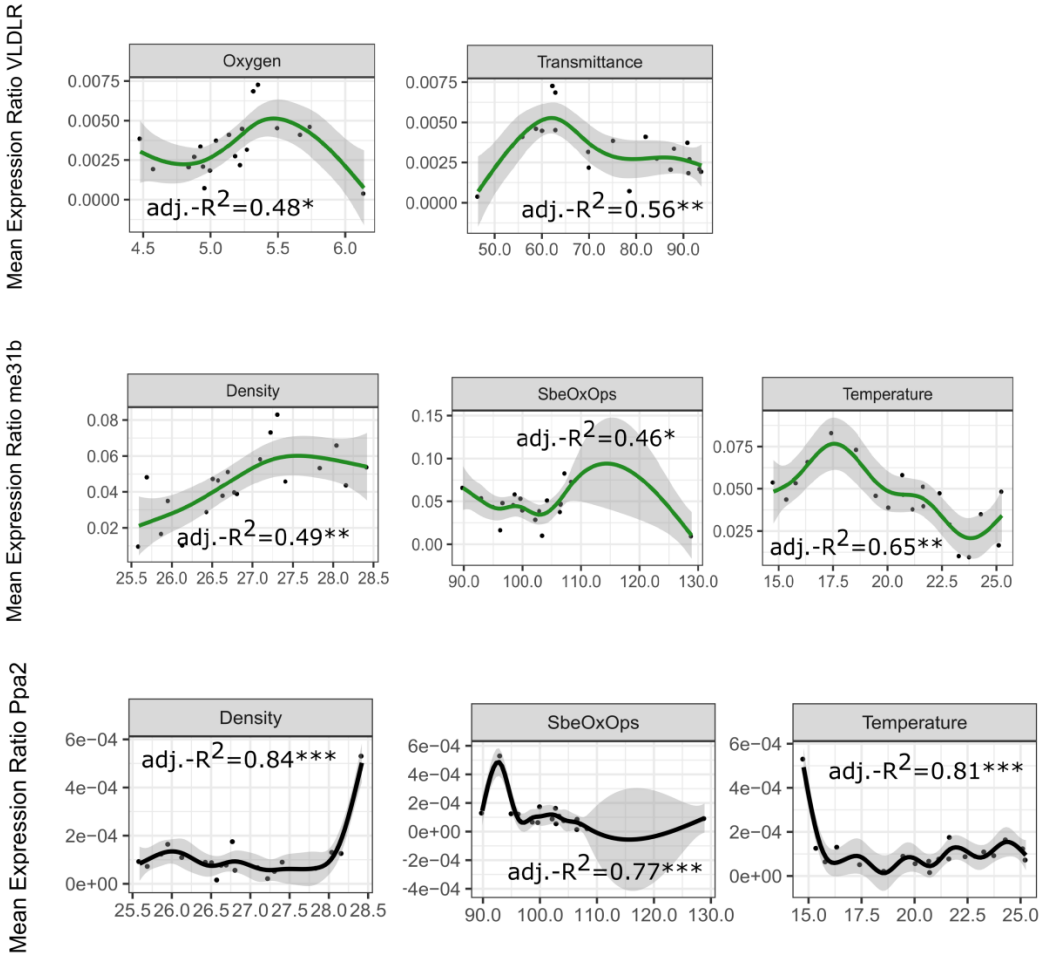

Figure 3. 24. Output of single GAM analyses inspecting the relationship between the expression of selected GOIs (MNE) in *Temora stylifera* and environmental variables measured at LTER-MC along 2017. Only significant relations are depicted. The R^2 of the regression and respective significance values are indicated. Line colours indicate gene clustering.

Expression rates of *Ppa2* and *CREBL* were not significantly explained by cell abundance variations of the four main phytoplankton groups (i.e. diatoms, dinoflagellates, coccolithophores and phytoflagellates; Figure 3.25). Expression of *me31b* was negatively related to coccolithophores (R^2=0.32; p<0.01), while *VLDLR* was significantly dependent on the abundance of coccolithophores (R^2=0.4; p<0.05), dinoflagellates (R^2=0.56; p<0.05)

and phytoflagellates (R^2=0.6; p<0.01). *ARSB* was significantly related to diatoms, dinoflagellates and phytoflagellates (R^2=0.6, 0.7 and 0.3; p<0.05, p<0.001 and p<0.01, respectively).

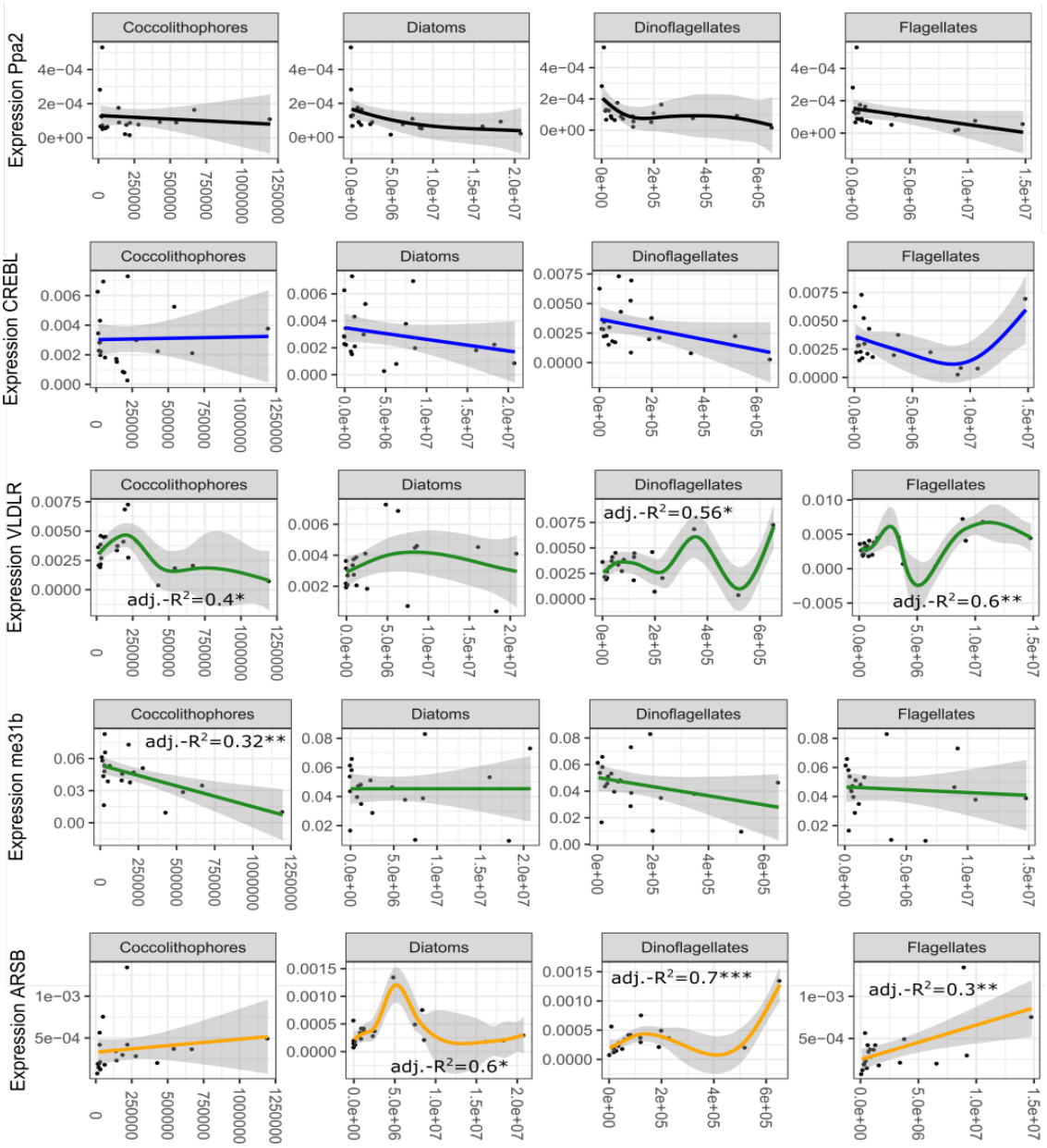

Figure 3. 25. Output of single GAM analyses inspecting the relationship between the expression of 5 selected GOIs (MNE) in *Temora stylifera* and the cell abundance (cells/L) of the four main phytoplankton taxonomic groups. When significant, the value and the significance level of the regression are shown. Line colours indicate gene clustering.

No significant regression was detected when considering NVO/L concentrations. Only the expression of *Ppa2* significantly varied along with variations in NVOs/diatom-cell concentrations (R^2=0.66; p<0.01; data not shown). Expression variations of this gene

were further investigated in relation to the concentrations of the six oxylipin species separately (NVOs/diatom-cell; Figure 3.26).

The hydroxy-acids deriving from DHA and EPA (i.e. HDoHE and HEPE) significantly related to the expression of *Ppa2* (R2=0.56 and 0.57, respectively; p<0.01 and 0.05, respectively), even though the strongest relationship was observed between the expression of this gene and the cellular concentration of HEpETE (R2=0.71; p<0.001)

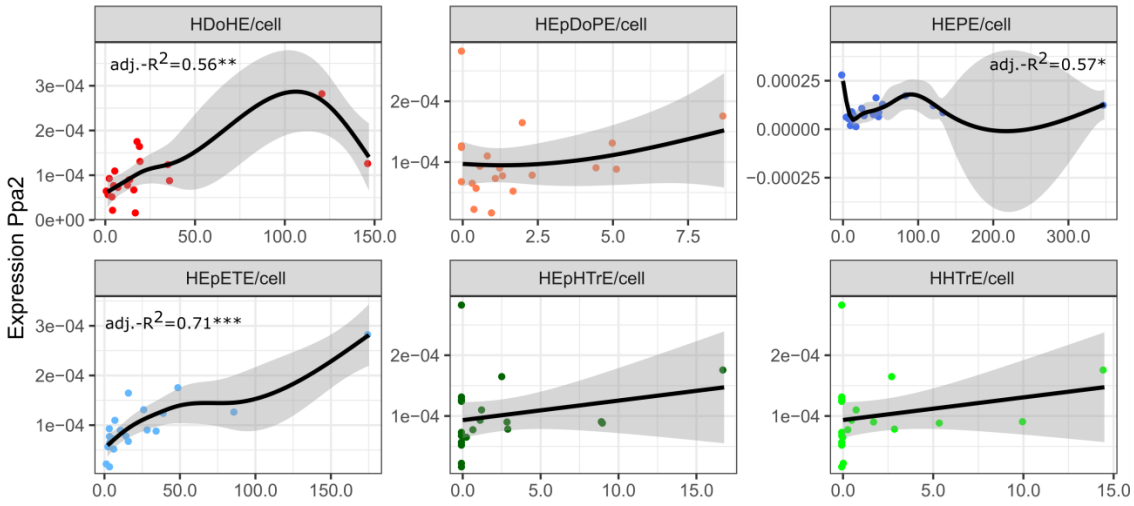

Figure 3. 26. Output of GAM analyses applied to inspect variations in the expression of *Temora stylifera Ppa2* (MNE) along concentrations of the six NVO species (fg-NVOs/diatom-cell). Colours of the dots reflect the different FA precursors leading to the synthesis of the six oxylipin species (red for DHA, blue for EPA and green for HTA). When significant, the value of the regression is provided along with its significance.

3.4 Discussion

3.4.1 Physiological responses and population dynamics of Temora stylifera *at LTER-MC*

Temora stylifera abundance observed in 2017 at LTER-MC well mirrored the annual cycle usually described for this species in the Gulf of Naples (Mazzocchi et al., 2012). Maximal population densities occurred in autumn, from October to November. Egg production rates measured along 2017 were also in line with previous information collected at LTER-MC. Between 2000 and 2001, in fact, the number of eggs laid daily by each *T. stylifera* female varied from less than 20 eggs/female-day to the maximum of

almost 120 eggs/female-day (in spring) (Carotenuto et al., 2006). Moreover, as in the present survey, a rather constantly high hatching success (%) was reported and survival rates (%) of NI nauplii were observed to dramatically oscillate at a weekly basis (Carotenuto et al., 2006).

One aim of this survey is to understand whether the physiological responses of copepod females collected weekly at LTER-MC in 2017 can offer an explanation of the annual population dynamics of the copepod *T. stylifera*. Interestingly, although egg production rates were higher in spring (mainly April) than autumn (Figure 3.2), total population abundance started to increase only from September onwards (Figure 3.3). This result suggests that factors other than egg production determine final recruitment of *T. stylifera* population. While hatching success of eggs did not show marked variations along the year, naupliar survival rates drastically oscillated in winter and spring (Figure 3.1 and Figure 3.2), maybe partially explaining the lack of population abundance peaks in winter, spring and summer. For example, the high nauplair recruitment calculated on 26th of September could have supported the high abundance of *T. stylifera* juveniles observed two weeks later, on 10th of October, in line with copepod developmental rates (Allan, 1997). As a result, understanding which factors drove variations in egg production rates and naupliar survival might be of key importance to predict *T. stylifera* population dynamics at LTER-MC.

Faecal pellet and egg production well correlated with each other, thus defecation rates can mirror the egg production rates of the copepod. Faecal pellets reached a plateau as chl-a, phaeo-a and fluorescence increased. These environmental variables are predictors of primary producer biomass and this result was confirmed by significant variations in faecal pellet production in function of phytoplankton concentrations. Little information is available about the feeding preferences of *T. stylifera* at sea, but this calanoid copepod has been described as a preferentially broadcasting herbivorous species (Benedetti et al., 2018, Benedetti et al., 2015). This result is confirmed by the relations observed between faecal

pellets and the four main phytoplankton groups (Figure 3.20), which could have constituted the main food source of this copepod species at LTER-MC along 2017. Recent findings suggest that *T. stylifera* can modify its feeding behaviour to maximize ingestion of phytoplankton preys (Mahadik et al., 2017). Regression curves describing production of faecal pellets as function of phytoplankton cell abundance also suggest that food saturation can occur at high phytoplankton densities, because faecal pellet production stabilized at the highest phytoplankton concentrations.

Differently from faecal pellets, biotic variables did not play major roles in determining egg production rate variations. In fact, when major phytoplankton taxa were considered, a weak significant relation was observed only between the number of eggs and diatom abundance. This result is in contrast with those laboratory experiments which have reported negative effects of diatoms and their secondary metabolites on production rates of copepod eggs (Ianora et al., 2011, Buttino et al., 2008, Ceballos and Ianora, 2003, Ban et al., 1997) and rather suggests that multi-specific phytoplankton communities could slightly elicit egg production in *T. stylifera* females, at sea (Vehmaa et al., 2011). The lack of a negative effect of diatoms on copepod egg production is also supported by the positive relation observed with the oxylipin-per-litre concentrations as well as by the non-significant relation with the oxylipin-per-cell production. Among biotic variables, the groups of the saturated fatty acids, C14:0, C16:0 and C18:0, also explained little positive variation in egg production rates. Possibly, these compounds provided useful energy sources for copepods to improve their reproductive output (Peters et al., 2007, Castellani and Altunbas, 2006, Jónasdóttir et al., 2002). Interestingly, a positive correlation between Docosa-hexaenoic acid 22:6 and egg production rates of the copepods *Acartia hudsonica* and *Temora longicornis* was reported (Jónasdóttir et al., 1995), but this relation was not evident in *T. stylifera* from the Gulf of Naples. This discrepancy may indicate that copepods could utilize different energy sources to improve their reproductive potential, depending on the nutritional traits of the available preys. Alternatively, saturated fatty

acids, which represent precursors for the synthesis of PUFAs (Brett and Müller-Navarra, 1997), can be substrates subsequently converted by the animals to maximize their fitness.

Temperature, density, oxygen and transmittance well related to egg production and were the only abiotic variables significantly affecting this physiological response. In particular, the highest number of eggs was observed at low temperature and transmittance values and at high oxygen concentrations (Figure 3.19). The effect of temperature on egg production potential has been previously reported for other copepod species. For example, (Holste et al., 2006) observed that egg production rates in the copepod *Acartia tonsa* from the Baltic Sea increased to the optimum of 24 °C, then decreasing at higher temperatures. The highest egg production rates were observed at 23 °C in the same copepod species collected in Chesapeake Bay (White and Roman, 1992) and a similar trend was observed also for the copepod *Temora longicornis* (Holste et al., 2009, Castellani and Altunbas, 2006). Results collected in the Gulf of Naples in the present survey indicated that *T. stylifera* produced the highest number of eggs between 18-20 °C, at temperature ranges already observed for *T. longicornis* by (Holste et al., 2009). Present results also highlighted a significant influence of dissolved oxygen concentrations on egg production, possibly mirroring lower reproductive outputs in response to hypoxic conditions (Marcus et al., 2004, Jónasdóttir and Kiørboe, 1996) or to oxidative stress, at low and high oxygen concentrations, respectively.

Few biotic and abiotic factors significantly described the little variations observed in hatching success for *T. stylifera* eggs along 2017. In fact, among the environmental variables, a high chl-a concentration was the only factor driving slight reduction in egg hatching. This relation was likely due to the negative pattern describing lower hatching success at higher dinoflagellate concentrations. No other major phytoplankton taxa significantly related to this physiological variable. This result is in contrast with laboratory experiments (Ianora et al., 2004, Ban et al., 1997) and field surveys (Ianora et al., 2008, Ianora et al., 2004, Miralto et al., 2003) reporting negative influence of diatoms and

positive effects of dinoflagellates on copepod egg viability (Chen et al., 2012). Field surveys have provided contrasting evidence about direct negative influence of diatoms and their secondary metabolites on the reproductive potential of planktonic copepods, so far (Wichard et al., 2008, Koski, 2007, Carotenuto et al., 2006, Ianora et al., 2004, Pond et al., 1996). These discrepancies are probably related to the study system, because negative effects of diatoms on copepod reproduction were mainly observed in the eutrophic Northern Adriatic Sea, where mono-specific blooms of PUA-producing diatoms (such as *Skeletonema marinoi*) occur (Ianora et al., 2004). Instead, clear relationships between copepod physiology and their diet were more difficult to detect in more heterogeneous marine systems. The Gulf of Naples is a mutable oligotrophic embayment and results collected in the present survey suggest that diatom density and oxylipin concentrations are not accurate predictors of copepod egg hatching success in this area. By contrast, significant negative effects on hatching seemed to be mediated by high concentrations of few fatty acid species (C14:0, C16:0, C18:0 and C22:6), while oscillatory patterns were observed in response to the Hexadecenoic acid (C16:1). The negative relation between egg viability and fatty acid concentration is surprising, because positive effects of long-chain fatty acids on egg production rates and hatching of copepods were reported in laboratory (Chen et al., 2012, Arendt et al., 2005) and confirmed in the field (Arendt et al., 2005).

Variations in naupliar survival rates probably represent the most interesting physiological response of *T. stylifera*, because they can help explain why high egg production rates observed in spring did not result in higher population recruitment. Effects of salinity on survival rates of nauplii of several copepod species have been already reported (Chinnery and Williams, 2004, Devreker et al., 2004). Evidence arising from the present survey may indicate salinity tolerance limits for *T. stylifera* eggs and nauplii. Considering that few fatty acid species may have mediated also low hatching success, these results could suggest that food quality rather than quantity can determine reproductive success and final recruitment in the copepod *T. stylifera*.

An additional aspect that merits further exploration is the possible delayed effect of phytoplankton. In fact, *Chaetoceros* significantly drove reductions of larval survivorship at t+1 (i.e. one week later). Potential delayed effects of diatoms on copepod naupliar survival rates were also proposed by (Halsband-Lenk et al., 2005) and could be the key to unveil copepod physiology in response to biological interactions. The genus *Chaetoceros* dominates phytoplankton community at LTER-MC (Ribera-D'Alcalá et al., 2004), encompassing species known to synthesize both PUAs (Wichard et al., 2005a) and NVOs (Fontana et al., 2007b). Nonetheless, these chemicals were likely not involved in naupliar survival reductions, because no delayed effect was observed when oxylipins were considered. This result indicates that oxylipin quantification is not sufficient to explain effects on *T. stylifera* naupliar survival at NI stage and population dynamics in the Gulf of Naples. Possibly, teratogenic effects could be evident at subsequent developmental stages than the NI nauplii; alternatively, other secondary metabolites synthesized by diatoms may act as defensive compounds.

In general, the present results support the view that egg production and naupliar survival variations can determine oscillations in recruitment rates of *T. stylifera* in the Gulf of Naples. Different factors seem to affect these two physiological responses. Environmental variables, such as temperature and oxygen, can play major roles in determining egg production potential, which seems to be supported by high diatom concentrations. Although salinity could play an important role in regulating naupliar survival rates, major effects on this physiological response may be mediated by discrete food items at delayed time scales. In this perspective, potential effects of nutritional resources and defensive compounds can occur and need further exploration.

3.4.2 De novo *transcriptome assembly and differential analysis*

Measuring naupliar survival rates at sea is crucial to estimate final recruitment in copepod populations, because wide oscillations in the viability of non-feeding larval stages

can occur (Carotenuto et al., 2006, Halsband-Lenk et al., 2005). As discussed in the previous section (3.4.1), population abundance of *T. stylifera* in the Gulf of Naples along 2017 was partially determined by naupliar survival rate variations. In this perspective, understanding which molecular mechanisms contributed to naupliar viability could help predict reproductive responses of this copepod species. Since *T. stylifera* females collected on 23rd and 30th of May only differed for naupliar survival rates, the transcriptomic analysis could allow elucidating molecular mechanisms involved in the maternal effect on early naupliar fitness. Also, this *de novo* assembled transcriptome contributes to enlarge the publicly available genomic resources for copepods (Bron et al., 2011).

The present transcriptome analysis resulted in 268,665 transcripts and 120,749 unigenes. These numbers were sensibly higher than results reported by (Lenz et al., 2014) for the calanoid copepod *Calanus finmarchicus* (206,041 contigs and 96,090 unique components), by (Ning et al., 2013) for the copepod *Calanus sinicus* (56,809 tags), by (Semmouri et al., 2018) for the copepod *Temora longicornis* (179,569 transcripts and 22,000 genes) and by (Zhou et al., 2018) for the copepod *Acartia tonsa* (113,786 transcripts and 53,619 genes). Rather, the *de novo* transcriptome assembly for *T. stylifera* was much closer to results presented by (Tarrant et al., 2014) for *C. finmarchicus*, because these authors reported 124,157 components and 241,140 transcripts. One positive aspect of the present transcriptome assembly is that the vast majority of the 20 top-hits BLAST species was represented by crustaceans and the first two top-hit species were the copepods *Eurytemora affinis* and *Acartia pacifica*. High affinity of the blasted copepod sequences to crustaceans and arthropods is increasing in the last years (Semmouri et al., 2018, Almada and Tarrant, 2016) and this indicates that publicly available copepod genomic resources are improving. Nonetheless, only nearly 50% of *T. stylifera* transcripts and unigenes found hits in BLASTx and around 25% of these sequences received GO annotation. These low percentages demonstrate that much effort still needs to be produced to put forward copepod genomic resources, even if the present results suggest improvements from

previous *de novo* transcriptomic analyses (Lee et al., 2015, Lenz et al., 2014, Ning et al., 2013).

Most unigenes were annotated in metabolic and cellular processes BP sub-categories (both 10.7%) and in cell or cell part (both 7%) CC sub-categories, in good agreement with previous transcriptomic studies on calanoid copepods (Semmouri et al., 2019, Zhou et al., 2018, Lenz et al., 2014, Ning et al., 2013). Among the total 268,665 transcripts, GO annotation indicated that 6.15% of these sequences were clustered in the BP sub-category codifying for organic substance metabolic process, while most sequences annotated in the MF category were assigned to organic cyclic and heterocyclic compound binding (5%).

Concerning differential expression analysis, more specific and wider functional annotations were reported for transcript isoforms. Therefore, these data will be mainly considered to discuss possible influence of up- and down-regulated sequences on lower naupliar survival rates observed in treated versus control copepod samples.

Differential expression analysis revealed that most of down-regulated transcripts were described as *putative Odorant-Binding Proteins*. Many of them were *A5-binding proteins*, which belong to the Phosphatidylethanolamine-Binding Proteins (Biessmann et al., 2005). These authors found expression of *A5* proteins in palps and antenna of the mosquito *Anopheles gambiae*, highlighting their role as chemosensory organs (Pikielny et al., 1994). Copepods base their feeding behaviour on mechanosensory setae, chemosensory sensilla (i.e. aesthetascs) or bimodal sensilla, present on antennules A1, antennas and the maxilliped. Such sensory organs allow copepods to distinguish different prey morphology, to detect foraging stimuli and avoid food items on the basis of chemicals (Heuschele and Selander, 2014). For example, (Leising et al., 2005) reported that *Calanus pacificus* can actively avoid *Skeletonema costatum* because of the high oxylipin synthesis potential reported for this diatom species (d'Ippolito et al., 2003). Nonetheless, other studies indicate that zooplankton cannot distinguish prey on the basis of their oxylipin synthesis potential

and that these chemicals are not feeding deterrents (Carotenuto and Lampert, 2004). Recently it has been demonstrated that copepods are able to detect dissolved PUAs and to respond positively to their presence (Kâ et al., 2014, Michalec et al., 2013). Differential expression of *Odorant Binding Proteins* in *T. stylifera* thus suggests altered feeding behaviour. However, it is difficult to discern whether this response depends on deleterious effects mediated by harmful molecules assimilated through the diet or whether it is part of a mechanism activated by the animal to avoid unsuitable preys.

The enzyme *Methylenetetrahydrofolate Dehydrogenase* (*MTHFD*) was listed among the up-regulated transcripts (log_2-FC of 4.45). Folate one-carbon metabolism plays a fundamental role in development and disease response of animals (Lee et al., 2012, Affleck et al., 2005). The folate metabolism is complex, because it involves the activity of several enzymes. The active folate form is the Tetrahydrofolate (THF) (Stanisławska-Sachadyn et al., 2008), which is a cofactor involved in the biosynthesis of thymidylate, purines, glycine, serine and homocysteine (Kompis et al., 2005). The enzyme Methylenetetrahydrofolate Dehydrogenase (MTHFD) converts Tetrahydrofolate (THF) into 10-Formyl, 5,10-Methenyl and 5,10-Methylene derivatives which are key cofactors in the *de novo* synthesis of DNA (Figure 3.27) (Steck et al., 2008). For example, altered folate expression has been shown to drastically reduce fecundity of *D. melanogaster* females (Affleck et al., 2005). Therefore, up-regulation of *MTHFD* suggests that *T. stylifera* females activated molecular pathways to counteract negative effects mediated by biotic or abiotic factors on their reproductive success.

Among the differentially expressed (DE) transcripts annotated in the Biological Process (BP) GO category and showing exclusive down-regulation after GO annotation, five sequences encoded for proteins involved in the oxidative phosphorylation chain for ATP production (log_2-FC ranging from -2.73 to -5.75). Several studies have reported that oocyte mitochondrial dysfunction in terms of respiration and electron transport can alter fertility and embryo development (Chakrabarti et al., 2009, Ramalho-Santos et al., 2009).

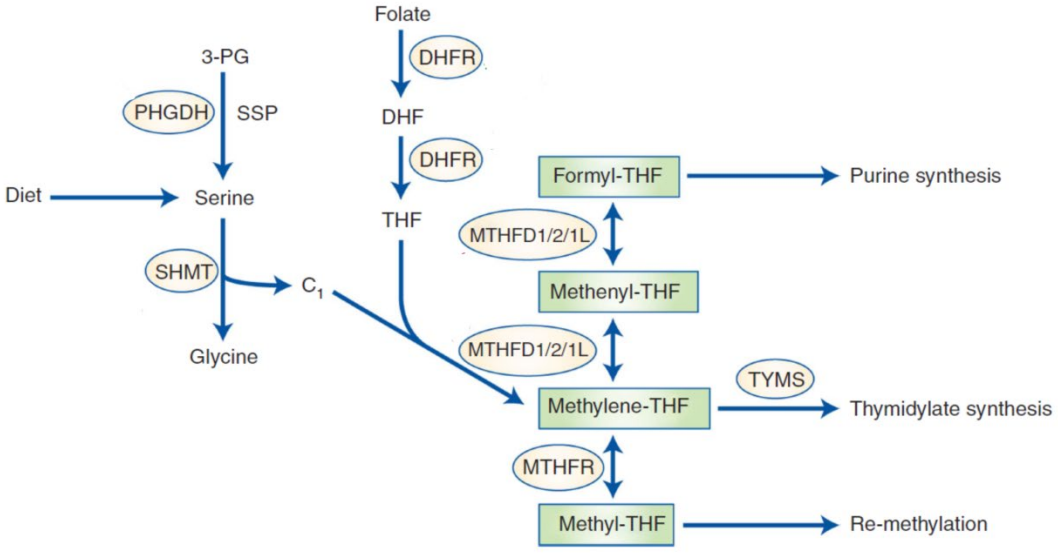

Figure 3. 27. One carbon metabolism pathway. Green and red text indicates established and potential chemotherapeutics, respectively. Enzymes are indicated in circles. Image modified from (Newman and Maddocks, 2017).

Possibly, down-regulation of the expression of the sequence codifying for the *Serine/Threonine Protein Phosphatase 2A* (*Ppa2*) was another relevant factor correlating with different naupliar survival rates. In fact, the important role of this enzyme in regulation of apoptosis has been documented (Klumpp and Krieglstein, 2002). These authors, in particular, reviewed that de-phosphorylation of BAD, a pro-apoptotic protein, by Pp1, Ppa2 and Ppb2 initiates cell death. On the other hand, (Fladmark et al., 1999) demonstrated that *Ppa2* inhibitors led to caspase-dependent apoptosis. Phosphodiesterases (PDEs) are enzymes influencing oocyte maturation in pre-ovulatory follicles (Tsafriri et al., 1996) and meiosis in oocytes (Richard et al., 2001). PDEs play a crucial role in acting as repressors of Ppa2 (Leslie and Nairn, 2019) through regulation of cAMP levels. As a result, down-regulation of PDE activity, as highlighted by differential expression analysis, could have led to higher cAMP levels and stronger stimulation of *Ppa2* as compensatory mechanism to re-equilibrate apoptosis regulation.

One further down-regulated sequence was the *Trinucleotide repeat-containing gene 18* (*Tnrc18*), which is involved in cell differentiation. In the last two decades, experimental

evidence has been reported about inhibitory effects of diatoms and their secondary metabolites on the embryonic development of planktonic copepods (Ianora et al., 2004, Poulet et al., 1995). Contribution of *Tnrc18* to development of copepod larvae is realistic, because this gene is known to have a chromatin binding activity and has been proposed as a new marker gene for development in zebrafish embryos (Armant et al., 2013).

Moreover, the sequence codifying for *Adaptor Protein Complex 2* (*AP-2*) showed a significant down-regulation (log_2-FC of -7.41) in *T. stylifera* showing low naupliar survival rates. AP-2 is involved in clathrin-dependent endocytosis in which proteins are incorporated into vesicles surrounded by clathrin (CVV) (McMahon and Boucrot, 2011). *AP-2* is therefore strictly related to both the endosomal and the lysosomal systems (Lau and Chou, 2008) and is essential to higher eukaryotic life (McMahon and Boucrot, 2011).

Dermatopontin (*DPT*), another significantly down-regulated protein, is involved in collagen fibril orientation (Catherino et al., 2004), thus its down-regulation and consequent impaired function could have led to negative effects on correct tissue formation in *T. stylifera* nauplii (Mizuta et al., 1994).

Among the four additional sequences classified in the signal transduction BP sub-category and down-regulated in wild *T. stylifera* females, the *1-Phosphatidylinositol 3-Phosphate 5-Kinase* (*FAB1B*) showed the strongest down-regulation (log_2-FC of -10.34). This enzyme catalyzes phosphorylation of the Phosphatidylinositol 3-Phosphate to synthesize Phosphatidylinositol 3,5-Bisphosphate, $PI(3,5)P_2$. This molecule is one of the seven regulatory Polyphosphoinositides (PPIn) that are ubiquitous in eukaryotes, where they regulate membrane trafficking in endosomes and lysosomes (Dove et al., 2009). Alteration in intracellular levels of $PI(3,5)P_2$ has been demonstrated to induce embryonic and neonatal lethality in animals (Ikonomov et al., 2011). Moreover, the fundamental role of Phosphatidylinositol-3,4,5-Triphosphate ($PI(3,4,5)P_3$) for survival rates of animal embryos has been reviewed by (O'Neill, 2008).

In support to the down-regulation of *FAB1B*, the significant up-regulation of the *Platelet-Activating Factor Acetyl Hydrolase* (*PAFAH*) suggests repression of the PPIn pathway. In fact, PAFAH is a particular type of Phospholipase A2 that deacetylates the Platelet-Activating Factor (PAF), inducing loss in its activity (Kordan et al., 2003, Arai et al., 2002). PAF is one of the most potent lipid mediators and occurs in membrane phospholipids. In mammals, PAF is supposed to importantly regulate reproductive cycle and pregnancy (Kordan et al., 2003). As shown in Figure 3.28, PAF initiates the enzymatic reactions leading to activation of PIP3, which determines high survival of offspring (O'Neill, 2008). Therefore, up-regulation of *PAFAH* in *T. stylifera* females collected on 23rd of May could have represented a synergic response with the strong down-regulation of *FAB1B*. In addition to PAF, PAFAH can target phospholipids and participate to oxidative-stress responses as well as to regulation of fertility and apoptosis (Kono and Arai, 2019).

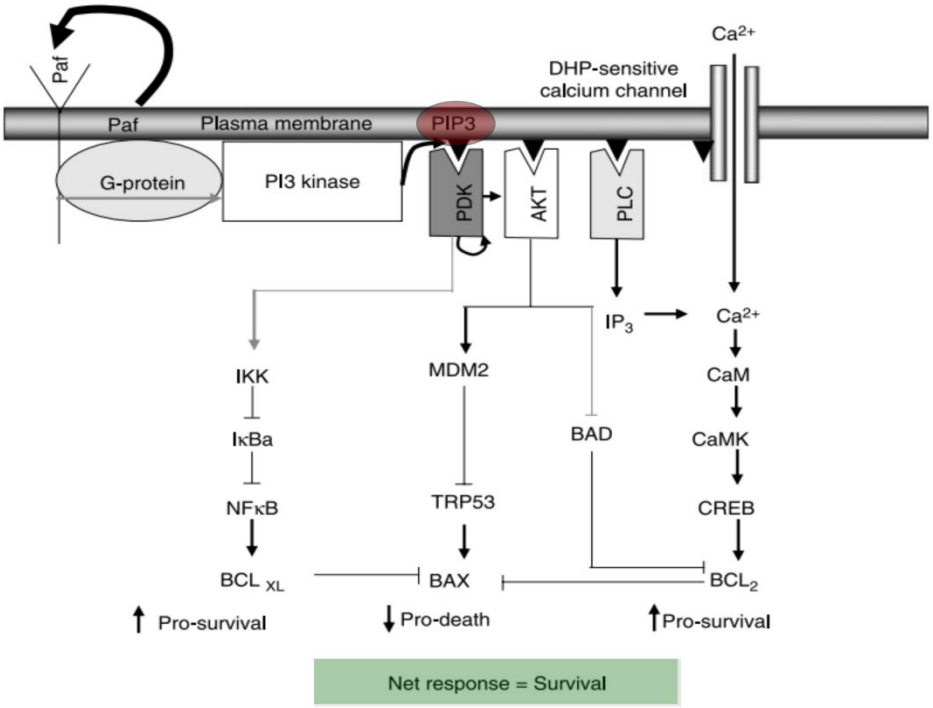

Figure 3. 28. Downstream consequences of PIP3 formation. PIP3 synthesized after enzymatic reactions creates a binding site for proteins containing the PH domain. Effectors can have effects on downstream targets. In the embryo, the net effect of PIP3 formation is the survival of the cells. Image modified from (O'Neill, 2008).

β-Tubulin was an exclusively up-regulated transcript. Previous laboratory experiments have reported variations in the expression of *α*- and *β-tubulin* genes in

copepods fed oxylipin-producing diatoms (Lauritano et al., 2015, Lauritano et al., 2011a, Lauritano et al., 2011b) and similar responses were quantified in the field for the copepod *Calanus helgolandicus* (Lauritano et al., 2016). Down-regulation of these genes was discussed as one of the factors leading to reproductive impairment mediated by diatoms on grazer copepods, because deficient tubulin polymerization affects spindle formation and cell division. The up-regulation of this sequence then suggests an active response of *T. stylifera* females to biotic and abiotic factors impairing reproductive success.

Significant up-regulation of the *protein maelstrom* (*mael*) is in line with the up-regulation of *β-tubulin*. In fact, mael has been reported as a required factor for the correct positioning of the microtubule-organizing centre (MTOC), in *D. melanogaster* (Clegg et al., 2001). Moreover, not only mael acts as a repressor for micro-RNA-7 in the nucleus, guaranteeing proper differentiation of germline cells (Siomi et al., 2011), but also contributes to oocyte determination (Pek et al., 2012).

Other sequences relevant for cell development and reproduction were selected from the differentially expressed unigenes and were further considered for the annual expression analysis at LTER-MC. Among them, *me31b* (*ATP-Dependent RNA Helicase*), *VLDLR* (*Very Low-Density Lipoprotein Receptor*) and *Vasa* (*ATP-Dependent RNA Helicase Vasa*) were up-regulated in *T. stylifera*. These three genes are involved in oocyte development and differentiation and could be part of pathways activated by *T. stylifera* females to counteract negative effects mediated by biotic and abiotic factors. *Me31b* is a gene expressed in polar granules and is involved in germ cell formation (Thomson et al., 2008). In particular, it has been shown to participate in mRNAs silencing in *D. melanogaster* oocytes (Nakamura et al., 2001). Similarly to *me31b*, *VLDLR* gene plays a crucial role in oocyte development, because it is a receptor that mediates the uptake of lipoproteins and vitellogenin in the developing oocytes (Khan et al., 2018). Similarly, also *Vasa* is known to be a fundamental regulator of oocyte differentiation and germline cyst development in animals (Styhler et al., 1998, Tomancak et al., 1998). In contrast to *me31b*, *VLDLR* and

Vasa, the gene *CREBL*-2 (*cAMP-Responsive Element-Binding Protein 2*), a transcription factor that can have important roles in cell cycle and cell differentiation (Hoornaert et al., 1998), was down-regulated.

Down-regulation was observed also for other sequences coding for key functions for development and reproduction. Among them, *Obst-E* (*Protein Obstructor E*) is known to code for a chitin-binding protein (Behr and Hoch, 2005) and is crucial for the correct cuticle development in arthropods (Tajiri et al., 2017). *ARIH-1* (*E3 Ubiquitin Protein Ligase*) is an E3 ubiquitin-protein ligase and, together with *Obst*-E, was included by (Legrand et al., 2016) in the list of the 31 genes involved in reproduction, growth and development in the calanoid copepod *Eurytemora affinis*, where ubiquitin genes were reported to affect gametogenesis. The down-regulated protein *Hsp-70 (Heat-Shock Protein 70)* has close affinity with E3 ubiquitin ligase proteins and it has been demonstrated to have a critical role in preventing apoptosis (Ravagnan et al., 2001). *Hsp-70* expression is also involved in thermo-tolerance mechanisms as well as in protection to xenobiotic exposure and to general stress in copepods (Lauritano and Procaccini, 2011, Aruda et al., 2011, Rhee et al., 2009, Voznesensky et al., 2004). Finally, the gene codifying for *ARSB* (*Arylsulfatase B*), mainly related to digestion of polysaccharides (Lyu et al., 2016) was an additional down-regulated sequence. This protein plays a central role in degradation of glycosaminoglycans (GAG) and altered *ARSB* activities can result in lysosomal excretion of these molecules (Karageorgos et al., 2007).

In general, information collected at the transcriptomic level revealed that *T. stylifera* females showing low naupliar viability responded by down- or up-regulating sequences coding for proteins involved in metabolic processes crucial for final reproductive success. In particular, key genes involved in ATP synthesis, cell differentiation and signal transduction could explain at a molecular level the low naupliar (NI) viability observed in the treated samples as well as molecular pathways regulated by *T. stylifera* females to counteract the low reproductive potential.

In this perspective, some differentially expressed genes are known to code for interconnected proteins participating in cellular biochemical patterns finally regulating apoptosis, cell cycle, yolk protein precursors (YPP), gene expression and autophagy. For example, up-regulation of *PAFAH*, as highlighted by the differential analysis, regulates apoptosis and cell cycle, while the gene codifying for *VLDLR* (also up-regulated) facilitates the ingression of lipoproteins in the cell, activating PPIn cascades (Santana and Marzolo, 2017). The differentially expressed sequences codifying for *FAB1B*, *Beta-amyloid protein* (*Aβ*), *Ppa2* and *CREBL* could indirectly play a central role in the regulation of yolk protein precursors (Dittmer et al., 2003). Moreover, the up-regulation of the *Trehalose-transporter 1* (*Tret1*), also supports negative regulation of autophagy in *T. stylifera*. These processes could partially disentangle coordinated molecular pathways leading to stress recovery and the high reproductive success observed on 30th of May.

3.4.3 Temporal variations of selected GOIs and relations with biotic and abiotic variables

Thirteen sequences (9 unigenes and 4 transcripts) were selected as genes of interest (GOIs) to inspect temporal expression variations along the sampling year 2017. These sequences were selected on the basis of several features, i.e. function, length, E-value, similarity, log_2-FC and significance (p-value).

Variations in the expression of these sequences in *T. stylifera* adult females collected along 2017 were inspected in the attempt to explain the molecular machinery possibly influencing the reproductive output of the copepod. In addition, possible effects of external biotic and abiotic variables on the expression levels of these 13 sequences were analysed. This study probably represents the first survey investigating temporal variations of 13 genes along one sampling year in a copepod species.

Obst-E and *Hsp-70* showed the highest expression values (MNE) along the year. Therefore, the role of *Obst*-E for cuticle development (Tajiri et al., 2017, Behr and Hoch,

2005) and of *Hsp-70* for stress responses (Aruda et al., 2011, Rhee et al., 2009, Voznesenski et al., 2004) might be molecular pathways modulated by the animals to cope with generic stress conditions. In contrast, the low MNE of *Ppa2*, *ARSB* and *MTHFD* suggests that expression of these three genes could be regulated in response to more specific stimuli or to overcome negative effects of factors acting on specific pathways. As highlighted by the PCA analysis, the 13 genes selected could already provide information about seasonal changes in the molecular responses of wild *T. stylifera* females. In fact, gene expression changed in particular from winter to spring, while summer and autumn were less separated.

GAM analyses are particularly useful to understand which factors could have driven different expression rates of the 13 genes, because they help to reveal non-linear relationships among variables. Overall, expression of 5 sequences out of the 13 selected were well related to *T. stylifera* physiological responses (faecal pellet production, egg deposition, egg hatching and naupliar survival rates). The *odorant-binding protein A5* was expected to drive variations in faecal pellet production, because of their role in arthropod chemosensory organs (Pikielny et al., 1994). This relation was not found and this result could indicate that the synergistic activity of other proteins might play important roles in regulating the feeding activity of copepods.

CREBL, *me31b* and *VLDLR* significantly predicted egg production. While the relation was negative with the first gene (low egg production at high expression), the number of eggs increased almost linearly along higher MNEs of *me31b* and *VLDLR*. This result is in line with previous evidence, because expression of *CREBL* has been proposed as a repressor of yolk protein precursors (YPP), such as vitellogenin and carboxypeptidase (Dittmer et al., 2003). YPP are essential for correct egg development and formation, thus low egg production at high MNE of *CREBL* is realistic. In this perspective, also the positive relationships between *me31b* and *VLDLR* with egg production may describe actual direct effects of these genes on the reproductive output of *T. stylifera* (Khan et al., 2018,

Thomson et al., 2008). On this basis, expression rates of *CREBL*, *me31b* and *VLDLR* proteins could represent sentinel genes to predict egg production of *T. stylifera* and potenetially of other copepod species in the field.

The genes codifying for *ARSB* and *Ppa2* were the only sequences, whose expression was significantly related to hatching success (*ARSB*) and naupliar viability (*ARSB* and *Ppa2*). Relations of egg hatching and larval survival to *ARSB* expression were oscillatory, but lower percentages were observed at high MNE of this gene. *ARSB* is involved in the degradation process of glycosaminoglycans (Karageorgos et al., 2007). High expression of this gene and consequent degradation of polysaccharides could then contribute to lower viability of eggs and larvae, likely due to low energy supplement to the embryos. *Ppa2* is a key gene for apoptosis regulation (Klumpp and Krieglstein, 2002). Naupliar survival rates in response to *Ppa2* MNE were oscillatory and of difficult interpretation, but variations in the expression of this gene could have contributed to the altered naupliar viability.

Among the 13 sequences selected, these five genes were considered as possible early warning signals for copepod physiological responses. Therefore, their expression was analysed in relation to biotic and abiotic factors to understand whether external variables could have affected copepod reproduction through alteration of molecular pathways related to these genes. While no environmental variable drove significant changes in *CREBL* expression, oxygen and transmittance significantly related to *VLDLR* MNE. Similarly, temperature, density and oxygen saturation well related to the MNE of *me31b*. This suggests that expression of *VLDLR* and *me31b* could have been modulated in response to environmental variables to maximize egg production at discrete values of temperature and oxygen, explaining production peaks along gradients of these variables (Holste et al., 2009, Marcus et al., 2004). Additionally, temperature, density and oxygen saturation were related to *Ppa2* expression. As discussed before, this gene is involved in apoptosis regulation (Klumpp and Krieglstein, 2002). *Ppa2* was significantly related to naupliar survival rates,

but no environmental variable drove significant variations of this physiological response. This could mean that expression of *Ppa2* was directly related to naupliar survival and was independent of environmental factors.

Expression of *VLDLR* and *me31b* was significantly related also with phytoplankton. *VLDLR* expression, in particular, decreased at high concentrations of coccolithophores, while showing oscillatory variations in relation to dinoflagellates and phytoflagellates. Oscillatory patterns are difficult to explain; a possible explanations for the expression variations of *VLDLR* should probably be discussed in relation to dinoflagellate and phytoflagellate composition. In contrast, low egg production rates have been reported for *C. helgolandicus* feeding on a coccolithophore diet (Huskin et al., 2000). High concentrations of this prey could have led to reduced *VLDLR* and *me31b* expression in *T. stylifera*. However, the number of eggs did not significantly vary in relation to coccolithophores; therefore, phytoplankton-mediated negative effects on *VLDLR* could have been counteracted through the expression of other genes.

Diatoms, dinoflagellates and phytoflagellates were significantly related to *ARSB* expression, which was more expressed at higher dinoflagellate and phytoflagellate concentrations, showing a unique peak at intermediate diatom densities. This gene is related to the digestion of polysaccharides (Karageorgos et al., 2007) and regulation of its expression along phytoplankton concentrations could be due to nutritional resources assimilated by *T. stylifera* after feeding. However, correlation of this gene to naupliar viability remains unclear.

Interestingly, *Ppa2* was the only gene whose expression was significantly related to oxylipin-per-cell concentrations. In particular, up-regulation of this gene at high HDoPE and HEpETE concentrations could constitute a copepod response to these teratogenic chemicals.

Chapter 4

Effects of diatom monospecific diets on physiological and molecular responses of *Temora stylifera*

4.1 Introduction

Since the first reports of negative effects of diatom mono-algal diets on the reproductive success of copepods (Ban et al., 1997), many laboratory experiments have been performed to better describe diatom-copepod interactions. Characterization of anti-proliferative molecules of diatom origin, such as PUAs (Miralto et al., 1999) and NVOs (Fontana et al., 2007b), offered a plausible explanation for the reduced fitness of copepod grazers after feeding on diatom preys (Wolfram et al., 2014, Md Amin et al., 2011, Ianora et al., 2011b, Buttino et al., 2008, Fontana et al., 2007b, Ianora et al., 2004).

Ingestion of oxylipin producing diatoms by adult copepod females leads to a maternal apoptotic effect on the offspring (Carotenuto et al., 2011, Adolph et al., 2004, Ianora et al., 2004) and direct mortality of nauplii, when these larval stages actively ingest oxylipin producing diatoms (Carotenuto et al., 2011). More recently, laboratory experiments started to encompass molecular analyses to investigate differential expression of genes in adult copepods after diatom ingestion (Lauritano et al., 2015, Carotenuto et al., 2014, Lauritano et al., 2011a, Lauritano et al., 2011b). Molecular techniques are advantageous in these experiments, because they can unveil intimate responses of the animals irrespective of physiological variations. For example, the different effects of oxylipins on adult and larval copepod stages might rely on the ability of adult females to activate molecular pathways counteracting negative effects mediated by harmful diatoms (Carotenuto et al., 2014).

Temora stylifera is a globally distributed neritic calanoid copepod (Bradford-Grieve et al., 1999) showing seasonal dominance of the copepod community in the Gulf of Naples (Mazzocchi et al., 2012, Mazzocchi et al., 2011). Although environmental variables, such as temperature, have been proposed to drive oscillations in the population dynamics of this copepod (Lindley and Daykin, 2005, Di Capua and Mazzocchi, 2004), life-history traits also represent useful predictors of such variations (Mazzocchi et al., 2006).

T. stylifera is usually described as a broadcast filter feeder privileging herbivory (Benedetti et al., 2018) and several laboratory experiments have highlighted sensitivity of this copepod species to diatom monospecific diets and pure oxylipins, which impaired egg production, egg viability and naupliar survival rates. (Ianora et al., 1995) tested the effects of the diatoms *Chaetoceros curvisetum* (CHA), *Phaeodactylum tricornutum* (PHA), *Thalassiosira rotula* (THA) and *Skeletonema costatum* (SKE) on *T. stylifera* in comparison to the flagellates *Prorocentrum minimum* (PRO) and *Isochrysis galbana* (ISO), reporting impaired egg viability in CHA, PHA and THA. Similarly, (Ceballos and Ianora, 2003) concluded that the diatoms THA, PHA, SKE and *Thalassiosira weissflogii* (TWEI) caused significant reductions in *T. stylifera* fitness because of reduced egg production and viability. Influence of diatom ingestion on copepods is not limited to maternal effects, because direct feeding of *T. stylifera* nauplii on oxylipin producing diatoms has been demonstrated to arrest development of larval stages as well as to influence the sex ratio of this species (Carotenuto et al., 2011, Carotenuto et al., 2002). As highlighted through laboratory setups, such negative effects are most likely mediated by secondary metabolites synthesized by the diatoms (Kâ et al., 2014, Buttino et al., 2008, Fontana et al., 2007b).

Despite this background information, many other experiments are still needed to unravel the complex interactions among copepods and their diets. In fact, not only diatoms show different oxylipin synthesis potential among genera, species and clones (Gerecht et al., 2011, Gerecht et al., 2013, Paffenhöfer et al., 2005), but also copepod responses differ among species and populations (Lauritano et al, 2015, Lauritano et al., 2012). Moreover, most laboratory setups tested the effects of diatoms at saturating concentrations, which often do not mirror natural occurrences in the field. In addition, no experiments included the contemporary analyses of copepod physiological and molecular responses as well as the chemical characterization of the algal species.

In this perspective, a series of laboratory experiments was performed to investigate physiological and molecular responses of the copepod *Temora stylifera* after feeding on

four diatom species in comparison to a dinoflagellate (*Prorocentrum minimum*) control diet. The diatoms *Asterionellopsis glacialis*, *Leptocylindrus* cf. *danicus*, *Chaetoceros curvisetus* and *Chaetoceros pseudocurvisetus* (Figure 4.1) were isolated from the Gulf of Naples and offered to adult *T. stylifera* females collected in the same area. *P. minimum* has been usually adopted as the ideal control diet to investigate the effects of diatoms on copepods, because of the low harmful potential of this dinoflagellate (Fontana et al., 2007b, Ianora et al., 1995). Oxylipin synthesis from Docosa-hexaenoic acid (DHA) has been recently documented in the Leptocylindraceae from the Gulf of Naples, but no laboratory setup has tested the effects of these diatoms on grazer copepods, so far. In particular, *L*. cf. *danicus* is among the dominating diatom species at LTER-MC (Ribera D'Alcalà et al., 2004), thus it was selected for the experiments. *A. glacialis*, although not occurring at high concentrations in the Gulf of Naples, was selected because it has been previously reported as a PUA-producing diatom species in the English Channel (Wichard et al., 2005a). Considering the limited number of PUA-producing diatoms in the Gulf of Naples (among the documented PUA-producing species, only *Thalassiosira rotula* is known to occur in this area), this diatom was offered to the copepod to investigate whether its harmful potential could have differed from other non-PUA producing species. Finally, the two *Chaetoceros*, *C. curvisetus* and *C. pseudocurvisetus*, were selected because this genus often constitutes the dominant fraction of diatoms at LTER-MC (Ribera D'Alcalà et al., 2004) (Chapter 2 of this thesis). Previous laboratory experiments have tested the effects of *C. affinis*, *C. socialis* and *C. curvisetum* on *T. stylifera* from the Gulf of Naples (Fontana et al., 2007b, Ianora et al., 1995), reporting negative influence of these algae on the reproductive success of the copepod. In this perspective, these two *Chaetoceros* species were selected to widen our understanding about the effects of this genus on *T. stylifera* in this area.

Effects on the reproductive potential of *T. stylifera* were estimated along 15 experimental days providing the four diatom diets at two concentrations. Differential

expression of 13 selected genes of interest (GOIs) was measured in copepods after 24 h and 48 h of feeding at the highest diatom concentration tested.

Figure 4. 1. Pictures (light microscope) of the algal diets offered to the copepod *Temora stylifera*. Top, left to right: *Chaetoceros pseudocurvisetus, Leptocylindrus* cf. *danicus* (2 cells); Bottom, left to right: *Chaetoceros curvisetus, Asterionellopsis glacialis, Prorocentrum minimum*.

4.2 Materials and methods

4.2.1 Feeding experiments

Temora stylifera specimens were collected at the Long-Term Ecological Research Station- MareChiara (LTER-MC, Gulf of Naples, Italy), from September 2017 to December 2017 during the early morning (09:00-11:00 h), by towing a 200 µm mesh nylon net with a non-filtering cod-end obliquely from ~50 m to the surface. Samples were poured in an insulated box and transported to the laboratory, within few hours after collection.

Healthy adult females and males were sorted under a stereomicroscope and transferred, as individual couples (N=10-24), to crystallizing dishes containing 100 ml of 50 µm filtered seawater collected at LTER-MC the same day. Females and males were incubated as individual pairs to ensure re-mating and the production of fertilized eggs (Ianora et al., 1989). After 24 h, faecal pellets, eggs and crumpled membranes (due to egg

cannibalism) were counted under a Zeiss Axiovert inverted microscope (25x magnification) to measure in istu pellet and egg production rates. Each couple was then transferred to new containers filled with 100 ml of 0.2 µm filtered seawater enriched with unialgal cultures. In total, the effects of four diatoms (*Asterionellopsis glacialis*-SZN FE355, *Leptocylindrus* cf. *danicus*-SZN FE354, *Chaetoceros curvisetus*-SZN FE330 and *Chaetoceros pseudocurvisetus*-SZN FE331) were tested in comparison to the dinoflagellate *P. minimum*-SZN FE100. *P. minimum* was used as control diet because this alga has been shown to induce high and stable hatching success in *T. stylifera* (Turner et al., 2001). Cell concentrations offered to copepods were adjusted depending on the algal diet to obtain similar carbon concentrations. In particular, two concentrations were tested: ≈1 µg-C/ml (high, H) and ≈0.1 µg-C/ml (low, L). Such values (H/L, respectively) corresponded to: ≈45,000/4500 cells/ml of *A. glacialis* (AST-H/AST-L), ≈25,000/2500 cells/ml of *L. danicus* (LEP-H/LEP-L), ≈6000/600 cells/ml of *C. curvisetus* (CUR-H/CUR-L), ≈8000/800 cells/ml of *C. pseudocurvisetus* (PSE-H/PSE-L) and ≈6000/600 cells/ml of *P. minimum* (PRO-H/PRO-L). The "low" concentration treatment allowed evaluating copepod responses after feeding on diatoms at cell densities much closer to natural occurrence. Mean biomass (pg-C/cell) of the four diatoms and *P. minimum* was calculated following standardized formulas for bio-volume calculation (Menden-Deuer and Lessard, 2000). Bio-volumes were in line with other biomass measurements on the same species (Mahadik et al., 2017, Wichard et al, 2005) (Table 4.1). The "high" carbon concentration used for the experiments was selected on the basis of previous laboratory setups and is considered the food saturating threshold (Carotenuto et al., 2011, Ceballos and Ianora, 2003, Carotenuto et al., 2002).

Table 4. 1. Morphological features of the algal species offered to *Temora stylifera*. Bio-volume is reported as mean value (±SE).

Species	Cell bio-volume (μm^3)	Morphology	State	Setae
P. minimum	1161.1 ± 118	Thecate	Non-colonial	Absent
A. glacialis	211.9 ± 8.6	Pennate	Colonial	Absent
L. danicus	492.7 ± 87.8	Centric	Colonial	Absent
C. curvisetus	1183.9 ± 71.8	Centric	Colonial	Present
C. pseudocurvisetus	913.3 ± 154.5	Centric	Colonial	Present

Each day, copepods were transferred to new containers with fresh media, keeping a daily record of eggs and faecal pellets produced by each copepod female. Hatching success and percentages of abnormal nauplii were determined 48 h later by adding ~10 ml of absolute ethyl alcohol to crystallizing dishes and counting the number of hatched and abnormal nauplii, respectively, settled to container bottoms. Egg cannibalism was accounted for by including crumpled egg membranes in daily egg production counts (Ianora et al., 1995). Hatching success was calculated as the percentage of nauplii with regard to egg production excluding crumpled egg membrane counts. Abnormality was calculated on the basis of hatched nauplii. Final fitness was calculated as the product of the number of eggs and the percentage of healthy nauplii and indicates the number of healthy nauplii/female-day, as described by (Ceballos and Ianora, 2003). Experiments were run for 15 days by maintaining animals at controlled temperature (20 °C) and photoperiod (12 h:12 h dark:light).

4.2.2 Algal isolation and culturing

The four diatom species were isolated from the natural phytoplankton community sampled at LTER-MC. Phytoplankton was collected at this sampling site by gently towing a 20 µm mesh plankton net for 10 min from the boat. The concentrated phytoplankton cells were then transferred to plastic bottles and brought to the laboratory within a few hours. Here, few drops of the concentrated natural phytoplankton sample were diluted in a Petri

dish filled with 10 ml of f/2medium (Guillard and Ryther, 1962). Single cells of each species were isolated with a glass capillary and transferred to sterile well plates to verify mono-specific isolation.

The four diatom species were grown in semi-continuous cultures in 2 L polycarbonate bottles containing f/2 medium (Guillard and Ryther, 1962), while the dinoflagellate *P. minimum* in f/2 medium without silica. All algae were subjected to a 12 h:12 h dark:light cycle and a light intensity of 110 µmol (m^2/s). Algal cell concentration was determined on a daily basis, before diet addition to the incubation water, by counting the number of cells in random fields of a Sedgewick-Rafter counting chamber (1 ml) under a light microscope (Zeiss Axioskop2, 200x magnification). Cultures were offered to copepods in late exponential growth phase.

4.2.3 RT-qPCR analyses on selected GOIs

To investigate molecular responses of *T. stylifera* after feeding on the four diatom species, adult copepod females were captured from the field and were provided mono-algal diets administered at high concentration (≈1 µg-C/ml). Experimental setup followed procedures described in previous laboratory experiments (Lauritano et al., 2011a, Lauritano et al., 2011b). Around 300 specimens were isolated the same day from the zooplankton samples collected at LTER-MC (see section 4.2.1 for sampling method). An equal number of females was distributed in six polycarbonate 2 L bottles filled with 0.22 µm filtered seawater.

Copepods were left to acclimatize for 24 h at controlled temperature (20 °C) and photoperiod (12 h:12 h, dark:light). After acclimatization, *T. stylifera* females were provided fresh 0.22 µm filtered seawater and algal cells at a concentration of ≈1 µg-C/ml. In particular, three polycarbonate bottles were filled with the diatom diets and the other three with *P. minimum* for control (algae were grown as described in section 4.2.2). The experimental medium was renewed daily. A variable number of copepods (N=5-20) was

collected after 2 days and 7 days of feeding. Specimens collected from each bottle were stored separately in six 1.5 ml eppendorf tubes. Therefore, three replicates for treatment and control diets were available at the two sampling times.

RNA extraction and subsequent analyses were performed following procedures described in Chapter 3. In particular, RNA was extracted using the RNeasy Micro extraction kit (Qiagen, Hilden, Germany). RNA concentration (ng/µl) and purity were quantified through Nanodrop ND-1000 (Marshall Scientific, Hampton, USA). 1 µg of RNA was used for reverse-transcription to cDNA using the iScriptTM cDNA Synthesis Kit (Bio-Rad, Hercules, USA). Expression of the 13 genes selected during the field survey (i.e. *A5*, *CREBL*, *PPA2*, *me31b*, *Obst*-E, *ARIH1*, *ARSB*, *HSP70*, *VLDLR*, *MOB1B*, *Vasa*, *PAFAH* and *MTHFD*) was assessed using the genes codifying for 18S RNA and UBI as reference genes. Expression rates were quantified through RT-qPCR performed with a Viia7 Real Time PCR system (Applied Biosystem, Foster City, USA). The final PCR volume for each sample was 10 µl, with 5 µl of SensiFAST SYBR Green Master Mix (Meridian Inc., Cincinnati, USA), 1 µl of cDNA template (1:5 dilution in Milli-Q water) and 4 µl (concentration of 0.7 pmol/µl) of each primer pair F+R. All RT-qPCR reactions were carried out in triplicate with additional three negative controls (consisting of 1 µl of Milli-Q water instead of the cDNA template).

To evaluate whether molecular responses of *T. stylifera* females explained the physiological responses observed and reflected chemical traits of diatom diets, mean normalized expression (MNE) of each gene was calculated with QGene software (Simon, 2003), according to formula (2), as described in Chapter 3. MNE was obtained after normalization with both the *18S* and *UBI* genes, then calculating the average MNE between the two RGs. Expression stability of these two RGs was confirmed by the low differences in Ct values of both 18S (17.3±0.79) and UBI (17.68±0.78) at the different experimental condition. Average MNEs were considered for the three samples collected after feeding on each diet after 2 and 7 experimental days. Significance in the expression of

each gene between treated and control samples was analysed by applying t-tests, adopting Welch's correction when necessary. Because some genes were constitutively more expressed than others, multivariate analyses were conducted after a log-transformation of the MNE values. To allow log-transformation from decimal MNE values, MNEx10^6 were calculated. PCA and cluster analyses on the log-transformed MNE were performed to investigate multivariate distribution of replicates depending on diatom diets.

4.2.4 Chemical analyses

To characterize the chemical profile of the four diatoms, the species were grown in triplicate in 2 L polycarbonate bottles at the same conditions as the cultures used for feeding experiments. Cell concentration was daily monitored. Once cultures reached late exponential/initial stationary phase, they were split in two aliquots and centrifuged with a Beckman Allegra 6R centrifuge (10 min, 4 °C, 700 RCF). One aliquot was exploited for oxylipin and fatty acid analysis, while the other one for elemental composition analysis.

Extraction and quantification of oxylipins were performed following standardized protocols (for further methodological details, refer to) (d'Ippolito et al., 2018, Cutignano et al., 2011), using 16-Hydroxyhexadecanoic acid (1 mg:10 ml, dissolved in methanol) and 4-decenale (1 mg:1 ml, dissolved in methanol) as internal standards for non-volatile oxylipins and poly-unsaturated aldehydes, respectively. Briefly, Milli-Q water was added to the pellet (1 ml/g pellet). Cells were broken through sonication (1 min in ice bath) and left for 30 min at room temperature. Subsequently, enzymatic reactions were stopped by adding acetone (C_3H_6O) in equal volume as water. Samples were then centrifuged with a Beckman Allegra 6R centrifuge (6 min, 4 °C, 1452 RCF) and the supernatant was extracted twice with dichloromethane (CH_2Cl_2). Organic phase was collected in a round-bottomed flask, dried and finally weighted. One third of the extract was methylated with diazomethane (30 min in ice bath) for non-volatile oxylipin characterization, while the rest

was derivatized with Carbethoxyethylidene triphenylphosphorane (CET, 20 h at room temperature) for PUA analysis.

Non-volatile oxylipin analysis was carried out with a Q-Exactive Hybrid Quadrupole-Orbitrap mass spectrometer as indicated in Chapter 2. Poly-unsaturated aldehydes were quantified through Ion-trap GC-MS/MS (Thermo ITQ 700 Mass spectrometer interfaced with Thermo Focus GC Polaris Q) in EI^+ mode (70eV) and mounting a 5% diphenil-polysiloxane (OV-5) column. Thermal gradient was set in accordance to methods described by (d'Ippolito et al., 2018).

The six most abundant non-volatile oxylipin species deriving from diatom PUFAs were targeted for the analysis. The oxylipin species were the same targeted during the field survey described in Chapter 2. When possible, lipoxygenase activity was inferred through MS/MS fragmentation of epoxy-alcohols (Cutignano et al., 2011). Oxylipin quantification followed the same calculation described in Chapter 2, but for these experiments oxylipin concentration was standardized by dividing the weight (ng_x) by the mg C measured for each species through CHN analysis (see later).

For fatty acid analysis, an aliquot of oxylipin extracts was collected and treated for transesterification to favour free fatty acid lysis from the glycerol group. Briefly, 5 mg of the dry extract were re-suspended in methanol. Sodium carbonate (Na_2CO_3) was then added to the sample. After 24 h of continuous agitation at room temperature, 1 ml of Milli-Q water was added, then adjusting pH to 7 with few drops of acetic acid (CH_3COOH). Fatty acids were extracted adding ethyl ether ($C_4H_{10}O$) in the same volume of water (1 ml:1 ml) and transferring the organic phase to a new vial. The extracts were dried and re-suspended in methanol for GC-MS/MS analysis. Thermal gradient followed settings described by (d'Ippolito et al., 2018). Fatty acids were identified on the basis of their retention time and mass spectra, comparing MS/MS fragmentations with those available on the NIST MS Search 2.0 online library. Fatty acids were quantified comparing peak areas of the fatty acids identified in the sample with the area of the standard (Nona-decanoic

acid, 1 mg:1 ml, dissolved in DMSO), which was added to the sample before oxylipin extraction.

For the analysis of diatom elemental composition, pellets were ice-dried and a minimum of 3 mg of each pellet was transferred to tin cups (N=3). Elemental composition was characterized with a CHNS/O analyser Flash 2000 (Thermo Scientific, Waltham, USA). Concentration of carbon and nitrogen was calculated in comparison to the internal standard Sulfanilamide and elemental abundance was reported as N:C ratio for the four diatoms.

4.2.5 Data analysis

To test for effects of the four diatoms on pellet and egg production, hatching success, naupliar abnormality and final fitness, two-way ANOVA tests considering interaction (experimental design consisting of two fixed and orthogonal factors, i.e. diet and concentration) were applied for every diet. To avoid temporal dependency, mean values of faecal pellets, eggs, hatching success, naupliar abnormality and fitness were calculated for each female along the 15 experimental days. Therefore, the number of *T. stylifera* females represented the experimental replicates for each diet (N=10-24). To produce balanced tests, group means were considered as missing replicates, when necessary (Underwood, 1997). The number of substitutions was then subtracted from the total degrees of freedom of the test to calculate the respective p-value. In case of heteroscedasticity at d.f.<40, significance was considered at $p<0.01$ to avoid type I error, because data transformation was not successful in respecting ANOVA assumption (Underwood, 1997). Post-hoc comparisons were performed applying Tukey HSD tests.

Significant variations in elemental composition (C, H, N and N:C ratio) among the four diatom diets were assessed through Kruskal-Wallis tests followed by t-tests to compare each single diet (AST, LEP, CUR and PSE).

PCA analyses were performed on log-transformed oxylipin data to inspect chemical trait similarity among the four diatoms as well as on copepod physiological and molecular responses to compare effects mediated by diatoms. When considering copepod physiological response variables, data were standardized, because of the different measurement units (N/couple-day and %), following the formula: $Z = (\mathrm{X} - \mu)/\sigma$, where Z is the standardized value, X is the raw value, μ is the population mean and σ is the standard deviation.

Cluster analyses were also performed to better investigate clustering of the four diatoms on the basis of their chemical traits as well as clustering of *T. stylifera* responses depending on physiological and molecular variables. For cluster analyses on chemical traits (i.e. oxylipins and fatty acids) of diatoms, similarity was calculated on the basis of Bray-Curtis index. Dendrograms for copepod physiological responses were built considering standardized values of pellets, eggs, hatching and abnormality after feeding on diatoms at high and low carbon concentrations and were built on Euclidean distance measure. Differences in molecular responses were performed considering log-transformed MNE of the 13 genes at day 2, day 7, in treated and control samples (in this case day 2 and day 7 were considered together). Differences in molecular responses were based on Euclidean distance.

To verify whether molecular responses of *T. stylifera* observed after experimental feeding reflected natural conditions, a Redundancy Analysis (RDA) was performed on field data (see Chapter 2 and 3). In particular, natural concentrations of the four diatom species selected were considered as the drivers of different MNE measured in the respective dates for *T. stylifera*. RDA is an interpretative multivariate technique that inspects how a multivariate matrix of constraining variables (in this case the diatom species) explains variations of a set of depending variables (in this case the 13 genes) (Paliy and Shankar, 2016).

Statistical analyses were carried out in R (version 3.5.0) and GraphPad Prism 4.

4.3 Results

4.3.1 Feeding experiments

Figure 4.2 and Table 4.2 show temporal variations in *T. stylifera* physiological responses along the 15 experimental days. While Figure 4.2 reports variations among females for each experimental day and for each physiological variable, Table 4.2 shows the average values calculated along the 15 experimental days.

Depending on the diet and the concentration provided, production of faecal pellets and eggs varied in *T. stylifera*. Different patterns in hatching success and naupliar abnormality were also observed.

The highest pellet production was observed in the CUR-H treatment (103.29 ±7.52), while the lowest in PRO-L (29.87 ±1.34). The control diet represented the best food for egg production, as the highest number of eggs was observed in treatment PRO-H (25.02 ±1.93). However, PRO-L treatment led to the lowest egg production (7.67 ±2.3). In general, lower egg production rates were detected at low food concentration, but *T. stylifera* feeding on *L. danicus* showed an opposite pattern. The highest hatching success rates were recorded in the control diet (86.11 ±1.49 PRO-H; 78.3 ±3.01 PRO-L), while the lowest value was observed in the PSE-H treatment (34.06 ±13.45). *P. minimum* did not induce abnormality in the hatched nauplii; in contrast, the highest percentage was measured in the AST-H treatment (28.86 ±10.31). In general, higher abnormality values were recorded in all diatom diets compared to controls, at high concentration. However, the opposite trend was true for the diatom *C. curvisetus*.

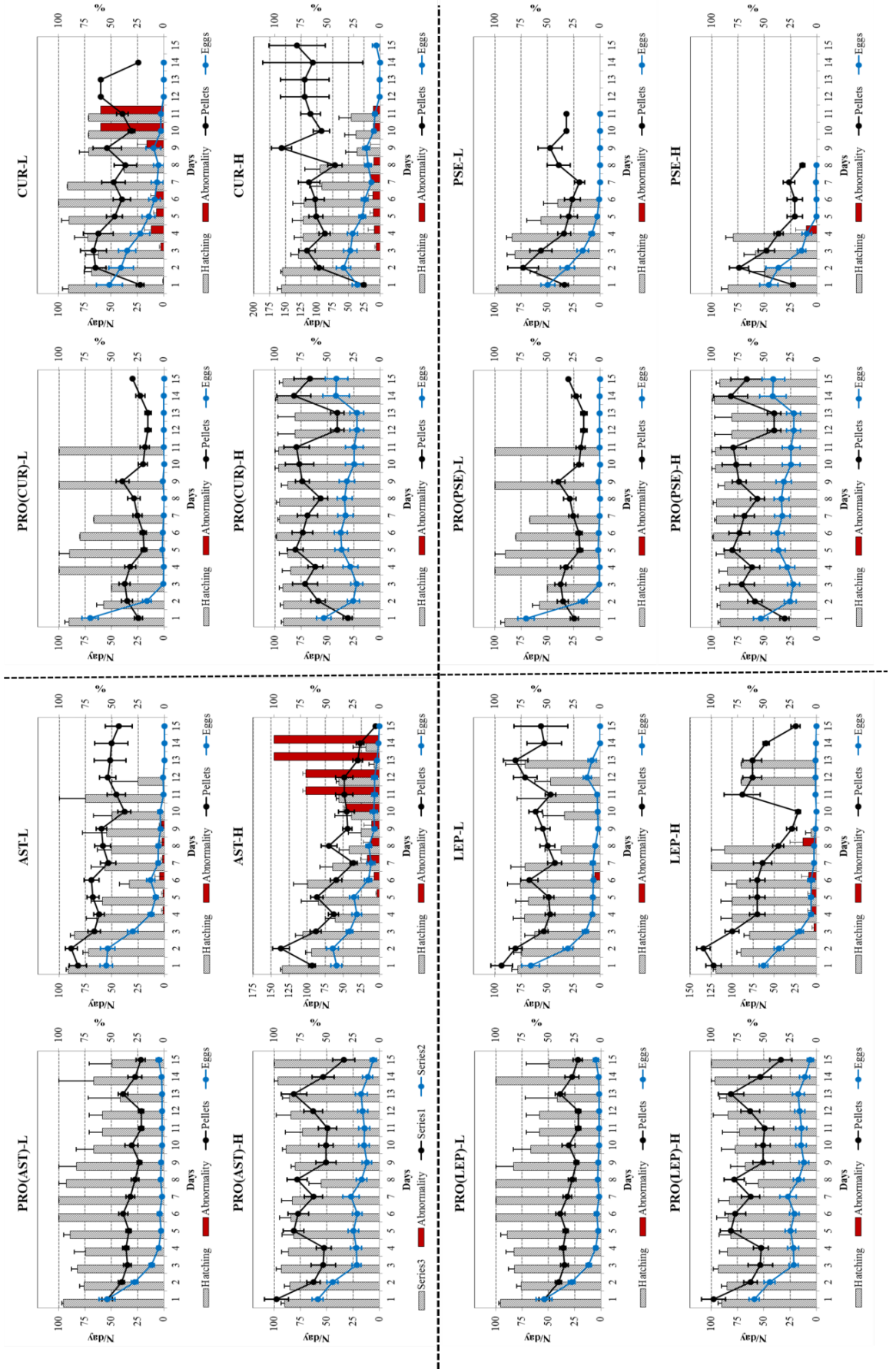

Figure 4. 2. Temporal physiological responses of *Temora stylifera* adult females to diatom and control diets provided at high (1 µg-C/ml) and low (0.1 µg-C/ml) concentrations.

Table 4. 2. Mean (±SE) values of pellets, eggs, hatching success (%) and abnormality (%) calculated for all females over the experimental period (max. 15 days). The four diet treatments at the two concentrations are shown. Diets: PRO=*P. minimum*, AST=*A. glacialis*, LEP=*L. danicus*, CUR=*C. curvisetus*, PSE=*C. pseudocurvisetus*. Concentrations ("Conc."): L=low (≈0.1 µgC/ml), H=high (≈1 µgC/ml). The lowest and the highest values measured are indicated in bold for each variable.

Diet	Conc.	Pellets Mean (±SE)	Eggs Mean (±SE)	Hatching Mean (±SE)	Abnormality Mean (±SE)
PRO	***L***	**29.87 (±1.34)**	**7.67 (±2.3)**	78.3 (±3.01)	**0**
	H	63.45 (±2.4)	**25.02 (±1.93)**	**86.11 (±1.49)**	**0**
AST	***L***	59.41 (±3.6)	12.92 (±4.81)	59.74 (±5.63)	1.08 (±0.4)
	H	58.63 (±8.42)	20.27 (±5.46)	43.4 (±6.71)	**28.86 (±10.31)**
LEP	***L***	60.42 (±3.84)	11.17 (±4.37)	56.91 (±6.31)	0.43 (±0.43)
	H	70.05 (±8.45)	10.35 (±4.8)	66.86 (±9.19)	2.9 (±1.24)
CUR	***L***	46.69 (±4.02)	14.08 (±4.47)	75.08 (±5.23)	15.02 (±6.89)
	H	**103.29 (±7.52)**	20.9 (±4.72)	55.52 (±8.83)	4.42 (±0.95)
PSE	***L***	38.42 (±4.59)	9.82 (±4.94)	69.6 (±8.61)	**0**
	H	32.8 (±6.98)	13.42 (±6.39)	**34.06 (±13.45)**	2.5 (±2.5)

In order to avoid temporal dependency in data analysis, ANOVA tests were based on average values calculated separately for each female along the 15 experimental days. *Asterionellopsis glacialis* was the only diatom that significantly affected all variables in *T. stylifera*, depending on the concentration it was provided to the copepod (Figure 4.3). The concentration effect of this diatom was less pronounced on hatching success, but still significant in its interaction with the first factor (i.e. diet) (Table 4.3).

In particular, lower concentrations of *A. glacialis* sustained higher production of faecal pellets and eggs than the control (PRO-L vs AST-L: diff.=-29.6, $p<0.001$; PRO-L vs AST-L: diff.=-8.5, $p<0.001$, respectively), while similar outputs were observed at high concentrations (PRO-H vs AST-H: diff.=-2.7, $p>0.05$; PRO-H vs AST-H: diff.=-0.3, $p>0.05$, respectively). Hatching success decreased when the higher concentration of *A. glacialis* was provided (AST-L vs AST-H: diff.=14.81, $p<0.01$), while similar high hatching percentages were detected after copepods fed on *P. minimum* at both concentrations (PRO-L vs PRO-H: diff.=-0.6, $p>0.05$). No abnormal nauplii were detected when females fed on the dinoflagellate. In contrast, abnormality increased along with concentration of this diatom (AST-L vs AST-H: diff.=-4.56, $p<0.01$). Fitness was

significantly influenced by the interaction of the two factors (i.e. diet and concentration; $p<0.001$). In particular, higher fitness after feeding on AST than PRO was calculated at low concentrations (PRO-L vs AST-L: diff.=-5.29; $p<0.05$), while the opposite pattern was observed at the highest carbon concentration (PRO-H vs AST-H: diff.=8.94; $p<0.001$).

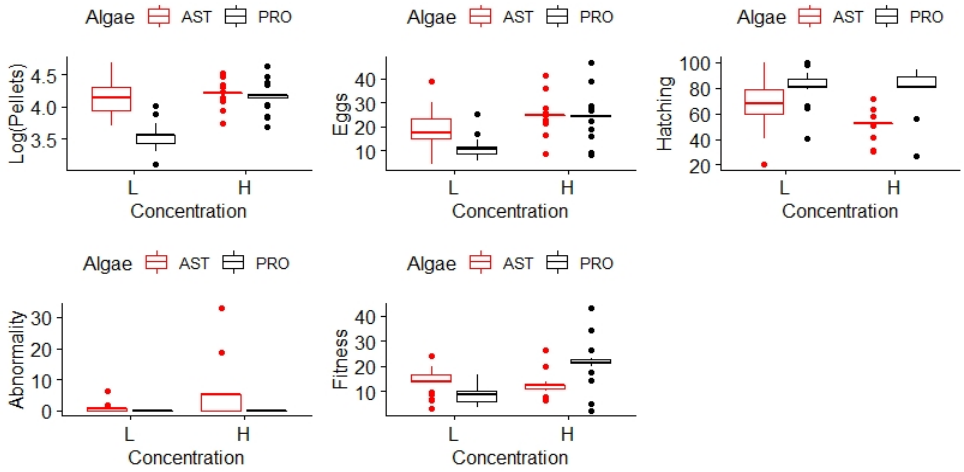

Figure 4. 3. Boxplot showing differences in faecal pellet, egg production, hatching succes, naupliar abnormality and final fitness measured for the copepod *T. stylifera* after feeding on the diatom *A. glacialis* (AST) in comparison to the control diet *P. minimum* (PRO). Values observed at the two concentrations (H and L) are shown.

Depending on concentration, the diatom *Leptocylindrus* cf. *danicus* also showed significant effects on all physiological variables measured for *T. stylifera* (Figure 4.4, Table 4.3). However, hatching success was only affected by the diet and not by concentration or the interactive effect of these two factors. Faecal pellet production significantly varied depending on diatom concentration only in comparison to the control diet (PRO-L vs LEP-L: diff.=-29.92, $p<0.001$; PRO-L vs LEP-H: diff.=-36.74, $p<0.001$) and not depending on concentration, because no significant difference was revealed between LEP-L and LEP-H treatments (diff.=-9.81, $p>0.05$). High egg production in the PRO-H treatment drove the significant result observed for this variable. In fact, no significant differences were detected between PRO-L and LEP-L (diff.=-4.83, $p>0.05$), PRO-L and LEP-H (diff.=-2.41, $p>0.05$) and LEP-L and LEP-H (diff.=2.42, $p>0.05$). As for the experiment with *A. glacialis*, no significant difference in hatching success was

observed in the control at the two concentrations. By contrast, *L.* cf. *danicus* provided at low concentrations induced lower hatching than the control diet (LEP-L vs PRO-H: diff.=-17.1, $p<0.05$; LEP-L vs PRO-L: diff.=-16.55, $p<0.05$). Significant abnormality rates were driven by LEP-H treatment, which differed from LEP-L (diff.=-2.39, $p<0.001$) and the control diet. The high fitness observed in the PRO-H treatment also drove the significant interaction among the two experimental factors. In fact, all post-hoc comparisons involving PRO-H were highly significant ($p<0.001$).

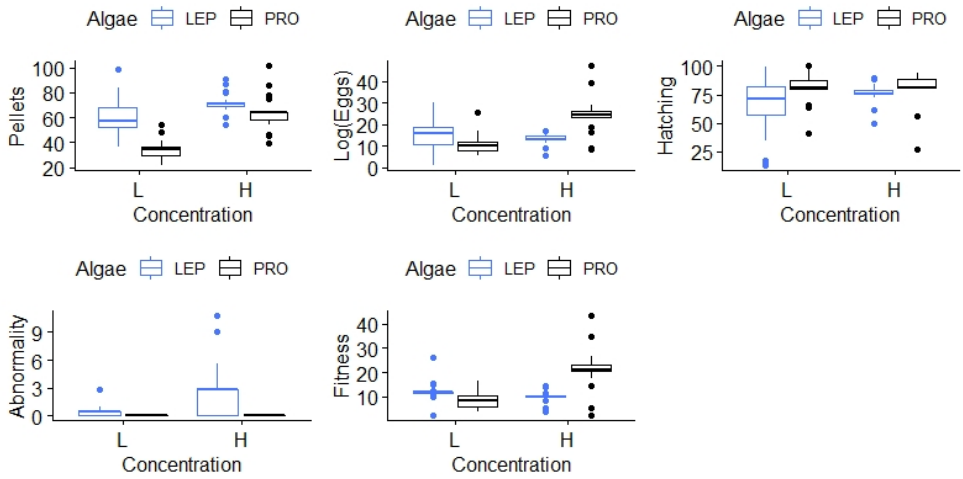

Figure 4. 4. Boxplot showing differences in faecal pellet, egg production, hatching succes, naupliar abnormality and final fitness measured for the copepod *T. stylifera* after feeding on the diatom *L. danicus* (LEP) in comparison to the control diet *P. minimum* (PRO). Values observed at the two concentrations (H and L) are shown.

The diatom *Chaetoceros curvisetus* showed significant interactive effects only on egg production (Figure 4.5, Table 4.3). Faecal pellet production was higher in the diatom treatment (PRO-L vs CUR-L: diff.=-1.8, $p<0.01$; PRO-H vs CUR-H: diff.=-1.74, $p<0.01$) and at the high concentrations (PRO-L vs PRO-H: diff.=-3, $p<0.001$; CUR-L vs CUR-H: diff.=-2.94, $p<0.001$). The interactive effects on egg production rates were mainly driven by the difference in the control (PRO-L vs PRO-H: diff.=-20.44, $p<0.01$). Hatching success significantly varied depending only on diet, because differences were significant between the diatom and the control (PRO-H vs CUR-H: diff.=26, $p<0.01$; PRO-H vs CUR-L: diff.=21.4, $p<0.05$), but not between the two concentrations (CUR-H vs CUR-L:

diff.=4.6, p>0.05). Fitness variations were significant when the interactive effect of the two factors was considered.

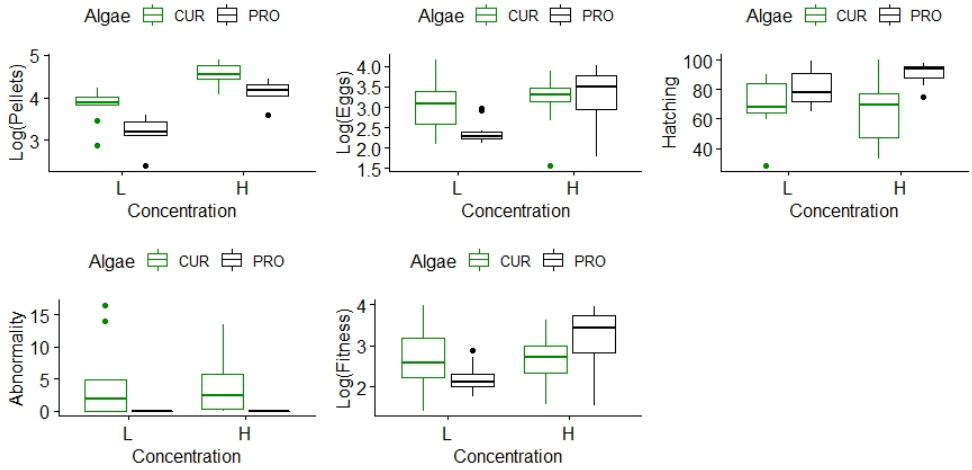

Figure 4. 5. Boxplot showing differences in faecal pellet, egg production, hatching succes, naupliar abnormality and final fitness measured for the copepod *T. stylifera* after feeding on the diatom *C. curvisetus* (CUR) in comparison to the control diet *P. minimum* (PRO). Values observed at the two concentrations (H and L) are shown.

Chaetoceros pseudocurvisetus drove significant variations in faecal pellet production in relation to its concentration (Figure 4.6, Table 4.3). Egg production was affected by algal concentration irrespective of the diet provided (the diatom or the control diet), even if the concentration effect could have been biased by the "type I" error (d.f.<40 and heteroscedasticity). Hatching success was significantly lower when the diatom was offered at the high concentration (PRO-H vs PSE-H: diff.=27.9, p<0.01). Interaction of diet and concentration was slightly significant (p<0.05), but possibly subjected to "type I" error. Final fitness was significantly affected by the interaction of diet and concentration in all treatments. Such response was less significant in the *Chaetoceros* (both *curvisetus* and *pseudocurvisetus*) treatments. For the experiment with *C. pseudocurvisetus*, in particular, heteroscedasticity could have affected final significance of the test.

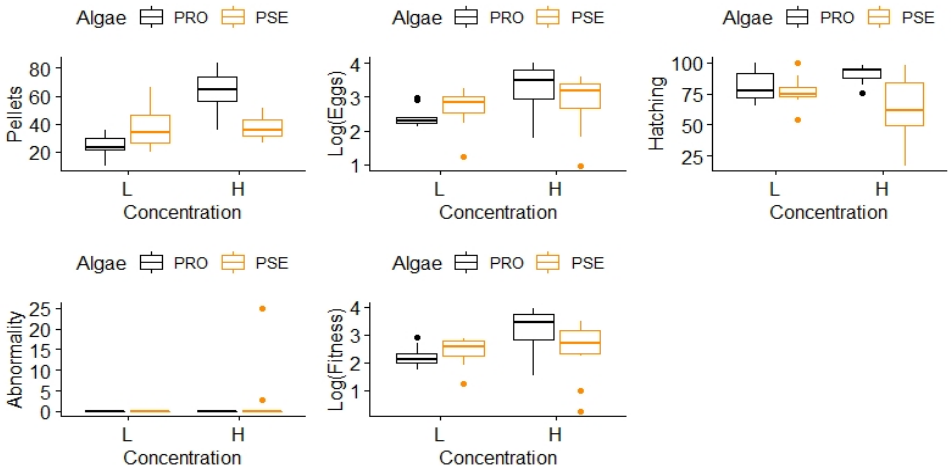

Figure 4. 6. Boxplot showing differences in faecal pellet, egg production, hatching succes, naupliar abnormality and final fitness measured for the copepod *T. stylifera* after feeding on the diatom *C. pseudocurvisetus* (PSE) in comparison to the control diet *P. minimum* (PRO). Values observed at the two concentrations (H and L) are shown.

Table 4. 3. Two-way ANOVA results for the four variables measured in *Temora stylifera* during laboratory feeding experiments, in comparison to the control diet *P. minimum*. Diets: PRO=*P. minimum*, AST=*A. glacialis*, LEP=*L. danicus*, CUR=*C. curvisetus*, PSE=*C. pseudocurvisetus*. Factors: D=Diet, C=Concentration, DxC=Interaction between the two factors. Asterisks indicate significance level: p<0.05(*), p<0.01(**), p<0.001(***); *!=significance at d.f.<40 and heteroscedasticity (Bartlett's test: p<0.05); n.s.: not significant.

Diet	Factors	F. Pellets	Eggs	Hatching	Abnormality	Fitness
	D	***	**	***	***	n.s.
AST	***C***	***	***	*	**	***
	DxC	***	**	*	**	***
	D	***	n.s.	**	***	**
LEP	***C***	***	***	n.s.	***	***
	DxC	***	***	n.s.	***	***
	D	***	n.s.	***	**	n.s.
CUR	***C***	***	*	n.s.	n.s.	*
	DxC	n.s.	*	n.s.	n.s.	*
	D	n.s.	n.s.	**	n.s.	n.s.
PSE	***C***	***	*!	n.s.	n.s.	*!
	DxC	***	n.s.	*!	n.s.	*!

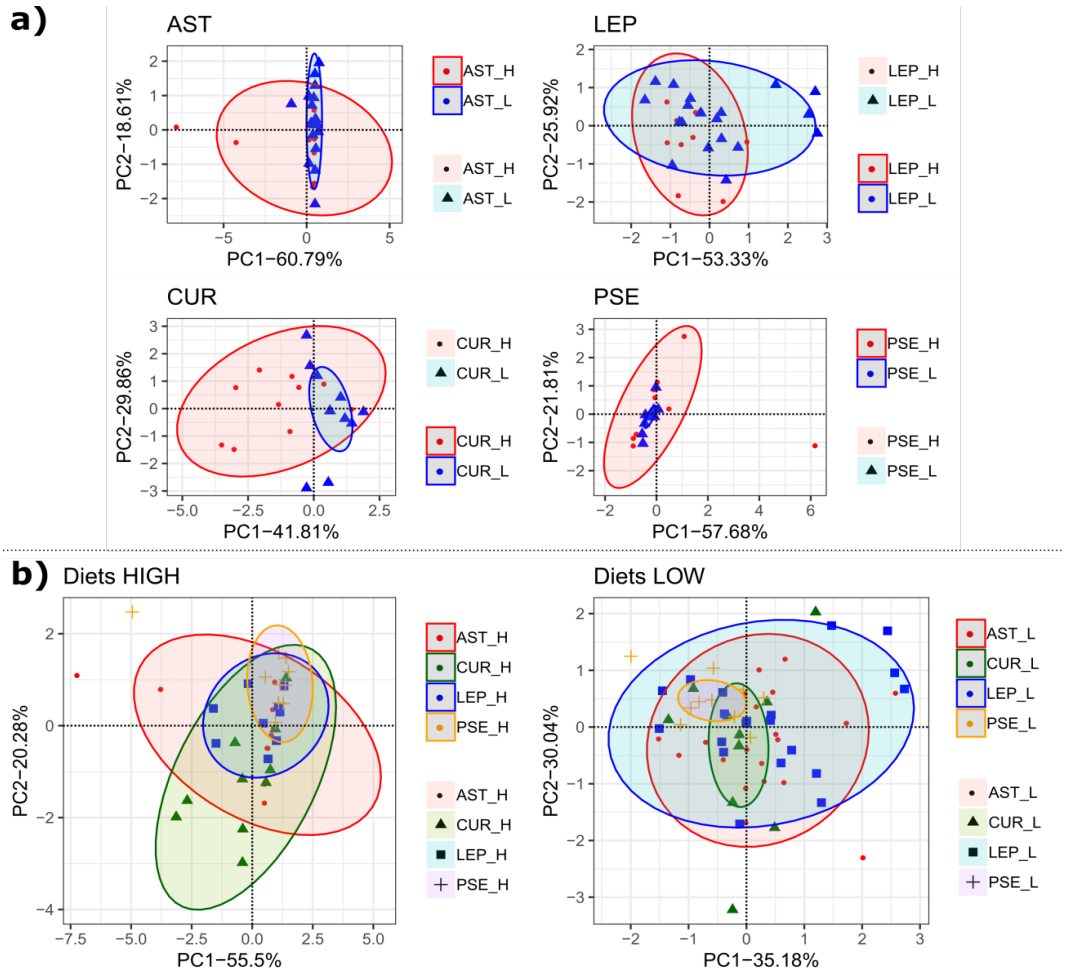

Figure 4. 7. a) PCA representations of *T. stylifera* responses (pellet and egg production, hatching success and abnormality) after feeding on the four diatoms (AST, LEP, CUR and PSE) at the two concentrations considered (HIGH and LOW). b) PCA representations of *T. stylifera* responses (pellet and egg production, hatching success and abnormality) feeding on diatoms administered at the HIGH and LOW concentrations. Data were standardized before analysis.

PCA analyses allowed multivariate comparisons of copepod responses to each diet and concentration. When responses to each diet were compared, first two PC axes offered an effective representation, explaining around 80% of total variation (Figure 4.7a). Main drivers of copepod responses after feeding on AST and PSE, in particular, were abnormality (PC1: corr.=0.98 and 0.89, respectively) and hatching success (PC2: corr.=0.99 and -0.91, respectively). In LEP treatment, instead, main drivers were hatching success (PC1: corr.=-0.99) and pellet production (PC2: corr.=-0.73) and in CUR treatment were pellets (PC1: corr.=-0.87) and abnormality (PC2: corr.=-0.83) (Table 4.4).

When copepod responses were compared at the high diet concentration (Figure 4.7b), first two components resumed 75.78% of total variation, suggesting that abnormality (PC1: corr.=-0.95) and pellet production (PC2: corr.=-0.85) mainly drove the observed differences. PCA analysis performed at low concentration also provided an effective representation, even if the total variation explained by the first two axes (65.22%) was lower than that observed for the "high" concentration diets. Main differences in copepod responses after feeding on diatoms at "low" concentrations were driven by hatching (PC1: corr.=-0.9) and egg production (PC2: corr.=-0.78) (Table 4.4).

Table 4. 4. PCA loadings of the first two principal components (PC1 and PC2). Comparisons between *T. stylifera* responses at high and low concentrations of the same diatom are shown (AST=*A. glacialis*, LEP=*L. danicus*, CUR=*C. curvisetus*, PSE=*C. pseudocurvisetus*). Comparisons among *T. stylifera* responses to the four diatoms provided at high (HIGH) or low (LOW) concentration are also displayed. Highest correlation values observed for each variable with the respective PC are highlighted in bold.

	AST				**HIGH**			
	Pellets	*Eggs*	*Hatching*	*Abnormality*	*Pellets*	*Eggs*	*Hatching*	*Abnormality*
PC1	0.07	0.15	0.04	**0.98**	-0.24	-0.09	0.15	**-0.95**
PC2	0.12	0.09	**0.99**	-0.07	**-0.85**	-0.43	0.16	0.28
	LEP				**LOW**			
	Pellets	*Eggs*	*Hatching*	*Abnormality*	*Pellets*	*Eggs*	*Hatching*	*Abnormality*
PC1	0.07	-0.04	**-0.99**	-0.004	0.42	0.09	**-0.9**	-0.08
PC2	**-0.73**	-0.43	-0.04	-0.53	-0.53	**-0.78**	-0.32	-0.07
	CUR							
	Pellets	*Eggs*	*Hatching*	*Abnormality*				
PC1	**-0.87**	-0.32	0.25	-0.28				
PC2	0.09	0.55	0.08	**-0.83**				
	PSE							
	Pellets	*Eggs*	*Hatching*	*Abnormality*				
PC1	0.1	-0.22	-0.39	**0.89**				
PC2	0.09	-0.07	**-0.91**	-0.4				

Cluster analyses generally confirmed results of PCA because the data highlighted that physiological responses of *T. stylifera* females were peculiar to feeding on PSE and CUR at 0.1 µg-C/ml. In fact, responses of specimens treated with these diets showed close similarity among each other, well separating from the other experimental conditions. In contrast, responses observed for the other diets at "low" concentration were not univocal.

Weak separation was evident also among replicates fed the four diatom diets provided at high carbon concentrations (1 µg-C/ml; Figure 4.8).

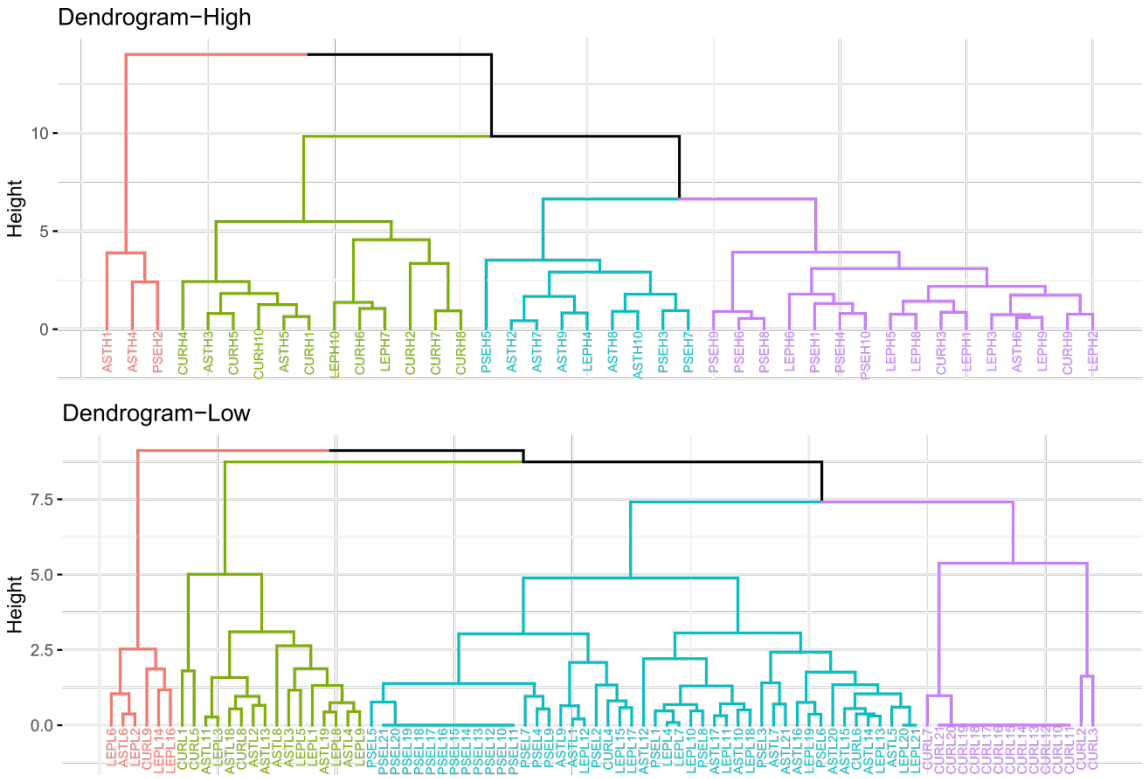

Figure 4. 8. Cluster analysis considering the physiological responses of *Temora stylifera* adult females after feeding on the four diatoms at high (top plot) and low (bottom plot) concentrations.

4.3.2 Chemical analyses

Elemental composition in terms of carbon (C), hydrogen (H), nitrogen (N) and N:C ratio significantly varied among the four diatom species (Table 4.5). Single t-tests highlighted that *A. glacialis* significantly differed from both *C. curvisetus* and *C. pseudocurvisetus* (Figure 4.9). Moreover, LEP differed from AST and PSE in terms of C and H content. Different concentrations of H and N were evident also between LEP and CUR. The only significant differences of N:C ratio were observed between AST and CUR, AST and PSE and LEP and PSE.

Table 4. 5. Kruskal-Wallis tests on carbon (C), hydrogen (H), nitrogen (N) and N:C ratio among the four diets.

Carbon			***Hydrogen***			***Nitrogen***			***Nitrogen:Carbon***		
H	*d.f.*	*p*	*H*	*d.f.*	*p*	*H*	*d.f.*	*p*	*H*	*d.f.*	*p*
10.4	3	<0.05	10.4	3	<0.05	9.4	3	<0.05	10.4	3	<0.05

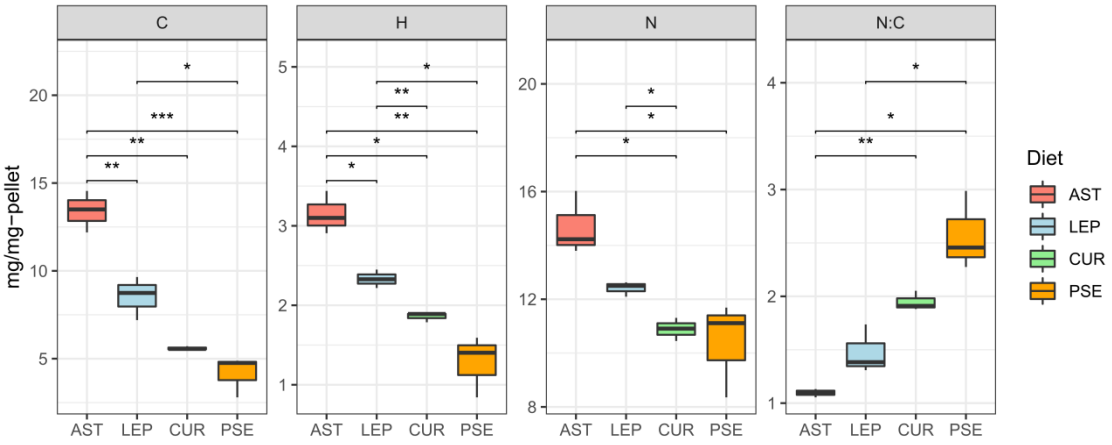

Figure 4. 9. Boxplots showing differences in elemental composition (C, H, N, N:C ratio) of the four diatom diets. Asterisks indicate significance of the t-tests applied to evaluate variations (*:p<0.05; **:p<0.01; ***:p<0.001).

No poly-unsaturated aldehydes were detected in the four algal samples. By contrast, the four diatom species showed distinct NVO synthesis potentials. In particular, the highest oxylipin concentrations were detected in *C. curvisetus* (8.54 ng-NVOs/mg-C) and *L.* cf. *danicus* (5.25 ng-NVOs/mg-C), while the lowest in *A. glacialis* (0.45 ng-NVOs/mg-C) and *C. pseudocurvisetus* (0.92 ng-NVOs/mg-C) (Table 4.6). Moreover, these four diatom species were characterized by distinct NVO composition. In fact, no DHA derivatives were detected in *A. glacialis* and very little in *C. pseudocurvisetus* (0.2 ng/mg-C), while lower concentrations of HTrA derivatives were observed in *A. glacialis* and *L. danicus* than the other two species. EPA derivatives (both hydroxy-acid and epoxy-alcohol), represented the largest fraction of the oxylipins in all diatoms.

MS/MS fragmentation of HEpDoPE and HEpETE indicated that *L.* cf. *danicus* and *C. pseudocurvisetus* were characterized by the presence of a 15-LOX, while *C. curvisetus* by the presence of a 18-LOX (Table 4.6).

Table 4. 6. Mean non-volatile oxylipin (NVO ±SD) concentrations (ng-NVOs/mg-C) measured in the four diatom species. Precursor fatty acids (FA) of the respective oxylipin are indicated. The highest value for each NVO species is highlighted in bold, while the most abundant NVO in each diatom species is underlined. NVOs: HEpDoPE=Hydroxy-epoxy docosapentanoic acid, HDoHE=Hydroxy docosaphexanoic acid, HEpETE=Hydroxy-epoxy eicosapentanoic acid, HEPE=Hydroxy eicosapentanoic acid, HHTrE=Hydroxy hexadecatrienoic acid, HEpHTrE=Hydroxy-epoxy hexadecatrienoic acid.

Precursor FA	**NVO**	***AST***	***LEP***	***CUR***	***PSE***
DHA	*HEpDoPE*	0	0.76 (±0.46)[a]	**0.79** (±0.12)[b]	0.02 (±0.002)
	HDoHE	0	**1.09** (±0.76)	0.84 (±0.21)	0.02 (±0.001)
EPA	*HEpETE*	0.21 (±0.09)	1.71 (±1)[a]	**3.79** (±0.59)[b]	0.19 (±0.03)[a]
	HEPE	0.22 (±0.05)	1.49 (±0.9)	**2.43** (±0.64)	0.31 (±0.05)
HTrA	*HHTrE*	0.01 (±0.01)	0.1 (±0.01)	**0.39** (±0.09)	0.31 (±0.11)
	HEpHTrE	0.01 (±0.01)	0.11 (±0.08)	**0.29** (±0.03)	0.08 (±0.03)
	TOTAL	***0.45***	***5.25***	***8.54***	***0.92***

[a]: 15-LOX; [b]: 18-LOX.

PCA was effective in synthesizing NVO production variability in the four diatoms, because PC1 explained 94.1% of total variance and PC2 explained 4.3% (Figure 4.10). Variability driven by EPA derivatives, in particular, was synthesized by PC1 (HEpETE: corr.=0.45 and HEPE: corr.=0.45). PC2 synthesized variance driven by HHTrE (corr.=-0.82). On the basis of their oxylipin profiles, the four diatom species were well separated from the other, each of which was distributed in one quadrant of the PCA plot. Nonetheless, AST and PSE appeared sensibly closer to each other than LEP and CUR. Separation of the four diatom species on the basis of their oxylipin synthesis potential and fatty acid composition was confirmed by the cluster analyses (Figure 4.11). Interestingly, the dendrogram built considering oxylipins demonstrated that the three replicates of each alga were similar among each other and that the diatoms LEP and CUR were close in terms of oxylipin synthesis potential and composition. In contrast, PSE and AST clearly separated from the other two species and also slightly with each other. The dendrogram, in

fact, resulted in three clusters, the first encompassing LEP and CUR and the other two represented by PSE and AST.

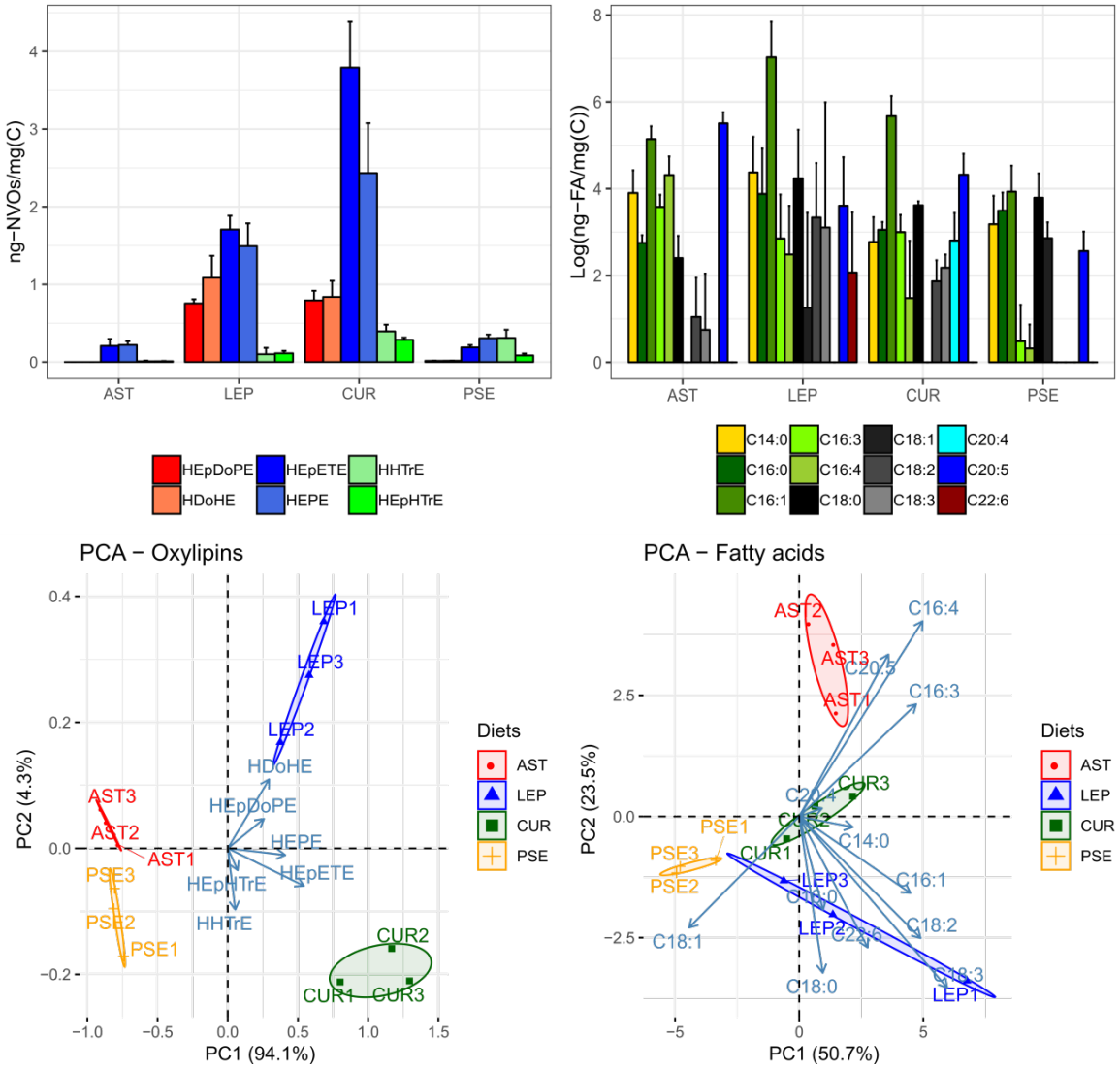

Figure 4. 10. Chemical characterization of the four diatom species and multivariate analyses. Top-left: non-volatile oxylipin concentration (ng/mg-C); top-right: fatty acid concentration (ng/mg-C) at logarithmic scale. Bottom-left: PCA based on oxylipin concentrations (ng/mg-C); bottom-right: PCA based on log-transformed fatty acid concentrations (ng/mg-C).

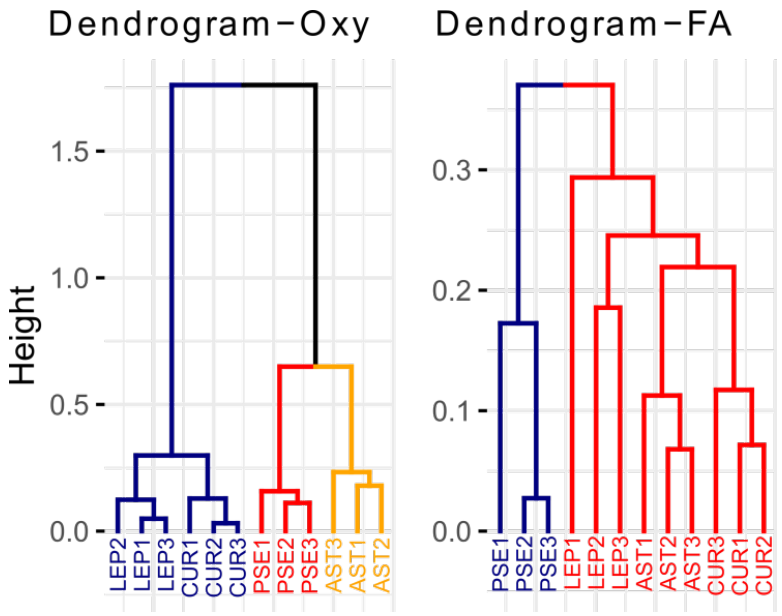

Figure 4. 11. Cluster analysis showing differences in diatom oxylipin ("Dendrogram-Oxy") and fatty acid ("Dendrogram-FA") synthesis potential and composition. The three replicates considered for each diatom species are shown. Height indicates distance among clusters; colours vary depending on cluster.

The four diatoms also differed in terms of fatty acid concentration and composition (Table 4.7). LEP showed the highest concentration of total FA (1.99 µg/mg-C), followed by AST (0.62 µg/mg-C), CUR (0.52 µg/mg-C) and PSE (less than 0.2 µg/mg-C). The fatty acid C16:1 was the most abundant FA species in all diatoms but AST, in which the most concentrated FA species was EPA (250.52 ng/mg-C). No C18:1 was detected in AST and CUR, while detectable levels of the arachidonic acid (C20:4) were present only in CUR. DHA was observed only in LEP (13.78 ng/mg-C). Other than C20:4 and C22:6, no C18:2 and 18:3 were detected in PSE, differently than the other three species. LEP generally showed the highest concentrations of all the FA species; however, HTrA and HTA (i.e. C16:3 and C16:4) were mostly abundant in AST.

Table 4. 7. Fatty acid (mean FA ±SE) concentrations (ng-FAs/mg-C) measured in the four diatom species. The most abundant FA species in each diatom species is underlined (n.d.: not detected).

FA	*AST*	*LEP*	*CUR*	*PSE*
C14:0	52.71(±13.82)	98.52(±46.76)	16.84(±5.8)	27.10(±11.59)
C16:0	14.83(±1.65)	70.29(±44.44)	20.40(±2.33)	33.98(±8.83)
C16:1	175.19(±28.13)	1433.59(±728.81)	310.90(±83)	57.01(±21.86)
C16:3	35.77(±5.46)	22.91(±12.73)	20.22(±5.24)	1.09(±1.09)
C16:4	78.54(±19.62)	17.42(±11.78)	5.79(±3.4)	0.53(±0.53)
C18:0	10.93(±2.97)	107.18(±71.91)	36.35(±1.97)	48.57(±17.38)
C18:1	n.d.	14.30(±14.3)	n.d.	17.28(±4.17)
C18:2	2.53(1.27)	46.30(±32.29)	6.02(±2.09)	n.d.
C18:3	2.81(±2.81)	111.54(±94.08)	8.12(±1.64)	n.d.
C20:4	n.d.	n.d.	17.89(±6.74)	n.d.
C20:5	250.52(±38.89)	56.42(±37.92)	80.84(±24.7)	12.86(±3.53)
C22:6	n.d.	13.78(±10.75)	n.d.	n.d.
TOTAL	**623.83**	**1992.25**	**523.38**	**198.41**

In the PCA analysis, the first two PC axes well represented inter-species variability in terms of fatty acid composition, because they comprised 74.2% of total variability (PC1: 50.7%; PC2: 23.5%) (Figure 4.10). The FAs C18:1, C18:2 and C18:3 well correlated with the first component (corr.=-0.33, 0.37 and 0.45, respectively). Also C16:1 and C16:3 well correlated with this component (corr.=0.34 and 0.36, respectively). By contrast, differences comprised by the second component (PC2) were mostly explained by HTA (C16:4; corr.=0.45), followed by EPA (corr.=0.37) and C18:0 (corr.=-0.36). The three replicates of each diatom species clustered together, but a weaker separation than the one observed considering the oxylipin profiles was also evident. This difference was confirmed by the cluster analysis. The three replicates of each species showed close similarity among each other, but PSE clearly differed from the other three diatoms, which were clustered in a single group (LEP, AST, CUR) (Figure 4.11).

4.3.3 Molecular responses of Temora stylifera

T-tests demonstrated that after two days of feeding on AST, *T. stylifera* females showed significant down-regulation of *ARIH1* and *me31b* with respect to *P. minimum*

(MNE=0.01 and 0.1, respectively; $p<0.05$). After 7 days of feeding on AST, *ARIH1* (MNE=$5x10^{-4}$; $p<0.05$) and *Vasa* (MNE=$1.5x10^{-3}$; $p<0.001$) were up-regulated.

At day 2, females fed LEP showed significant down-regulation of *A5* (MNE=$8x10^{-4}$; $p<0.05$) and *Pafah* (MNE=$2.5x10^{-5}$; $p<0.05$) as well as up-regulation of *ARSB* (MNE=0.002; $p<0.01$) and *CREBL* (MNE=0.0075; $p<0.05$). After 7 days of feeding on LEP, *CREBL* and *VLDLR* were significantly down-regulated (MNE=0.0025 and 0.005; $p<0.05$ respectively), while *A5* (MNE=0.0027; $p<0.01$), *ARSB* (MNE=0.0045; $p<0.01$) and *Hsp70* (MNE=0.08; $p<0.01$) were significantly up-regulated.

In contrast to LEP, *T. stylifera* females up-regulated *A5* after 2 days of feeding on CUR (MNE=0.0018; $p<0.05$). Also, up-regulation of *CREBL* (MNE=0.0025; $p<0.05$) and down-regulation of *Obst* (MNE=0.15; $p<0.05$) were observed after the same feeding period. After 7 days, *ARIH1* (MNE=0.005; $p<0.05$), *CREBL* (MNE=0.005; $p<0.01$) and *Ppa2* (MNE=$2x10^{-4}$; $p<0.05$) were significantly up-regulated, in contrast to the significant down-regulation of *me31b* (MNE=0.03; $p<0.01$), *Obst* (MNE=0.2; $p<0.05$), *Vasa* (MNE=0.0008; $p<0.05$) and *VLDLR* (MNE=0.004; $p<0.01$). No significant variations in the expression of the 13 GOIs were observed after feeding on PSE (Figure 4.12).

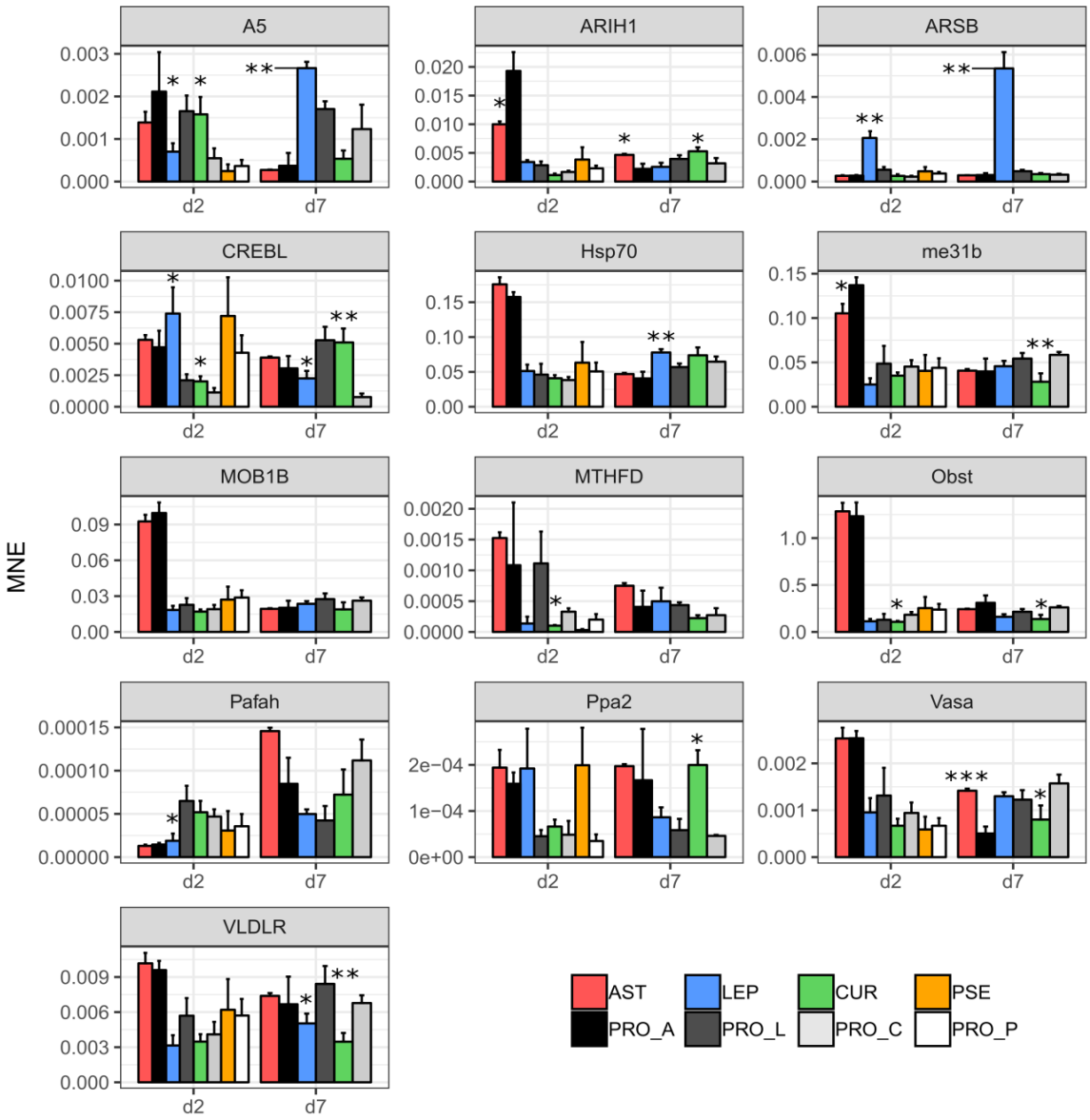

Figure 4. 12. Mean Normalized Expression of the 13 selected GOIs analysed in *T. stylifera* adult females fed *A. glacialis* (AST), *L.* cf. *danicus* (LEP), *C. curvisetus* (CUR) and *C. pseudocurvisetus* (PSE) in comparison to the respective controls (*P. minimum*, PRO). Asterisks indicate significance values calculated after t-tests with Welch's correction for non-homogeneity of the variances (*:p<0.05; **:p<0.01; ***:p<0.001).

In general, a higher number of genes showed significant variations after feeding on LEP and CUR, while only two genes were differentially expressed after feeding on AST. More in particular, 4 genes (2 up-regulated and 2 down-regulated) were differentially expressed after 2 days of feeding on LEP and CUR, while 2 genes (both down-regulated) after feeding on AST. After 7 days, 3 genes were significantly up-regulated and 4 significantly down-regulated in copepod females fed CUR (total of 7 differentially expressed genes), while 5 genes (3 up-regulated and 2 down-regulated) were differentially

expressed in LEP. AST led to significant variations in the expression of 2 genes (both up-regulated; Figure 4.13).

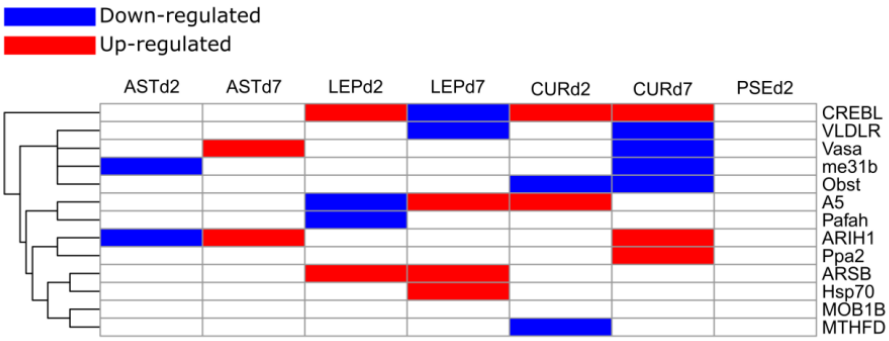

Figure 4. 13. Map showing significantly up- or down-regulated genes measured in *T. stylifera* females fed the four diatom diets for 2 days and 7 days. Blue: down-regulated; red: up-regulated; no fill: no significant variation in comparison to the respective control (*P. minimum*, PRO).

Molecular responses of *T. stylifera* females differed depending on diet and feeding period (2 days and 7 days). In fact, as revealed by PCA, replicates analysed for each diatom treatment clustered together, showing a separation between samples collected after 2 and 7 days of feeding (Figure 4.14). In total, 63.26% of total variance in all treated samples was explained by the first two components (PC1: 40.1%; PC2: 23.2%). Variation along PC1 was mainly explained by *MTHFD* (corr.=-0.66) and *Obst* (corr=-0.39), while variation along PC2 by *ARSB* (corr.=0.69) and *A5* (corr.=0.54). To verify whether such separation could have been effectively mediated by feeding on diatoms or if it was rather constitutive of the copepods, the PCA analysis was repeated on control samples available for each diatom diet. Total variance explained by the first two components (total 64.67%; PC1: 43.9%; PC2: 20.78%) was similar to that observed in the previous analysis. For control samples, variation along the first component was mainly explained by *ARIH1* (corr.=-0.47), *Obst* (corr.=-0.34) and *MOB1B* (corr.=-0.31), while variation along PC2 by *A5* (corr.=0.53), *Ppa2* (corr.=-0.47) and *MTHFD* (corr.=0.41). In contrast to PCA results obtained with treated samples, clustering of control samples was less clear and some groups slightly overlapped.

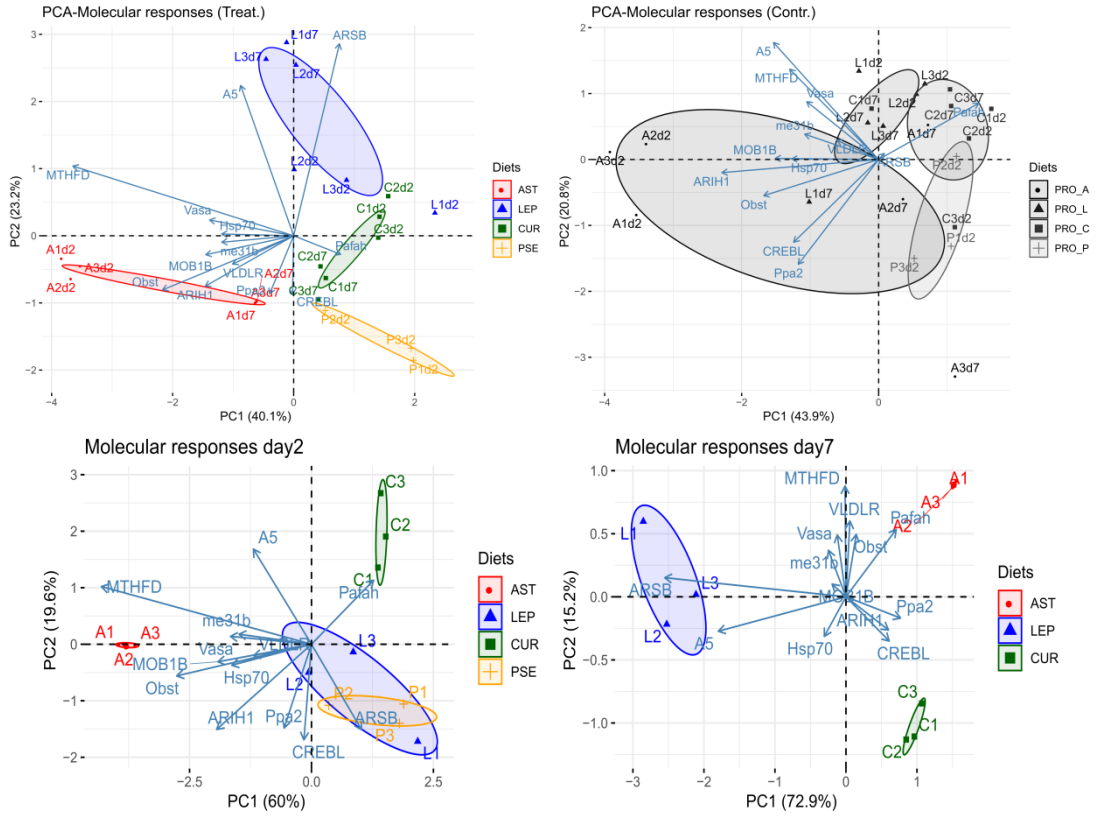

Figure 4. 14. PCA analyses. Differences in molecular responses of treated and control samples are summarized in top plots. Differences among treated samples after 2 and 7 days of feeding are summarized in bottom plots.

Molecular responses of treated *T. stylifera* females sensibly differed at the two feeding periods and depending on the diatom provided. After 2 days of feeding, females fed AST and CUR well separated from LEP and PSE treatments, which instead overlapped. The first two components explained 79.56% of total variance (PC1: 60%; PC2:19.6%) and PC1 correlated with *MTHFD* and *Obst* (corr.=-0.63 and -0.4, respectively), while PC2 with *CREBL* (corr.=-0.43), *A5* (corr.=0.43), *ARSB* (corr.=-0.39), *ARIH1* (corr.=-0.38) and *Ppa2* (corr.=-0.38). After 7 days of feeding, separation of treatments was more pronounced. First two components of PCA explained 88.1% of total variance (PC1: 72.9%; PC2: 15.2%). First component well correlated with *ARSB* and *A5* (corr.=-0.74 and -0.52, respectively) and the second component with *MTHFD* (corr.=0.56), *VLDLR* (corr.=0.38), *Pafah* (corr.=0.34), *Obst* (corr.=0.32) and *Vasa* (corr.=0.31; Figure 4.14).

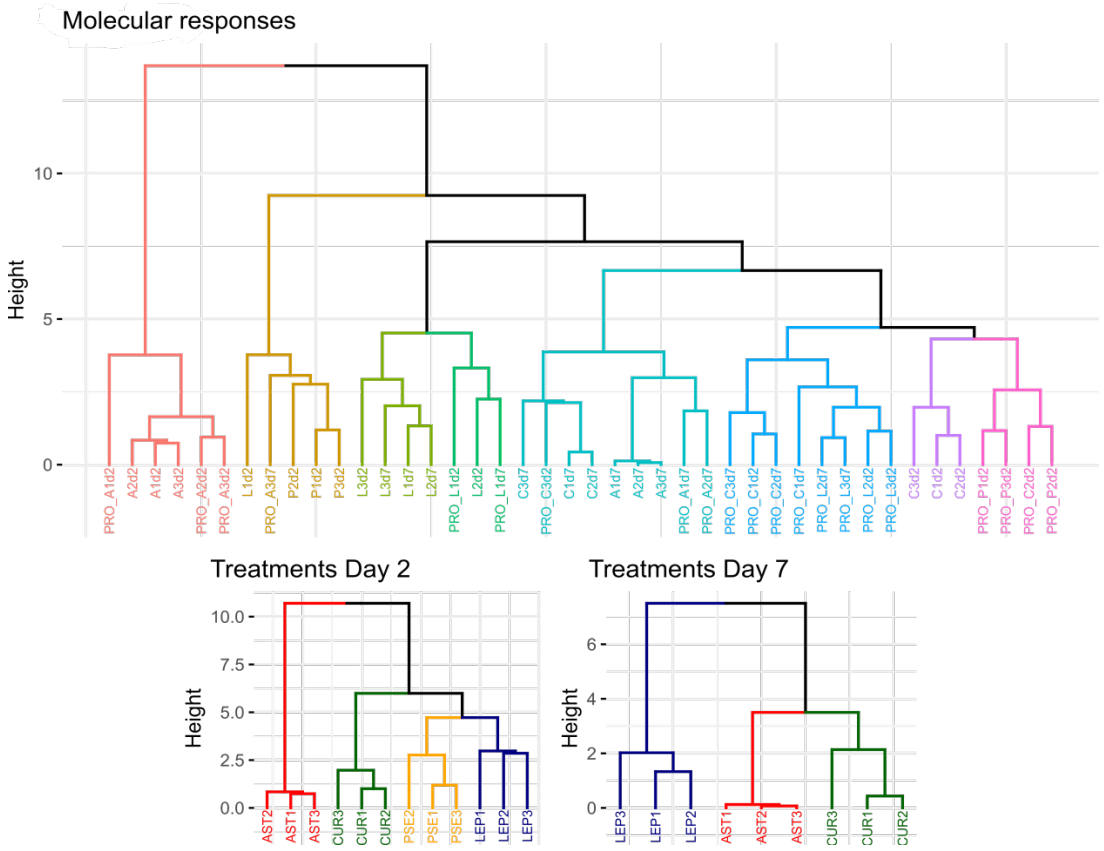

Figure 4. 15. Dendrograms showing clustering of *T. stylifera* samples depending on molecular responses measured in control and treated samples (top panel) as well as after 2 and 7 days of feeding on diatom diets (bottom panel).

Results obtained from PCA were confirmed by cluster analyses. When performed considering all samples, dendrograms allowed evaluating whether group separation observed in treated samples was effectively driven by diatom ingestion or if it was due to constitutive responses of the copepod specimens sampled. The output showed that control samples generally differed from treated ones and that a clear separation was not evident among them. However, *T. stylifera* females collected and analysed after 2 days of feeding on AST were very close to the respective control samples and well separated from the other groups. Molecular responses were neatly separated in treated samples analysed separately after 2 and 7 days of feeding. At day 2, AST represented the most distant group, because the three replicates analysed after feeding on this diatom showed the highest distance from the other samples, with responses that were closer to each other. In contrast,

on day 7, LEP was the most distant group from the other two (AST and CUR) (Figure 4.15).

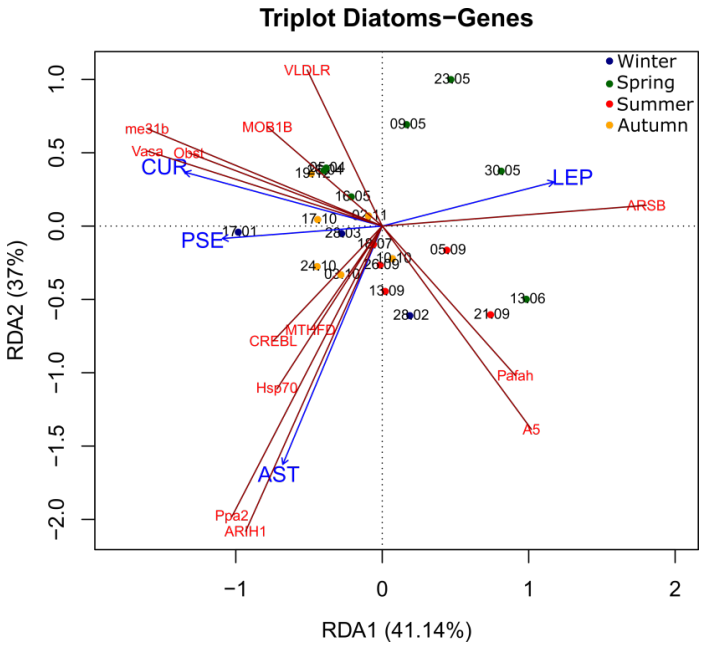

Figure 4. 16. RDA plot showing distribution of the four diatom species and the MNE levels measured in the sampling dates at LTER-MC. Dates are also plotted and the respective season is indicated by coloured dots. The closer the constraining variables (blue arrows) distribute to the dependent ones (red lines), the highest the relationships among these variables.

Redundancy analysis (RDA) allowed evaluating whether molecular responses observed in *T. stylifera* fed mono-algal cultures of AST, LEP, CUR and PSE could reflect molecular responses in the natural population of the Gulf of Naples. In fact, the four diatom species were originally isolated from LTER-MC and the molecular responses of *T. stylifera* from the same area were measured analysing MNE of the same genes inspected in the present laboratory experiments. The hypothesis was that wild copepod females could show similar molecular responses to specimens fed the experimental diets, because laboratory results showed clear separation depending on the diet provided. The first two axes of the RDA summarized 78.15% of total variance (Figure 4.16) and the first (41.14%) was mainly related to *ARSB* (corr.=0.6), *me31b* (corr.=-0.53) and *Vasa* (corr.=-0.53), while the second (37%) to *ARIH1* (corr.=0.66) and *Ppa2* (corr.=0.63). However, constraining

variables (i.e. the four diatom species) drove significant variations of dependent variables (i.e. genes) only at probability α=0.1 (F=1.48; p=0.09).

4.4 Discussion

The four diatom monospecific diets significantly affected physiological responses of adult *T. stylifera* females. Depending on the diatom species provided, different effects were measured in response to a single factor or the interaction of the two factors considered. As suggested by egestion rates, copepods actively fed on the diatoms provided, because pellet production was constantly higher after feeding on diatoms than *P. minimum*, both at the "low" and the "high" concentrations, except for the PSE treatment. These results seem to contrast with previous reports about negative selective feeding of copepods towards oxylipin producing diatoms (Maibam et al., 2015, Leising et al., 2005), but at the same time cannot confirm that oxylipins can act as attractive feeding cues for copepods (Kâ et al., 2014).

Variations in egg production and hatching success observed in the treatment diets in comparison to PRO at high carbon concentration (1 µg-C/mL) resembled some responses previously reported for the same copepod species after feeding on diatom species provided at similar carbon densities. Negative effects of diatom mono-algal diets on egg production rates of grazer copepods have been demonstrated (Vehmaa et al., 2012, Vehmaa et al., 2011). Also, (Ianora et al., 2011) measured temporal reduction in egg production rates and hatching success in *T. stylifera* females fed *S. marinoi* and *Pseudo-nitzschia delicatissima* (a non-PUA-producing diatom) provided at 0.98 µg-C/ml. Similarly, (Barreiro et al., 2011) fed the copepod *T. stylifera* from the Gulf of Naples with the PUA-producing diatoms *S. marinoi* and *T. rotula* as well as with the non-PUA-producing diatom *Skeletonema pseudocostatum*, provided at similar concentration to the present experiments. These authors reported reduced hatching success in all diatom treatments in comparison to the

dinoflagellate *P. minimum*, proposing that the negative effects on the reproductive success of the copepod were driven by NVOs. In the present experiments, reduced hatching success was observed after ingesting *A. glacialis*, *L.* cf. *danicus*, *C. curvisetus* and *C. pseudocurvisetus*, in comparison to the control diet. At the "high" carbon concentration, also egg production was generally lower in diatom treatments than PRO, even if, on average, egg production rates measured in AST and CUR were more similar to the control. Abnormal nauplii were not frequently observed in experimental treatments. Progressive increments in the percentage of abnormal nauplii along time occurred only in AST-H and CUR-L treatments, while in the others naupliar abnormality was low. These results differ from previous evidence demonstrating that diatom mono-algal diets induce progressive increase in percentage of abnormal nauplii (Ianora et al., 2004) and these discrepancies could be due to different chemical traits of the diatom diets. Interestingly, the general fitness calculated for each diatom diet at the "high" carbon concentration was always reduced in comparison to the control, suggesting potential negative effects of the four diatom species on the population dynamics of *T. stylifera* in the Gulf of Naples, at the "high" carbon density. These results are in line with higher recruitment rates observed in *T. stylifera* fed the dinoflagellate *P. minimum* in comparison to diatoms provided at 0.98 µg-C/mL (Ceballos and Ianora, 2003).

However, the number of algal cells offered to *T. stylifera* at the "high" carbon concentration level was largely above natural cellular densities observed for the four diatom species at LTER-MC, along 2017. In fact, the maximal concentration of *A. glacialis* at LTER-MC was 131,744 cells/L (on 17th of October), of *L.* cf. *danicus* was 2.04x10^{6} cells/L (on 6th of June), of *C. curvisetus* was 265,882 (on 4th of July) and of *C. pseudocurvisetus* was 23,000 (on 14th of February). Low carbon concentration treatments resembled more accurately natural cellular concentrations of the four diatom species in the Gulf of Naples. In particular, the number of *L.* cf. *danicus* cells at 0.1 µg-C/mL was well within the concentration ranges observed in the field. This is the first time that laboratory

experiments compare the effects of diatom monospecific diets on the physiological responses of copepods at two carbon concentrations. Results obtained from this treatment are interesting, because they show that moderate diatom densities can instead affect positively the final fitness of copepods in comparison to a dinoflagellate diet. Even though fitness was the highest at 1 µg-C/mL of PRO because of high egg production rates associated to no impairment of hatching and no induction of naupliar abnormality, higher fitness was measured for copepods fed the four diatoms than those fed PRO at the "low" carbon concentration. This result is mainly driven by the reduced egg production rates expressed by copepod females after feeding on *P. minimum* at 0.1 µg-C/mL. Therefore, PRO diet was probably unsuitable to provide sufficient energetic resources to support egg production, which tended to zero after the first 3-4 experimental days. Egg production rates progressively diminished along time also after feeding on diatoms, at the same carbon concentration, but these algae supported egg production for longer time. This information suggests that copepod physiological responses measured at 0.1 µg-C/mL were mainly driven by nutritional deficiency. In this perspective, low carbon densities of dinoflagellates could be more deleterious for the final fitness of grazer copepods than the ingestion of diatoms synthesizing harmful chemicals. Nonetheless, no abnormal nauplii occurred in PRO-L treatments in comparison to the diatom diets at 0.1 µg-C/mL. Thus, while egg production probably depended on nutritional resources assimilated by copepod females from the diet, the lowered egg hatching and higher naupliar abnormality observed in diatom treatments could have been caused by apoptosis mediated by the ingestion of diatom-derived harmful chemicals. Irrespective of potential teratogenic effects mediated by diatoms, final fitness calculated at the "low" carbon concentration was always higher than the control. This pattern suggests that egg production potential could play a major role in determining final recruitment in copepod populations, when little teratogenic effects occur. Therefore, moderate feeding on diatom diets could improve naupliar recruitment despite

lower hatching and higher larval abnormalities, as also suggested by (Carotenuto et al., 2012).

In this perspective, physiological responses of *T. stylifera* need to be discussed also in relation to diatom chemical traits. The four diatom species selected were sensibly different in terms of their chemical features, including mineral and fatty acid concentration and composition as well as oxylipin synthesis potential. Assessing if and how chemical traits of the diatoms drove different physiological responses of *T. stylifera* is difficult. Interactive effects of measured chemical variables (such as fatty acids and oxylipins) could have occurred and other molecules, not characterized in the present experiments, could have affected copepod physiology.

Copepods have been described to actively select food items that more closely match their energetic requirements (Meunier et al., 2016). In particular, adult copepods can select nitrogen-enriched preys to sustain high nitrogen demand. *A. glacialis* was the diatom showing the highest mineral concentrations of C and N and a N:C ratio close to one. In contrast, the lowest concentration of C and N and the highest N:C ratios were observed in *C. pseudocurvisetus* and *C. curvisetus*. Despite apparent favourable mineral composition of AST, low fitness was observed in *T. stylifera* after feeding on this diatom. Also, percentage of abnormal nauplii progressively increased along time. These results indicate that mineral composition of diatoms could have played a marginal role for the reproductive potential of copepods.

Rather, the effects of other chemicals could be more relevant. Multivariate analyses of both fatty acids and NVOs revealed that the four diatoms well separated among each other. AST and PSE were both characterized by low oxylipin synthesis potentials, in contrast to the high synthesis potentials expressed by CUR and LEP. Also, PSE was characterized by the lowest concentration of total fatty acids and well separated from the other three diatom species depending on composition and abundance of these molecules. As a result, negative effects of PSE on the physiological responses of *T. stylifera* could

have been mediated by poor energetic resources assimilated after feeding on this diatom (Jones and Flynn, 2005) and these effects could have been particularly evident at the low carbon concentration treatment. The low oxylipin synthesis potential associated to the low amount of fatty acid substrates available supports this interpretation.

In contrast, oxylipin-mediated teratogenic effects more likely influenced copepod responses to CUR and LEP. Between these two diatoms, *C. curvisetus* showed a clearly higher oxylipin synthesis potential, despite a total fatty acid concentration slightly lower than *A. glacialis* (523.38 vs 623.83 ng-FA/mg-C, respectively). *L.* cf. *danicus*, instead, showed high tendency to synthesize oxylipins in line with the high fatty acid content (1992.25 ng-FA/mg-C). This means that, at similar ingestion rates, *T. stylifera* females take a much higher amount of oxylipins after feeding on CUR than LEP. Potential teratogenic effects mediated by the high oxylipin synthesis potentials expressed by these two diatoms are also suggested by the two-way ANOVA results. Hatching success in these two treatments was not dependent on the interaction of the two experimental factors, but only varied depending on diet. When abnormality was measured, instead, LEP effects resulted significantly different depending on diet and carbon concentration, while interaction was no longer significant in CUR. This suggests that the lower oxylipin synthesis potential of LEP could lead to differential effects on larval abnormality (but not on egg viability) depending on the carbon concentration provided. That is, teratogenic effects mediated by oxylipins at 0.1 µg-C/mL of LEP do not show the same intensity at the "high" carbon concentration treatment. Chemical traits of *L.* cf. *danicus* strain in terms of NVO species and LOX pathways involved in their synthesis well mirrored previous chemical characterization of *L.* cf. *danicus* collected in the Gulf of Naples (Nanjappa et al., 2014). Interestingly, *L.* cf. *danicus* was indicated as the species showing the highest oxylipin synthesis potential together with *L. hargravesii* (Nanjappa et al., 2014); this suggests that effects of *L.* cf. *danicus* measured on *T. stylifera* females in the present laboratory setup

could represent the most powerful influences of the genus *Leptocylindrus* on *T. stylifera* in the Gulf of Naples.

In contrast to LEP, the very high oxylipin synthesis potential of CUR drives ingestion of high amounts of teratogenic molecules by the copepod after feeding on this diatom, irrespective of the carbon concentration offered.

Despite clear discrepancies in diatom chemical traits, physiological responses of *T. stylifera* did not differentiate among the four diatom treatments, because multivariate analyses revealed weak clustering. A neat separation of copepod physiological responses was observed only in CUR-L and PSE-L treatments. This result could be driven by the peculiar chemical traits of these diatom species: while effects of PSE-L may have represented copepod responses to low nutritional resources availability assimilated from this diet, effects of CUR-L could have differed from the other treatments because of the high oxylipin synthesis potential. This separation was lost at the "high" carbon concentrations, may be as a consequence of the homogenization of copepod physiological responses at saturating food concentrations. In this condition, high fitness of copepods could have been expected after feeding on PSE, because this diatom showed low oxylipin synthesis potential. However, fitness in the PSE-H treatment was lower than the control. Possible explanations may be related to the selectivity and the ingestion rates of *T. stylifera* while feeding on this diatom or to the low mineral and fatty acid contents observed for this diet.

While physiological responses of *T. stylifera* to CUR, LEP and PSE seem plausible in an oxylipin production and in a nutritional perspective, responses observed after feeding on AST likely require a different discussion. *A. glacialis* was characterized by the second highest total amount of fatty acids (623.83 ng-FA/mg-C), after *L.* cf. *danicus* (1992.25 ng-FA/mg-C). Despite the high availability of fatty acid substrates, oxylipin synthesis potential of *A. glacialis* was even lower than the fatty acid-depleted *C. pseudocurvisetus* (0.45 and 0.92 ng-NVOs/mg-C, respectively). Such chemical features suggest that *A.*

glacialis represented a very favourable diet for *T. stylifera* reproduction because it could have provided high nutritional resources associated with low teratogenic potential mediated by oxylipins. Nonetheless, physiological responses of the copepod females resembled the effects observed for the other diatoms. In particular, the final recruitment at 1 µg-C/mL was significantly lower than the PRO treatment. More surprisingly, progressive increments in the percentage of abnormal nauplii were observed only in this diatom treatment, resembling patterns reported in previous experiments testing physiological responses of copepods to PUA-producing diatoms (Ianora et al., 2004) or to pure oxylipin compounds (Ianora et al., 2011). Actually, *A. glacialis* from the English Channel has been reported as a PUA-producing diatom (Wichard et al., 2005a), but no PUAs were detected in the strain isolated from the Gulf of Naples. This information points at a possible harmful effect mediated by other molecules of diatom origin. For example, it has been recently demonstrated that sterol sulphates are constitutive enzymatic products that can trigger diatom bloom termination (Gallo et al., 2017). Apoptotic events mediated by diatom secondary metabolites other than oxylipins still need thorough exploration. Sterol sulphates could represent relevant molecules involved in maternal effects in grazer copepods.

Further resolution to discriminate responses of *T. stylifera* to the four diatoms was provided by the expression analyses of the 13 selected GOIs. In general, the number of differentially expressed genes after feeding on the four diatom diets was in line with the oxylipin synthesis potentials measured in the diatom species. In fact, after 2 days of feeding, LEP and CUR ingestion led to differential expression of four genes, while 5 genes were differentially expressed in LEP and 7 genes in CUR, after 7 days. Different molecular responses of *C. helgolandicus* were previously reported, after two days of feeding on the diatoms *S. marinoi* and *Chaetoceros socialis* (Lauritano et al., 2011b). Such discrepancies were probably related to the higher oxylipin synthesis potential expressed by *S. marinoi* than *C. socialis* (Fontana et al., 2007b) and differential gene expression measured in the present experiment could mirror copepod responses to diatoms depending on their

chemical traits. In contrast to LEP and CUR, no genes were differentially expressed in PSE after 2 days of feeding and 2 genes were down-regulated in AST. Interestingly, AST showed a lower oxylipin synthesis potential than PSE; therefore, the differential expression of 2 selected GOIs after feeding on this diet further suggests that molecules other than NVOs could have mediated *T. stylifera* responses to *A. glacialis*.

As shown by multivariate PCA and cluster analyses, molecular responses of *T. stylifera* adult females varied depending on the diet provided. Since controls were run separately, comparisons among diatom treatments could have been influenced by constitutive differences in the gene expression of sampled females. This drawback probably occurred mainly for AST samples analysed at day 2, because these replicates clustered together and were well separated from the other treatments. Even if interpretation about the effects of AST in comparison to PRO at day 2 was not affected, this indicates that separation of AST replicates from the other treatments was likely mediated by constitutive differences in the expression of the 13 GOIs and not by differential effects mediated by this diatom. Constitutive differences in gene expression were lost at day 7 and the marked multivariate distances among AST, CUR and LEP effectively mirrored discrepancies in the molecular responses of *T. stylifera* to the diatom diets. Thus, the information collected suggests that *T. stylifera* differentially regulated different sets of genes depending on food preys.

After 2 days of feeding on AST, *ARIH1* and *me31b* were significantly down-regulated. *ARIH1* is a gene codifying for ubiquitin E3 proteins and silencing of this gene has been shown to sensitize cells to genotoxic compounds (von Stechow et al., 2015). These authors also showed that *ARIH1* expression increases after DNA damage; therefore, up-regulation of this gene after 7 days of feeding on AST could indicate the effect of genotoxic compounds transmitted by AST to the copepod females. After 2 days of feeding on AST, *me31b* was also down-regulated. This gene is expressed in polar granules and codifies for an ATP-dependent RNA helicase, thus being involved in germ cell formation

(Thomson et al., 2008). However, at day 7 no differential expression was observed for this gene, possibly indicating recovery from putative stressors driving its down-regulation at day 2. In addition to *ARIH1*, the only up-regulated gene at day 7 after feeding on AST was *Vasa*, which also codifies for an ATP-dependent RNA helicase fundamental for oocyte differentiation and germline cyst development in animals (Styhler et al., 1998, Tomancak et al., 1998). The up-regulation of this gene could further reveal molecular responses activated by *T. stylifera* with time, but molecular and physiological mechanisms explaining why *Vasa* was significantly up-regulated and *me31b* was not remain unclear.

After 2 days of feeding on LEP, *A5* and *Pafah* genes were down-regulated. Expression of *A5* proteins has been reported in chemosensory organs of insects (Biessmann et al., 2005, Pikielny et al., 1994), highlighting the role of this gene for animal feeding. Down-regulation of *A5* in LEP diet after 2 days of feeding could indicate either a potential effect of harmful chemicals on food localization efficiency or active prey avoidance by *T. stylifera*. Deficiencies in food perception could then be counteracted by the up-regulation of *A5* with time, as demonstrated by the high MNE at day 7. LEP was the only diet driving down-regulation of *Pafah* at day 2. This gene codifies for a phospholipase A_2 that inhibits PAF (the platelet-activating factor) through deacetylation (Kordan et al., 2003, Arai et al., 2002). PAF regulates the reproductive cycle and pregnancy (O'Neill, 2008, Kordan et al., 2003). The response observed after 2 days of feeding on LEP could then indicate immediate reactions of *T. stylifera* females to harmful effects mediated by the diatom diet. Significant up-regulation of *CREBL*, a repressor of yolk protein precursors (YPP) such as vitellogenin and carboxypeptidase (Dittmer et al., 2003), seems to conflict with the interpretation that molecular responses are activated to maximize final reproduction. However, it is likely that up-regulation of this gene is part of a more complex molecular pathway involved in early reactions to stressors, because significant down-regulation of *CREBL* occurred on day 7, presumably favouring reproductive success of *T. stylifera*. At this sampling time, *T. stylifera* seemed to try to maximize ingestion of LEP (*A5* was up-

regulated) and to digest organic material assimilated (up-regulation of *ARSB*, involved in polysaccharide metabolism, increased from day 2 to 7), coordinating molecular responses involved in stress response. In fact, *T. stylifera* females up-regulated Hsp-70 on day 7. This protein is involved in thermo-tolerance, protection to xenobiotic exposure and to general stress responses in copepods (Aruda et al., 2011, Rhee et al., 2009, Voznesensky et al., 2004). Overall, the observed regulation of the 13 GOIs suggests molecular responses aiming at favouring both adult survival and reproductive output. In fact, the up-regulation of *ARSB* might help adult females to maximize nutritional storage in their tissues to cope with stressful physiological conditions mediated by the diatom diet, whereas down-regulation of *CREBL*, and hence increased production of yolk proteins, might compensate for the down-regulation of *VLDLR*, a receptor protein that favours ingression of lipoproteins in developing oocytes (Kahn et al., 2018) at day 7. Such responses could be also mediated by the extremely high lipid content of *L.* cf. *danicus* observed after the chemical characterization provided.

The higher oxylipin production potential observed in CUR possibly mediated the differential expression of a different number of genes in *T. stylifera*. As a consequence of the active feeding of the copepod, demonstrated by the high number of pellets and the up-regulation of *A5* at day2, *CREBL*, *me31b* and *VLDLR* were expressed to regulate egg production and hatching success. In fact, at day 2 and 7 *CREBL* was up-regulated, while the other two genes showed down-regulation only at day 7. Additionally, over-expression of *Ppa2* at day 7 could stress this pattern. Ppa2, in fact, regulates apoptosis and its stimulation initiates cell death (Klumpp and Krieglstein, 2002). Moreover, *MTHFD* was down-regulated at day 2, *Vasa* gene at day 7 and *Obst* at both experimental times. Differential regulation of *MTHFD* was observed only in response to CUR and not in the other algal treatments. Folate malfunctions are known to induce apoptosis and alter fertility in adult individuals (Forges et al., 2007), as well as embryo development (Affleck et al., 2005). *Obst* gene, instead, is involved in the gene cluster of chitin binding (Behr and Hoch,

2005), thus its down-regulation could induce structural damages in larval copepod stages (Tajiri et al., 2017). Overall, molecular responses of *T. stylifera* to CUR indicate stressful conditions perceived by copepod females and suggest regulation of genes possibly aimed at maximizing adult survival.

Non-significant effects of PSE could indicate that expression of the 13 selected genes depends on the synthesis potential of harmful molecules synthesized by the diatoms. In fact, oxylipins have been shown to accumulate in the copepod female ovary (Wolfram et al., 2014), where regulation of stress-mediated genes can occur. PSE showed low oxylipin synthesis potential and low levels of fatty acids. Therefore, molecular effects mediated by nutritional deficiency could concern differential expression of genes related to starvation, rather than to stress response.

In general, clear deciphering of molecular responses to the four diatom diets depending on their chemical traits remains difficult. However, the present results demonstrated that oxylipin synthesis potentials of diatoms could mirror different molecular responses in *T. stylifera*, as highlighted by the increasing number of differentially expressed genes in PSE, AST, LEP and CUR treatments.

One of the clearest responses was the differential regulation of *ARSB* after feeding on LEP. In fact, this gene was clearly up-regulated and its MNE increased from day 2 to 7. RDA analysis performed considering natural algal concentrations and MNE measured in wild *T. stylifera* females suggests that up-regulation of *ARSB* could be specifically activated when *L.* cf. *danicus* occurs. In contrast, regulation of the other genes in the field did not mirror expression patterns observed in the present laboratory experiments. However, this discrepancy could be due to the sensibly different abundances of the four diatoms at sea. In particular, *L.* cf. *danicus* was the only species reaching natural concentrations close to cell numbers offered to *T. stylifera* in the present laboratory experiments. The other three species, instead, occurred in lower amounts and were not highly persistent along time, at LTER-MC (Figure 4.17).

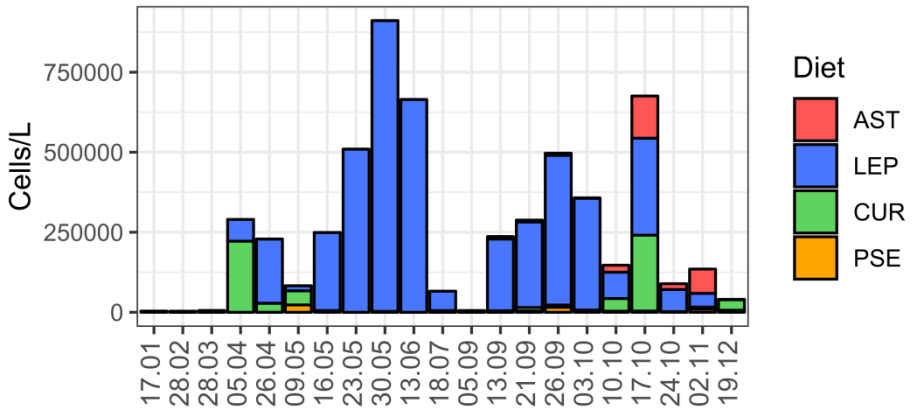

Figure 4. 17. Cell abundances of the four diatom species considered in laboratory experiments. Only the dates at which molecular responses of wild *T. stylifera* females are available are displayed.

Laboratory experiments demonstrated that physiological responses of *T. stylifera* to the diatoms *A. glacialis*, *L.* cf. *danicus*, *C. curvisetus* and *C. pseudocurvisetus* significantly differ from the dinoflagellate control diet *P. minimum* and depended on the carbon concentration provided. These responses could be related to the synthesis potential of harmful molecules or the nutritional resources assimilated from diatoms. In this perspective, ingestion of species showing higher oxylipin synthesis potential can lead to stronger stress-related molecular responses in adult copepod females, which could strive to maximize their own survival and then their reproductive output. Much effort is still needed to reach sound chemical characterization of diatoms so as to better assess the effects of these algae on copepod grazers. In fact, as demonstrated by physiological, chemical and molecular analyses, effects of the diatom *A. glacialis* on copepods were likely mediated by molecules other than NVOs. These laboratory experiments also clarify that diatoms can impair copepod recruitment mainly when they occur at saturating food densities. On the contrary, at low carbon concentrations, naupliar recruitment could increase after feeding on diatoms, despite little impairment of egg hatching and survival of NI nauplii.

Chapter 5

General conclusions

Results presented in this thesis offer new insights in plankton chemical ecology. Even if experimental activities only involved organisms collected in the Gulf of Naples, broader considerations about marine ecology dynamics can be proposed.

The targeted-metabolomics analyses performed on natural nano- and micro-plankton communities (2 μm - 200 μm) allowed fine chemical characterization of fatty acids and lipid peroxidation products (non-volatile oxylipins, NVOs), in these organisms. Generalized Additive Models (GAM) applied were particularly suitable to describe non-linear relationships so as to reveal biotic and abiotic drivers influencing plankton chemical features.

One-year data concerning fatty acid and oxylipin profiles can be helpful to unveil plankton dynamics at LTER-MC, along 2017 (Chapter 2). For example, information provided about fatty acid abundance and composition can be useful to estimate nutritional resources available for grazers and, in turn, to decipher food web dynamics in the sampling area. In the Gulf of Naples, saturated and mono-unsaturated fatty acids represented the most abundant fraction, while poly-unsaturated fatty acids (PUFAs) were less abundant. Fatty acid signatures are often described as trophic markers in marine systems, because specific fatty acid classes are characteristic of different organisms (Brett and Müller-Navarra, 1997). Fatty acid composition analysed in the Gulf of Naples, however, did not allow clearly relating fatty acid composition to the phytoplankton groups identified. In this perspective a clearer signature was observed only between the Hexadecanoic acid, the Octadecanoic acid and phytoflagellates.

One of the most striking results obtained after the targeted-metabolomics survey was the important relationship found between diatoms/L and NVOs/L. This point is of particular relevance because previous field surveys had failed in finding such regression and in ascribing oxylipin synthesis to diatoms in natural plankton communities. On this ground, present results could be a reference point for subsequent experiments focusing on diatom chemical traits. More in particular, sampling methodology and analytical procedure

were highly suitable for the purposes of the thesis and can now be applied to other experimental procedures. Additionally, the linear regression equation describing NVOs/L increase at higher diatoms/L concentrations could be compared with slopes observed in other systems to quantitatively assess oxylipin synthesis potential in other areas. More interestingly, oxylipin-per-diatom-cell production decreased along diatom concentration (cells/L) and this suggested a potential role of these molecules as info-chemicals in diatom populations. Although the role of oxylipins as info-chemicals was already proposed by other authors after laboratory evidence, no clear information was available from natural communities. The proposed mechanism of oxylipin synthesis modulation depending on diatom density is new and still needs to be supported by further experimental evidence.

Even though previous laboratory information highlighted the negative effects of diatoms and oxylipins on the reproductive potential of several copepod species, no effect of these molecules was observed on the copepod *Temora stylifera* at LTER-MC (Chapter 3). In fact, neither concentrations of NVOs/L or NVOs/diatom-cell significantly related to physiological and molecular responses measured in the target copepod species in situ. This suggests that factors other than NVO concentration can influence population dynamics of *T. stylifera* in the Gulf of Naples; also, the selected species can more effectively counteract the deleterious effects of these chemicals when offered a mixed natural food assemblage (i.e. dilution effect).

Among the physiological variables, the interactive effect of egg production rates and naupliar recruitment seem to be of primary importance for the population dynamics of *T. stylifera*. In fact, high egg production sustained high recruitment only at favourable survival rates of NI nauplii in autumn, at LTER-MC. The high number of eggs observed in spring did not support high population densities in the same season, likely because of oscillatory survival rates of the nauplii. In this perspective, it is of particular importance assessing which biotic and abiotic drivers influenced egg production and naupliar survival rates. As highlighted by GAM regressions, abiotic factors, such as temperature and oxygen

concentration, could have played a major role in determining egg production rates in *T. stylifera*. Reductions in naupliar survival rates mainly related to salinity and fatty acid concentrations, but not to NVOs/L or NVOs/diatom-cell. However delayed effects mediated by the ingestion of diatoms seem also plausible and realistic. Delayed effects on naupliar survival rates were already proposed by (Halsband-Lenk et al, 2005), after a field survey conducted in Dabob Bay (Washington, USA). Data collected in the Gulf of Naples indicated a significant negative relation between the genus *Chaetoceros* and NI survival. *Chaetoceros* is a diatom genus that often dominates the diatom community along the year at LTER-MC (Ribera D'Alcalà et al., 2004) and negative effects of these diatoms on naupliar survival could contribute regulating *T. stylifera* population abundance in this area. Effects of biotic and abiotic variables on copepod physiology are mediated by molecular responses at the gene level, and the ultimate effect on copepod population dynamics will depend on the trade-off between direct impairment of key physiological processes and defensive mechanisms activated by the copepod to counteract such negative effects. In this perspective, the *de novo* transcriptome assembly and differential gene expression analysis performed in *T. stylifera* could be of help to decipher molecular pathways affected by or activated by the copepods to recover from stressful environmental conditions impairing naupliar survival. As discussed in Chapter 3, in fact, up-regulated and down-regulated genes could describe molecular pathways leading to both low larval viability and subsequent recovery. The differential expression analysis was also useful to select those sequences codifying for functions most likely involved in copepod reproductive and developmental processes.

Five sequences out of the 13 selected for RT-qPCR analyses significantly related to copepod physiological responses and could represent potential early-warning or biomarker genes for copepod physiology in further field survey (Chapter 3). In particular, co-expression of genes involved in cell development and reproduction such as the cAMP-Responsive Element-Binding Protein 2 (*CREBL*), the ATP-Dependent RNA Helicase

(*me31b*) and the Very Low-Density Lipoprotein Receptor (*VLDLR*) could have mainly regulated egg production rates in *T. stylifera*. An intriguing perspective is that these three genes could be differentially expressed in response to distinct pressures, because oxygen and transmittance related to *VLDLR*, while temperature and oxygen saturation to *me31b*. Relationships of the genes *ARSB* and *Ppa2* to hatching and naupliar survival rates still remains difficult to interpret and explain, but they could also represent useful marker for further laboratory and field investigations.

Laboratory experiments performed in this thesis also allowed testing the effects of four diatoms isolated from the phytoplankton community at LTER-MC (Chapter 4) on the copepod *T. stylifera*. Also, this was the first time that an integrative approach encompassing physiological and molecular characterization of copepod responses as well as chemical analysis of the diatom diets was applied. Further information deriving from the perforemed laboratory experiments is supported by the treatments, because no previous laboratory experiment tested the effects of diatoms on copepods at saturating and non-saturating carbon concentrations. This point seems to be of particular importance to understand the effects of diatoms con copepods, because higher naupliar recruitment than in the presence of the control dinoflagellate diet was always observed after feeding on diatoms at 0.1 µg-C/mL. This suggests that low teratogenic effects mediated by diatom ingestion at non-saturating food conditions could be less deleterious than low nutritional resources for the final fitness of copepod grazers. Moreover, clearer distinction between the effects mediated by teratogenic molecules or by nutritional resources was observed at low carbon concentrations. In particular, the high oxylipin synthesis potential displayed by *Chaetoceros curvisetus* could have led to teratogenic-mediated responses, while the low fatty acid contents of *C. pseudocurvisetus* to nutritional-mediated effects. Interestingly, the four diatoms selected (*Asterionellopsis glacialis*, *Leptocylindrus* cf. *danicus*, *Chaetoceros curvisetus* and *Chaetoceros pseudocurvisetus*) showed distinct chemical features, especially in terms of oxylipin synthesis potential and composition. Similarly, molecular

responses of *T. stylifera* differed among treatments, suggesting that genes could be differentially regulated by copepods depending on the chemical traits of their prey.

Although relevant in a chemical ecology perspective, results collected in the present thesis likely constitute an intermediate step in plankton ecology. In fact, laboratory and field experiments are needed to confirm *in situ* dynamics about oxylipin variations along diatom gradients. Moreover, despite analytical improvements in the present *de novo* transcriptome assembly, much effort is still needed to enlarge functional annotation of genomic resources available for copepods so as to unveil the most intimate responses of these animals to biotic and abiotic stressors. Similar approaches should be also applied to other copepod species that can show different sensitivity to the factors considered. An intriguing perspective is to apply laboratory and field approaches investigating diatom-copepod interactions to micro-zooplankton organisms. In fact, micro-zooplankton likely represents the plankton compartment most actively feeding on diatoms (Clabet and Saiz, 2005), but studies evaluating oxylipin-mediated effects on these organisms are still few (Lavrentyev et al., 2015, Franzè et al. 2017). In the meanwhile, it is worth continuing to report on the sensitivity of copepods to diatoms by the application of integrative studies encompassing physiological, molecular and chemical analyses of the species considered.

In conclusion, non-volatile oxylipins could have evolved as a communication strategy in diatoms and do not seem to directly affect the reproductive success of the copepod *T. stylifera* at LTER-MC. While abiotic factors could have major effects on egg production, *Chaetoceros* could have lead to negative delayed effects on naupliar survival rates. However, the ultimate cause of the negative relation between *Chaetoceros* and larval viability is unknown. This is a clear demonstration that our understanding of plankton food web dynamics is highly limited and that it is still necessary to widen our knowledge about secondary metabolites synthesized by phytoplankton and their effects on copepods.

References

- ADOLPH, S., BACH, S., BLONDEL, M., CUEFF, A., MOREAU, M., POHNERT, G., POULET, S. A., WICHARD, T. & ZUCCARO, A. 2004. Cytotoxicity of diatom-derived oxylipins in organisms belonging to different phyla. The Journal of Experimental Biology, 207, 2935-46.

- AFFLECK, J. G., NEUMANN, K., WONG, L. & WALKER, V. K. 2005. The Effects of Methotrexate on Drosophila Development, Female Fecundity, and Gene Expression. Toxicological Sciences, 89, 495-503.

- ALLAN, J. D., 1976. Life history patterns in zooplankton. American Naturalist, 110, 165–180.

- ALMADA, A. A. & TARRANT, A. M. 2016. Vibrio elicits targeted transcriptional responses from copepod hosts. FEMS microbiology ecology, 92, fiw072.

- ALTSCHUL, S. F., GISH, W., MILLER, W., MYERS, E. W. & LIPMAN, D. J. 1990. Basic local alignment search tool. Journal of Molecular Biology, 215, 403-410.

- ALVAIN, S., MOULIN, C., DANDONNEAU, Y. & LOISEL, H. 2008. Seasonal distribution and succession of dominant phytoplankton groups in the global ocean: A satellite view. Global Biogeochemical Cycles, 22, GB3001.

- AMATO, A. & CAROTENUTO, Y. 2018. Planktonic calanoids embark into the "Omics Era". In: UTTIERI, M. (ed.) Trends in copepod studies: distribution, biology and ecology. Nova Science Publisher, Hauppage, p287-314.

- AMATO, A., DELL'AQUILA, G., MUSACCHIA, F., ANNUNZIATA, R., UGARTE, A., MAILLET, N., CARBONE, A., RIBERA D'ALCALÀ, M., SANGES, R., IUDICONE, D. & FERRANTE, M. I. 2017. Marine diatoms change their gene expression profile when exposed to microscale turbulence under nutrient replete conditions. Scientific Reports, 7, 3826.

- ANDERSEN, C. L., JENSEN, J. L. & ØRNTOFT, T. F. 2004. Normalization of Real-Time Quantitative Reverse Transcription-PCR Data: A Model-Based Variance Estimation Approach to Identify Genes Suited for Normalization, Applied to Bladder and Colon Cancer Data Sets. Cancer Research, 64, 5245-5250.

- ANDERSON, M. J. & WALSH, D. C. I. 2013. PERMANOVA, ANOSIM, and the Mantel test in the face of heterogeneous dispersions: What null hypothesis are you testing? Ecological Monographs, 83, 557-574.

- ARAI, H., KOIZUMI, H., AOKI, J. & INOUE, K. 2002. Platelet-Activating Factor Acetylhydrolase (PAF-AH). The Journal of Biochemistry, 131, 635-640.

- ARENDT, K. E., JÓNASDÓTTIR, S. H., HANSEN, P. J. & GÄRTNER, S. 2004. Effects of dietary fatty acids on the reproductive success of the calanoid copepod *Temora longicornis*. Marine Biology, 146, 513-530.

- ARMANT, O., MARZ, M., SCHMIDT, R., FERG, M., DIOTEL, N., ERTZER, R., BRYNE, J. C., YANG, L., BAADER, I., REISCHL, M., LEGRADI, J., MIKUT, R., STEMPLE, D., VAN, I. W., VAN DER SLOOT, A., LENHARD, B., STRAHLE, U. & RASTEGAR, S. 2013. Genome-wide, whole mount in situ analysis of transcriptional regulators in zebrafish embryos. Developmental biology, 380, 351-62.

- ARMBRUST, E. V. 2009. The life of diatoms in the world's oceans. Nature, 459, 185-92.

- ARUDA, A. M., BAUMGARTNER, M. F., REITZEL, A. M. & TARRANT, A. M. 2011. Heat shock protein expression during stress and diapause in the marine copepod Calanus finmarchicus. Journal of insect physiology, 57, 665-75.

- ARYA, M., SHERGILL, I. S., WILLIAMSON, M., GOMMERSALL, L., ARYA, N. & PATEL, H. R. H. 2005. Basic principles of real-time quantitative PCR. Expert Review of Molecular Diagnostics, 5, 209-219.

- ASAI, S., IANORA, A., LAURITANO, C., LINDEQUE, P. K. & CAROTENUTO, Y. 2015. High-quality RNA extraction from copepods for Next Generation Sequencing: A comparative study. Marine genomics, 24, 115-8.

- ASK, J., REINIKAINEN, M. & BÅMSTEDT, U. 2006. Variation in hatching success and egg production of *Eurytemora affinis* (Calanoida, Copepoda) from the Gulf of Bothnia, Baltic Sea, in relation to abundance and clonal differences of diatoms. Journal of Plankton Research, 28, 683-694.

- BALESTRA, C., ALONSO-SÁEZ, L., GASOL, J. M. & CASOTTI, R. 2011. Group-specific effects on coastal bacterioplankton of polyunsaturated aldehydes produced by diatoms. Aquatic Microbial Ecology, 63, 123-131.

- BAN, S., BURNS, C., CASTEL, J., CHAUDRON, Y., CHRISTOU, E., ESCRIBANO, R., UMANI, S. F., GASPARINI, S., RUIZ, F. G., HOFFMEYER, M., IANORA, A., KANG, H.-K., LAABIR, M., LACOSTE, A., MIRALTO, A., NING, X., POULET, S., RODRIGUEZ, V., RUNGE, J., SHI, J., STARR, M., UYE, S.-I. & WANG, Y. 1997. The paradox of diatom-copepod interactions. Marine Ecology Progress Series, 157, 287-293.

- BAROFSKY, A., SIMONELLI, P., VIDOUDEZ, C., TROEDSSON, C., NEJSTGAARD, J. C., JAKOBSEN, H. H. & POHNERT, G. 2009. Growth phase of the diatom *Skeletonema marinoi* influences the metabolic profile of the cells and

the selective feeding of the copepod *Calanus* spp. Journal of Plankton Research, 32, 263-272.

- BARREIRO, A., CAROTENUTO, Y., LAMARI, N., ESPOSITO, F., D'IPPOLITO, G., FONTANA, A., ROMANO, G., IANORA, A., MIRALTO, A. & GUISANDE, C. 2011. Diatom induction of reproductive failure in copepods: The effect of PUAs versus non volatile oxylipins. Journal of Experimental Marine Biology and Ecology, 401, 13-19.

- BARTUAL, A., ARANDIA-GOROSTIDI, N., CÓZAR, A., MORILLO-GARCÍA, S., ORTEGA, M., VIDAL, M., CABELLO, A., GONZÁLEZ-GORDILLO, J. & ECHEVARRÍA, F. 2014. Polyunsaturated Aldehydes from Large Phytoplankton of the Atlantic Ocean Surface (42°N to 33°S). Marine Drugs, 12, 682.

- BAUMEISTER, T. U. H., VALLET, M., KAFTAN, F., SVATOS, A. & POHNERT, G. 2019. Live Single-Cell Metabolomics With Matrix-Free Laser/Desorption Ionization Mass Spectrometry to Address Microalgal Physiology. Frontiers in Plant Science, 10, 172.

- BEAUGRAND, G., BRANDER, K. M., ALISTAIR LINDLEY, J., SOUISSI, S. & REID, P. C. 2003. Plankton effect on cod recruitment in the North Sea. Nature, 426, 661.

- BEHR, M. & HOCH, M. 2005. Identification of the novel evolutionary conserved *Obst*ructor multigene family in invertebrates. FEBS letters, 579, 6827-33.

- BENEDETTI, F., GASPARINI, S. & AYATA, S.-D. 2016. Identifying copepod functional groups from species functional traits. Journal of Plankton Research, 38, 159-166.

- BENEDETTI, F., VOGT, M., RIGHETTI, D., GUILHAUMON, F. & AYATA, S.-D. 2018. Do functional groups of planktonic copepods differ in their ecological niches? Journal of Biogeography, 45, 604-616.

- BENJAMINI, Y. & HOCHBERG, Y. 1995. Controlling the False Discovery Rate: A Practical and Powerful Approach to Multiple Testing. Journal of the Royal Statistical Society. Series B (Methodological), 57, 289-300.

- BIDLE, K. D. 2015. The molecular ecophysiology of programmed cell death in marine phytoplankton. Annual review of marine science, 7, 341-75.

- BIDLE, K. D. 2016. Programmed Cell Death in Unicellular Phytoplankton. Current Biology, 26, R594-R607.

- BIESSMANN, H., NGUYEN, Q. K., LE, D. & WALTER, M. F. 2005. Microarray-based survey of a subset of putative olfactory genes in the mosquito Anopheles gambiae. Insect molecular biology, 14, 575-89.

- BOXSHALL, G. A. & DEFAYE, D. 2007. Global diversity of copepods (Crustacea: Copepoda) in freshwater. Hydrobiologia, 595, 195-207.

- BRADFORD-GRIEVE, J. M., MARKHASEVA, E. L., ROCHA, C. E. F., ABIAHY, B., 1999. Copepoda. In BOLTOVSKOY, D. (Ed.). *South Atlantic Zooplankton,* Leiden: Backhuys Publishers. p. 869-1098.

- BRETT, M. & MÜLLER-NAVARRA, D. 1997. The role of highly unsaturated fatty acids in aquatic foodweb processes. Freshwater Biology, 38, 483-499.

- BROMKE, M. A., SABIR, J. S., ALFASSI, F. A., HAJARAH, N. H., KABLI, S. A., AL-MALKI, A. L., ASHWORTH, M. P., MERET, M., JANSEN, R. K. & WILLMITZER, L. 2015. Metabolomic Profiling of 13 Diatom Cultures and Their Adaptation to Nitrate-Limited Growth Conditions. PloS one, 10, e0138965.

- BRUGNANO, C., GRANATA, A., GUGLIELMO, L., MINUTOLI, R., ZAGAMI, G. & IANORA, A. 2016. The deleterious effect of diatoms on the biomass and growth of early stages of their copepod grazers. Journal of Experimental Marine Biology and Ecology, 476, 41-49.

- BUTTINO, I., DE ROSA, G., CAROTENUTO, Y., MAZZELLA, M., IANORA, A., ESPOSITO, F., VITIELLO, V., QUAGLIA, F., LA ROTONDA, M. I. & MIRALTO, A. 2008. Aldehyde-encapsulating liposomes impair marine grazer survivorship. The Journal of Experimental Biology, 211, 1426-33.

- CAGLIARI, A., MARGIS, R., DOS SANTOS MARASCHIN, F., TURCHETTO-ZOLET, A., LOSS, G. & MARGIS-PINHEIRO, M. 2011. Biosynthesis of Triacylglycerols (TAGs) in plants and algae. International Journal of Plant Biology, 2, e10.

- CALDWELL, G. S. 2009. The influence of bioactive oxylipins from marine diatoms on invertebrate reproduction and development. Marine Drugs, 7, 367-400.

- CAROTENUTO, Y. & LAMPERT, W. 2004. Ingestion and incorporation of freshwater diatoms by Daphnia pulicaria: do morphology and oxylipin production matter? Journal of Plankton Research, 26, 563-569.

- CAROTENUTO, Y. 1999. Morphological analysis of larval stages of *Temora stylifera* (Copepoda, Calanoida) from the Mediterranean Sea. Journal of Plankton Research, 21, 1613-1632.

- CAROTENUTO, Y., DATTOLO, E., LAURITANO, C., PISANO, F., SANGES, R., MIRALTO, A., PROCACCINI, G. & IANORA, A. 2014. Insights into the transcriptome of the marine copepod *Calanus helgolandicus* feeding on the oxylipin-producing diatom Skeletonema marinoi. Harmful Algae, 31, 153-162.

- CAROTENUTO, Y., ESPOSITO, F., PISANO, F., LAURITANO, C., PERNA, M., MIRALTO, A. & IANORA, A. 2012. Multi-generation cultivation of the copepod *Calanus helgolandicus* in a re-circulating system. Journal of Experimental Marine Biology and Ecology, 418-419, 46-58.

- CAROTENUTO, Y., IANORA, A. & MIRALTO, A. 2011. Maternal and neonate diatom diets impair development and sex differentiation in the copepod *Temora stylifera*. Journal of Experimental Marine Biology and Ecology, 396, 99-107.

- CAROTENUTO, Y., IANORA, A., BUTTINO, I., ROMANO, G. & MIRALTO, A. 2002. Is postembryonic development in the copepod *Temora stylifera* negatively affected by diatom diets? Journal of Experimental Marine Biology and Ecology, 276, 49-66.

- CAROTENUTO, Y., IANORA, A., BUTTINO, I., ROMANO, G. & MIRALTO, A. 2002. Is postembryonic development in the copepod Temora stylifera negatively affected by diatom diets? Journal of Experimental Marine Biology and Ecology, 276, 49-66.

- CAROTENUTO, Y., IANORA, A., DI PINTO, M., SARNO, D. & MIRALTO, A. 2006. Annual cycle of early developmental stage survival and recruitment in the copepods Temora stylifera and Centropages typicus. Marine Ecology Progress Series, 314, 227-238.

- CASOTTI, R., MAZZA, S., BRUNET, C., VANTREPOTTE, V., IANORA, A. & MIRALTO, A. 2005. Growth Inhibition and Toxicity of the Diatom Aldehyde 2-Trans, 4-Trans-Decadienal On *Thalassiosira weissflogii* (Bacillariophyceae). Journal of phycology, 41, 7-20.

- CATHERINO, W. H., LEPPERT, P. C., STENMARK, M. H., PAYSON, M., POTLOG-NAHARI, C., NIEMAN, L. K. & SEGARS, J. H. 2004. Reduced dermatopontin expression is a molecular link between uterine leiomyomas and keloids. Genes, chromosomes & cancer, 40, 204-17.

- CEBALLOS, S. & IANORA, A. 2003. Different diatoms induce contrasting effects on the reproductive success of the copepod Temora stylifera. Journal of Experimental Marine Biology and Ecology, 294, 189-202.

- CHAKRABARTI, R., SHEPARDSON, S., KARMAKAR, M., TRDAN, R., WALKER, J., SHANDILYA, R., STEWART, D., VIJAYARAGHAVAN, S. & HOEH, W. 2009. Extra-mitochondrial localization and likely reproductive function

of a female-transmitted cytochrome c oxidase subunit II protein. Development, growth & differentiation, 51, 511-9.

- CHRISTIE, A. E., FONTANILLA, T. M., RONCALLI, V., CIESLAK, M. C. & LENZ, P. H. 2014a. Diffusible gas transmitter signaling in the copepod crustacean Calanus finmarchicus: identification of the biosynthetic enzymes of nitric oxide (NO), carbon monoxide (CO) and hydrogen sulfide (H2S) using a de novo assembled transcriptome. General and comparative endocrinology, 202, 76-86.

- CHRISTIE, A. E., FONTANILLA, T. M., RONCALLI, V., CIESLAK, M. C. & LENZ, P. H. 2014b. Identification and developmental expression of the enzymes responsible for dopamine, histamine, octopamine and serotonin biosynthesis in the copepod crustacean Calanus finmarchicus. General and comparative endocrinology, 195, 28-39.

- CIANELLI, D., UTTIERI, M., BUONOCORE, B., FALCO, P., ZAMBARDINO, G., ZAMBIANCHI, E. 2012. Dynamics of a very special mediterranean cosatal area: the Gulf of Naples. In: Williams, G. S. (Ed.). Mediterranean Ecosystems: Dynamics, Management & Conservation, Nova Science Publisher, Inc., p129-150.

- CIANELLI, D., FALCO, P., IERMANO, I., MOZZILLO, P., UTTIERI, M., BUONOCORE, B., ZAMBARDINO, G. & ZAMBIANCHI, E. 2015. Inshore/offshore water exchange in the Gulf of Naples. Journal of Marine Systems, 145, 37-52.

- CLEGG, N., FINDLEY, S., MAHOWALD, A. & RUOHOLA-BAKER, H. 2001. maelstrom is required to position the MTOC in stage 2–6 Drosophila oocytes. Development Genes and Evolution, 211, 44-48.

- CONESA, A. & GÖTZ, S. 2008. Blast2GO: A Comprehensive Suite for Functional Analysis in Plant Genomics. International journal of plant genomics, 2008, 619832.

- CONESA, A., GÖTZ, S., GARCÍA-GÓMEZ, J. M., TEROL, J., TALÓN, M. & ROBLES, M. 2005. Blast2GO: a universal tool for annotation, visualization and analysis in functional genomics research. Bioinformatics, 21, 3674-3676.

- COPEMAN, L. A. & PARRISH, C. C. 2003. Marine lipids in a cold coastal ecosystem: Gilbert Bay, Labrador. Marine Biology, 143, 1213-1227.

- CÓZAR, A., MORILLO-GARCÍA, S., ORTEGA, M. J., LI, Q. P. & BARTUAL, A. 2018. Macroecological patterns of the phytoplankton production of polyunsaturated aldehydes. Scientific Reports, 8, 12282.

- CUTIGNANO, A., LAMARI, N., D'IPPOLITO, G., MANZO, E., CIMINO, G. & FONTANA, A. 2011. Lipoxygenase Products in Marine Diatoms: A Concise

Analytical Method to Explore the Functional Potential of Oxylipins. Journal of phycology, 47, 233-43.

- D'ALELIO, D., MAZZOCCHI, M. G., MONTRESOR, M., SARNO, D., ZINGONE, A., DI CAPUA, I., FRANZÈ, G., MARGIOTTA, F., SAGGIOMO, V. & RIBERA D'ALCALÀ, M. 2015. The green-blue swing: plasticity of plankton food-webs in response to coastal oceanographic dynamics. Marine Ecology, 36, 1155-1170.

- DALSGAARD, J., ST. JOHN, M., KATTNER, G., MÜLLER-NAVARRA, D. & HAGEN, W. 2003. Fatty acid trophic markers in the pelagic marine environment. Advances in Marine Biology, 46, 225-340.

- DE RUGGIERO, P., NAPOLITANO, E., IACONO, R. & PIERINI, S. 2016. A high-resolution modelling study of the circulation along the Campania coastal system, with a special focus on the Gulf of Naples. Continental Shelf Research, 122, 85-101.

- DESCHUTTER, Y., EVERAERT, G., DE SCHAMPHELAERE, K. & DE TROCH, M. 2017. Relative contribution of multiple stressors on copepod density and diversity dynamics in the Belgian part of the North Sea. Marine Pollution Bulletin, 125, 350-359.

- DI CAPUA, I. & MAZZOCCHI, M. G. 2004. Population structure of the copepods *Centropages typicus* and *Temora stylifera* in different environmental conditions. ICES Journal of Marine Science, 61, 632-644.

- DIATCHENKO, L., LAU, Y.-F. C., AARON, P.C., CHENCHIK, A., MOQADAM, F., HUANG, B., LUKYANOV, S., LUKYANOV, K., GURSKAYA, N., SVERRDLOV, E. D., SIEBERT, P. D., 1996. Suppression subtractive hybridization: a method for generating differentially regulated or tissue-specific cDNA probes and libraries. Proc. Natl. Acad. Sci. U. S. A., 93 (12), 6025–6030.

- DIJKMAN, N. A. & KROMKAMP, J. C. 2006. Phospholipid-derived fatty acids as chemotaxonomic markers for phytoplankton: application for inferring phytoplankton composition. Marine Ecology Progress Series, 324, 113-125.

- D'IPPOLITO, G., CUTIGNANO, A., BRIANTE, R., FEBBRAIO, F., CIMINO, G. & FONTANA, A. 2005. New C16 fatty-acid-based oxylipin pathway in the marine diatom *Thalassiosira rotula*. Organic & Biomolecular Chemistry, 3, 4065-70.

- D'IPPOLITO, G., CUTIGNANO, A., TUCCI, S., ROMANO, G., CIMINO, G. & FONTANA, A. 2006. Biosynthetic intermediates and stereochemical aspects of aldehyde biosynthesis in the marine diatom *Thalassiosira rotula*. Phytochemistry, 67, 314-22.

- D'IPPOLITO, G., LAMARI, N., MONTRESOR, M., ROMANO, G., CUTIGNANO, A., GERECHT, A., CIMINO, G. & FONTANA, A. 2009. 15S-lipoxygenase metabolism in the marine diatom *Pseudo-nitzschia delicatissima*. The New Phytologist, 183, 1064-71.

- D'IPPOLITO, G., NUZZO, G., SARDO, A., MANZO, E., GALLO, C. & FONTANA, A. 2018. Chapter Four - Lipoxygenases and Lipoxygenase Products in Marine Diatoms. In: MOORE, B. S. (ed.) Methods in Enzymology. Academic Press.

- D'IPPOLITO, G., ROMANO, G., CARUSO, T., SPINELLA, A., CIMINO, G. & FONTANA, A. 2003. Production of Octadienal in the Marine Diatom *Skeletonema costatum*. Organic Letters, 5, 885-887.

- D'IPPOLITO, G., ROMANO, G., CARUSO, T., SPINELLA, A., CIMINO, G. & FONTANA, A. 2003. Production of Octadienal in the Marine Diatom Skeletonema costatum.

- D'IPPOLITO, G., ROMANO, G., IADICICCO, O., MIRALTO, A., IANORA, A., CIMINO, G. & FONTANA, A. 2002. New birth-control aldehydes from the marine diatom *Skeletonema costatum*: characterization and biogenesis. Tetrahedron Letters, 43, 6133-6136.

- D'IPPOLITO, G., TUCCI, S., CUTIGNANO, A., ROMANO, G., CIMINO, G., MIRALTO, A. & FONTANA, A. 2004. The role of complex lipids in the synthesis of bioactive aldehydes of the marine diatom *Skeletonema costatum*. Biochimica et Biophysica Acta, 1686, 100-7.

- DITTMER, N. T., SUN, G., WANG, S. F. & RAIKHEL, A. S. 2003. CREB isoform represses yolk protein gene expression in the mosquito fat body. Molecular and cellular endocrinology, 210, 39-49.

- DOBIN, A., DAVIS, C. A., SCHLESINGER, F., DRENKOW, J., ZALESKI, C., JHA, S., BATUT, P., CHAISSON, M. & GINGERAS, T. R. 2012. STAR: ultrafast universal RNA-seq aligner. Bioinformatics, 29, 15-21.

- DOVE, S. K., DONG, K., KOBAYASHI, T., WILLIAMS, F. K. & MICHELL, R. H. 2009. Phosphatidylinositol 3,5-bisphosphate and Fab1p/PIKfyve underPPIn endo-lysosome function. The Biochemical journal, 419, 1-13.

- EDLER, L. & ELBRÄCHTER, M. 2010. The Utermöhl method for quantitative phytoplankton analysis. In: KARLSON, B., CUSACK, C., BRESNAN, E. (eds.). Microscopic and Molecular Methods for Quantitative Phytoplankton Analyses. UNESCO (Paris), p13-20.

- EDWARDS, B. R., BIDLE, K. D. & VAN MOOY, B. A. 2015. Dose-dependent regulation of microbial activity on sinking particles by polyunsaturated aldehydes: Implications for the carbon cycle. Proceedings of the National Academy of Sciences of the United States of America, 112, 5909-14.

- FALCIATORE, A., D'ALCALÀ, M. R., CROOT, P. & BOWLER, C. 2000. Perception of Environmental Signals by a Marine Diatom. Science, 288, 2363-2366.

- FERRARI & DAHMS, H. U. 2007. Post-Embryonic Development of the Copepoda. In: BRILL (ed.). Crustaceana Monographs. Leiden (Boston).

- FIELD, C. B., BEHRENFELD, M. J., RANDERSON, J. T. & FALKOWSKI, P. 1998. Primary Production of the Biosphere: Integrating Terrestrial and Oceanic Components. Science, 281, 237-240.

- FIORE, C. L., LONGNECKER, K., KIDO SOULE, M. C. & KUJAWINSKI, E. B. 2015. Release of ecologically relevant metabolites by the cyanobacterium *Synechococcus elongatus* CCMP 1631. Environmental Microbiology, 17, 3949-63.

- FLADMARK, K. E., BRUSTUGUN, O. T., HOVLAND, R., BØE, R., GJERTSEN, B. T., ZHIVOTOVSKY, B. & DØSKELAND, S. O. 1999. Ultrarapid caspase-3 dependent apoptosis induction by serine/threonine phosphatase inhibitors. Cell Death & Differentiation, 6, 1099-1108.

- FLYNN, K. J. & IRIGOIEN, X. 2009. Aldehyde-induced insidious effects cannot be considered as a diatom defence mechanism against copepods. Marine Ecology Progress Series, 377, 79-89.

- FONTANA, A., D'IPPOLITO, G., CUTIGNANO, A., MIRALTO, A., IANORA, A., ROMANO, G. & CIMINO, G. 2007a. Chemistry of oxylipin pathways in marine diatoms. Pure and Applied Chemistry, 79, 481-490.

- FONTANA, A., D'IPPOLITO, G., CUTIGNANO, A., ROMANO, G., LAMARI, N., MASSA GALLUCCI, A., CIMINO, G., MIRALTO, A. & IANORA, A. 2007b. LOX-induced lipid peroxidation mechanism responsible for the detrimental effect of marine diatoms on zooplankton grazers. Chembiochem : a European Journal of Chemical Biology, 8, 1810-8.

- FORGES, T., MONNIER-BARBARINO, P., ALBERTO, J. M., GUEANT-RODRIGUEZ, R. M., DAVAL, J. L. & GUEANT, J. L. 2007. Impact of folate and homocysteine metabolism on human reproductive health. Human reproduction update, 13, 225-38.

- FRANZÈ, G., PIERSON, J. J., STOECKER, D. K. & LAVRENTYEV, P. J. 2017. Diatom-produced allelochemicals trigger trophic cascades in the planktonic food web. Limonology and Oceanography, 0, 1-16.

- GALLO, C., D'IPPOLITO, G., NUZZO, G., SARDO, A. & FONTANA, A. 2017. Autoinhibitory sterol sulfates mediate programmed cell death in a bloom-forming marine diatom. Nature Communications, 8, 1292.

- GALLOWAY, A. W. & WINDER, M. 2015. Partitioning the Relative Importance of Phylogeny and Environmental Conditions on Phytoplankton Fatty Acids. PloS one, 10, e0130053.

- GERECHT, A., CAROTENUTO, Y., IANORA, A., ROMANO, G., FONTANA, A., D'IPPOLITO, G., JAKOBSEN, H. H. & NEJSTGAARD, J. C. 2013. Oxylipin production during a mesocosm bloom of *Skeletonema marinoi*. Journal of Experimental Marine Biology and Ecology, 446, 159-165.

- GERECHT, A., ROMANO, G., IANORA, A., D'IPPOLITO, G., CUTIGNANO, A. & FONTANA, A. 2011. Plasticity of Oxylipin Metabolism among Clones of the Marine Diatom *Skeletonema marinoi* (Bacillariophyceae). Journal of phycology, 47, 1050-6.

- GIORDANO, G., CARBONE, M., CIAVATTA, M. L., SILVANO, E., GAVAGNIN, M., GARSON, M. J., CHENEY, K. L., MUDIANTA, I. W., RUSSO, G. F., VILLANI, G., MAGLIOZZI, L., POLESE, G., ZIDORN, C., CUTIGNANO, A., FONTANA, A., GHISELIN, M. T. & MOLLO, E. 2017. Volatile secondary metabolites as aposematic olfactory signals and defensive weapons in aquatic environments. Proceedings of the National Academy of Sciences, 114, 3451.

- GLUD, R. N., GROSSART, H.-P., LARSEN, M., TANG, K. W., ARENDT, K. E., RYSGAARD, S., THAMDRUP, B. & GISSEL NIELSEN, T. 2015. Copepod carcasses as microbial hot spots for pelagic denitrification. Limnology and Oceanography, 60, 2026-2036.

- GRABHERR, M. G., HAAS, B. J., YASSOUR, M., LEVIN, J. Z., THOMPSON, D. A., AMIT, I., ADICONIS, X., FAN, L., RAYCHOWDHURY, R., ZENG, Q., CHEN, Z., MAUCELI, E., HACOHEN, N., GNIRKE, A., RHIND, N., DI PALMA, F., BIRREN, B. W., NUSBAUM, C., LINDBLAD-TOH, K., FRIEDMAN, N. & REGEV, A. 2011. Full-length transcriptome assembly from RNA-Seq data without a reference genome. Nature biotechnology, 29, 644-652.

- GRAHAM, M. H. 2003. Confronting multicollinearity in ecological multiple regression. Ecology, 84, 2809-2815.

- GROSSART, H. P., KIØRBOE, T., TANG, K. W., ALLGAIER, M., YAM, E. M. & PLOUG, H. 2006. Interactions between marine snow and heterotrophic bacteria: aggregate formation and microbial dynamics. Aquatic Microbial Ecology, 42, 19-26.

- GROSSE, J., BRUSSAARD, C. & BOSCHKER, H. 2018. Nutrient limitation driven dynamics of amino acids and fatty acids in coastal phytoplankton: Compound synthesis under N and P limitation. Limnology and Oceanography 64, 302-316.

- GUILLARD, R. R. L., RYTHER, J. H. 1962. Studies on Marine Planktonic Diatoms I. Cyclotella nana Hustedt and Detonula confervacea (Cleve) Gran. Canadian Journal of Microbiology 8, 229-239.

- GUISAN, A., EDWARDS, T. C. & HASTIE, T. 2002. Generalized linear and generalized additive models in studies of species distributions: setting the scene. Ecological Modelling, 157, 89-100.

- GUSCHINA, I. A. & HARWOOD, J. L. 2006. Lipids and lipid metabolism in eukaryotic algae. Progress in Lipid Research, 45, 160-86.

- HALSBAND-LENK, C. 2005. Metridia pacifica in Dabob Bay, Washington: The diatom effect and the discrepancy between high abundance and low egg production rates. Progress in Oceanography, 67, 422-441.

- HALSBAND-LENK, C., NIVAL, S., CARLOTTI, F. & HIRCHE, H.-J. 2001. Seasonal Cycles of Egg Production of Two Planktonic Copepods, *Centropages typicus* and *Temora stylifera*, in the North-western Mediterranean Sea. Journal of Plankton Research, 23, 597-609.

- HALSBAND-LENK, C., PIERSON, J. J. & LEISING, A. W. 2005. Reproduction of *Pseudocalanus newmani* (Copepoda: Calanoida) is deleteriously affected by diatom blooms – A field study. Progress in Oceanography, 67, 332-348.

- HAMMER, O., HARPER, D. & RYAN, P. 2001. PAST: Paleontological Statistics Software Package for Education and Data Analysis. Paleontologia Electroinica, p4-9.

- HAVIRD, J. C. & SANTOS, S. R. 2016. Here We Are, But Where Do We Go? A Systematic Review of Crustacean Transcriptomic Studies from 2014-2015. Integrative and comparative biology, 56, 1055-1066.

- HAZZARD, S. E. & KLEPPEL, G. S. 2003. Egg production of the copepod *Acartia tonsa* in Florida Bay: role of fatty acids in the nutritional composition of the food environment. Marine Ecology Progress Series, 252, 199-206.

- HEUSCHELE, J. & SELANDER, E. 2014. The chemical ecology of copepods. Journal of Plankton Research, 36, 895-913.

- HOLSTE, L., JOHN, M. & PECK, M. 2009. The effects of temperature and salinity on reproductive success of Temora longicornis in the Baltic Sea. Marine Biology, 156, 527-540.

- HOORNAERT, I., MARYNEN, P. & BAENS, M. 1998. *CREBL2* a novel transcript from the chromosome 12 region flanked by ETV6 and CDKN1B. Genomics, 51, 154-7.

- HUSKIN, I., ANADÓN, R., ÁLVAREZ-MARQUÉS, F. & HARRIS, R. 2000. Ingestion, faecal pellet and egg production rates of Calanus helgolandicus feeding coccolithophorid versus non-coccolithophorid diets. Journal of Experimental Marine Biology and Ecology, 248, 239-254.

- IANORA, A. & MIRALTO, A. 2010. Toxigenic effects of diatoms on grazers, phytoplankton and other microbes: a review. Ecotoxicology, 19, 493-511.

- IANORA, A., BASTIANINI, M., CAROTENUTO, Y., CASOTTI, R., RONCALLI, V., MIRALTO, A., ROMANO, G., GERECHT, A., FONTANA, A. & TURNER, J. T. 2015. Non-volatile oxylipins can render some diatom blooms more toxic for copepod reproduction. Harmful Algae, 44, 1-7.

- IANORA, A., BASTIANINI, M., CAROTENUTO, Y., CASOTTI, R., RONCALLI, V., MIRALTO, A., ROMANO, G., GERECHT, A., FONTANA, A. & TURNER, J. T. 2015. Non-volatile oxylipins can render some diatom blooms more toxic for copepod reproduction. Harmful algae, 44, 1-7.

- IANORA, A., CASOTTI, R., BASTIANINI, M., BRUNET, C., D'IPPOLITO, G., ACRI, F., FONTANA, A., CUTIGNANO, A., TURNER, J. T. & MIRALTO, A. 2008. Low reproductive success for copepods during a bloom of the non-aldehyde-producing diatom *Cerataulina pelagica* in the North Adriatic Sea. Marine Ecology, 29, 399-410.

- IANORA, A., MIRALTO, A. & ROMANO, G. 2012a. Antipredatory Defensive Role of Planktonic Marine Natural Products. In: FATTORUSSO, E., GERWICK, W. H. & TAGLIALATELA-SCAFATI, O. (eds.) Handbook of Marine Natural Products. Dordrecht: Springer Netherlands.

- IANORA, A., MIRALTO, A., A POULET, S., CAROTENUTO, Y., BUTTINO, I., ROMANO, G., CASOTTI, R., POHNERT, G., WICHARD, T., COLUCCI D'AMATO, L., TERRAZZANO, G. & SMETACEK, V. 2004. Aldehyde suppression of copepod recruitment in blooms of a ubiquitous planktonic diatom. Nature. 2004;429: 403-407.

- IANORA, A., POULET, S. A. & MIRALTO, A. 1995. A comparative study of the inhibitory effect of diatoms on the reproductive biology of the copepod Temora stylifera. Marine Biology, 121, 533-539.

- IANORA, A., ROMANO, G., CAROTENUTO, Y., ESPOSITO, F., RONCALLI, V., BUTTINO, I. & MIRALTO, A. 2011. Impact of the diatom oxylipin 15S-HEPE on the reproductive success of the copepod *Temora stylifera*. Hydrobiologia, 666, 265-275.

- IANORA, A., SCOTTO DI CARLO, B. & MASCELLARO, P. 1989. Reproductive biology of the planktonic copepod Temora stylifera. Marine biology, 101, 187-194.

- IKONOMOV, O. C., SBRISSA, D., DELVECCHIO, K., XIE, Y., JIN, J. P., RAPPOLEE, D. & SHISHEVA, A. 2011. The phosphoinositide kinase PIKfyve is vital in early embryonic development: preimplantation lethality of PIKfyve-/- embryos but normality of PIKfyve+/- mice. The Journal of biological chemistry, 286, 13404-13.

- IRIGOIEN, X., HARRIS, R. P., VERHEYE, H. M., JOLY, P., RUNGE, J., STARR, M., POND, D., CAMPBELL, R., SHREEVE, R., WARD, P., SMITH, A. N., DAM, H. G., PETERSON, W., TIRELLI, V., KOSKI, M., SMITH, T., HARBOUR, D. & DAVIDSON, R. 2002. Copepod hatching success in marine ecosystems with high diatom concentrations. Nature, 419, 387.

- JÓNASDÓTTIR, S. H., VISSER, A. W. & JESPERSEN, C. 2009. Assessing the role of food quality in the production and hatching of *Temora longicornis* eggs. Marine Ecology Progress Series, 382, 139-150.

- JÓNASDÓTTIR, S., GUDFINNSSON, H., GISLASON, A. & ASTTHORSSON, O. 2002. Diet composition and quality for *Calanus finmarchicus* egg production and hatching success off south-west Iceland. Marine Biology, 140, 1195-1206.

- JONES, R. & FLYNN, K. 2005. Nutritional Status and Diet Composition Affect the Value of Diatoms as Copepod Prey. Science (New York, N.Y.), 307, 1457-9.

- KÂ, S., CAROTENUTO, Y., ROMANO, G., HWANG, J.-S., BUTTINO, I. & IANORA, A. 2014. Impact of the diatom-derived polyunsaturated aldehyde 2-trans,4-trans decadienal on the feeding, survivorship and reproductive success of the calanoid copepod Temora stylifera. Marine Environmental Research, 93, 31-37.

- KAINZ, M., ARTS, M. T. & MAZUMDER, A. 2004. Essential fatty acids in the planktonic food web and their ecological role for higher trophic levels. Limnology and Oceanography, 49, 1784-1793.

- KARAGEORGOS, L., BROOKS, D. A., POLLARD, A., MELVILLE, E. L., HEIN, L. K., CLEMENTS, P. R., KETTERIDGE, D., SWIEDLER, S. J., BECK,

M., GIUGLIANI, R., HARMATZ, P., WRAITH, J. E., GUFFON, N., LEAO TELES, E., SA MIRANDA, M. C. & HOPWOOD, J. J. 2007. Mutational analysis of 105 mucopolysaccharidosis type VI patients. Human mutation, 28, 897-903.

- KHAN, M. T., DALVIN, S., WAHEED, Q., NILSEN, F. & MALE, R. 2018. Molecular characterization of the lipophorin receptor in the crustacean ectoparasite Lepeophtheirus salmonis. PloS one, 13, e0195783.

- KIDO SOULE, M. C., LONGNECKER, K., JOHNSON, W. M. & KUJAWINSKI, E. B. 2015. Environmental metabolomics: Analytical strategies. Marine Chemistry, 177, 374-387.

- KLUMPP, S. & KRIEGLSTEIN, J. 2002. Serine/threonine protein phosphatases in apoptosis. Current opinion in pharmacology, 2, 458-62.

- KOMPIS, I. M., ISLAM, K. & THEN, R. L. 2005. DNA and RNA Synthesis: Antifolates. Chemical Reviews, 105, 593-620.

- KONO, N. & ARAI, H. 2019. Platelet-activating factor acetylhydrolases: An overview and update. Biochimica et biophysica acta. Molecular and cell biology of lipids, 1864, 922-931.

- KORDAN, W., STRZEŻEK, J. & FRASER, L. 2003. Functions of platelet activating factor (PAF) in mammalian reproductive processes: A review. Polish journal of veterinary sciences, 6, 55-60.

- KOSKI, M. 2007. High reproduction of Calanus finmarchicus during a diatom-dominated spring bloom. Marine Biology, 151, 1785-1798.

- KUHLISCH, C. & POHNERT, G. 2015. Metabolomics in chemical ecology. Natural Product Reports, 32, 937-955.

- LAMARI, N., RUGGIERO, M. V., D'IPPOLITO, G., KOOISTRA, W. H., FONTANA, A. & MONTRESOR, M. 2013. Specificity of lipoxygenase pathways supports species delineation in the marine diatom genus *Pseudo-nitzschia*. PloS one, 8, e73281.

- LANG, I., HODAC, L., FRIEDL, T. & FEUSSNER, I. 2011. Fatty acid profiles and their distribution patterns in microalgae: a comprehensive analysis of more than 2000 strains from the SAG culture collection. BMC Plant Biology, 11, 124.

- LAU, A. W. & CHOU, M. M. 2008. The adaptor complex AP-2 regulates post-endocytic trafficking through the non-clathrin Arf6-dependent endocytic pathway. Journal of Cell Science, 121, 4008-4017.

- LAURITANO, C. & PROCACCINI, G. 2011. Gene expression patterns and stress response in marine copepods. Marine environmental research, 76, 22-31.

- LAURITANO, C., BORRA, M., CAROTENUTO, Y., BIFFALI, E., MIRALTO, A., PROCACCINI, G. & IANORA, A. 2011a. First molecular evidence of diatom effects in the copepod *Calanus helgolandicus*. Journal of Experimental Marine Biology and Ecology, 404, 79-86.

- LAURITANO, C., BORRA, M., CAROTENUTO, Y., BIFFALI, E., MIRALTO, A., PROCACCINI, G. & IANORA, A. 2011b. Molecular Evidence of the Toxic Effects of Diatom Diets on Gene Expression Patterns in Copepods. PloS one, 6, e26850.

- LAURITANO, C., CAROTENUTO, Y., MIRALTO, A., PROCACCINI, G. & IANORA, A. 2012. Copepod population-specific response to a toxic diatom diet. PloS one, 7, e47262.

- LAURITANO, C., CAROTENUTO, Y., VITIELLO, V., BUTTINO, I., ROMANO, G., HWANG, J. S. & IANORA, A. 2015. Effects of the oxylipin-producing diatom *Skeletonema marinoi* on gene expression levels of the calanoid copepod *Calanus sinicus*. Marine genomics, 24, 89-94.

- LAURITANO, C., ROMANO, G., RONCALLI, V., AMORESANO, A., FONTANAROSA, C., BASTIANINI, M., BRAGA, F., CAROTENUTO, Y. & IANORA, A. 2016. New oxylipins produced at the end of a diatom bloom and their effects on copepod reproductive success and gene expression levels. Harmful Algae, 55, 221-229.

- LAVRENTYEV, P. J., FRANZE, G., PIERSON, J. J. & STOECKER, D. K. 2015. The effect of dissolved polyunsaturated aldehydes on microzooplankton growth rates in the Chesapeake Bay and Atlantic coastal waters. Marine drugs, 13, 2834-56.

- LEE, B.-Y., KIM, H.-S., CHOI, B.-S., HWANG, D.-S., CHOI, A. Y., HAN, J., WON, E.-J., CHOI, I.-Y., LEE, S.-H., OM, A.-S., PARK, H. G. & LEE, J.-S. 2015. RNA-seq based whole transcriptome analysis of the cyclopoid copepod Paracyclopina nana focusing on xenobiotics metabolism. Comparative Biochemistry and Physiology Part D: Genomics and Proteomics, 15, 12-19.

- LEE, D. S., NIOCHE, P., HAMBERG, M. & RAMAN, C. S. 2008. Structural insights into the evolutionary paths of oxylipin biosynthetic enzymes. Nature, 455, 363-8.

- LEE, M. S., BONNER, J. R., BERNARD, D. J., SANCHEZ, E. L., SAUSE, E. T., PRENTICE, R. R., BURGESS, S. M. & BRODY, L. C. 2012. Disruption of the

folate pathway in zebrafish causes developmental defects. BMC Developmental Biology, 12, 12.

- LEGRAND, E., FORGET-LERAY, J., DUFLOT, A., OLIVIER, S., THOME, J. P., DANGER, J. M. & BOULANGE-LECOMTE, C. 2016. Transcriptome analysis of the copepod Eurytemora affinis upon exposure to endocrine disruptor pesticides: Focus on reproduction and development. Aquatic toxicology, 176, 64-75.

- LEISING, A. W., PIERSON, J. J., HALSBAND-LENK, C., HORNER, R. & POSTEL, J. 2005. Copepod grazing during spring blooms: Does Calanus pacificus avoid harmful diatoms? Progress in Oceanography, 67, 384-405.

- LENZ, P. H., RONCALLI, V., HASSETT, R. P., WU, L.-S., CIESLAK, M. C., HARTLINE, D. K. & CHRISTIE, A. E. 2014. De Novo Assembly of a Transcriptome for Calanus finmarchicus (Crustacea, Copepoda) – The Dominant Zooplankter of the North Atlantic Ocean. PloS one, 9, e88589.

- LESLIE, S. N. & NAIRN, A. C. 2019. cAMP regulation of protein phosphatases PP1 and PP2A in brain. Biochimica et biophysica acta. Molecular cell research, 1866, 64-73.

- LEU, E., DAASE, M., SCHULZ, K. G., STUHR, A. & RIEBESELL, U. 2013. Effect of ocean acidification on the fatty acid composition of a natural plankton community. Biogeosciences, 10, 1143-1153.

- LEU, E., FALK-PETERSEN, S., KWAŚNIEWSKI, S., WULFF, A., EDVARDSEN, K. & HESSEN, D. O. 2006. Fatty acid dynamics during the spring bloom in a High Arctic fjord: importance of abiotic factors versus community changes. Canadian Journal of Fisheries and Aquatic Sciences, 63, 2760-2779.

- LEU, E., WIKTOR, J., SØREIDE, J. E., BERGE, J. & FALK-PETERSEN, S. 2010. Increased irradiance reduces food quality of sea ice algae. Marine Ecology Progress Series, 411, 49-60.

- LI, B. & DEWEY, C. N. 2011. RSEM: accurate transcript quantification from RNA-Seq data with or without a reference genome. BMC Bioinformatics, 12, 323.

- LIMA-MENDEZ, G., FAUST, K., HENRY, N., DECELLE, J., COLIN, S., CARCILLO, F., CHAFFRON, S., IGNACIO-ESPINOSA, J. C., ROUX, S., VINCENT, F., BITTNER, L., DARZI, Y., WANG, J., AUDIC, S., BERLINE, L., BONTEMPI, G., CABELLO, A. M., COPPOLA, L., CORNEJO-CASTILLO, F. M., D'OVIDIO, F., DE MEESTER, L., FERRERA, I., GARET-DELMAS, M.-J., GUIDI, L., LARA, E., PESANT, S., ROYO-LLONCH, M., SALAZAR, G., SÁNCHEZ, P., SEBASTIAN, M., SOUFFREAU, C., DIMIER, C., PICHERAL, M., SEARSON, S., KANDELS-LEWIS, S., GORSKY, G., NOT, F., OGATA, H., SPEICH, S., STEMMANN, L., WEISSENBACH, J., WINCKER, P., ACINAS, S.

G., SUNAGAWA, S., BORK, P., SULLIVAN, M. B., KARSENTI, E., BOWLER, C., DE VARGAS, C. & RAES, J. 2015. Determinants of community structure in the global plankton interactome. Science, 348, 1262073.

- LINDLEY, J. A. & DAYKIN, S. 2005. Variations in the distributions of Centropages chierchiae and Temora stylifera (Copepoda: Calanoida) in the north-eastern Atlantic Ocean and western European shelf waters. ICES Journal of Marine Science, 62, 869-877.

- LLEWELLYN, C. A., SOMMER, U., DUPONT, C. L., ALLEN, A. E. & VIANT, M. R. 2015. Using community metabolomics as a new approach to discriminate marine microbial particulate organic matter in the western English Channel. Progress in Oceanography, 137, 421-433.

- LOVE, M. I., HUBER, W., ANDERS, S. 2014. Moderated estimation of fold change and dispersion for RNA-seq data with DESeq2. Genome Biol., 15, 550.

- LU, N., WEI, D., CHEN, F. & YANG, S.-T. 2013. Lipidomic profiling reveals lipid regulation in the snow alga *Chlamydomonas nivalis* in response to nitrate or phosphate deprivation. Process Biochemistry, 48, 605-613.

- LUTZ, S., ANESIO, A. M., FIELD, K. & BENNING, L. G. 2015. Integrated 'Omics', Targeted Metabolite and Single-cell Analyses of Arctic Snow Algae Functionality and Adaptability. Frontiers in Microbiology, 6, 1323.

- LYU, Q., JIAO, W., ZHANG, K., BAO, Z., WANG, S. & LIU, W. 2016. Proteomic analysis of scallop hepatopancreatic extract provides insights into marine polysaccharide digestion. Scientific reports, 6, 34866.

- MAHADIK, G. A., CASTELLANI, C., MAZZOCCHI, M. G., 2017. Effect of diatom morphology on the small-scale behavior of the copepod Temora stylifera (Dana, 1849). Journal of Experimental Marine Biology and Ecology, 493, 41-48.

- MALVIYA, S., SCALCO, E., AUDIC, S., VINCENT, F., VELUCHAMY, A., POULAIN, J., WINCKER, P., IUDICONE, D., DE VARGAS, C., BITTNER, L., ZINGONE, A. & BOWLER, C. 2016. Insights into global diatom distribution and diversity in the world's ocean. Proceedings of the National Academy of Sciences of the United States of America, 113, E1516-25.

- MARCUS, N., RICHMOND, C., SEDLACEK, C., MILLER, G. & OPPERT, C. 2004. Impact of hypoxia on the survival, egg production and population dynamics of Acartia tonsa Dana. Journal of Experimental Marine Biology and Ecology, 301, 111-128.

- MAUSZ, M. A. & POHNERT, G. 2015. Phenotypic diversity of diploid and haploid *Emiliania huxleyi* cells and of cells in different growth phases revealed by comparative metabolomics. Journal of plant physiology, 172, 137-48.

- MAZZOCCHI, M. G., BUFFONI, G., CAROTENUTO, Y., PASQUALI, S. & RIBERA D'ALCALÀ, M. 2006. Effects of food conditions on the development of the population of Temora stylifera: A modeling approach. Journal of Marine Systems, 62, 71-84.

- MAZZOCCHI, M. G., BUFFONI, G., CAROTENUTO, Y., PASQUALI, S. & RIBERA D'ALCALÀ, M. 2006. Effects of food conditions on the development of the population of Temora stylifera: A modeling approach. Journal of Marine Systems, 62, 71-84.

- MAZZOCCHI, M. G., DUBROCA, L., GARCÍA-COMAS, C., CAPUA, I. D. & RIBERA D'ALCALÀ, M. 2012. Stability and resilience in coastal copepod assemblages: The case of the Mediterranean long-term ecological research at Station MC (LTER-MC). Progress in Oceanography, 97-100, 135-151.

- MAZZOCCHI, M. G., DUBROCA, L., GARCÍA-COMAS, C., CAPUA, I. D. & RIBERA D'ALCALÀ, M. 2012. Stability and resilience in coastal copepod assemblages: The case of the Mediterranean long-term ecological research at Station MC (LTER-MC). Progress in Oceanography, 97-100, 135-151.

- MAZZOCCHI, M. G., LICANDRO, P., DUBROCA, L., DI CAPUA, I. & SAGGIOMO, V. 2011. Zooplankton associations in a Mediterranean long-term time-series. Journal of Plankton Research, 33, 1163-1181.

- MCMAHON, H. T. & BOUCROT, E. 2011. Molecular mechanism and physiological functions of clathrin-mediated endocytosis. Nature reviews. Molecular cell biology, 12, 517-33.

- MD AMIN, R., KOSKI, M., BAMSTEDT, U. & VIDOUDEZ, C. 2011. Strain-related physiological and behavioral effects of *Skeletonema marinoi* on three common planktonic copepods. Marine biology, 158, 1965-1980.

- MENDEN-DEUER, S. & LESSARD, E. 2000. Carbon to volume relationships for dinoflagellates, diatoms, and other protest plankton. Limnology and Oceanography, 45, 569-579.

- MEUNIER, C. L., BOERSMA, M., WILTSHIRE, K. H. & MALZAHN, A. M. 2016. Zooplankton eat what they need: copepod selective feeding and potential consequences for marine systems. Oikos, 125, 50-58.

- MICHALEC, F.-G., KÂ, S., HOLZNER, M., SOUISSI, S., IANORA, A. & HWANG, J.-S. 2013. Changes in the swimming behavior of Pseudodiaptomus

annandalei (Copepoda, Calanoida) adults exposed to the diatom toxin 2-trans, 4-trans decadienal. Harmful algae, 30, 56-64.

- MIRALTO, A., BARONE, G., ROMANO, G., POULET, S. A., IANORA, A., RUSSO, G. L., BUTTINO, I., MAZZARELLA, G., LAABIR, M., CABRINI, M. & GIACOBBE, M. G. 1999. The insidious effect of diatoms on copepod reproduction. Nature, 402, 173.

- MIZUTA, S., YOSHINAKA, R., SATO, M. & SAKAGUCHI, M. 1994. Characterization of collagen in muscle of several crustacean species. Comparative Biochemistry and Physiology Part B: Comparative Biochemistry, 107, 365-370.

- MONTAGNES, D. J. S. & FRANKLIN, M. 2001. Effect of temperature on diatom volume, growth rate, and carbon and nitrogen content: Reconsidering some paradigms. Limnology and Oceanography, 46, 2008-2018.

- MORABITO, G., MAZZOCCHI, M. G., SALMASO, N., ZINGONE, A., BERGAMI, C., FLAIM, G., ACCORONI, S., BASSET, A., BASTIANINI, M., BELMONTE, G., BERNARDI AUBRY, F., BERTANI, I., BRESCIANI, M., BUZZI, F., CABRINI, M., CAMATTI, E., CAROPPO, C., CATALETTO, B., CASTELLANO, M., DEL NEGRO, P., DE OLAZABAL, A., DI CAPUA, I., ELIA, A. C., FORNASARO, D., GIALLAIN, M., GRILLI, F., LEONI, B., LIPIZER, M., LONGOBARDI, L., LUDOVISI, A., LUGLIÈ, A., MANCA, M., MARGIOTTA, F., MARIANI, M. A., MARINI, M., MARZOCCHI, M., OBERTEGGER, U., OGGIONI, A., PADEDDA, B. M., PANSERA, M., PISCIA, R., POVERO, P., PULINA, S., ROMAGNOLI, T., ROSATI, I., ROSSETTI, G., RUBINO, F., SARNO, D., SATTA, C. T., SECHI, N., STANCA, E., TIRELLI, V., TOTTI, C. & PUGNETTI, A. 2018. Plankton dynamics across the freshwater, transitional and marine research sites of the LTER-Italy Network. Patterns, fluctuations, drivers. Science of The Total Environment, 627, 373-387.

- MORILLO-GARCÍA, S., VALCÁRCEL-PÉREZ, N., CÓZAR, A., ORTEGA, M., MACÍAS, D., RAMÍREZ-ROMERO, E., GARCÍA, C., ECHEVARRÍA, F. & BARTUAL, A. 2014. Potential Polyunsaturated Aldehydes in the Strait of Gibraltar under Two Tidal Regimes. Marine Drugs, 12, 1438.

- MOROZOVA, O., HIRST, M. & MARRA, M. A. 2009. Applications of New Sequencing Technologies for Transcriptome Analysis. Annual Review of Genomics and Human Genetics, 10, 135-151.

- MÜLLER-NAVARRA, D. C. 2008. Food Web Paradigms: The Biochemical View on Trophic Interactions. International Review of Hydrobiology, 93, 489-505.

- MÜLLER-NAVARRA, D. C., BRETT, M. T., PARK, S., CHANDRA, S., BALLANTYNE, A. P., ZORITA, E. & GOLDMAN, C. R. 2004. Unsaturated fatty acid content in seston and tropho-dynamics coupling in lakes. Nature, 427, 69-72.

- NAKAMURA, A., AMIKURA, R., HANYU, K. & KOBAYASHI, S. 2001. *Me31b* silences translation of oocyte-localizing RNAs through the formation of cytoplasmic RNP complex during Drosophila oogenesis. Development, 128, 3233-3242.

- NANJAPPA, D., D'IPPOLITO, G., GALLO, C., ZINGONE, A. & FONTANA, A. 2014. Oxylipin diversity in the diatom family Leptocylindraceae reveals DHA derivatives in marine diatoms. Marine Drugs, 12, 368-84.

- NAPOLITANO, G. E., POLLERO, R. J., GAYOSO, A. M., MACDONALD, B. A. & THOMPSON, R. J. 1997. Fatty acids as trophic markers of phytoplankton blooms in the Bahía Blanca estuary (Buenos Aires, Argentina) and in Trinity Bay (Newfoundland, Canada). Biochemical Systematics and Ecology, 25, 739-755.

- NEWMAN, A. C. & MADDOCKS, O. D. K. 2017. One-carbon metabolism in cancer. British journal of cancer, 116, 1499-1504.

- NING, J., WANG, M., LI, C. & SUN, S. 2013. Transcriptome Sequencing and De Novo Analysis of the Copepod Calanus sinicus Using 454 GS FLX. PloS one, 8, e63741.

- O'NEILL, C. 2008. Phosphatidylinositol 3-kinase signaling in mammalian preimplantation embryo development. Reproduction, 136, 147-56.

- PAFFENHÖFER, G. A. 1998. On the relation of structure, perception and activity in marine planktonic copepods. Journal of Marine Systems, 15, 457-473.

- PAFFENHÖFER, G. A., IANORA, A., MIRALTO, A., TURNER, J. T., KLEPPEL, G. S., D'ALCALÀ, M. R., CASOTTI, R., CALDWELL, G. S., POHNERT, G., FONTANA, A., MÜLLER-NAVARRA, D., JÓNASDÓTTIR, S., ARMBRUST, V., BÅMSTEDT, U., BAN, S., BENTLEY, M. G., BOERSMA, M., BUNDY, M., BUTTINO, I., CALBET, A., CARLOTTI, F., CAROTENUTO, Y., D'IPPOLITO, G., FROST, B., GUISANDE, C., LAMPERT, W., LEE, R. F., MAZZA, S., MAZZOCCHI, M. G., NEJSTGAARD, J. C., POULET, S. A., ROMANO, G., SMETACEK, V., UYE, S., WAKEHAM, S., WATSON, S. & WICHARD, T. 2005. Colloquium on diatom-copepod interactions. Marine Ecology Progress Series, 286, 293-305.

- PAFFENHÖFER, G.-A. & KNOWLES, S. C. 1980. Omnivorousness in marine planktonic copepods. Journal of Plankton Research, 2, 355-365.

- PALIY, O. & SHANKAR, V. 2016. Application of multivariate statistical techniques in microbial ecology. Molecular ecology, 25, 1032-57.

- PALOMERA, I., OLIVAR, M. P., SALAT, J., SABATÉS, A., COLL, M., GARCÍA, A. & MORALES-NIN, B. 2007. Small pelagic fish in the NW Mediterranean Sea: An ecological review. Progress in Oceanography, 74, 377-396.

- PATTI, G. J., YANES, O. & SIUZDAK, G. 2012. Innovation: Metabolomics: the apogee of the omics trilogy. Nature reviews. Molecular Cell Biology, 13, 263-9.

- PAUL, C., MAUSZ, M. A. & POHNERT, G. 2012. A co-culturing/metabolomics approach to investigate chemically mediated interactions of planktonic organisms reveals influence of bacteria on diatom metabolism. Metabolomics, 9, 349-359.

- PEK, J. W., NG, B. F. & KAI, T. 2012. Polo-mediated phosphorylation of Maelstrom regulates oocyte determination during oogenesis in Drosophila. Development, 139, 4505-13.

- PÉREZ-PORTELA, R. & RIESGO, A. 2013. Optimizing preservation protocols to extract high-quality RNA from different tissues of echinoderms for next-generation sequencing. Molecular Ecology Resources, 13, 884-889.

- PFAFFL, M. W., HORGAN, G. W. & DEMPFLE, L. 2002. Relative expression software tool (REST) for group-wise comparison and statistical analysis of relative expression results in real-time PCR. Nucleic acids research, 30, e36-e36.

- PFAFFL, M. W., TICHOPAD, A., PRGOMET, C. & NEUVIANS, T. P. 2004. Determination of stable housekeeping genes, differentially regulated target genes and sample integrity: BestKeeper – Excel-based tool using pair-wise correlations. Biotechnology Letters, 26, 509-515.

- PIERSON, J. J., HALSBAND-LENK, C. & LEISING, A. W. 2005. Reproductive success of *Calanus pacificus* during diatom blooms in Dabob Bay, Washington. Progress in Oceanography, 67, 314-331.

- PIKIELNY, C. W., HASAN, G., ROUYER, F. & ROSBASH, M. 1994. Members of a family of drosophila putative odorant-binding proteins are expressed in different subsets of olfactory hairs. Neuron, 12, 35-49.

- POHNERT, G. 2002. Phospholipase A2 activity triggers the wound-activated chemical defense in the diatom *Thalassiosira rotula*. Plant Physiology, 129, 103-11.

- POHNERT, G. 2005. Diatom/copepod interactions in plankton: the indirect chemical defense of unicellular algae. Chembiochem : a European Journal of Chemical Biology, 6, 946-59.

- POHNERT, G. 2009. Chemical noise in the silent ocean. Journal of Plankton Research, 32, 141-144.

- POND, D., HARRIS, R., HEAD, R. & HARBOUR, D. 1996. Environmental and nutritional factors determining seasonal variability in the fecundity and egg viability of *Calanus helgolandicus* in coastal waters off Plymouth, UK. Marine Ecology Progress Series, 143, 45-63.

- POPENDORF, K. J., TANAKA, T., PUJO-PAY, M., LAGARIA, A., COURTIES, C., CONAN, P., ORIOL, L., SOFEN, L. E., MOUTIN, T. & VAN MOOY, B. A. S. 2011. Gradients in intact polar diacylglycerolipids across the Mediterranean Sea are related to phosphate availability. Biogeosciences, 8, 3733-3745.

- POPKO, J., HERRFURTH, C., FEUSSNER, K., ISCHEBECK, T., IVEN, T., HASLAM, R., HAMILTON, M., SAYANOVA, O., NAPIER, J., KHOZIN-GOLDBERG, I. & FEUSSNER, I. 2016. Metabolome Analysis Reveals Betaine Lipids as Major Source for Triglyceride Formation, and the Accumulation of Sedoheptulose during Nitrogen-Starvation of *Phaeodactylum tricornutum*. PloS one, 11, e0164673.

- POULET, S. A., CUEFF, A., WICHARD, T., MARCHETTI, J., DANCIE, C. & POHNERT, G. 2007a. Influence of diatoms on copepod reproduction. III. Consequences of abnormal oocyte maturation on reproductive factors in *Calanus helgolandicus*. Marine biology, 152, 415-428.

- POULET, S. A., ESCRIBANO, R., HIDALGO, P., CUEFF, A., WICHARD, T., AGUILERA, V., VARGAS, C. A. & POHNERT, G. 2007b. Collapse of *Calanus chilensis* reproduction in a marine environment with high diatom concentration. Journal of Experimental Marine Biology and Ecology, 352, 187-199.

- POULET, S. A., LAABIR, M., IANORA, A. & MIRALTO, A. 1995. Reproductive response of Calanus helgolandicus. I. Abnormal embryonic and naupliar development. Marine Ecology Progress Series, 129, 85-95.

- POULET, S. A., WICHARD, T., LEDOUX, J. B., LEBRETON, B., MARCHETTI, J., DANCIE, C., BONNET, D., CUEFF, A., MORIN, P. & POHNERT, G. 2006. Influence of diatoms on copepod reproduction. I. Field and laboratory observations related to *Calanus helgolandicus* egg production. Marine Ecology Progress Series, 308, 129-142.

- POULIN, R. X. & POHNERT, G. 2019. Simplifying the complex: metabolomics approaches in chemical ecology. Analytical and Bioanalytical Chemistry, 411, 13-19.

- POULIN, R. X., POULSON-ELLESTAD, K. L., ROY, J. S. & KUBANEK, J. 2018. Variable allelopathy among phytoplankton reflected in red tide metabolome. Harmful Algae, 71, 50-56.

- POULSON-ELLESTAD, K. L., JONES, C. M., ROY, J., VIANT, M. R., FERNÁNDEZ, F. M., KUBANEK, J. & NUNN, B. L. 2014. Metabolomics and proteomics reveal impacts of chemically mediated competition on marine plankton. Proceedings of the National Academy of Sciences, 111, 9009.

- RAMALHO-SANTOS, J., VARUM, S., AMARAL, S., MOTA, P. C., SOUSA, A. P. & AMARAL, A. 2009. Mitochondrial functionality in reproduction: from gonads and gametes to embryos and embryonic stem cells. Human reproduction update, 15, 553-72.

- RAVAGNAN, L., GURBUXANI, S., SUSIN, S., MAISSE-PARADISI, C., DAUGAS, E., ZAMZAMI, N., DUNCAN, G., JAATTELA, M., PENNINGER, J., GARRIDO, C. & KROEMER, G. 2001. Heat-shock protein 70 antagonizes apoptosis-inducing factor. Nature cell biology, 3, 839-43.

- RAY, J. L., ALTHAMMER, J., SKAAR, K. S., SIMONELLI, P., LARSEN, A., STOECKER, D., SAZHIN, A., IJAZ, U. Z., QUINCE, C., NEJSTGAARD, J. C., FRISCHER, M., POHNERT, G. & TROEDSSON, C. 2016. Metabarcoding and metabolome analyses of copepod grazing reveal feeding preference and linkage to metabolite classes in dynamics microbial plankton communities. Molecular Ecology, 25, 5585-5602.

- RENBERG, L., JOHANSSON, A. I., SHUTOVA, T., STENLUND, H., AKSMANN, A., RAVEN, J. A., GARDESTROM, P., MORITZ, T. & SAMUELSSON, G. 2010. A metabolomic approach to study major metabolite changes during acclimation to limiting CO2 in *Chlamydomonas reinhardtii*. Plant Physiology, 154, 187-96.

- REUSS, N. & POULSEN, L. 2002. Evaluation of fatty acids as biomarkers for a natural plankton community. A field study of a spring bloom and a post-bloom period off West Greenland. Marine Biology, 141, 423-434.

- RHEE, J. S., RAISUDDIN, S., LEE, K. W., SEO, J. S., KI, J. S., KIM, I. C., PARK, H. G. & LEE, J. S. 2009. Heat shock protein (Hsp) gene responses of the intertidal copepod Tigriopus japonicus to environmental toxicants. Comparative biochemistry and physiology. Toxicology & pharmacology : CBP, 149, 104-12.

- RIBALET, F., BASTIANINI, M., VIDOUDEZ, C., ACRI, F., BERGES, J., IANORA, A., MIRALTO, A., POHNERT, G., ROMANO, G., WICHARD, T. & CASOTTI, R. 2014. Phytoplankton Cell Lysis Associated with Polyunsaturated Aldehyde Release in the Northern Adriatic Sea. PLOS ONE, 9, e85947.

- RIBALET, F., BERGES, J. A., IANORA, A. & CASOTTI, R. 2007a. Growth inhibition of cultured marine phytoplankton by toxic algal-derived polyunsaturated aldehydes. Aquatic toxicology, 85, 219-27.

- RIBALET, F., INTERTAGLIA, L., LEBARON, P. & CASOTTI, R. 2008. Differential effect of three polyunsaturated aldehydes on marine bacterial isolates. Aquatic Toxicology, 86, 249-255.

- RIBALET, F., VIDOUDEZ, C., CASSIN, D., POHNERT, G., IANORA, A., MIRALTO, A. & CASOTTI, R. 2009. High Plasticity in the Production of Diatom-derived Polyunsaturated Aldehydes under Nutrient Limitation: Physiological and Ecological Implications. Protist, 160, 444-451.

- RIBALET, F., WICHARD, T., POHNERT, G., IANORA, A., MIRALTO, A. & CASOTTI, R. 2007b. Age and nutrient limitation enhance polyunsaturated aldehyde production in marine diatoms. Phytochemistry, 68, 2059-2067.

- RIBERA D'ALCALÀ, M., CONVERSANO, F., CORATO, F., LICANDRO, P., MANGONI, O., MARINO, D., MAZZOCCHI, M. G., MODIGH, M., MONTRESOR, M., NARDELLA, M., SAGGIOMO, V., SARNO, D., ZINGONE, A. 2004. Seasonal patterns in plankton communities in a pluriannual time series at a coastal Mediterranean site (Gulf of Naples): an attempt to discern recurrences and trends. Scientia Marina 68, 65-83.

- RICHARD, F. O. J., TSAFRIRI, A. & CONTI, M. 2001. Role of Phosphodiesterase Type 3A in Rat Oocyte Maturation1. Biology of Reproduction, 65, 1444-1451.

- ROMBOUTS, I., BEAUGRAND, G., IBANEZ, F., GASPARINI, S., CHIBA, S. & LEGENDRE, L. 2009. Global latitudinal variations in marine copepod diversity and environmental factors. Proceedings. Biological Sciences, 276, 3053-62.

- ROMBOUTS, I., BEAUGRAND, G., IBAÑEZ, F., GASPARINI, S., CHIBA, S. & LEGENDRE, L. 2010. A multivariate approach to large-scale variation in marine planktonic copepod diversity and its environmental correlates. Limnology and Oceanography, 55, 2219-2229.

- RUSSO, E., IANORA, A. & CAROTENUTO, Y. 2018. Re-shaping marine plankton communities: effects of diatom oxylipins on copepods and beyond. Marine Biology, 166.

- SADLER, T., KUSTER, C. & VON ELERT, E. 2014. Seasonal dynamics of chemotypes in a freshwater phytoplankton community – A metabolomic approach. Harmful Algae, 39, 102-111.

- SCHROEDER, A., MUELLER, O., STOCKER, S., SALOWSKY, R., LEIBER, M., GASSMANN, M., LIGHTFOOT, S., MENZEL, W., GRANZOW, M. & RAGG, T. 2006. The RIN: an RNA integrity number for assigning integrity values to RNA measurements. BMC molecular biology, 7, 3-3.

- SEMMOURI, I., ASSELMAN, J., VAN NIEUWERBURGH, F., DEFORCE, D., JANSSEN, C. R. & DE SCHAMPHELAERE, K. A. C. 2018. The transcriptome of the marine calanoid copepod Temora longicornis under heat stress and recovery. Marine Environmental Research.

- SILVER, N., BEST, S., JIANG, J. & THEIN, S. L. 2006. Selection of housekeeping genes for gene expression studies in human reticulocytes using real-time PCR. BMC molecular biology, 7, 33.

- SIMON, P. 2003. Q-Gene: processing quantitative real-time RT-PCR data. Bioinformatics, 19, 1439-40.

- SIOMI, M. C., SATO, K., PEZIC, D. & ARAVIN, A. A. 2011. PIWI-interacting small RNAs: the vanguard of genome defence. Nature Reviews Molecular Cell Biology, 12, 246.

- SOMMER, U., ADRIAN, R., DE SENERPONT DOMIS, L., ELSER, J. J., GAEDKE, U., IBELINGS, B., JEPPESEN, E., LÜRLING, M., MOLINERO, J. C., MOOIJ, W. M., VAN DONK, E. & WINDER, M. 2012. Beyond the Plankton Ecology Group (PEG) Model: Mechanisms Driving Plankton Succession. Annual Review of Ecology, Evolution, and Systematics, 43, 429-448.

- STANISŁAWSKA-SACHADYN, A., BROWN, K. S., MITCHELL, L. E., WOODSIDE, J. V., YOUNG, I. S., SCOTT, J. M., MURRAY, L., BOREHAM, C. A., MCNULTY, H., STRAIN, J. J. & WHITEHEAD, A. S. 2008. An insertion/deletion polymorphism of the dihydrofolate reductase (DHFR) gene is associated with serum and red blood cell folate concentrations in women. Human Genetics, 123, 289-295.

- STECK, S. E., KEKU, T., BUTLER, L. M., GALANKO, J., MASSA, B., MILLIKAN, R. C. & SANDLER, R. S. 2008. Polymorphisms in Methionine Synthase, Methionine Synthase Reductase and Serine Hydroxymethyltransferase, Folate and Alcohol Intake, and Colon Cancer Risk. Lifestyle Genomics, 1, 196-204.

- STEINBERG, D. K. & LANDRY, M. R. 2017. Zooplankton and the Ocean Carbon Cycle. Annual review of marine science, 9, 413-444.

- STYHLER, S., NAKAMURA, A., SWAN, A., SUTER, B. & LASKO, P. 1998. *Vasa* is required for GURKEN accumulation in the oocyte, and is involved in oocyte differentiation and germline cyst development. Development, 125, 1569-1578.

- TAIPALE, S., STRANDBERG, U., PELTOMAA, E., GALLOWAY, A. W. E., OJALA, A. & BRETT, M. T. 2013. Fatty acid composition as biomarkers of

freshwater microalgae: analysis of 37 strains of microalgae in 22 genera and in seven classes. Aquatic Microbial Ecology, 71, 165-178.

- TAJIRI, R., OGAWA, N., FUJIWARA, H. & KOJIMA, T. 2017. Mechanical Control of Whole Body Shape by a Single Cuticular Protein *Obst*ructor-E in Drosophila melanogaster. PLoS genetics, 13, e1006548.

- TARRANT, A. M., BAUMGARTNER, M. F., HANSEN, B. H., ALTIN, D., NORDTUG, T. & OLSEN, A. J. 2014. Transcriptional profiling of reproductive development, lipid storage and molting throughout the last juvenile stage of the marine copepod Calanus finmarchicus. Frontiers in Zoology, 11, 91.

- TARRANT, A., BAUMGARTNER, M., LYSIAK, N., ALTIN, D., STØRSETH, T. & HANSEN, B. 2016. Transcriptional Profiling of Metabolic Transitions during Development and Diapause Preparation in the Copepod Calanus finmarchicus. Integrative and comparative biology, 56, icw060.

- THOMPSON, P. A., GUO, M.-X., HARRISON, P. J. & WHYTE, J. N. C. 1992. Effects of variation in temperature. II. On the fatty acid composition of eight species of marine phytoplankton. Journal of Phycology, 28, 488-497.

- THOMPSON, P. A., HARRISON, P. J. & WHYTE, J. N. C. 1990. Influence of irradiance on the fatty acid composition of phytoplankton. Journal of Phycology, 26, 278-288.

- THOMSON, T., LIU, N., ARKOV, A., LEHMANN, R. & LASKO, P. 2008. Isolation of new polar granule components in Drosophila reveals P body and ER associated proteins. Mechanisms of development, 125, 865-73.

- TOMANCAK, P., GUICHET, A., ZAVORSZKY, P. & EPHRUSSI, A. 1998. Oocyte polarity depends on regulation of gurken by *Vasa*. Development, 125, 1723-1732.

- TRÉGUER, P. & PONDAVEN, P. 2000. Silica control of carbon dioxide. Nature, 406, 358-359.

- TRÉGUER, P., BOWLER, C., MORICEAU, B., DUTKIEWICZ, S., GEHLEN, M., AUMONT, O., BITTNER, L., DUGDALE, R., FINKEL, Z., IUDICONE, D., JAHN, O., GUIDI, L., LASBLEIZ, M., LEBLANC, K., LEVY, M. & PONDAVEN, P. 2017. Influence of diatom diversity on the ocean biological carbon pump. Nature Geoscience, 11, 27-37.

- TSAFRIRI, A., CHUN, S.-Y., ZHANG, R., HSUEH, A. J. W. & CONTI, M. 1996. Oocyte Maturation Involves Compartmentalization and Opposing Changes of cAMP Levels in Follicular Somatic and Germ Cells: Studies Using Selective Phosphodiesterase Inhibitors. Developmental biology, 178, 393-402.

- TURNER, J. T. 2015. Zooplankton fecal pellets, marine snow, phytodetritus and the ocean's biological pump. Progress in Oceanography, 130, 205-248.

- TURNER, J., IANORA, A., MIRALTO, A., LAABIR, M. & ESPOSITO, F. 2001. Decoupling of copepod grazing rates, fecundity and egg-hatching success on mixed and alternating diatom and dinoflagellate diets. Marine Ecology Progress Series, 220, 187-199.

- UITZ, J., CLAUSTRE, H., GENTILI, B. & STRAMSKI, D. 2010. Phytoplankton class-specific primary production in the world's oceans: Seasonal and interannual variability from satellite observations. Global Biogeochemical Cycles, 24, GB3016.

- UNDERWOOD, A.J. 1997. Experiments in ecology: Their logical design and interpretation using analysis of variance. Cambridge University Press, Cambridge.

- UTTIERI, M., CIANELLI, D., NARDELLI, B. B., BUONOCORE, B., FALCO, P., COLELLA, S. & ZAMBIANCHI, E. 2011. Multiplatform observation of the surface circulation in the Gulf of Naples (Southern Tyrrhenian Sea). Ocean Dynamics, 61, 779-796.

- VAN MOOY, B. A. S. & FREDRICKS, H. F. 2010. Bacterial and eukaryotic intact polar lipids in the eastern subtropical South Pacific: Water-column distribution, planktonic sources, and fatty acid composition. Geochimica et Cosmochimica Acta, 74, 6499-6516.

- VANDESOMPELE, J., DE PRETER, K., PATTYN, F., POPPE, B., VAN ROY, N., DE PAEPE, A. & SPELEMAN, F. 2002. Accurate normalization of real-time quantitative RT-PCR data by geometric averaging of multiple internal control genes. Genome biology, 3, RESEARCH0034-RESEARCH0034.

- VARDI, A., BIDLE, K. D., KWITYN, C., HIRSH, D. J., THOMPSON, S. M., CALLOW, J. A., FALKOWSKI, P. & BOWLER, C. 2008. A diatom gene regulating nitric-oxide signaling and susceptibility to diatom-derived aldehydes. Current Biology : CB, 18, 895-9.

- VARDI, A., FORMIGGINI, F., CASOTTI, R., DE MARTINO, A., RIBALET, F., MIRALTO, A. & BOWLER, C. 2006. A Stress Surveillance System Based on Calcium and Nitric Oxide in Marine Diatoms. PloS Biology, 4, e60.

- VARGAS, C. A., ESCRIBANO, R. & POULET, S. 2006. Phytoplankton Food Quality Determines Time Windows for Successful Zooplankton Reproductive Pulses. Ecology, 87, 2992-2999.

- VEHMAA, A., LARSSON, P., VIDOUDEZ, C., POHNERT, G., REINIKAINEN, M. & ENGSTRÖM-ÖST, J. 2011. How will increased dinoflagellate:diatom ratios

affect copepod egg production? — A case study from the Baltic Sea. Journal of Experimental Marine Biology and Ecology, 401, 134-140.

- VERITY, P. G. & SMETACEK, V. 1996. Organism life cycles, predation, and the structure of marine pelagic ecosystems. Marine Ecology Progress Series, 130, 277-293.

- VIANT, M. R. 2008. Recent developments in environmental metabolomics. Molecular bioSystems, 4, 980-6.

- VIDOUDEZ, C. & POHNERT, G. 2008. Growth phase-specific release of polyunsaturated aldehydes by the diatom *Skeletonema marinoi*. Journal of Plankton Research, 30, 1305-1313.

- VIDOUDEZ, C. & POHNERT, G. 2012. Comparative metabolomics of the diatom *Skeletonema marinoi* in different growth phases. Metabolomics, 8, 654-669.

- VIDOUDEZ, C., CASOTTI, R., BASTIANINI, M. & POHNERT, G. 2011. Quantification of dissolved and particulate polyunsaturated aldehydes in the Adriatic sea. Marine Drugs, 9, 500-13.

- VON STECHOW, L., TYPAS, D., CARRERAS PUIGVERT, J., OORT, L., SIDDAPPA, R., PINES, A., VRIELING, H., VAN DE WATER, B., MULLENDERS, L. H. & DANEN, E. H. 2015. The E3 ubiquitin ligase *ARIH1* protects against genotoxic stress by initiating a 4EHP-mediated mRNA translation arrest. Molecular and cellular biology, 35, 1254-68.

- VOZNESENSKY, M., LENZ, P. H., SPANINGS-PIERROT, C. & TOWLE, D. W. 2004. Genomic approaches to detecting thermal stress in Calanus finmarchicus (Copepoda: Calanoida). Journal of Experimental Marine Biology and Ecology, 311, 37-46.

- WAKEHAM, S. G., HEDGES, J. I., LEE, C., PETERSON, M. L., HERNES, P. J. 1997. Composition and transport of lipid biomarkers through the water column and surficial sediments of the equatorial Pacific Ocean. Deep-Sea Research Part II: Topical Studies in Oceanography 44, 2131-2162.

- WHITE, D. A., WIDDICOMBE, C. E., SOMERFIELD, P. J., AIRS, R. L., TARRAN, G. A., MAUD, J. L. & ATKINSON, A. 2015. The combined effects of seasonal community succession and adaptive algal physiology on lipid profiles of coastal phytoplankton in the Western English Channel. Marine Chemistry, 177, 638-652.

- WICHARD, T., GERECHT, A., BOERSMA, M., POULET, S. A., WILTSHIRE, K. & POHNERT, G. 2007. Lipid and fatty acid composition of diatoms revisited: rapid wound-activated change of food quality parameters influences herbivorous

copepod reproductive success. Chembiochem : a European Journal of Chemical Biology, 8, 1146-53.

- WICHARD, T., POULET, S. A. & POHNERT, G. 2005b. Determination and quantification of α,β,γ,δ-unsaturated aldehydes as pentafluorobenzyl-oxime derivates in diatom cultures and natural phytoplankton populations: application in marine field studies. Journal of Chromatography B, 814, 155-161.

- WICHARD, T., POULET, S. A., BOULESTEIX, A.-L., LEDOUX, J. B., LEBRETON, B., MARCHETTI, J. & POHNERT, G. 2008. Influence of diatoms on copepod reproduction. II. Uncorrelated effects of diatom-derived α,β,γ,δ-unsaturated aldehydes and polyunsaturated fatty acids on Calanus helgolandicus in the field. Progress in Oceanography, 77, 30-44.

- WICHARD, T., POULET, S. A., HALSBAND-LENK, C., ALBAINA, A., HARRIS, R., LIU, D. & POHNERT, G. 2005a. Survey of the Chemical Defence Potential of Diatoms: Screening of Fifty Species for α,β,γ,δ-unsaturated aldehydes. Journal of Chemical Ecology, 31, 949-958.

- WOLFRAM, S., NEJSTGAARD, J. C. & POHNERT, G. 2014. Accumulation of polyunsaturated aldehydes in the gonads of the copepod *Acartia tonsa* revealed by tailored fluorescent probes. PloS one, 9, e112522.

- WÖRDENWEBER, R., ROKITTA, S. D., HEIDENREICH, E., CORONA, K., KIRSCHHÖFER, F., FAHL, K., KLOCKE, J. L., KOTTKE, T., BRENNER-WEIß, G., ROST, B., MUSSGNUG, J. H. & KRUSE, O. 2018. Phosphorus and nitrogen starvation reveal life-cycle specific responses in the metabolome of *Emiliania huxleyi* (Haptophyta). Limnology and Oceanography, 63, 203-226.

- ZHOU, C., CAROTENUTO, Y., VITIELLO, V., WU, C., ZHANG, J. & BUTTINO, I. 2018. De novo transcriptome assembly and differential gene expression analysis of the calanoid copepod Acartia tonsa exposed to nickel nanoparticles. Chemosphere, 209, 163-172.

- ZINGONE, A., DUBROCA, L., IUDICONE, D., MARGIOTTA, F., CORATO, F., RIBERA D'ALCALÀ, M., SAGGIOMO, V. & SARNO, D. 2009. Coastal Phytoplankton Do Not Rest in Winter. Estuaries and Coasts, 33, 342-361.

- ZÖLLNER, E., HOPPE, H.-G., SOMMER, U. & JÜRGENS, K. 2009. Effect of zooplankton-mediated trophic cascades on marine microbial food web components (bacteria, nanoflagellates, ciliates). Limnology and Oceanography, 54, 262-275.

7

APPENDIX I

Table AI. 1. ANOSIM results (permutation N=9999, Euclidean distance) of diatom monthly differences in diatom community. Abbreviations: Jan=January, Feb=February, Mar=March, Apr=April, Jun=June, Jul=July, Sep=September, Oct=October, Nov-Dec=November-December. Asterisks indicate significance levels: *=p<0.05, **=p<0.01, ns=not significant. Log-transformed data and Euclidean distance are considered.

R=0.67 p<0.001	Feb	Mar	Apr	May	Jun	Jul	Sep	Oct	Nov-Dec
Jan	*	**	**	**	**	**	**	**	**
Feb		ns	*	**	**	**	*	**	ns
Mar			**	**	**	**	*	**	*
Apr				*	**	**	**	**	**
May					**	*	**	**	**
Jun						ns	**	**	**
Jul							**	*	**
Sep								*	*
Oct									ns

Table AI. 2. ANOSIM results (permutation N=9999, Bray-Curtis dissimilarity) of monthly differences in fatty acid species composition and concentration. Abbreviations: Jan=January, Feb=February, Mar=March, Apr=April, Jun=June, Jul=July, Sep=September, Oct=October, Nov-Dec=November-December. Asterisks indicate significance levels: *=p<0.05, **=p<0.01, ns=not significant. Log-transformed data and Bray-Curtis dissimilarity are considered.

R=0.47 p<0.001	Feb	Mar	Apr	May	Jun	Jul	Sep	Oct	Nov-Dec
Jan	*	**	**	**	**	**	**	**	**
Feb		*	**	**	**	**	**	**	*
Mar			*	**	**	**	*	**	ns
Apr				ns	ns	*	*	ns	ns
May					ns	*	*	*	*
Jun						ns	ns	ns	ns
Jul							ns	ns	ns
Sep								ns	ns
Oct									ns

Table AI. 3. ANOSIM results (permutation N=9999, Bray-Curtis dissimilarity) of monthly differences in NVO species composition and concentration. Abbreviations: Jan=January, Feb=February, Mar=March, Apr=April, Jun=June, Jul=July, Sep=September, Oct=October, Nov-Dec=November-December. Asterisks indicate significance levels: *=p<0.05, **=p<0.01, ns=not significant. Log-transformed data and Bray-Curtis dissimilarity are considered.

R=0.14 p<0.05	Feb	Mar	Apr	May	Jun	Jul	Sep	Oct	Nov-Dec
Jan	*	ns	**	**	*	**	*	*	*
Feb		ns	ns	ns	ns	ns	ns	ns	*
Mar			**	**	ns	**	*	*	ns
Apr				ns	ns	ns	*	*	*
May					ns	ns	*	*	**
Jun						ns	ns	ns	ns
Jul							ns	ns	*
Sep								ns	ns
Oct									ns

8

APPENDIX II

Table AII. 1. List of differentially expressed unigenes after differential expression analysis from transcriptomic analysis in Temora stylifera females collected on 23rd May 2017 (treated) and 30th May 2017 (control). Sequence name, log_2 fold-change, adjusted p-value (p-adj.), sequence length and sequence description are reported. Down-regulated sequences are reported in green text; up-regulated sequences are reported in red text.

Trinity name	log_2FoldChange	p-adj.	Length	Description
TRINITY_DN48953_c0_g1	-9.92	0.00000	1140	*---NA---*
TRINITY_DN56306_c2_g1	-7.10	0.00039	435	*putative odorant-binding protein A5*
TRINITY_DN46479_c0_g2	-6.06	0.02748	490	*TPA: hypothetical protein BOS_23229*
TRINITY_DN54322_c1_g1	-5.18	0.01537	202	*OV-16 antigen-like*
TRINITY_DN56306_c3_g2	-5.04	0.00000	426	*---NA---*
TRINITY_DN56306_c2_g2	-4.79	0.00000	256	*putative odorant-binding protein A5*
TRINITY_DN56306_c0_g1	-4.76	0.00000	279	*protein D3*
TRINITY_DN47252_c1_g3	-4.60	0.01527	622	*collagen alpha-1(I) chain-like*
TRINITY_DN56306_c3_g1	-4.51	0.00000	749	*putative odorant-binding protein A5*
TRINITY_DN44842_c0_g1	-4.46	0.04323	603	*collagen alpha-1(I) chain-like*
TRINITY_DN59703_c3_g3	-4.43	0.00000	422	*---NA---*
TRINITY_DN54322_c1_g2	-4.30	0.00145	758	*protein D2*
TRINITY_DN40295_c1_g1	-4.03	0.01381	287	*protein GVQW1-like*
TRINITY_DN57986_c1_g1	-3.82	0.04360	348	*alpha-l1 nicotinic acetyl choline receptor*
TRINITY_DN51020_c2_g1	-3.76	0.03377	861	*---NA---*
TRINITY_DN47801_c76_g1	-3.74	0.02770	255	*---NA---*

TRINITY_DN50358_c0_g1	-3.72	0.00117	2126	*serine/threonine protein phosphatase Ppa2*
TRINITY_DN50277_c3_g1	-3.52	0.00393	3180	*hypothetical protein*
TRINITY_DN48256_c0_g1	-3.39	0.02827	1552	*cell wall-associated hydrolase*
TRINITY_DN47115_c1_g1	-3.32	0.03158	1556	*cell wall-associated hydrolase*
TRINITY_DN56650_c0_g2	-3.30	0.00000	2522	*uncharacterized protein LOC111708691*
TRINITY_DN48918_c10_g1	-3.13	0.00094	214	*putative odorant-binding protein A5*
TRINITY_DN42279_c0_g1	-3.04	0.00003	502	*collagen-like protein*
TRINITY_DN41737_c0_g1	-2.95	0.01807	490	*---NA---*
TRINITY_DN42313_c0_g1	-2.93	0.00000	319	*---NA---*
TRINITY_DN48948_c2_g1	-2.85	0.00000	220	*putative odorant-binding protein A5*
TRINITY_DN48918_c8_g1	-2.83	0.00060	223	*39S ribosomal protein L38, mitochondrial*
TRINITY_DN59703_c2_g3	-2.81	0.00000	372	*---NA---*
TRINITY_DN48067_c0_g1	-2.81	0.00000	220	*uncharacterized protein LOC111712488 isoform X2*
TRINITY_DN59703_c2_g1	-2.80	0.00000	445	*putative odorant-binding protein A5*
TRINITY_DN59703_c3_g1	-2.79	0.00000	345	*---NA---*
TRINITY_DN50915_c1_g1	-2.79	0.04331	2990	*IS1 transposase InsAB*
TRINITY_DN52417_c2_g3	-2.78	0.01707	4052	*conserved hypothetical protein*
TRINITY_DN59703_c2_g2	-2.69	0.00001	239	*protein D2-like*
TRINITY_DN48788_c0_g2	-2.68	0.00961	1966	*dentin sialophosphoprotein isoform X2*
TRINITY_DN46462_c2_g1	-2.67	0.00000	676	*---NA---*
TRINITY_DN48918_c6_g2	-2.64	0.00000	866	*---NA---*
TRINITY_DN51686_c3_g3	-2.64	0.01319	821	*---NA---*
TRINITY_DN46462_c2_g2	-2.62	0.00008	382	*OV-16 antigen-like*
TRINITY_DN51574_c1_g2	-2.61	0.04331	2162	*23S rRNA (guanosine(2251)-2'-O)-methyltransferase RlmB*
TRINITY_DN48918_c11_g1	-2.55	0.01093	229	*OV-16 antigen-like*
TRINITY_DN52057_c0_g1	-2.54	0.00019	1291	*---NA---*

TRINITY_DN56306_c1_g1	-2.54	0.00000	499	*OV-16 antigen-like*
TRINITY_DN48918_c5_g1	-2.54	0.00000	499	*putative odorant-binding protein A5*
TRINITY_DN48918_c6_g1	-2.53	0.00000	477	*OV-16 antigen-like*
TRINITY_DN48948_c0_g1	-2.52	0.01864	202	*OV-16 antigen-like*
TRINITY_DN54592_c0_g1	-2.51	0.00393	1887	*uncharacterized protein LOC111700481*
TRINITY_DN50660_c0_g2	-2.45	0.03286	357	*---NA---*
TRINITY_DN43949_c0_g2	-2.44	0.00145	323	*---NA---*
TRINITY_DN48948_c1_g2	-2.40	0.00076	216	*putative odorant-binding protein A5*
TRINITY_DN50660_c0_g1	-2.37	0.00001	1081	*protein D3*
TRINITY_DN45228_c5_g1	-2.37	0.00002	281	*---NA---*
TRINITY_DN53544_c0_g3	-2.34	0.01923	1552	*altered inheritance of mitochondria protein 3-like*
TRINITY_DN48948_c1_g1	-2.32	0.00000	718	*---NA---*
TRINITY_DN44278_c0_g1	-2.31	0.03292	204	*cytochrome c oxidase subunit I (mitochondrion)*
TRINITY_DN60327_c0_g1	-2.23	0.02143	239	*---NA---*
TRINITY_DN38350_c0_g1	-2.19	0.00832	300	*collagen alpha-1(XI) chain-like*
TRINITY_DN60534_c0_g1	-2.16	0.02757	965	*---NA---*
TRINITY_DN48918_c5_g2	-2.13	0.00000	367	*protein D3*
TRINITY_DN56133_c1_g4	-2.05	0.00094	333	*sequestosome-1-like*
TRINITY_DN43949_c3_g1	-2.05	0.01584	201	*---NA---*
TRINITY_DN46002_c0_g1	-2.03	0.00163	370	*cAMP-responsive element-binding protein-like 2*
TRINITY_DN55139_c4_g1	-1.95	0.00070	759	*---NA---*
TRINITY_DN53118_c0_g1	-1.95	0.00045	1205	*cytochrome b5-like*
TRINITY_DN46104_c2_g1	-1.95	0.03531	2150	*hypothetical protein T11_14937*
TRINITY_DN59998_c0_g2	-1.88	0.02236	1293	*uncharacterized protein LOC111714070*
TRINITY_DN48367_c6_g8	-1.87	0.04258	224	*malate dehydrogenase, mitochondrial*
TRINITY_DN50562_c0_g1	-1.87	0.00225	1183	*cytochrome P450 2C9-like*

TRINITY_DN55139_c4_g2	-1.84	0.00341	292	*---NA---*
TRINITY_DN43949_c1_g1	-1.83	0.00060	243	*---NA---*
TRINITY_DN48564_c3_g1	-1.80	0.02987	509	*---NA---*
TRINITY_DN61944_c3_g2	-1.78	0.03094	569	*DNA ligase 1-like isoform X2*
TRINITY_DN58322_c1_g1	-1.76	0.01707	430	*heat shock protein 70*
TRINITY_DN60002_c1_g1	-1.76	0.00163	2872	*ariadne protein*
TRINITY_DN53340_c0_g1	-1.76	0.00327	2014	*Leukocyte receptor cluster member 9*
TRINITY_DN55139_c4_g3	-1.75	0.03978	236	*---NA---*
TRINITY_DN50562_c0_g2	-1.74	0.00224	1177	*cytochrome P450 CYP3034A1*
TRINITY_DN58203_c2_g2	-1.71	0.03908	3609	*---NA---*
TRINITY_DN44347_c0_g1	-1.71	0.00001	2339	*Carboxylic ester hydrolase*
TRINITY_DN59831_c1_g3	-1.70	0.04484	1335	*sterile alpha and TIR motif-containing protein 1 isoform X1*
TRINITY_DN51606_c3_g1	-1.67	0.04896	201	*heat shock protein beta-1*
TRINITY_DN46142_c0_g1	-1.62	0.00009	228	*peritrophins 3-A1 precursor*
TRINITY_DN49225_c2_g1	-1.55	0.02029	497	*---NA---*
TRINITY_DN54543_c0_g1	-1.54	0.00783	244	*peroxidase, putative*
TRINITY_DN45036_c0_g1	-1.53	0.00350	1409	*---NA---*
TRINITY_DN60327_c0_g3	-1.53	0.02769	431	*E3 ubiquitin-protein ligase Mdm2-like isoform X1*
TRINITY_DN55139_c3_g1	-1.53	0.00504	358	*---NA---*
TRINITY_DN61324_c6_g2	-1.49	0.02694	274	*arylsulfatase B-like*
TRINITY_DN37862_c0_g1	-1.45	0.04730	318	*arylsulfatase B-like*
TRINITY_DN46682_c4_g1	-1.41	0.01400	301	*ubiquitin*
TRINITY_DN55897_c0_g1	-1.38	0.00721	2619	*sodium-dependent nutrient amino acid transporter 1-like*
TRINITY_DN58435_c6_g2	-1.37	0.00980	1170	*---NA---*
TRINITY_DN51606_c2_g1	-1.33	0.03887	204	*heat shock protein beta-1-like*
TRINITY_DN57765_c0_g1	-1.32	0.03946	923	*---NA---*

TRINITY_DN49317_c3_g1	-1.32	0.00083	1120	*---NA---*
TRINITY_DN51502_c2_g2	-1.31	0.00961	815	*heat shock protein 70 B2*
TRINITY_DN57961_c5_g1	-1.30	0.03377	370	*heat shock protein beta-1*
TRINITY_DN48866_c0_g1	-1.29	0.03479	475	*uncharacterized protein LOC111717104*
TRINITY_DN61324_c6_g3	-1.29	0.00202	663	*arylsulfatase B-like*
TRINITY_DN61324_c6_g1	-1.29	0.00350	1527	*arylsulfatase B-like*
TRINITY_DN50806_c1_g2	-1.27	0.02769	2402	*phosphatidylserine decarboxylase proenzyme, mitochondrial-like*
TRINITY_DN46430_c2_g2	-1.25	0.02694	763	*heat shock 70 kDa protein 1-like*
TRINITY_DN57961_c4_g1	-1.20	0.03946	395	*heat shock protein beta-1*
TRINITY_DN51606_c1_g1	-1.19	0.04999	946	*heat shock protein beta-1-like*
TRINITY_DN54808_c0_g1	-1.14	0.03531	1485	*arginine kinase*
TRINITY_DN56814_c0_g1	-1.13	0.00497	1639	*arylsulfatase B-like*
TRINITY_DN56639_c0_g1	-1.05	0.03495	3285	*protein unc-45 homolog B*
TRINITY_DN59770_c0_g1	-0.96	0.01998	2778	*solute carrier organic anion transporter family member 2A1*
TRINITY_DN48929_c1_g2	1.00	0.01829	439	*---NA---*
TRINITY_DN48585_c5_g2	1.02	0.00086	467	*---NA---*
TRINITY_DN50261_c1_g1	1.07	0.01527	526	*---NA---*
TRINITY_DN46130_c0_g2	1.08	0.01783	565	*transforming growth factor-beta-induced protein ig-h3-like*
TRINITY_DN58926_c0_g1	1.12	0.00538	2475	*organic cation transporter protein-like*
TRINITY_DN47352_c0_g1	1.12	0.00261	1119	*uncharacterized protein LOC111697309*
TRINITY_DN44753_c2_g1	1.13	0.00327	652	*---NA---*
TRINITY_DN46080_c1_g2	1.23	0.00350	514	*---NA---*
TRINITY_DN47755_c1_g1	1.34	0.00163	314	*---NA---*
TRINITY_DN39167_c0_g1	1.44	0.03531	858	*vitellogenin receptor*
TRINITY_DN49031_c4_g1	1.45	0.00225	214	*---NA---*
TRINITY_DN56235_c0_g1	1.50	0.00224	976	*facilitated trehalose transporter Tret1-like*

TRINITY_DN48929_c1_g1	1.57	0.00040	406	*---NA---*
TRINITY_DN53823_c0_g4	1.58	0.01973	2294	*Facilitated trehalose transporter Tret1*
TRINITY_DN50724_c4_g1	1.68	0.00350	404	*---NA---*
TRINITY_DN47273_c4_g1	1.78	0.00225	201	*---NA---*
TRINITY_DN47638_c5_g1	2.09	0.00401	269	*---NA---*
TRINITY_DN46792_c0_g1	2.16	0.00194	1107	*---NA---*
TRINITY_DN48936_c0_g1	2.17	0.00348	2363	*uncharacterized protein LOC111698428*
TRINITY_DN46832_c5_g1	2.24	0.04890	401	*---NA---*
TRINITY_DN46134_c9_g2	2.34	0.01998	396	*---NA---*
TRINITY_DN44649_c1_g3	2.43	0.00000	439	*---NA---*
TRINITY_DN48983_c0_g1	2.61	0.03241	2068	*uncharacterized protein LOC111696662*
TRINITY_DN47725_c0_g1	2.75	0.01783	668	*---NA---*
TRINITY_DN57759_c4_g3	3.11	0.00000	224	*---NA---*
TRINITY_DN43876_c0_g1	3.42	0.00000	885	*---NA---*
TRINITY_DN26125_c0_g1	3.56	0.02336	1469	*probable serine/threonine-protein kinase samkA*
TRINITY_DN47135_c3_g1	3.58	0.00000	532	*---NA---*
TRINITY_DN41595_c0_g1	3.63	0.02261	1708	*uncharacterized protein LOC111704026 isoform X2*
TRINITY_DN44116_c1_g1	3.76	0.00035	1536	*neuronal acetylcholine receptor subunit alpha-10-like isoform X1*
TRINITY_DN54042_c0_g1	4.08	0.01707	2309	*---NA---*
TRINITY_DN57931_c1_g6	5.11	0.01059	814	*N-acylglucosamine 2-epimerase*
TRINITY_DN40267_c0_g1	5.42	0.00363	315	*putative ATP-dependent RNA helicase me31b*
TRINITY_DN52242_c0_g2	6.73	0.00000	1534	*---NA---*
TRINITY_DN52242_c0_g1	7.13	0.00039	439	*---NA---*
TRINITY_DN49250_c2_g3	8.76	0.01403	201	*---NA---*

Table AII. 2. List of differentially expressed transcripts after differential expression analysis from transcriptomic analysis in Temora stylifera females collected on 23rd May 2017 (treated) and 30th May 2017 (control). Sequence name, log_2 fold-change, adjusted p-value (p-adj.), sequence length and sequence description are reported. Down-regulated sequences are reported in green text; up-regulated sequences are reported in red text.

Trinity name	log2FoldChange	padj	Description
TRINITY_DN61915_c1_g1_i2	-10.34	9.55E-12	*1-phosphatidylinositol 3-phosphate 5-kinase-like*
TRINITY_DN56306_c3_g1_i4	-4.61	9.55E-12	*putative odorant-binding protein A5*
TRINITY_DN56306_c3_g1_i5	-4.24	9.55E-12	*putative odorant-binding protein A5*
TRINITY_DN59703_c2_g1_i2	-2.87	9.55E-12	*putative odorant-binding protein A5*
TRINITY_DN56306_c3_g2_i5	-5.07	1.63E-11	*---NA---*
TRINITY_DN56306_c3_g2_i2	-5.20	4.46E-11	*OV-16 antigen-like*
TRINITY_DN62889_c0_g1_i1	-9.72	6.51E-11	*zinc finger SWIM domain-containing protein 8-like*
TRINITY_DN59703_c3_g1_i2	-2.90	6.51E-11	*---NA---*
TRINITY_DN59703_c3_g1_i1	-2.71	6.51E-11	*OV-16 antigen-like*
TRINITY_DN56306_c0_g1_i1	-4.75	9.98E-11	*OV-16 antigen-like*
TRINITY_DN42313_c0_g1_i3	-2.81	1.81E-10	*---NA---*
TRINITY_DN52078_c1_g1_i5	-9.48	4.26E-10	*MOB kinase activator 1B*
TRINITY_DN58707_c1_g1_i11	-9.95	9.23E-10	*amyloid-beta-like protein*
TRINITY_DN58691_c0_g1_i4	-9.63	9.83E-10	*BRCA2-interacting transcriptional repressor EMSY-like*
TRINITY_DN54322_c1_g2_i5	-4.46	9.83E-10	*putative odorant-binding protein A5*
TRINITY_DN59703_c2_g3_i1	-2.92	2.12E-09	*---NA---*
TRINITY_DN61508_c0_g1_i2	-9.72	3.24E-09	*uncharacterized protein Dere_GG13897, isoform C*
TRINITY_DN61841_c6_g1_i4	-9.29	1.73E-08	*protein trapped in endoderm-1-like*
TRINITY_DN48953_c0_g1_i2	-9.91	2.28E-08	*---NA---*
TRINITY_DN56306_c3_g1_i1	-4.47	4.16E-08	*putative odorant-binding protein A5*
TRINITY_DN48918_c6_g1_i6	-2.83	6.08E-08	*putative odorant-binding protein A5*
TRINITY_DN61595_c2_g1_i1	-9.39	1.01E-07	*serine/threonine-protein phosphatase 2A 56 kDa regulatory subunit gamma isoform-*

			like isoform X1
TRINITY_DN48067_c0_g1_i1	-2.81	1.01E-07	*uncharacterized protein LOC111712488 isoform X2*
TRINITY_DN51343_c0_g1_i2	-8.83	1.44E-07	*monocarboxylate transporter 2-like*
TRINITY_DN46462_c2_g1_i3	-2.64	1.65E-07	*OV-16 antigen-like*
TRINITY_DN59703_c2_g1_i1	-2.56	2.56E-07	*putative odorant-binding protein A5*
TRINITY_DN46462_c2_g1_i1	-2.15	6.13E-07	*OV-16 antigen-like*
TRINITY_DN56306_c3_g1_i2	-4.78	6.56E-07	*---NA---*
TRINITY_DN47549_c0_g2_i1	-8.48	7.40E-07	*---NA---*
TRINITY_DN52432_c2_g1_i3	-5.23	1.93E-06	*uncharacterized protein LOC111718103*
TRINITY_DN51709_c0_g1_i5	-8.38	2.72E-06	*SET and MYND domain-containing protein 4-like*
TRINITY_DN56306_c3_g1_i7	-4.92	3.49E-06	*putative odorant-binding protein A5*
TRINITY_DN54322_c1_g2_i2	-4.20	3.49E-06	*putative odorant-binding protein A5*
TRINITY_DN44995_c9_g1_i6	-5.44	5.75E-06	*ferritin heavy chain A-like*
TRINITY_DN48918_c6_g2_i10	-2.84	5.75E-06	*putative odorant-binding protein A5*
TRINITY_DN48918_c6_g2_i5	-2.51	6.97E-06	*putative odorant-binding protein A5*
TRINITY_DN59824_c0_g1_i9	-7.91	9.86E-06	*uncharacterized protein LOC111704961*
TRINITY_DN59703_c3_g3_i1	-4.62	1.01E-05	*---NA---*
TRINITY_DN48918_c6_g2_i11	-2.67	1.05E-05	*putative odorant-binding protein A5*
TRINITY_DN48918_c5_g1_i2	-2.59	1.15E-05	*putative odorant-binding protein A5*
TRINITY_DN52419_c1_g1_i4	-8.08	1.58E-05	*trinucleotide repeat-containing gene 18 protein-like*
TRINITY_DN56306_c1_g1_i2	-2.70	1.58E-05	*OV-16 antigen-like*
TRINITY_DN54322_c1_g2_i1	-4.51	1.58E-05	*OV-16 antigen-like*
TRINITY_DN56306_c3_g2_i1	-5.61	1.66E-05	*putative odorant-binding protein A5*
TRINITY_DN56306_c2_g2_i2	-4.67	1.76E-05	*putative odorant-binding protein A5*
TRINITY_DN51438_c1_g2_i4	-8.09	1.97E-05	*14-3-3zeta, partial*
TRINITY_DN46462_c2_g1_i4	-2.66	1.97E-05	*OV-16 antigen-like*

TRINITY_DN44347_c0_g1_i1	-1.71	1.97E-05	*fatty acyl-CoA hydrolase precursor, medium chain-like*
TRINITY_DN51778_c4_g1_i2	-5.62	2.32E-05	*putative odorant-binding protein A5*
TRINITY_DN51778_c4_g1_i12	-4.89	2.49E-05	*---NA---*
TRINITY_DN48918_c5_g2_i1	-2.14	3.44E-05	*putative odorant-binding protein A5*
TRINITY_DN56306_c3_g2_i3	-4.52	5.07E-05	*OV-16 antigen-like*
TRINITY_DN56306_c3_g2_i4	-5.90	5.28E-05	*putative odorant-binding protein A5*
TRINITY_DN57618_c0_g1_i12	-8.09	5.65E-05	*uncharacterized protein LOC111704154*
TRINITY_DN63585_c4_g1_i2	-2.73	5.65E-05	*cytochrome oxidase subunit 1 (mitochondrion)*
TRINITY_DN48918_c6_g2_i4	-2.65	5.65E-05	*putative odorant-binding protein A5*
TRINITY_DN48948_c1_g1_i17	-1.97	5.65E-05	*OV-16 antigen-like*
TRINITY_DN58203_c2_g2_i2	-7.56	8.20E-05	*---NA---*
TRINITY_DN54322_c1_g1_i1	-5.18	8.41E-05	*OV-16 antigen-like*
TRINITY_DN49317_c3_g1_i1	-1.35	1.02E-04	*---NA---*
TRINITY_DN48819_c0_g1_i1	-1.94	1.05E-04	*---NA---*
TRINITY_DN56650_c0_g2_i4	-3.90	1.10E-04	*uncharacterized protein LOC111708691*
TRINITY_DN48948_c1_g1_i1	-4.07	1.15E-04	*putative odorant-binding protein A5*
TRINITY_DN61324_c6_g3_i3	-1.28	1.43E-04	*arylsulfatase B-like*
TRINITY_DN56650_c0_g2_i1	-7.73	1.58E-04	*uncharacterized protein LOC111708691*
TRINITY_DN48918_c6_g2_i7	-3.48	1.58E-04	*putative odorant-binding protein A5*
TRINITY_DN48948_c2_g1_i1	-2.86	1.58E-04	*putative odorant-binding protein A5*
TRINITY_DN51429_c3_g1_i3	-8.03	1.69E-04	*---NA---*
TRINITY_DN48918_c6_g1_i3	-2.65	1.69E-04	*OV-16 antigen-like*
TRINITY_DN50660_c0_g1_i2	-2.35	1.69E-04	*putative odorant-binding protein A5*
TRINITY_DN59703_c2_g2_i1	-2.69	1.80E-04	*putative odorant-binding protein A5*
TRINITY_DN48948_c1_g1_i6	-2.81	2.08E-04	*OV-16 antigen-like*
TRINITY_DN48948_c1_g1_i13	-2.34	2.73E-04	*OV-16 antigen-like*

TRINITY_DN46462_c2_g1_i9	-3.71	2.93E-04	*---NA---*
TRINITY_DN59576_c0_g1_i1	-8.17	2.95E-04	*ATP-dependent RNA helicase p62-like*
TRINITY_DN46462_c2_g1_i5	-2.77	2.96E-04	*---NA---*
TRINITY_DN46142_c0_g1_i1	-1.63	2.96E-04	*protein Obstructor-E-like*
TRINITY_DN48918_c6_g1_i1	-2.48	3.10E-04	*OV-16 antigen-like*
TRINITY_DN54349_c0_g1_i3	-8.18	3.15E-04	*melanization protease 1-like isoform X2*
TRINITY_DN48918_c6_g1_i2	-2.09	3.39E-04	*OV-16 antigen-like*
TRINITY_DN47040_c1_g1_i13	-5.81	3.69E-04	*uncharacterized protein LOC111707931*
TRINITY_DN48918_c6_g2_i6	-2.71	4.08E-04	*putative odorant-binding protein A5*
TRINITY_DN60795_c6_g1_i2	-7.41	4.26E-04	*AP-2 complex subunit alpha-like*
TRINITY_DN43949_c0_g2_i1	-3.29	4.26E-04	*---NA---*
TRINITY_DN48918_c6_g2_i14	-2.70	4.29E-04	*putative odorant-binding protein A5*
TRINITY_DN60146_c0_g1_i1	-7.77	4.78E-04	*E3 ubiquitin-protein ligase UHRF1-like isoform X1*
TRINITY_DN48918_c6_g2_i1	-2.60	6.18E-04	*putative odorant-binding protein A5*
TRINITY_DN45761_c1_g1_i4	-3.39	6.39E-04	*cytochrome oxidase subunit I (mitochondrion)*
TRINITY_DN63629_c3_g1_i3	-1.65	6.39E-04	*uncharacterized protein LOC111699091 isoform X1*
TRINITY_DN46462_c2_g2_i4	-3.44	6.46E-04	*OV-16 antigen-like*
TRINITY_DN54322_c1_g2_i6	-6.98	6.92E-04	*putative odorant-binding protein A5*
TRINITY_DN48918_c6_g2_i2	-2.78	7.38E-04	*putative odorant-binding protein A5*
TRINITY_DN48948_c1_g1_i12	-2.22	7.79E-04	*OV-16 antigen-like*
TRINITY_DN58090_c0_g1_i4	-7.34	8.17E-04	*---NA---*
TRINITY_DN48918_c6_g1_i4	-2.20	9.49E-04	*putative odorant-binding protein A5*
TRINITY_DN46462_c2_g1_i8	-3.25	1.00E-03	*---NA---*
TRINITY_DN63868_c1_g1_i2	-9.59	1.15E-03	*16797*
TRINITY_DN53590_c0_g1_i1	-7.67	1.41E-03	*RNA 3'-terminal phosphate cyclase-like*
TRINITY_DN42279_c0_g1_i1	-2.97	1.46E-03	*---NA---*

TRINITY_DN57870_c0_g2_i2	-6.69	1.74E-03	*RUN and FYVE domain-containing protein 2-like isoform X2*
TRINITY_DN55139_c4_g1_i4	-2.58	1.74E-03	*---NA---*
TRINITY_DN55139_c4_g1_i5	-1.83	1.74E-03	*---NA---*
TRINITY_DN60491_c0_g1_i3	-6.99	1.77E-03	*---NA---*
TRINITY_DN53118_c0_g1_i2	-1.97	1.85E-03	*uncharacterized protein LOC111705033*
TRINITY_DN50801_c1_g2_i4	-6.96	1.85E-03	*uncharacterized protein LOC111699566*
TRINITY_DN44114_c1_g1_i1	-7.17	2.22E-03	*---NA---*
TRINITY_DN43949_c1_g1_i1	-1.84	2.45E-03	*---NA---*
TRINITY_DN43771_c0_g1_i3	-6.99	2.74E-03	*---NA---*
TRINITY_DN55850_c0_g2_i2	-6.94	3.19E-03	*ribokinase-like isoform X1*
TRINITY_DN56814_c0_g1_i3	-1.13	3.56E-03	*arylsulfatase B-like isoform X2*
TRINITY_DN46511_c3_g3_i2	-8.02	3.86E-03	*---NA---*
TRINITY_DN55139_c4_g2_i1	-1.76	3.94E-03	*---NA---*
TRINITY_DN48918_c6_g1_i5	-2.64	4.12E-03	*OV-16 antigen-like*
TRINITY_DN56133_c1_g4_i1	-2.11	4.30E-03	*sequestosome-1-like*
TRINITY_DN56306_c3_g1_i6	-5.01	4.35E-03	*putative odorant-binding protein A5*
TRINITY_DN55139_c4_g1_i2	-2.18	4.78E-03	*---NA---*
TRINITY_DN56306_c2_g1_i1	-7.03	4.86E-03	*putative odorant-binding protein A5*
TRINITY_DN43307_c0_g1_i2	-6.79	4.86E-03	*uncharacterized protein LOC111703668 isoform X1*
TRINITY_DN51778_c4_g1_i5	-4.70	4.87E-03	*---NA---*
TRINITY_DN57836_c7_g3_i3	-7.12	5.24E-03	*---NA---*
TRINITY_DN35563_c0_g1_i8	-6.64	5.31E-03	*collagen alpha-1(V) chain-like*
TRINITY_DN60002_c1_g1_i1	-1.70	5.96E-03	*E3 ubiquitin-protein ligase ARIH1-like*
TRINITY_DN48041_c0_g2_i3	-1.98	6.10E-03	*---NA---*
TRINITY_DN44787_c0_g1_i11	-5.75	7.28E-03	*AF484038_1cytochrome oxidase subunit II (mitochondrion)*
TRINITY_DN57113_c0_g1_i2	-6.55	7.54E-03	*dermatopontin-like isoform X1*

TRINITY_DN46002_c0_g1_i1	-2.04	8.15E-03	*cAMP-responsive element-binding protein-like 2*
TRINITY_DN48948_c1_g2_i1	-2.40	9.46E-03	*putative odorant-binding protein A5*
TRINITY_DN45761_c1_g1_i10	-3.65	9.57E-03	*cytochrome oxidase subunit I (mitochondrion)*
TRINITY_DN54699_c0_g1_i3	-6.45	9.62E-03	*cAMP-specific 3',5'-cyclic phosphodiesterase 4C-like isoform X1*
TRINITY_DN52460_c0_g1_i4	-4.55	9.63E-03	*proton-associated sugar transporter A-like isoform X1*
TRINITY_DN48918_c8_g1_i1	-2.83	1.00E-02	*OV-16 antigen-like*
TRINITY_DN55590_c0_g2_i3	-3.51	1.06E-02	*uncharacterized protein LOC111699505*
TRINITY_DN54151_c0_g2_i2	-7.30	1.12E-02	*PREDICTED: ankyrin-2-like*
TRINITY_DN44295_c0_g1_i5	-4.21	1.16E-02	*hypothetical protein AN484_25455*
TRINITY_DN55897_c0_g1_i1	-1.38	1.18E-02	*sodium-dependent nutrient amino acid transporter 1-like*
TRINITY_DN48948_c1_g1_i4	-2.57	1.29E-02	*OV-16 antigen-like*
TRINITY_DN61324_c6_g1_i4	-1.14	1.30E-02	*arylsulfatase B-like*
TRINITY_DN52028_c0_g1_i1	-0.71	1.31E-02	*chitinase-3-like protein 1*
TRINITY_DN63004_c3_g1_i1	-6.00	1.35E-02	*uncharacterized protein LOC111699347*
TRINITY_DN56485_c0_g1_i1	-2.08	1.36E-02	*innexin inx2-like isoform X1*
TRINITY_DN55139_c4_g1_i8	-2.07	1.40E-02	*---NA---*
TRINITY_DN54543_c0_g1_i1	-1.55	1.41E-02	*UNKNOWN*
TRINITY_DN58044_c3_g1_i2	-4.70	1.43E-02	*NADH dehydrogenase subunit 4 (mitochondrion)*
TRINITY_DN46462_c2_g1_i7	-2.33	1.60E-02	*OV-16 antigen-like*
TRINITY_DN47580_c1_g1_i11	-6.88	1.62E-02	*hypothetical protein A7L40_19220*
TRINITY_DN59770_c0_g1_i3	-1.00	1.62E-02	*solute carrier organic anion transporter family member 5A1-like*
TRINITY_DN50562_c0_g2_i2	-1.71	1.64E-02	*cytochrome P450 2C15-like*
TRINITY_DN56306_c1_g1_i1	-2.42	1.67E-02	*OV-16 antigen-like*
TRINITY_DN45814_c4_g1_i8	-5.34	1.68E-02	*---NA---*
TRINITY_DN57765_c0_g1_i1	-1.61	1.69E-02	*putative uncharacterized protein DDB_G0290989*
TRINITY_DN47394_c2_g1_i3	-1.14	1.69E-02	*---NA---*

TRINITY_DN44842_c2_g1_i6	-3.55	1.74E-02	*hypothetical protein BKN39_10055*
TRINITY_DN42423_c2_g1_i6	-5.07	1.80E-02	*paramyosin, long form-like*
TRINITY_DN57961_c4_g1_i5	-1.89	1.80E-02	*heat shock protein beta-1-like*
TRINITY_DN46372_c1_g2_i11	-1.49	1.80E-02	*40S ribosomal protein S11*
TRINITY_DN57136_c0_g1_i3	-2.07	1.95E-02	*uncharacterized protein LOC111709168*
TRINITY_DN48918_c10_g1_i1	-3.14	2.17E-02	*putative odorant-binding protein A5*
TRINITY_DN55139_c3_g1_i1	-1.48	2.18E-02	*---NA---*
TRINITY_DN56639_c0_g1_i2	-1.06	2.18E-02	*protein unc-45 homolog B-like*
TRINITY_DN48918_c6_g2_i12	-2.23	2.38E-02	*putative odorant-binding protein A5*
TRINITY_DN48183_c1_g1_i7	-11.14	2.38E-02	*UNKNOWN*
TRINITY_DN48663_c0_g2_i3	-4.40	2.43E-02	*---NA---*
TRINITY_DN49074_c2_g2_i6	-3.45	2.55E-02	*hypothetical protein DAPPUDRAFT_119636*
TRINITY_DN46982_c0_g1_i2	-3.34	2.74E-02	*---NA---*
TRINITY_DN46137_c1_g1_i1	-3.58	2.76E-02	*---NA---*
TRINITY_DN58880_c2_g3_i1	-0.84	2.83E-02	*uncharacterized protein LOC111701982*
TRINITY_DN45964_c0_g1_i1	-6.56	2.94E-02	*carbohydrate sulfotransferase 11-like isoform X1*
TRINITY_DN42313_c0_g1_i1	-3.35	3.05E-02	*---NA---*
TRINITY_DN47748_c1_g1_i1	-4.01	3.05E-02	*---NA---*
TRINITY_DN47731_c3_g1_i6	-3.07	3.15E-02	*---NA---*
TRINITY_DN46682_c4_g1_i3	-1.42	3.17E-02	*ubiquitin-60S ribosomal protein L40*
TRINITY_DN55577_c0_g1_i7	-7.46	3.21E-02	*ice-structuring glycoprotein-like*
TRINITY_DN42279_c0_g1_i5	-6.50	3.22E-02	*---NA---*
TRINITY_DN48574_c9_g1_i9	-2.13	3.22E-02	*hypothetical protein WG66_6567*
TRINITY_DN58203_c2_g2_i18	-4.46	3.26E-02	*---NA---*
TRINITY_DN44989_c1_g1_i2	-4.34	3.26E-02	*60S ribosomal protein L27*
TRINITY_DN44725_c0_g2_i4	-3.46	3.28E-02	*hypothetical protein OXYTRI_13058 (macronuclear)*

TRINITY_DN46836_c0_g1_i7	-1.13	3.48E-02	*ribosomal protein S11*
TRINITY_DN58848_c2_g5_i3	-1.11	3.56E-02	*cytochrome b-c1 complex subunit 2, mitochondrial-like*
TRINITY_DN45228_c1_g1_i10	-1.92	3.64E-02	*---NA---*
TRINITY_DN46430_c2_g2_i2	-1.27	3.71E-02	*heat-shock protein Hsp70*
TRINITY_DN55678_c3_g1_i6	-4.74	3.83E-02	*hypothetical protein DAPPUDRAFT_119636*
TRINITY_DN49592_c0_g2_i10	-1.14	3.90E-02	*leukocyte surface antigen CD53-like*
TRINITY_DN46462_c2_g1_i6	-2.71	4.08E-02	*---NA---*
TRINITY_DN53513_c3_g1_i22	-1.33	4.10E-02	*cytochrome c oxidase subunit I (mitochondrion)*
TRINITY_DN43660_c0_g2_i1	-3.57	4.13E-02	*hypothetical protein AN484_25455*
TRINITY_DN48828_c0_g1_i6	-2.03	4.13E-02	*---NA---*
TRINITY_DN53513_c3_g1_i1	-3.10	4.15E-02	*cytochrome oxidase subunit I (mitochondrion)*
TRINITY_DN43792_c0_g1_i1	-3.30	4.16E-02	*predicted protein*
TRINITY_DN52728_c0_g1_i6	-4.47	4.17E-02	*---NA---*
TRINITY_DN46292_c1_g1_i6	-4.47	4.31E-02	*60S ribosomal protein L26-like*
TRINITY_DN54808_c0_g1_i1	-1.11	4.37E-02	*arginine kinase-like*
TRINITY_DN45142_c0_g1_i1	-3.68	4.53E-02	*putative uncharacterized protein ART2, partial*
TRINITY_DN48918_c6_g2_i13	-3.10	4.53E-02	*putative odorant-binding protein A5*
TRINITY_DN44582_c0_g3_i5	-3.34	4.55E-02	*hypothetical protein*
TRINITY_DN44720_c0_g1_i1	-4.10	4.68E-02	*hypothetical protein A7L46_19195, partial*
TRINITY_DN58726_c2_g1_i12	-6.00	4.80E-02	*uncharacterized protein LOC111717719*
TRINITY_DN54592_c0_g1_i1	-2.50	4.80E-02	*uncharacterized protein LOC111700481*
TRINITY_DN51606_c1_g1_i7	-1.40	4.92E-02	*heat shock protein beta-1-like*
TRINITY_DN46306_c0_g1_i7	9.84	4.82E-11	*ADP,ATP carrier protein 3*
TRINITY_DN58411_c0_g1_i2	9.57	3.73E-10	*cytochrome b (mitochondrion)*
TRINITY_DN51343_c0_g1_i5	8.76	1.54E-08	*monocarboxylate transporter 2-like*
TRINITY_DN63022_c3_g1_i6	9.52	3.26E-08	*tyrosine-protein phosphatase non-receptor type 9-like*

TRINITY_DN47419_c0_g1_i19	1.48	4.14E-08	*---NA---*
TRINITY_DN49892_c0_g1_i2	8.46	1.01E-07	*stomatin-4-like isoform X2*
TRINITY_DN44649_c1_g3_i5	8.78	2.49E-07	*vitellogenin-like*
TRINITY_DN47135_c3_g1_i1	4.42	2.54E-07	*---NA---*
TRINITY_DN52728_c0_g1_i13	8.32	2.54E-07	*---NA---*
TRINITY_DN44694_c0_g1_i4	2.78	3.96E-07	*---NA---*
TRINITY_DN62990_c0_g1_i1	8.40	4.89E-07	*protein TANC2 isoform X1*
TRINITY_DN63480_c0_g1_i1	8.41	6.12E-07	*serine/threonine-protein kinase SMG1-like*
TRINITY_DN57858_c0_g1_i6	9.31	7.22E-07	*ubiquitin carboxyl-terminal hydrolase 7 isoform X2*
TRINITY_DN47247_c2_g1_i17	1.98	1.47E-06	*---NA---*
TRINITY_DN63311_c0_g2_i2	8.03	2.41E-06	*uncharacterized protein LOC111703753 isoform X2*
TRINITY_DN62038_c7_g1_i2	7.37	3.19E-06	*heat shock 70 kDa protein cognate 4-like*
TRINITY_DN48585_c5_g2_i3	1.01	4.61E-06	*---NA---*
TRINITY_DN51709_c0_g1_i4	7.72	1.81E-05	*SET and MYND domain-containing protein 4-like*
TRINITY_DN57759_c4_g3_i1	3.11	1.92E-05	*---NA---*
TRINITY_DN44685_c4_g1_i4	7.82	2.09E-05	*tubulin beta-2C chain*
TRINITY_DN50724_c4_g1_i1	1.84	2.86E-05	*---NA---*
TRINITY_DN51872_c0_g1_i1	7.84	3.95E-05	*translocation protein SEC62-like*
TRINITY_DN59539_c0_g3_i2	2.33	6.55E-05	*sodium-coupled neutral amino acid transporter 9-like*
TRINITY_DN63479_c1_g1_i3	8.36	1.04E-04	*isoleucine--tRNA ligase, mitochondrial-like*
TRINITY_DN46736_c4_g1_i3	1.30	1.69E-04	*---NA---*
TRINITY_DN49250_c2_g3_i1	8.75	1.69E-04	*---NA---*
TRINITY_DN50801_c1_g2_i2	7.23	2.01E-04	*uncharacterized protein LOC111699566*
TRINITY_DN59211_c1_g1_i1	8.09	2.08E-04	*glutamyl aminopeptidase-like isoform X2*
TRINITY_DN53126_c0_g2_i1	7.45	2.31E-04	*zinc finger and BTB domain-containing protein 14-like isoform X2*
TRINITY_DN43876_c0_g1_i1	3.41	2.69E-04	*---NA---*

TRINITY_DN42960_c0_g2_i5	7.14	3.37E-04	*ATP-dependent RNA helicase Vasa-like*
TRINITY_DN54042_c0_g1_i1	3.97	3.39E-04	*---NA---*
TRINITY_DN44753_c2_g1_i8	1.37	4.85E-04	*---NA---*
TRINITY_DN57630_c0_g4_i2	7.21	6.20E-04	*uncharacterized protein LOC111697918*
TRINITY_DN54686_c2_g1_i2	5.02	6.25E-04	*twinkle protein, mitochondrial-like*
TRINITY_DN57354_c2_g2_i1	7.03	7.46E-04	*protein phosphatase 1H-like*
TRINITY_DN52500_c0_g1_i8	5.09	9.35E-04	*G-protein comlpex beta subunit CpcB*
TRINITY_DN54647_c1_g1_i3	0.86	1.15E-03	*---NA---*
TRINITY_DN57615_c1_g1_i7	7.42	1.58E-03	*uncharacterized protein LOC111709725*
TRINITY_DN50969_c0_g3_i2	6.88	1.63E-03	*uncharacterized protein LOC111702633 isoform X1*
TRINITY_DN57108_c1_g2_i7	8.03	1.63E-03	*transcription initiation factor TFIID subunit 5-like*
TRINITY_DN56355_c0_g1_i3	6.93	1.71E-03	*platelet-activating factor acetylhydrolase homolog 2-like*
TRINITY_DN41175_c0_g1_i7	6.93	1.74E-03	*conserved Plasmodium protein, unknown function*
TRINITY_DN50630_c0_g1_i1	7.52	1.74E-03	*zinc finger protein 431-like*
TRINITY_DN54252_c2_g4_i4	7.20	1.77E-03	*rhythmically expressed gene 2 protein-like*
TRINITY_DN46609_c0_g1_i13	0.92	1.83E-03	*---NA---*
TRINITY_DN54182_c0_g1_i1	7.00	1.83E-03	*uncharacterized protein LOC110459190*
TRINITY_DN52894_c0_g1_i4	6.88	2.49E-03	*glutathione hydrolase 2-like isoform X1*
TRINITY_DN60920_c2_g1_i3	6.83	2.74E-03	*autotransporter outer membrane beta-barrel domain-containing protein*
TRINITY_DN49250_c2_g1_i3	8.01	2.74E-03	*---NA---*
TRINITY_DN49053_c3_g3_i1	4.90	3.06E-03	*---NA---*
TRINITY_DN54686_c2_g1_i13	4.88	3.87E-03	*twinkle protein, mitochondrial-like*
TRINITY_DN48929_c1_g1_i1	2.32	3.92E-03	*---NA---*
TRINITY_DN47592_c5_g1_i2	1.34	3.92E-03	*---NA---*
TRINITY_DN52242_c0_g2_i2	6.32	3.92E-03	*---NA---*
TRINITY_DN60616_c2_g4_i2	7.18	3.92E-03	*WD and tetratricopeptide repeats protein 1-like*

TRINITY_DN58926_c0_g1_i1	1.16	4.12E-03	*organic cation transporter 1-like*
TRINITY_DN54042_c0_g1_i2	7.27	4.13E-03	*---NA---*
TRINITY_DN59517_c0_g1_i1	4.35	4.19E-03	*uncharacterized protein Dvir_GJ21895, isoform A*
TRINITY_DN49031_c4_g1_i1	1.44	4.36E-03	*---NA---*
TRINITY_DN55018_c3_g2_i7	6.62	4.86E-03	*Transposable element P transposase*
TRINITY_DN43983_c0_g1_i7	1.09	4.93E-03	*putative nuclease HARBI1*
TRINITY_DN47526_c2_g1_i11	5.22	5.41E-03	*40S ribosomal protein S3a*
TRINITY_DN60491_c0_g1_i10	6.92	5.50E-03	*---NA---*
TRINITY_DN45315_c0_g1_i1	4.45	5.71E-03	*hypothetical protein BOX15_Mlig011095g2, partial*
TRINITY_DN53791_c1_g1_i6	2.14	5.96E-03	*---NA---*
TRINITY_DN48128_c0_g1_i9	1.92	6.22E-03	*vitellogenin-1-like*
TRINITY_DN48929_c1_g2_i3	1.02	6.83E-03	*---NA---*
TRINITY_DN57863_c8_g1_i3	1.59	6.83E-03	*---NA---*
TRINITY_DN62476_c3_g1_i7	6.82	6.83E-03	*serine/arginine repetitive matrix protein 2-like*
TRINITY_DN45457_c7_g1_i2	3.47	6.90E-03	*---NA---*
TRINITY_DN51440_c1_g1_i6	1.22	7.41E-03	*---NA---*
TRINITY_DN46986_c3_g1_i4	4.98	7.72E-03	*---NA---*
TRINITY_DN55259_c0_g2_i2	7.03	7.99E-03	*dipeptidase 1-like*
TRINITY_DN59715_c1_g1_i2	6.49	8.09E-03	*uncharacterized protein C18orf8-like*
TRINITY_DN49250_c2_g1_i10	5.29	8.31E-03	*---NA---*
TRINITY_DN55457_c0_g1_i1	7.31	8.35E-03	*putative neutral sphingomyelinase*
TRINITY_DN49303_c3_g2_i2	1.79	8.44E-03	*---NA---*
TRINITY_DN47977_c1_g1_i14	4.19	8.83E-03	*uncharacterized protein LOC111708092*
TRINITY_DN46736_c4_g1_i4	1.48	9.78E-03	*---NA---*
TRINITY_DN48929_c1_g1_i2	1.55	9.86E-03	*---NA---*
TRINITY_DN63004_c3_g1_i9	6.59	1.09E-02	*uncharacterized protein LOC111699347*

TRINITY_DN55207_c2_g1_i4	6.88	1.09E-02	*cytochrome P450 3080A1*
TRINITY_DN52997_c0_g1_i9	6.67	1.12E-02	*uncharacterized protein LOC111712824 isoform X2*
TRINITY_DN47804_c2_g1_i3	10.23	1.12E-02	*---NA---*
TRINITY_DN59759_c0_g1_i7	0.98	1.16E-02	*collagen alpha-1(I) chain-like isoform X2*
TRINITY_DN47273_c4_g1_i1	1.77	1.29E-02	*---NA---*
TRINITY_DN63794_c0_g1_i1	6.52	1.29E-02	*uncharacterized protein LOC111712008*
TRINITY_DN56211_c0_g1_i4	1.62	1.30E-02	*uncharacterized protein LOC111698820 isoform X2*
TRINITY_DN57778_c0_g1_i5	6.47	1.31E-02	*uncharacterized protein LOC111702854*
TRINITY_DN63486_c4_g1_i3	7.71	1.36E-02	*phosphatidate phosphatase LPIN2-like isoform X1*
TRINITY_DN54885_c2_g2_i15	6.44	1.47E-02	*uncharacterized protein LOC111711709 isoform X1*
TRINITY_DN46471_c0_g1_i18	1.24	1.50E-02	*uncharacterized protein LOC111697309*
TRINITY_DN62176_c0_g1_i4	6.84	1.54E-02	*uncharacterized protein LOC111700460*
TRINITY_DN44753_c2_g1_i6	1.11	1.57E-02	*---NA---*
TRINITY_DN49250_c2_g1_i8	3.30	1.61E-02	*latent-transforming growth factor beta-binding protein 4-like*
TRINITY_DN58828_c12_g2_i2	1.16	1.62E-02	*replication protein A 70 kDa DNA-binding subunit-like*
TRINITY_DN46903_c1_g1_i9	1.25	1.68E-02	*---NA---*
TRINITY_DN62958_c2_g1_i14	7.16	1.74E-02	*---NA---*
TRINITY_DN47352_c0_g1_i10	1.93	1.80E-02	*uncharacterized protein LOC111697309*
TRINITY_DN49384_c5_g1_i3	2.84	1.80E-02	*---NA---*
TRINITY_DN62627_c7_g1_i1	4.60	1.80E-02	*---NA---*
TRINITY_DN48756_c1_g2_i3	6.39	1.80E-02	*hypothetical protein PTSG_05583*
TRINITY_DN56235_c0_g1_i2	1.51	1.87E-02	*facilitated trehalose transporter Tret1-like*
TRINITY_DN62669_c23_g1_i1	2.75	2.00E-02	*---NA---*
TRINITY_DN53649_c0_g1_i1	6.33	2.09E-02	*glucosidase 2 subunit beta-like*
TRINITY_DN52232_c0_g1_i1	6.28	2.18E-02	*phospholipase D alpha 1-like*
TRINITY_DN45976_c3_g1_i5	4.04	2.21E-02	*---NA---*

TRINITY_DN51616_c0_g1_i6	6.57	2.29E-02	*methyltransferase-like protein 4 isoform X1*
TRINITY_DN46511_c3_g1_i4	2.96	2.30E-02	*---NA---*
TRINITY_DN46134_c8_g1_i5	4.92	2.38E-02	*---NA---*
TRINITY_DN54004_c1_g1_i6	6.66	2.42E-02	*zinc finger protein 142-like isoform X2*
TRINITY_DN50261_c1_g1_i4	1.01	2.52E-02	*---NA---*
TRINITY_DN46134_c9_g2_i1	2.55	2.56E-02	*---NA---*
TRINITY_DN47645_c0_g1_i6	6.58	2.89E-02	*unnamed protein product, partial*
TRINITY_DN50261_c1_g1_i2	1.72	2.91E-02	*---NA---*
TRINITY_DN58138_c0_g4_i3	6.53	3.10E-02	*focal adhesion kinase 1-like isoform X2*
TRINITY_DN49250_c2_g2_i1	7.51	3.19E-02	*---NA---*
TRINITY_DN56524_c2_g4_i1	1.70	3.33E-02	*katanin p60 ATPase-containing subunit A-like 1*
TRINITY_DN47638_c5_g1_i1	2.09	3.55E-02	*---NA---*
TRINITY_DN59104_c0_g2_i1	6.22	3.91E-02	*protein maelstrom 2-like isoform X1*
TRINITY_DN48936_c0_g1_i1	2.17	4.13E-02	*uncharacterized protein LOC111698428*
TRINITY_DN54445_c0_g1_i3	6.10	4.16E-02	*---NA---*
TRINITY_DN50621_c1_g1_i1	0.99	4.42E-02	*---NA---*
TRINITY_DN57931_c1_g6_i1	5.11	4.48E-02	*uncharacterized protein LOC111709312*
TRINITY_DN60005_c0_g1_i5	4.97	4.65E-02	*---NA---*
TRINITY_DN44116_c1_g1_i1	3.77	4.67E-02	*ligand-gated ion channel 4-like precursor*
TRINITY_DN47795_c1_g1_i6	0.68	4.80E-02	*---NA---*
TRINITY_DN45706_c1_g1_i17	4.02	4.80E-02	*uncharacterized protein LOC111704217*
TRINITY_DN52242_c0_g1_i3	6.38	4.80E-02	*---NA---*
TRINITY_DN48889_c2_g1_i2	3.71	4.92E-02	*---NA---*
TRINITY_DN46289_c1_g3_i1	2.49	4.97E-02	*---NA---*